



Technical Guidelines for

**Seismic Evaluation of Existing Reinforced  
Concrete Buildings in Bangladesh for Extended  
Application of PWD Seismic Evaluation Manual**

February 2022

Prepared by

**SATREPS-TSUIB Project**

A Japan-Bangladesh Joint Research Project

The University of Tokyo  
&  
Housing and Building Research Institute



## Foreword

Natural hazards like earthquake focused in this technical report are inevitable, and disaster mitigation is a global issue that we should tackle. These problems and proposed strategies to reach their solutions for making society more disaster-resilient are not local to one country and should, therefore, be shared among related countries and regions.

Bangladesh is located in an earthquake-prone region and has been under the rapid growth of economy and urbanization, causing densely constructed and populated cities. Although the Bangladesh National Building Code (BNBC) including seismic provisions was first published in 1993 and the revised code BNBC 2020 was enforced very recently, older buildings and even some newer buildings have not been constructed with proper seismic design concept and/or supervisions, leaving a huge number of existing vulnerable buildings in urban centers to future earthquake events. Seismic evaluation and retrofitting of such vulnerable buildings are therefore of great urgency for a safer and more resilient society to future damaging earthquakes, which is also a key for a continued and sustainable development of the society.

Motivated by the imminent threat exposed to the society of Bangladesh, a research project collaborating with the Government of Bangladesh was proposed and launched in 2015 entitled “The Project for Technical Development to Upgrade Structural Integrity of Buildings in Densely Populated Urban Areas and Its Strategic Implementation towards Resilient Cities in Bangladesh (TSUIB)” under JICA(Japan International Cooperation Agency) and JST(Japan Science and Technology Agency) joint program for “Science and Technology Research Partnership for Sustainable Development (SATREPS)”. The major tasks and expected outputs from the SATREPS-TSUIB project include the development of seismic evaluation and retrofitting procedures that are suitable for reinforced concrete buildings in Bangladesh with scientific evidence and data, and this report offers evidence-based and practical guidelines and recommendations derived after the 6-year research project. Although Japan has repeatedly learned bitter lessons from damaging earthquakes and accordingly implemented seismic upgrading of existing vulnerable buildings, we do not have a cure-all medicine and the best solution in one area may not always be so in another area. It may often need to be customized to fit the needs and availability of each societal environment since the societal and design/construction practice background were different from those in Japan, and this is one of the most essential policies that we have emphasized and shared with research group members throughout the project. The implemented policy can be found in various parts of the guidelines.

Another feature that should be addressed is that the guidelines are designed to be cross-referred with closely related technical manuals for seismic evaluation and retrofit design, which were both developed in the preceded JICA CNCRP project (2011-2015) followed by the JICA BSPP project (2016-2021). These manuals provide the fundamental concept and methods of seismic evaluation and retrofitting of reinforced concrete buildings in Bangladesh while the guidelines cover extended data and/or information in detail for their practical application to those with low strength concrete, high axial loads, URM infills, flat-plate system, etc., which are often found in reinforced concrete buildings in Bangladesh and accordingly focused in the SATREPS-TSUIB project.

Our road to the goal was not flat and smooth; we faced significantly restricted activities due to a safety reason after a terror attack in Dhaka that occurred just at the beginning of the project and COVID-19 that caused the pandemic in the final corner of the project. Also, during the project, we lost the most valuable person, Dr. Jamilur Reza Choudhury, the Vice Chancellor of University of Asia Pacific and the Chairperson of the Joint Coordination Committee of the project, who had always provided us with clear and brilliant directions with compassionate suggestions. Nevertheless, both Bangladeshi and Japanese colleagues have been collaborating to successfully achieve the goal through finding a way out of such difficulties and crises, and we would like to express our sincere gratitude for their greatest efforts and contributions to the project. Their efforts have been definitely the source of our success and we are very proud of them. We do hope and believe that all the achievements including knowledge, skills, experiences, and confidence obtained and developed during the project can serve as a basis for making a more earthquake-resilient society of Bangladesh.

This project has been long supported by the Government of Bangladesh, JICA Headquarter, JICA Bangladesh Office, and JST, which fully understand the impact of the research outputs on the society of Bangladesh. Dr. Kaoru Takara, Professor of Kyoto University and Research Supervisor of SATREPS-TSUIB project, visited Dhaka and encouraged us for a fruitful and best achievement to the goal. Mr. Koichiro Miyara and Ms. Atsuko Himeno, Project Coordinators, have spared no effort to accommodate local arrangements for smooth implementation of on-site research activities in Bangladesh. Finally, we would like to take this opportunity to thank all of them for their valuable supports.

Yoshiaki Nakano  
SATREPS-TSUIB Project Japan side Leader  
Professor  
Institute of Industrial Science  
The University of Tokyo

Md. Ashraful Alam  
SATREPS-TSUIB Project Bangladesh side Leader  
Director General  
Housing and Building Research Institute  
Ministry of Housing and Public Works



## Preface

Recent earthquakes in and around Bangladesh have been highlighted the importance of preparedness of future catastrophic earthquake to make the society seismically resilient. Seismic evaluation of existing RC building and strengthening is urgent for future preparedness. Government of Bangladesh has initiated several research projects to develop seismic evaluation and strengthening methods. In this regards, a “**Manual for Seismic Evaluation of Existing Reinforced Concrete Buildings**” has been prepared by Publics Works Department (PWD) under CNCRP project, a PWD-JICA technical cooperation project (2011-2016). The PWD manual is mainly developed based on the Japanese seismic evaluation standard (JBDPA standard) and guidelines incorporating the seismic design standard in Bangladesh national building code (BNBC). Since the buildings’ structural system and characteristics are different from Japan, still there are several issues are being addressed and the development of the PWD manual is going on. The PWD seismic evaluation manual is being revised by PWD-JICA another technical cooperation project called **BSPP** project (2016-2021). The First revision of the PWD manual will be published soon. However, there is several issues that exists in RC building in Bangladesh, are addressed in the first version of PWD manual which is not incorporated in the BSPP manual. These issues are low strength concrete, inadequate beam-column joints and consideration of lateral strength of unreinforced masonry infill. In addition, the PWD manual does not consider the evaluation procedure of Flat plate structures which is also commonly found in Bangladesh. This current seismic evaluation guideline is developed to address the aforementioned issues and discusses the evaluation procedure considering these unsolved issues.

This seismic evaluation guideline is developed for extended application of PWD seismic evaluation manual that is developed thorough BSPP project. This guideline consists to six distinct chapters including the introduction chapters. Each chapter discusses about one unsolved issues and provide the evaluation procedure such as low strength concrete, beam column joint, effect of masonry infill. Chapter 2 and Chapter 6 discuss about classification of compressive strength of concrete and seismic evaluation procedure of flat plate structure. Flat plate structure is widely used and major structural system during recent development in Bangladesh. But this type of structural system is susceptible to earthquake. Seismic evaluation of flat plate structure is new concept which is very effective to conduct seismic evaluation for improving the lateral strength which is discussed in Chapter 6. Chapter 2 discusses about several procedures to understand the compressive strength of concrete. These methods are very useful screening the low concrete strength building without major destructive test. Also provides classification of concrete strength.

This current guideline and PWD manual should be used together. That why there are several cross-referencing for each chapter. However, seismic evaluation of flat plate structure is a new part and aspect for evaluation of existing RC buildings in Bangladesh.

This guideline is developed based on several research work in different direction within the duration of the project. The Working group 2 team are highly grateful to all Junior Consultants for their great effort to conduct the experiment, building investigation and also compilation the SATREPS-TSUIB guideline during the project tenure. This guideline also developed based on discussion in between Bangladesh and Japanese counterpart. The Working group 2 team are highly acknowledging to JICA for arranging such types of discussion meeting.

Finally, this guideline will be very helpful for future preparedness of earthquake disaster in Bangladesh.

Masaki Maeda  
SATREPS-TSUIB project WG2 Japan side leader  
Professor,  
Department of Architecture and building science  
Tohoku University, Sendai, Japan

Md Rafiqul Islam  
SATREPS-TSUIB project WG2 Bangladesh side leader  
Superintending Engineer  
Public Works Department, Bangladesh

## **Joint Coordination Committee**

### **Chairperson**

Jamilur Reza Choudhury

University of Asia Pacific (- April 2020)

Md. Jahangir Alam

University of Science and Technology Chittagong (December 2021-)

## **Working Groups of SATREPS-TSUIB project**

### **Working Group 1 (WG1): Data collection on building stock in Dhaka**

Co-Leader      Yoshiaki Nakano      The University of Tokyo

Co-Leader      Md Ashraful Alam      Housing and Building Research Institute

### **Working Group 2 (WG2): Development of seismic performance evaluation methodologies**

Co-Leader      Masaki Maeda      Tohoku University

Co-Leader      Rafiqul Islam      Public Works Department

### **Working Group 3 (WG3): Development of seismic retrofit schemes**

Co-Leader      Yasushi Sanada      Osaka University

Co-Leader      AFM Saiful Amin      Bangladesh University of Engineering and Technology

### **Working Group 4 (WG4): Development of efficient and effective urban planning strategies**

Co-Leader      Michio Ubaura      Tohoku University

Co-Leader      Md. Akter Mahmud      Jahangirnagar University

## Working Group 2 (WG2)

Co-Leader	Masaki Maeda	Tohoku University
Co-Leader	MD Rafiqul Islam	Public Works Department
	Yoshiaki Nakano	The University of Tokyo
	Yasushi Sanada	Osaka University
	Md. Abdul Malek Sikder	Senior Research Consultant, SATREPS-TSUIB project
	Iftexhar Anam	University of Asia Pacific
	AFM Saiful Amin	Bangladesh University of Engineering and Technology
	Matsutaro Seki	Building Research Institute
	Tomoya Nishiwaki	Tohoku University
	Kazuto Matsukawa	The University of Tokyo
	Susumu Takahashi	Daido University
	Md. Abdur Rahman Bhuiyan	Senior Research Consultant, SATREPS-TSUIB project
	Md. Mizanur Rahman	Bangladesh University of Engineering and Technology
	Sharmin Reza Chowdhury	Ahsanullah University of Engineering and Technology
	Hamood Alwahshali	Tohoku University
	Md Shafiul Islam	Tohoku University
	Debasish Sen	Ahsanullah University of Engineering and Technology
	Fatema-Tuz-Zahura	Ahsanullah University of Engineering and Technology
	Md. Jahidul Islam Khan	Public Works Department
	Humaira Binte Hasan	Public Works Department
	Md. Raquibul Hasan	Public Works Department
	Md. Iftexharul Islam	Public Works Department
	Fumio Kaneko	OYO Corporation
	Joji Sakuta	Horie Engg and Architectural Research Institute Co., Ltd
	Tsutomu Ohta	Horie Engg and Architectural Research Institute Co., Ltd
	Yuji Haga	The University of Tokyo
	Md. Ashraful Alam	Housing and Building Research Institute
	Md. Arifujjaman	Housing and Building Research Institute
	S.A.M Nassif Zubayer	Public Works Department
	Farjana Khanan	Junior Research Consultant, SATREPS-TSUIB project
	Anik Das	Junior Research Consultant, SATREPS-TSUIB project
	S. M. Muhaiminul Islam	Junior Research Consultant, SATREPS-TSUIB project
	Munirul Islam Saeed	Ahsanullah University of Engineering and Technology
	Sristi Das Gupta	Ahsanullah University of Engineering and Technology
	Md. Ibnul Warah	Housing and Building Research Institute

## **Authors**

Masaki Maeda	Tohoku University
Yoshiaki Nakano	The University of Tokyo
Yasushi Sanada	Osaka University
AFM Saiful Amin	Bangladesh University of Engineering and Technology
Matsutaro Seki	Building Research Institute
Tomoya Nishiwaki	Tohoku University
Kazuto Matsukawa	The University of Tokyo
Susumu Takahashi	Daido University
Hamood Alwashali	Tohoku University
Rokhyun Yoon	Osaka University
Md Shafiul Islam	Housing and Building Research Institute
Debasish Sen	Ahsanullah University of Engineering and Technology
HM Golam Samdani	Osaka University
Murshalin Ahmed	Osaka University

### **List of Authors by each chapter**

Chapter 1 General (Nakano)

Chapter 2 Classification of compressive strength of concrete (Nishiwaki, Amin)

Chapter 3 Columns with Low Strength Concrete and/or High Axial Load (Matsukawa, Amin)

Chapter 4 RC Frame with Masonry Infill Wall (Islam, Sen, Alwashali, Seki, Maeda)

Chapter 5 RC Beam-Column Joint (Sanada, Takahashi, Ahmed, Amin)

Chapter 6 Flat Plate Structures (Takahashi, Sanada, Yoon, Samdani)

Chapter 7 Example buildings

7.1 (Islam) / 7.2 (Ahmed) / 7.3 (Samdani)

## Table of Contents

<b>Foreword .....</b>	<b>i</b>
<b>Preface .....</b>	<b>iii</b>
<b>Joint Coordination Committee.....</b>	<b>v</b>
<b>Working Groups of SATREPS-TSUIB project .....</b>	<b>v</b>
<b>Working Group 1 (WG1): Data collection on building stock in Dhaka .....</b>	<b>v</b>
<b>Working Group 2 (WG2): Development of seismic performance evaluation methodologies.....</b>	<b>v</b>
<b>Working Group 3 (WG3): Development of seismic retrofit schemes .....</b>	<b>v</b>
<b>Working Group 4 (WG4): Development of efficient and effective urban planning strategies.....</b>	<b>v</b>
<b>Working Group 2 (WG2).....</b>	<b>vi</b>
<b>Authors .....</b>	<b>vii</b>
<b>Chapter 1 General.....</b>	<b>1</b>
1.1 General Principle .....	1
1.2 Scope of Application .....	5
1.3 Structural Modeling .....	8
1.4 Definitions .....	16
1.5 Notations.....	16
<b>Chapter 2 Classification of compressive strength of concrete.....</b>	<b>19</b>
2.1 General .....	19
2.2 Scope .....	20
2.3 Procedure to use the rebound hammer .....	22
2.4 Procedure to use the scratching test device .....	23
2.5 Determination of the classification of concrete .....	24
<b>Chapter 3 Columns with Low Strength Concrete and/or High Axial Load.....</b>	<b>29</b>
3.1 General .....	29
3.2 Calculation of Shear Strength ( $Q_{su}$ ) and Flexural Strength ( $M_u$ ).....	30
3.3 Example of application: An RC column of a five story office building in Dhaka constructed in 1985.	39

<b>Chapter 4 RC Frame with Masonry Infill Wall .....</b>	<b>43</b>
4.1 General .....	43
4.2 Classification of masonry infill wall .....	47
4.3 Judgement of failure mode .....	48
4.4 Strength index $C$ .....	55
4.5 Ductility index $F$ .....	63
4.6 Stiffness evaluation .....	66
4.7 Application examples .....	67
<b>Chapter 5 RC Beam-Column Joint.....</b>	<b>105</b>
5.1 General .....	105
5.2 Scope .....	106
5.3 Failure mechanism identification .....	107
5.4 $C$ -index .....	107
5.5 $F$ -index .....	107
<b>Chapter 6 Flat Plate Structures .....</b>	<b>119</b>
6.1 General .....	119
6.2 Scope .....	120
6.3 Judgement of failure mode .....	121
6.4 Strength index $C$ .....	126
6.5 Ductility index $F$ .....	126
6.6 Limitations.....	127
6.7 Example of Application.....	127
<b>Chapter 7 Example building .....</b>	<b>131</b>
7.1 General .....	131
7.2 Moment-resisting frame structure .....	147
7.3 Example calculation of flat plate structure .....	166

## List of Tables

Table C.2.1 Classification of concrete strength according to construction period (without testing).....	21
Table 2.1 Division of sample data into 4 zones with boundary values of Q .....	22
Table 2.2 Division of sample data into 4 zones with boundary values of GW .....	23
Table 4.3.1 Idealized Failure types of RC frame with masonry infill .....	49
Table C.4.3.1 Boundary for failure mechanism of RC frame with masonry infill.....	54
Table 4.4.1 Summary of strength .....	57
Table C.4.4.1 Past research database diagonal compression failure .....	63
Table 4.5.1 Ductility Index corresponding to Failure Mechanism.....	64
Table C 4.5.1 Idealized C-F relationship of Masonry infilled RC frame .....	65
Table C.4.6.1 Comparison between experimental initial stiffness and the proposed method.....	67
Table 4.7.1 Column dimension .....	68
Table 4.7.2 masonry infill-wall properties .....	68
Table 4.7.3 Material properties .....	69
Table C.4.2.1 A factor based on aspect ratio by Abram et al. (1996) .....	78
Table 4.3.1 Idealized Failure types of RC frame with masonry infill .....	81
Table C.4.3.1 Idealized C-F relationship of FC strengthened Masonry infilled RC frame.....	95
Table 4.3.4.1 Column dimension.....	96
Table 4.3.4.2 masonry infill-wall properties .....	96
Table 4.3.4.3 Material properties.....	97
Table 5.1. List of the C-index and F-index according to the CNCRP manual. ....	114
Table 5.2. List of the modified C-index and F-index. ....	117
Table A1 General Information .....	133
Table A2: Dimension and Reinforcement in X direction.....	134
Table A3: Tension and Shear rebar in x-direction.....	135
Table A4 Material properties.....	135
Table A5 Masonry infill-wall properties .....	138
Table A6 Failure mode of all wall in x-direction .....	140
Table A7: Strength index of all wall in x-direction.....	141
Table A8: Ductility index of wall in x-direction .....	141
Table A9: Basic seismic index ( $E_0$ ) using Equation 4 in x-direction .....	145
Table A10: Basic seismic index ( $E_0$ ) using Equation 5 in x-direction .....	146
Table A11: Seismic index of the building in both directions .....	146
Table 7.2.1 Summary .....	147
Table 7.2.2 Column Layout.....	149
Table 7.2.3 Material property .....	149
Table 7.2.3 Basic seismic index $E_0$ of 2 <sup>nd</sup> floor in the Y-Direction.....	160
Table 7.2.4 Basic seismic index $E_0$ of 2 <sup>nd</sup> floor in the Y-Direction up to $F_{limit}$ .....	161
Table 7.2.5 Basic seismic index $E_0$ of whole building .....	162
Table 7.2.6 Seismic performance judgment.....	163



Table C1 Summary of materials.....	168
Table C2 Summary of Floor weight of the structure.....	169
Table C3 Storey modification factor .....	170
Table C4 Summary of Sustaining Force of Columns.....	170
Table C5 Summary of the column lateral resistances .....	176
Table C6 Ductility index $F$ and strength index $C$ .....	178
Table C7 Summary of the seismic evaluation .....	180

## List of Figures

Figure C.1.1 CNCRP Manual [1] and BSPP Manual [2] for Seismic Evaluation of RC buildings in Bangladesh .....	1
Figure C.1.2 Cross-referred CNCRP/BSPP Manuals (PWD) and SATREPS-TSUIB Guidelines for Seismic Evaluation and Retrofit Design of Existing RC Buildings in Bangladesh .....	4
Figure C.1.3 Special issues addressed in the CNCRP Seismic Evaluation Manual (PWD) [1].....	5
Figure C.1.4 Damage to beam-column joints, losing a building's integrity (2005 Kashmir earthquake).....	7
Figure C.1.5 Example structure with partially beamless slab system .....	11
Figure C.1.6 Complex structure requiring comparison between whole and divided structure.....	13
Figure C.1.7 Effects of plain concrete on column height at ground floor .....	13
Figure C.1.8 Complicated lateral load path of a building with vertically irregular shape.....	14
Figure 2.1 Steps during non-destructive assessment of concrete .....	20
Figure C.2.1 Compressive strength of concrete in surveyed buildings according to the year of construction [2] .....	21
Figure 2.2 Classification of concrete into 4 classes depending on Q and GW boundary values.....	24
Figure C.2.2 Calibration equation for rebound hammer (Regression equation 1) .....	25
Figure C.2.3 Calibration equation for scratching test (Regression equation 1).....	25
Figure C.2.4 Normal distribution of compressive strength with upper and lower boundary values for surface hardness NDTs. ....	26
Figure C.3.1.1 Accuracy of the JBDPA shear strength calculation (Kabir et al., 2020) .....	32
Figure C.3.1.2 Accuracy of the CNCRP shear strength calculation.....	33
Figure C.3.1.3 Accuracy of the shear strength calculation with $\alpha_L$ (Kabir et al., 2020).....	33
Figure C.3.2.1 Accuracy of the flexural strength calculation using JBDPA equations.....	35
Figure C.3.2.2 Relation between $Q_{exp}$ and $Q_{mu}$ for column specimens with plain bars (Araki et al., 2011)....	35
Figure C.3.2.3 Improved accuracy of the flexural strength using enhancement factor, $e_h$ and reduction factor, $e_p$ .....	36
Figure C.3.3.1 Comparison of the calculated $cR_{mu}$ and $cR_{mu}$ in test.....	37
Figure C.3.3.2 Residual axial capacity ratio $\eta_r$ evaluation for extremely brittle column.....	37
Figure C.3.3.3 Residual axial capacity ratio $\eta_r$ evaluation for shear column .....	38
Figure C.3.3.4 Residual axial capacity ratio $\eta_r$ evaluation for flexural column.....	38
Figure C.4.1.1 Flow of seismic evaluation of RC frame with masonry infill .....	44
Figure C.4.2.2 Opening positions and partial masonry infill walls that could not be considered as a structural element .....	48
Figure 4.3.1 Contact length of masonry infill .....	50
Figure C.4.3.1 Idealization of masonry infilled RC frame .....	51
Figure C.4.3.2 Deformation of a beam on an elastic foundation.....	51
Figure C.4.3.3 Surrounding RC column (a) un-deformed shape, (b) deformed shape and (c) curvature distribution.....	52
Figure C.4.3.4 Idea to separate failure modes based on contact length.....	53

Figure C.4.3.5 Comparison of experimental failure modes and $a_c/h_o$ ratio .....	54
Figure C.4.3.6 (a) Distribution of normalized contact length and (b) Cumulative distribution of normalized contact length for different failure modes .....	54
Figure C.4.3.7 Prism compressive strength based on brick strength reported in the Code TMS 402/602-16. ....	55
Figure C.4.4.1 (a) Idealized load transfer mechanism of diagonal compression (Type I) (Sen 2020) and (b) concept of idealized diagonal strut width .....	59
Figure C 4.4.2 Surrounding RC column (a) un-deformed shape, (b) deformed shape and (c) curvature distribution.....	60
Figure C.4.4.3 Reduction in compressive strength of masonry infill due to orientation by A.W. Page (1981) .....	61
Figure C.4.4.4 Reduction in compressive strength of masonry infill due to orientation by Hamid et al (1980) .....	61
Figure C.4.4.5 Schematic drawing of sliding mechanism and axial load from strut.....	62
Figure C.4.4.6 Comparison between maximum lateral strength by experiment results and calculated results using this guideline.....	63
Figure C.4.5.1 Relationship between experimental $F$ -index and contact length ratio ( $a_c/h_o$ ) .....	64
Figure C.4.6.1 Idealization of masonry infilled RC frame as braced RC frame .....	66
Figure 4.7.1 Architectural plan (dimensions are in mm).....	68
Figure 4.7.2 Location of masonry infill.....	69
Figure 4.7.3 Masonry Infilled RC Frame $W_1$ .....	70
Figure 4.7.4 Masonry Infilled RC Frame $W_3$ .....	71
Figure C.4.1.1 Comparison between different methods proposed to calculate the reduction of strength due to openings.....	75
Figure 4.2.1 Out-of-plane failure considering the arching mechanism.....	76
Figure C.4.2.1 Relationship between boundary conditions and the out-of-plane capacity by Dawe and Seah (1989) .....	77
Figure C.4.3.1 Comparison of experimental results and calculated results based on Eq. (4.3.3) [Alwashali et al. (2018)] .....	83
Figure C.4.3.2 Comparison of experimental failure modes and $\beta$ -index.....	84
Figure C.4.3.3 (a) Distribution of $\beta$ index with different failure mode (b) Cumulative distribution of $\beta$ index for different failure modes.....	84
Figure C.4.3.4 Correlation between $\beta$ index and contact length ratio .....	85
Figure C.4.3.5 Strut width and contact length at maximum strength .....	88
Figure C.4.3.6 Reduction in compressive strength of masonry infill due to orientation <sup>89</sup> by A.W. Page (1981) .....	89
Figure C.4.3.7 Reduction in compressive strength of masonry infill due to orientation <sup>89</sup> by Hamid et al. (1980) .....	89
Figure C.4.3.8 Relationship between ratio of strut width to diagonal length and $\beta$ -index based on experimental results (Alwashali et al. 2018) .....	90
Figure C.4.3.9 Relationship between shear strength and $\beta$ -index based on other past experimental data .....	91

Figure C.4.3.10 Schematic drawing of sliding mechanism and axial load from strut.....	91
Figure C.4.3.11 Relationship between prism compressive strength and shear strength of masonry infill .....	93
Figure C.4.3.12 Relationship of experimental $F$ -index with relative strength ( $\beta$ ).....	94
Figure 4.3.4.1 Architectural plan (dimensions are in mm).....	96
Figure 4.3.4.2 Location of masonry infill.....	98
Figure 4.3.4.3 Masonry Infilled RC Frame W1 .....	98
Figure 4.3.4.4 Masonry Infilled RC Frame W3 .....	100
Figure C.5.1 Typical exterior beam-column joint under construction in 2017. ....	105
Figure C.5.2 Flow of the seismic performance evaluation considering existence of exterior beam-column joint with poor anchorage of beam longitudinal rebar.....	106
Figure C.5.3 Equilibrium of moment/force at beam-column joint for equation (1).....	109
Figure C.5.4 Test specimens and loading scheme.....	110
Figure C.5.5 Comparisons of the seismic performance.....	111
Figure C.5.6 Comparison between the experiment and FE analysis. ....	112
Figure 5.7 Sample building. ....	113
Figure 5.8 C-F relationship according to the CNCRP manual. ....	114
Figure 5.9 Modified C-F relationship.....	117
Figure 6.1.1 Flat plate structure.....	119
Figure 6.1.2 Flat slab structure .....	120
Figure 6.1.3 Flat-plate structure with beams in perimeter frame .....	120
Figure C.6.3.1 Outline of experiment.....	124
Figure C.6.3.2 Experimental result (Specimen FP-C1).....	124
Figure C. 6.3.3 Assumed moment diagram .....	125
Figure C.6.3.4 Capacity of vertical load.....	125
Figure C.6.3.5 Capacity of bending moment.....	126
Figure C.6.4.3 Experimental result (Specimen FP-C2).....	127
Figure: General flow of evaluation.....	132
Figure A3 Floor plan with column layout .....	134
Figure A5 C-F relationship in x direction at ground floor.....	136
Figure A6 Architectural plan (dimensions are in mm).....	138
Figure A7 Masonry infill wall W1 .....	139
Figure 7.2.1 Typical floor plan.....	148
Figure 7.2.2 Column schedule.....	148
Figure 7.2.3 Column layout.....	149
Figure 7.2.5 Seismic evaluation results according the CNCRP/BSPP Manuals. ....	160
Figure 7.2.6 Structural performance curve.....	163
Figure C1 Flow Diagram of Seismic Evaluation.....	167
Figure C2 Typical floor layout with exterior beams .....	168
Figure C3 Column schedule of the existing structure .....	169
Figure C4 Assumed moment diagram at slab yielding (Grid Y2).....	173

Figure C5 Assumed moment diagram for slab punching .....	175
Figure C6 Relationship between strength index $C$ and ductility index $F$ .....	179
Figure C7 Comparison between seismic demand and capacity .....	180

This Page is Intentionally Left Blank

## Chapter 1 General

### 1.1 General Principle

- (1) The Technical Guidelines shall apply to seismically evaluate the structural performance of existing reinforced concrete buildings in Bangladesh.
- (2) The Guidelines shall apply to obtain technically appropriate parameters and data for extended application of “Manual for Seismic Evaluation of Existing Reinforced Concrete Buildings (PWD 2021).”

#### [Commentary]

(1) Bangladesh is located in an earthquake-prone region and has been under the rapid growth of economy and urbanization, causing densely constructed and populated cities. Although the Bangladesh National Building Code (BNBC) including seismic provisions was first published in 1993 and the revised code BNBC 2020 was enforced very recently, older buildings and even some newer buildings have not been constructed with proper seismic design concept and/or supervisions, leaving a huge number of existing vulnerable buildings in urban centers to future earthquake events. Seismic evaluation and retrofit of such vulnerable buildings are therefore of great urgency for a safer and more resilient society to future damaging earthquakes.

In light of such an imminent threat to expanding cities in Bangladesh, a technical cooperation project for Capacity Development on Natural Disaster Resistant Techniques of Construction and Retrofitting for Public Buildings (CNCRP) started in 2011 focusing on seismic evaluation and retrofit of existing vulnerable reinforced concrete buildings (RC) in Bangladesh. It was a multi-fold project, emphasizing its major outputs of the development of a seismic evaluation manual and retrofit manual for existing RC buildings [1]. This project was followed by the Project on Promoting Building Safety for Disaster Risk Reduction (BSPP) and the manuals were revised and published in 2021[2] (*Figure C.1.1*). While compiling the manuals in the CNCRP project, the major problems were the lack of technical information and reliable data regarding structural

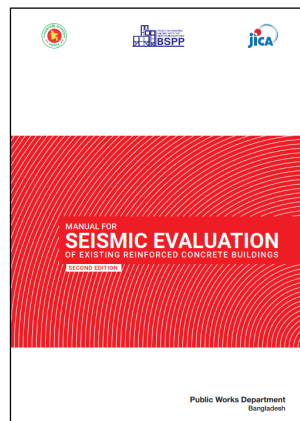
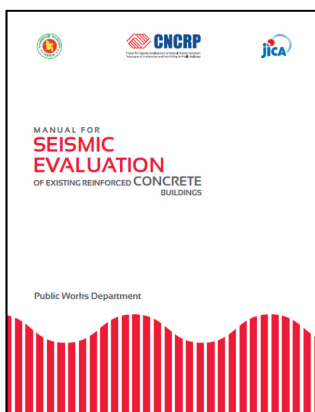


Figure C.1.1 CNCRP Manual [1] and BSPP Manual [2] for Seismic Evaluation of RC buildings in Bangladesh

performances of buildings in Bangladesh, especially those based on experimentally or numerically verified data and/or evidence. Some parameters or equations to evaluate structural performance were therefore tentatively determined and employed in the Manual, referring to the *Standard for Seismic Evaluation of Existing Reinforced Concrete Buildings*[3] that was exclusively developed for buildings in Japan, and further studies were highly expected to enrich the manual for more rational contents suitable for buildings in Bangladesh since the societal and design/construction practice background were different from those in Japan.

Motivated by these findings and experiences during the CNCRP project, a research project collaborating with the Government of Bangladesh was proposed and launched in 2015 entitled “*Technical Development to Upgrade Structural Integrity of Buildings in Densely Populated Urban Areas and Its Strategic Implementation towards Resilient Cities in Bangladesh (TSUIB)*” under JICA(Japan International Cooperation Agency) and JST(Japan Science and Technology Agency) joint program for “*Science and Technology Research Partnership for Sustainable Development (SATREPS)*”. The major tasks and expected outputs from the SATREPS-TSUIB project include the development of seismic evaluation and retrofit procedures that are suitable for buildings in Bangladesh with scientific evidence and data which did not appear in the CNCRP Manual. As can be found subsequently in Section 1.2 and Chapters 2 through 6, the Guidelines provide methods and parameters to evaluate the strength and ductility of RC buildings typically found in Bangladesh, which are essential to appropriately evaluate the seismic capacity index of a structure,  $I_s$ , but are not quantitatively described in the CNCRP/BSPP Manuals (PWD) [1] [2].

(2) As can be found in **Figure C.1.2**, the fundamental concept and calculation procedure (or basic flow) for seismic evaluation are found in the CNCRP/BSPP Manuals, and the Guidelines, therefore, provide essential and imperative procedures and parameters to appropriately calculate the strength and ductility index of a building with specific survey conditions and/or structural characteristics. The SATREPS-TSUIB Guidelines and CNCRP/BSPP Manuals are expected to be cross-referred because the Guidelines are designed to provide missing data and/or information in the CNCRP/BSPP Manuals while the Manual contains the fundamental concept and methods of the seismic evaluation procedure. For example, structural engineers can follow the basic procedure to calculate the seismic index of a structure,  $I_s$ , which appears in the CNCRP/BSPP Manuals, and they can refer to the SATREPS-TSUIB Guidelines to calculate the strength and ductility index for URM wall and boundary RC frames which are not specified in the CNCRP/BSPP Manuals if the target building concerned contains URM walls in the RC frame, as is often found in Bangladesh.



## References

- [1] Public Works Department “Manual for Seismic Evaluation of Existing Reinforced Concrete Buildings,” Prepared under the Project for Capacity Development on Natural Disaster Resistant Techniques of Construction and Retrofitting for Public Buildings (CNCRP), A Technical Cooperation Project between PWD and JICA, June 2015.
- [2] Public Works Department “Manual for Seismic Evaluation of Existing Reinforced Concrete Buildings (Second edition),” Prepared under the Project on Promoting Building Safety for Disaster Risk Reduction (BSPP), A Technical Cooperation Project between PWD and JICA, November 2021.
- [3] Japan Building Disaster Prevention Association (JBDPA), “Standard for Seismic Evaluation of Existing Reinforced Concrete Buildings, 2001, Guidelines for Seismic Retrofit of Existing Reinforced Concrete Buildings, 2001 and Technical Manual for Seismic Evaluation of Existing Reinforced Concrete Buildings, 2001” (English version), March 2004.

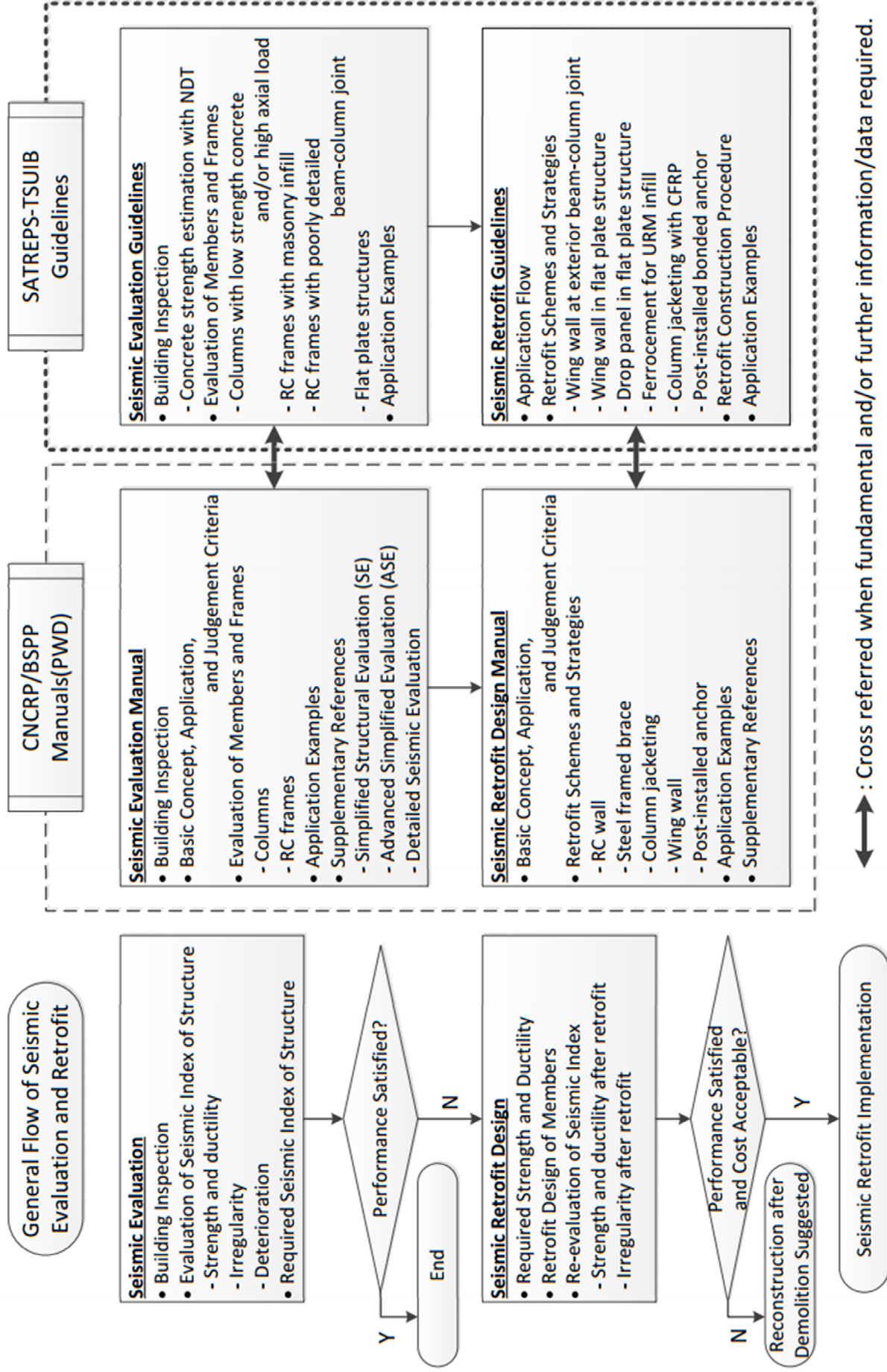


Fig. C.1.2 Cross-referred CNCRP/BSPP Manuals (PWD) and SATREPS-TSUIB Guidelines for Seismic Evaluation and Retrofit Design of Existing RC Buildings in Bangladesh

## 1.2 Scope of Application

The Guidelines shall apply to estimate the following structural parameters.

- (1) Compressive strength of concrete with non-destructive testing,
- (2) Lateral strength and ductility of RC columns with low strength concrete and/or high axial load,
- (3) Lateral strength and ductility of RC frame with masonry infill,
- (4) Lateral strength and ductility of RC frame with poorly detailed beam-column joint, and
- (5) Lateral strength and ductility of flat plate structures.

### [Commentary]

**Figure C.1.3** illustrates the typical problems identified in applying the CNCRP Manual (PWD) [1] and further studies recommended in the CNCRP project. Some parameters or values in the Manual were provisionally determined referring to those in the Japanese Standard for Seismic Evaluation since experimentally or numerically verified data and/or evidence were found limited in Bangladesh. The SATREPS-TSUIB project, therefore, was proposed and researches have been extensively carried out mainly focusing on experimental investigations to fill the gap between knowledge and practical applications. Based on the finding from the SATREPS-TSUIB project, the Technical Guidelines can provide reliable answers to such problems, although not to all, in the subsequent Chapters.

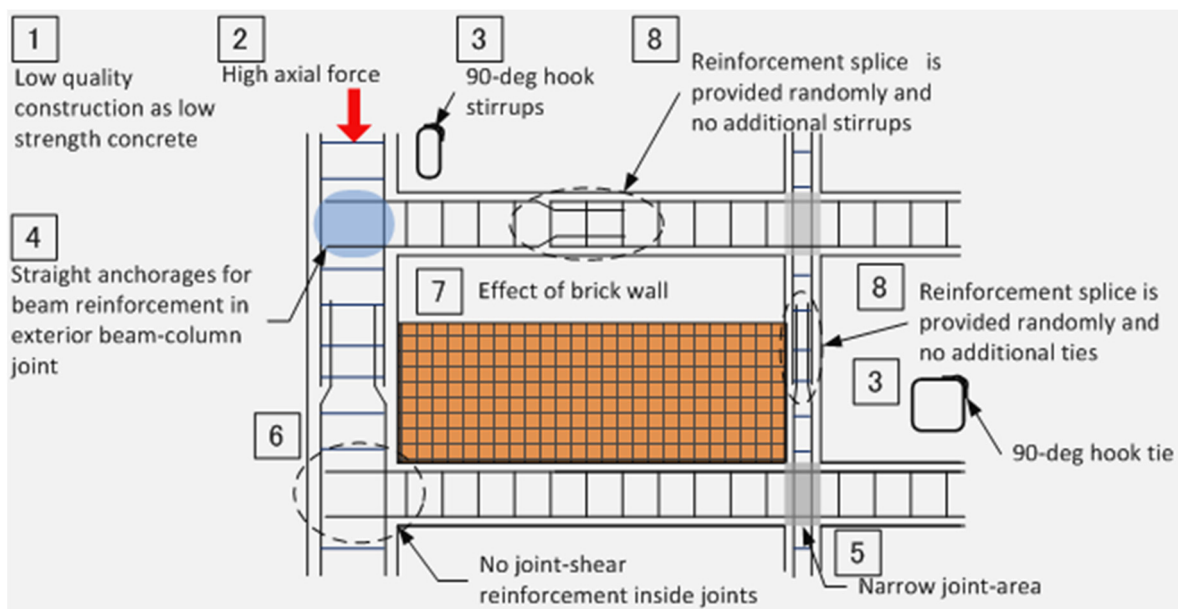


Figure C.1.3 Special issues addressed in the CNCRP Seismic Evaluation Manual (PWD) [1]

(1) Concrete core samplings from structural members undoubtedly provide the most reliable data to estimate the concrete strength to be used in estimating the strength and ductility of structural members. It is often found difficult, however, to obtain core samplings because the member is not large enough to drill the core or the

building owners do not agree with destructive testing. Non-destructive testing (NDT) procedures are therefore often practical options if reliable data can be obtained.

NDTs often show widely scattered test results, which may be more likely to be observed in concrete with low strength. Chapter 2 describes the application of NDTs and their limit to rationally apply the test results to a seismic evaluation of existing RC buildings.

(2) Low strength concrete and/or high axial loads acting on RC columns significantly affect their strength and ductility and this is especially so when the concrete strength  $F_c$  is low because it may significantly increase the concrete axial load ratio  $N/Ag F_c$  ( $N$ : axial load,  $Ag$ : sectional area of a column,  $F_c$ : compressive strength of concrete) leading to a premature failure under seismic loads. Buildings in Bangladesh are often found constructed with lower strength and/or much higher axial loads than those in Japan. Equations and their coefficients that are generally employed in the Seismic Evaluations Standard of existing RC buildings in Japan, to which the CNCRP/BSPP Manuals (PWD) [1] [2] refer, may not give appropriate predictions of structural behaviors of buildings in Bangladesh. To clarify whether or not the equations and coefficients conventionally used in the Standard can be applied to buildings in Bangladesh, statistical studies were made considering the effects of major structural differences found in buildings in Bangladesh, e.g., lower concrete strength, higher axial load ratio, different material properties of concrete, etc. and their applicability was examined. Also, an equation developed in the preceded researches that would better predict the shear strength of RC columns over a wider range of concrete strength lower than the scope of applications assumed in the Standard is proposed in Chapter 3.

(3) Frames with unreinforced masonry (URM) infill is a general construction practice of RC buildings in Bangladesh. To properly predict the structural behavior of such typical buildings is therefore of great importance to identify the vulnerability of densely constructed cities. As has been well accepted in the earthquake engineering community, the URM greatly contributes to the seismic performance of buildings, both positively and negatively although it has been generally neglected in the seismic design. Since the quantitatively verified data on the strength, ductility, failure modes, and their governing parameters of URM infilled RC frames are limited, they were experimentally examined and the evaluation procedure that can be directly applied to the seismic evaluation of URM infilled RC buildings is proposed in Chapter 4.

(4) Improperly designed or supervised RC buildings often have poorly detailed beam-column joints with insufficient embedment length and/or anchorage details of beam reinforcing bars into the joint, which leads to pull-out failure of reinforcing bars and eventually hampers the structure to reach its potential seismic performance expected in the design as shown in **Figure C.1.4**. To understand such weakness of a structure is also fundamental and essential to seek strategies to upgrade the seismic capacity of buildings with structural

integrity as well as to properly predict the as-is seismic performance of existing buildings expected during earthquake events. In general, computer software which is often used in structural design does not incorporate such structural deficit in structural analyses, and does not necessarily give correct but gives overestimated answers. Chapter 5 evaluates the seismic capacity of RC buildings considering the possible pull-out failure of beam longitudinal rebars.

(5) Flat-plate structures are another design and construction trend generally found in urban centers of Bangladesh because they can offer design-flexible interior space without beam sections and fashionable facade. Flat-plate structures, however, should be more carefully designed and constructed so that the joints with columns and slabs, generally much thinner than beams, should behave in a ductile manner under lateral loads, which often needs more engineering knowledge and experiences than ordinary buildings. Bangladeshi Engineers often point out, however, that even newer flat-plate buildings are questionable in their seismic performance, and they are also targeted buildings to be urgently evaluated and retrofitted if needed.

Since the flat-plate buildings are not a major construction style in Japan and the Standard for Seismic Evaluation does not include this structure, the structural behavior of typical flat-plate structures are experimentally examined, and their findings are incorporated in their seismic evaluation procedure in Chapter 6.



Figure C.1.4 Damage to beam-column joints, losing a building's integrity (2005 Kashmir earthquake)

### 1.3 Structural Modeling

Structures shall be properly modeled carefully considering their structural configuration, detailing, and resultant behaviors expected under earthquake ground motions.

#### [Commentary]

Proper structural modeling is another key issue to estimate a reliable structural performance of buildings as well as identifying rational parameters and values employed in the seismic evaluation procedure.

Seismic evaluation of an existing building is often much more difficult than the new design of a building because the building in concern already exists and engineers, who are generally not the original structural designers, need to predict its performance with a proper understanding of the original design concept and actual construction conditions. To properly evaluate the seismic capacity of a building, their structural behavior, therefore, should be first well examined. Bearing this in mind, it should be strongly emphasized that a careful examination of structural performance considering the rationally expected behavior of a building during earthquakes is the most essential key to obtain a reliable evaluation result and that this cannot be achieved just by calculating the seismic capacity index values.

An engineer may often encounter difficulties in evaluating the seismic capacity of a building in a rational way. This may arise from:

- 1) Lack of reliable data and/or observed evidence,
- 2) Application limit of the evaluation procedure, i.e., a discrepancy between basic assumptions in the evaluation procedure and expected behaviors considering structural conditions of the target building, and
- 3) Combined effects of 1) and 2) above.

#### (1) Lack of reliable data

As was pointed out earlier, experimentally or numerically verified data and/or evidence were quite limited to develop a rational seismic evaluation procedure that reflects the design and construction practices in Bangladesh. These practices significantly affect the seismic performance of buildings in earthquake events but their effects have not been fully considered in the CNCRP/BSPP Manuals (PWD) [1] [2] due to limited available data and evidence. The Guidelines are designed to provide structural engineers with methods, parameters, and values to properly evaluate the seismic capacity of existing RC buildings in Bangladesh which are derived from experimental and numerical examinations made in the SATREPS-TSUIB research project.

## (2) Application limit of the evaluation procedure

Another difficulty may result from a wide variety of structural systems in existing buildings, which can be found in many countries as well as in Japan. Less experienced engineers may find it significantly difficult to apply the evaluation procedure to such a building and it is often regarded as an out-of-scope building. Appropriate structural modeling and accordingly made structural analyses/calculations, however, may often greatly help engineers find a rational solution even under currently existing evaluation procedures.

In general, a structural calculation, which is a basic tool to evaluate the capacity and performance of a building, is not almighty and one may find it difficult to uniquely reach the right answer through a single and straightforward calculation. This is especially so when the building has a more complicated configuration and structural system. Even when using a sophisticated computer code, there is no exception to this, and this may more often happen as the target building stays farther from the basic assumptions employed in the evaluation procedure. For example, the CNCRP/BSPP Manuals, which follows the Japanese Standard for Seismic Evaluation of Existing RC Buildings (JBDPA, 2001), assumes that a building has the following structural system:

#1 Low- to medium-rise structural system (or not higher than 6 stories),

#2 Simple structural system with uniformly distributed mass,

#3 Rigid floor system,

#4 Well-balanced layout of structural members,

#5 Regular structural configuration in plan and elevation, etc.

### a) Major premise in the evaluation procedure (#1 and #2)

The basic calculation procedure in the JBDPA Standard is derived from the major premise of a building that i) the first mode is predominant during earthquakes, ii) its shape is linear, and iii) the mass is uniformly distributed along its height, all of which lead the story coefficient in calculating  $E_o$  to a simple form of  $(n+1)/(n+1)$ . Assumptions #1 and #2 play an important role to satisfy the premise above, and engineers should carefully judge the results whether or not they are on the safe side if the target building stays away from such basic assumptions.

### b) Rigid floor system and well-balanced layout of structural members (#3 and #4)

The rigid floor system is a convenient assumption and serves as the backbone principle in the manual because the capacity of a whole structure can be determined only from vertical elements. However, if a building has columns not connected to a strong beam, including those having a flat-plate system or weak-

beam system, this assumption cannot apply to the building and its lateral strength should be properly reduced considering the effects of weaker horizontal members. The weak beam system may also result from poor detailing of beam rebars straightly embedded in the beam-column joints, which can be often found in Bangladesh, and the beam strength in such a case should be determined from the smaller capacity at pull-out failure and yielding. Appropriate structural modeling and calculation procedure considering pull-out failure and the flat-plate system can be found in Chapters 5 and 6

If a structure has a discontinued beam system, it may also raise a question whether or not the rigid floor assumption can be applied. **Figure C.1.5(a)** shows an example of such a system subjected to an earthquake in EQy direction. In such a case, a rational answer cannot be given from a regular calculation targeting a regularly shaped and proportioned building but can only be provided after comparing results from case studies on different structural models under different assumptions. For example, a structure shown in **Figure C.1.5** can be modeled by a combination of one-mass systems, having a spring representing a beamless slab. One can assume that they behave either i) as a one-mass system if the spring is strong enough or ii) as two systems if the spring is not strong enough to transfer the load between two masses, and a rational answer may be derived by comparing these results based on the two different assumptions above as shown in the following case studies.

[Case 1: Strong beam-slab system]

If a spring representing the slab system between two masses is strong enough, the model structure can behave as a single structure, and the  $C$  index can be obtained as:

$$C = (V_1 + V_2) / (W_1 + W_2) \quad (C.1.1)$$

Where  $V_i$  and  $W_i$  are the strength and weight of frame  $i$ , respectively.

If the two frames are not identical, i.e.,  $C_1 (= V_1 / W_1) \neq C_2 (= V_2 / W_2)$ , the slab system must be strong and rigid enough to represent the structure's strength index by  $C$  defined in Eq. (C.1.1). Since the unbalanced force  $f$ , which should be transferred by the connecting slab system, can be obtained from the following Eqs. (C.1.2) of equilibrium of forces, one can judge whether or not the building meets the assumption of a rigid slab system by comparing  $f$  with slab yield strength in tension and/or buckling strength in compression.

$$\begin{aligned} C W_1 + f &= V_1 \\ C W_2 &= V_2 + f \end{aligned} \quad (C.1.2)$$

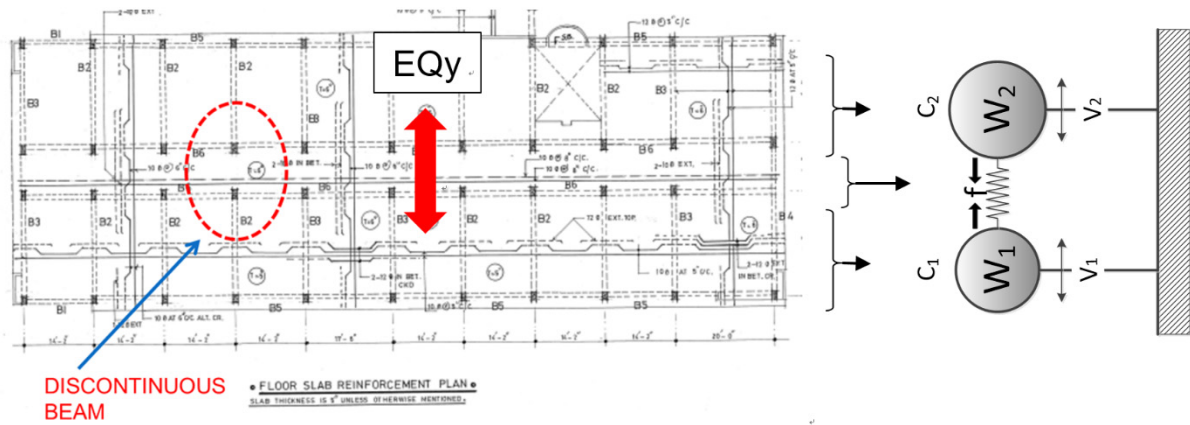


For example, the structure is deemed to have a rigid slab system and the structure's strength index can be obtained as  $C$  in Eq. (C.1.1) if  $f$  is small enough compared to  $(n \cdot f_y)$ , where  $n$  is the number of reinforcing bars in the slab and  $f_y$  is their specified yield strength, respectively.

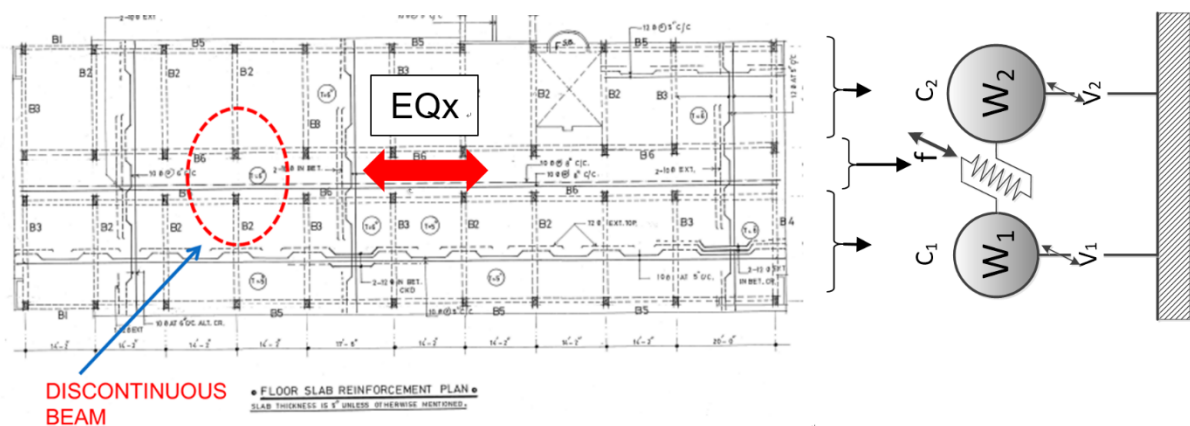
[Case 2: Weak beam-slab system]

However, if the slab system is not strong enough, the structure's strength index may lie between  $C$  and  $\min(C_1, C_2)$  calculated earlier. It should be also noted that engineers must recognize the building may eventually have damage such as residual cracks, spalling of concrete, etc. in slabs after an earthquake.

A system subjected to an earthquake in EQx direction, shown in **Figure C.1.5(b)**, can also be analogously examined as described earlier. If the obtained shear force  $f$  is small enough compared to the allowable strength of beamless slab, e.g., shear cracking strength, the structure is deemed to have a rigid slab system and the structure's strength index can be obtained analogously as described in [Case 1]. If the slab system is not strong enough, the structure's strength index can be obtained as described earlier in [Case 2].



(a) Building subjected to earthquake in EQy direction



(b) Building subjected to earthquake in EQx direction

Fig. C.1.5 Example structure with partially beamless slab system (courtesy of Mr. Rafiqul Islam, PWD)

Note that these examinations should be carefully made especially when  $V_1$  significantly differs from  $V_2$  due to the uneven distribution of lateral-load resisting members in frames.

**Figure C.1.6** shows another example of a complex building structure, which consists of several structural units with different story height connected. This structure also raises the question whether or not the slab can be assumed rigid enough, and the answer may give a critical impact on the judgment. Analogously as found in the example of **Figure C.1.5**, the unbalanced force  $f$  acting at critical slab sections between adjacent two units (e.g., shown in red in **Figure C.1.6**) can be compared to the shear strength ( $V$ ) and yield strength ( $T$ ) of the slab in the direction of applied force.

**Figure C.1.7** shows a much simpler structure than others described earlier, but engineers may have questions in their mind that “Can we ignore the effect of plain concrete on the ground floor in the assessment?” This is also a question that cannot be answered before numerical simulations are made under several structural models. The plain concrete slab is likely to restrain the lateral drift of columns during the initial small deformation stage, but the slab may fail in the ultimate stage and therefore may not be necessarily effective to keep shortening the column height until the ultimate state. The following approach, therefore, would be recommended to reach a rational answer:

- Calculate the column strengths, both considering and neglecting restraining effects of the plain slab,
- Compare the column strengths calculated above, slab buckling strength, slab bearing strength, and other potential strength if any, and
- Find the most-likely-to-occur failure mode.

A structural analysis does not necessarily have a unique prescription beforehand, and engineers should make every effort to find the deemed-to-be-right way to proceed after setting appropriate structural modeling and accordingly made calculations. As can be discussed herein, the capacity may not be always determined by a single value. For practical reasons, engineers may take the smallest value to represent the structure’s capacity, but they should spare no effort to minimize the range of values through appropriate

modeling. It should be also noted that a conservative evaluation may not always give a conservative solution because it may underestimate loads acting on a member expected not to fail during earthquakes, which

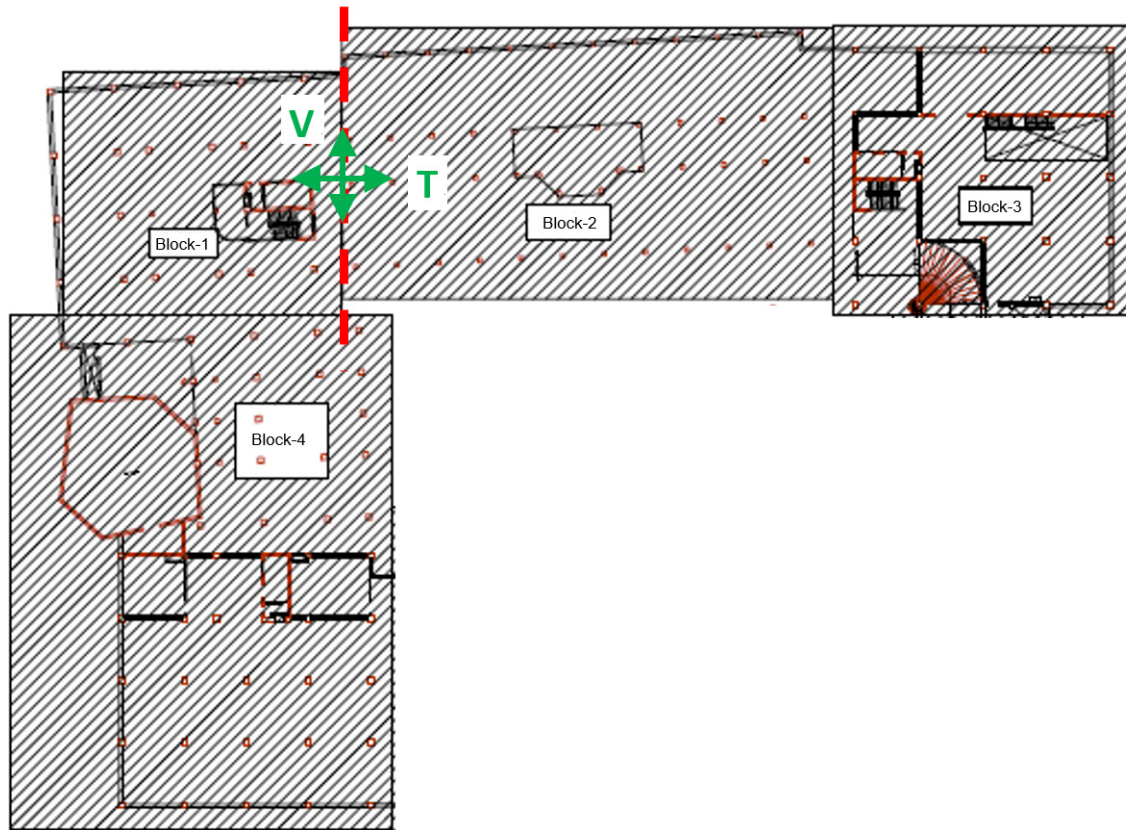


Fig. C.1.6 Complex structure requiring comparison between whole and divided structure  
(Courtesy of Mr. Rafiqul Islam, PWD)

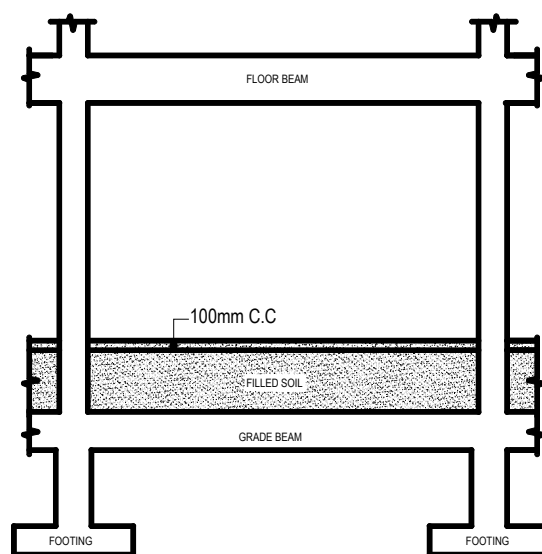


Fig. C.1.7 Effects of plain concrete on column height at ground floor  
(Courtesy of Mr. Rafiqul Islam, PWD)

leads to a misprediction of its failure mode. Also, a conservative evaluation may overestimate the required amount of retrofit, eventually imposing an over-strength on the structure if the conservative result lies below the required capacity criteria or demand.

c) Irregular structural configuration in plan and elevation (#5)

A building shown in **Figure C.1.8** has an irregular elevation along its height, having an extended floor plan in the lower story. A reduction factor to account for such irregularity of a building is considered in the  $S_D$  index in the CNCRP/BSPP Manuals as well as JBDPA Standard, and the second story may generally have the lowest seismic capacity index due to its discontinued stiffness and strength. This result may well correspond to the generally observed damage in past earthquakes. It should be also noted, however, that the capacity index in the first story may overestimate the performance if all columns (and walls, if any) are unconditionally taken into account for its capacity without any verification. As shown in the figure, the seismic actions would create a complicated load path in the plan and height of a building. To achieve successful performance, these actions should be well transferred to columns in the single-story block through the slab system so that all columns in the first story (ground floor) can effectively contribute to the whole structure's capacity. However, unless the slab is strong enough, the compatibility of deformation will not be satisfied and the columns would eventually result in heavier damage in the high tower block while lighter damage in the single-story block due to their less contribution to the story's lateral resistance. Careful examinations therefore should be made especially when stiffer and stronger members, e.g., due to the presence of brick (or RC) walls placed outside the high tower block as shown in the figure, are expected to contribute to the story resistance. Engineers should rationally find the final result after comparing the capacity of the high tower block (enclosed by a dotted box in **Figure C.1.8**) and the result obtained simply assuming all columns in the first story uniformly contribute to the capacity.

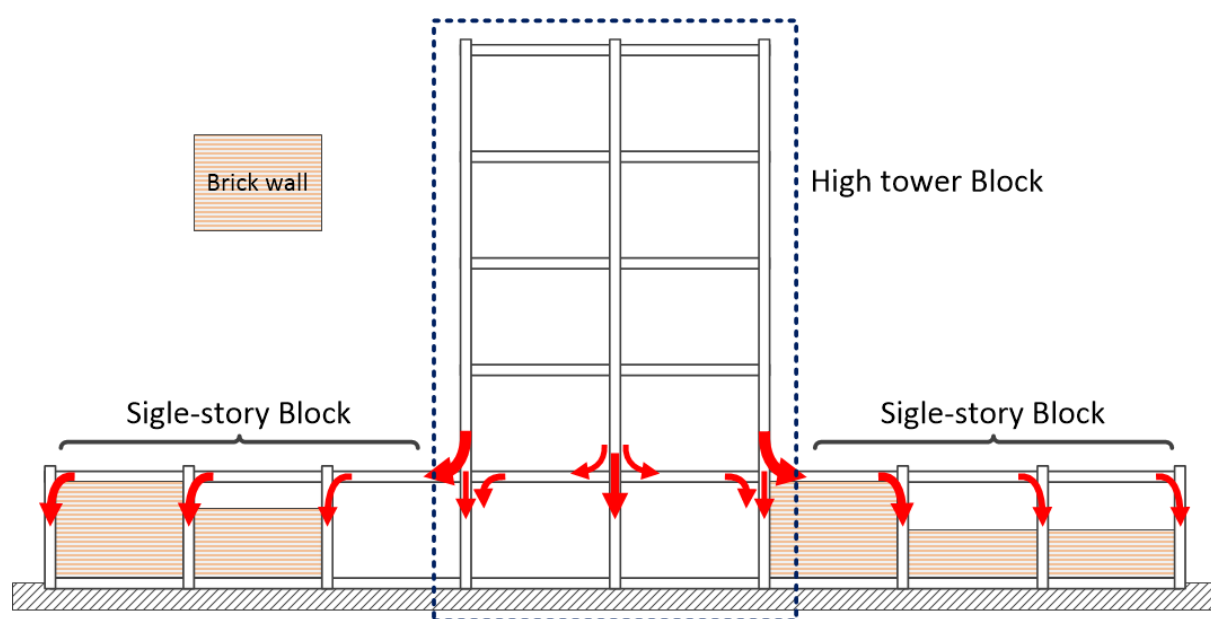


Fig. C.1.8 Complicated lateral load path of a building with vertically irregular shape

### (3) Important tips for successful seismic evaluation of existing structures

An existing building is often not regularly shaped and even consists of a structurally irregular framing system. This may cause difficulties in simply applying the evaluation procedure to such buildings. To obtain a rational result, engineers must try investigating its behavior from different but reasonable angles, i.e., comparing results based on properly made structural modeling, considering expected performance during earthquakes.

Just obtaining the seismic capacity index value is not the seismic evaluation that engineers are expected to perform. Properly understanding and predicting the expected failure mode/pattern is the most essential task in seismic evaluation. This is even more important than obtaining the values and one should recognize that rational evaluation results and values can be obtained only when such efforts are successfully made.

## 1.4 Definitions

**$\beta$ -Index:** The ratio of the boundary frame's lateral strength to masonry infill strength

**Strength index  $C$ :** The lateral-load carrying capacity of a member (masonry infill, or RC column) in terms of a shear coefficient, namely the shear capacity normalized by the weight of the building above.

**Ductility index  $F$ :** An index representing the deformation capacity of a structural member.

**$\beta$ -index:** An index representing the confinement of the RC frame defined by the ratio of the boundary frame's lateral strength to masonry infill's shear strength. A larger  $\beta$ -index represents a stronger surrounding RC frame relative to masonry strength.

**$a_o/h_o$  ratio:** The ratio of contact length of masonry infill to column height

**In-plane failure:** A failure mode of masonry infill caused by the load acting horizontally along the wall length.

**Out-of-plane failure:** A failure mode of masonry infill damaged in a perpendicular direction to the wall surface.

**Structural masonry element:** An infill that is deemed to contribute to the lateral capacity of a building.

## 1.5 Notations

${}_bM_{ba}$ : flexural strength of beam at pull-out failure

$D_c$ : column depth

$D_c$ : column depth

$L_b$ : Span length of beam

$L_c$ : column height (= story height)

$\sum W$ : total weight supported by the story concerned

${}_cQ_{ba}$ : column shear resistance at pull-out failure of beam connected to the column.

${}_cQ_{mu}$ : column shear resistance at the flexural yielding.

${}_cQ_{su}$ : column shear strength at the shear failure.

$d_b$ : diameter of beam longitudinal rebar

$l_{ba}$ : anchorage length of beam longitudinal rebar; when  $l_{ba}$  is unknown  $l_{ba} = \frac{2}{3}D_c$

$\sigma_0$ : axial force on the joint (N/mm<sup>2</sup>)

$\sigma_B$ : compressive strength of concrete (N/mm<sup>2</sup>)

$a_{ob}$ : sectional area of a reinforcing bar of slab bottom layer

$a_{ot}$ : sectional area of a reinforcing bar of slab top layer

$a_{t.col}$ : Area of steel of longitudinal reinforcement in tension column.

$a_t$ : total area of tensile longitudinal reinforcement  
 $b$ : width of column  
 $c_1$ : column depth  
 $c_2$ : column width  
 $C_{col}$ : The strength index of a boundary RC column attached to the infill wall.  
 $C_{inf}$ : The strength index of a masonry infill wall.  
 $d$ : beam effective depth  
 $D$ : depth of column  
 $d$ : effective depth of column (mm).  $D - 50\text{mm}$  shall be applied.  
 $d_{inf}$ : Diagonal length of masonry infill.  
 $E_c$ : Young's modulus of concrete.  
 $e_h$ : strength enhancement factor for high axial load  
 $E_{inf}$ : Young's modulus of masonry infill.  
 $e_p$ : strength reduction factor for plain bars and low strength concrete  
 $F_c$ : concrete compressive strength  
 $F_{col}$ : The ductility index of a boundary RC column attached to the infill wall.  
 $F_{inf}$ : The ductility index of a masonry infill wall.  
 $f_m$ : Prism compressive strength of masonry infill.  
 $h_0$ : clear height of column  
 $h_c$ : Height of RC column  
 $h_{inf}$ : Height of masonry infill.  
 $h_o$ : Clear height of RC column.  
 $I_b$  and  $I_c$ : Second moment of inertia of beam and column respectively.  
 $j$ : distance between centroids of tension and compression forces (mm),  $0.8D$  shall be applied.  
 $K_{frame}$ : Initial stiffness of RC frame  
 $K_{ini}$ : Initial stiffness for RC frame with masonry infill  
 $K_{strut}$ : Initial stiffness of masonry infill  
 $l_b$ : Length of RC beam  
 $l_{inf}$ : Length of masonry infill.  
 $l_o$ : Maximum width of opening measured across a horizontal plane  
 $l_w$ : Center to center span length of RC frame.  
 $M/Q$ : shear span length (mm).  $h_0/2$  shall be applied.  $1.0 \leq M/Qd \leq 3.0$ .  
 $M_0$ : capacity of bending moment  
 $M_s$ : bending moment due to the shear resistance of slab at the critical section  
 $M_u$ : Flexural yield moment of the column calculated based on the Japanese standard (JBDPA, 2001).  
 $M_{wmu}$ : Flexural Moment capacity for overall flexural failure  
 $N$ : axial load of column  
 $N_{max}$ : maximum axial strength of column  
 $N_{min}$ : minimum axial strength of column  
 $p_t$ : tensile reinforcement ratio (%)  
 $p_w$ : transverse reinforcement ratio  
 $Q_{dia}$ : Diagonal compression strength of masonry infill.  
 $Q_{expected}$ : Expected lateral strength of masonry infill.  
 $Q_{flex-wall}$ : Strength of frame calculated as flexural wall and masonry infill as a rigid panel.

$Q_{frame}$  : Lateral strength of column calculated as the minimum strength of  $Q_{su}$ ,  $Q_{mu}$ .  
 $Q_{fw}$ : Lateral strength for overall flexural failure  
 $Q_{inf}$ : Lateral in-plane strength of the masonry infill.  
 $Q_{jw}$ : Lateral strength of punching shear failure  
 $Q_{mu}$  : Shear force at the ultimate flexural strength of the column.  
 $Q_{mw}$ : Lateral strength of an RC frame with a masonry infill  
 $Q_{pc}$ : Punching shear strength of column  
 $Q_{punching}$ : Punching shear of an RC column  
 $Q_{slab}$  : column shear resistance based on the flexural yielding of slab  
 $Q_{sta}$ : Sliding lateral strength of masonry infill,  
 $Q_{su}$  : Ultimate shear strength of the column.  
 ${}_sM_y$ : flexural capacity of slab  
 $t_{inf}$  : Thickness of masonry infill.  
 $W$ : The weight of the building including live load for seismic calculation supported by the story concer  
 $W_{inf}$ : Strut width  
 $x_b$ : space of reinforcing bars of slab bottom layer  
 $x_t$ : space of reinforcing bars of slab top layer  
 $\alpha_L$ : reduction factor for low strength concrete  
 $\theta$  : Inclination angle of masonry wall`s diagonal from the horizontal axis.  
 $\lambda_{op}$  : Reduction factor to account for opening in masonry infill  
 $\sigma_0$ : axial stress in column (MPa), not exceeding 8 MPa  
 $\sigma_{wy}$ : yield strength of transverse reinforcing bars in column  
 $\sigma_y$  : Yield strength of tension reinforcement.  
 $\sigma_B$ : compressive strength of concrete



## Chapter 2 Classification of compressive strength of concrete

### 2.1 General

This section describes a classification method of compressive strength of existing reinforced concrete buildings by simple non-destructive testing method(s). If the compressive strength is classified very low ( $\leq 9$  MPa) [1], it is out of the scope of the seismic evaluation method described in later sections.

Note that this section explains a classification method and does not provide an accurate estimate of the compressive strength.

### C.2.1 [Commentary]

- In Bangladesh, recent surveys revealed that many old reinforced concrete buildings in the country have low-strength concrete. In the CNCRP manual of “Seismic Evaluation of Existing Reinforced Concrete Buildings” (Public Works Department, 2015), concrete compressive strength lower than 13.5 MPa was considered as low-strength concrete. However, Bangladeshi concrete has brick chips, and it has been observed that actual concrete strength of some of the buildings are less than 10 MPa. Information of concrete compressive strength is necessary during seismic evaluation of buildings. On the other hand, it is not practical to conduct a comprehensive seismic evaluation because the number of target buildings is enormous. Concrete with extremely low strength, e.g. less than 9 MPa, may let the structures very vulnerable. Screening out of the very low strength concrete can reduce the number of target buildings of detailed seismic evaluation. Therefore, it is necessary to identify the buildings with very low compressive strength of concrete in order to apply the proper guidelines of safety evaluations.
- The proposed non-destructive testing (NDT) method(s) is very simple and carried out for the classification of the concrete strength, in particular, finding very low strength concrete is the first priority. Therefore, the accurate estimation of the concrete strength is out of scope of this section’s target. If the accurate strength measurement is needed, it should be obtained by compressive test of the extruded core sample obtained from the target building.

## 2.2 Scope

The procedure presented in Figure 2.1 is applicable to identify the low-strength concrete buildings in Bangladesh with simple and prompt non-destructive testing (NDT) methods, rebound hammer type L, associated with a mushroom head, and scratching test device.

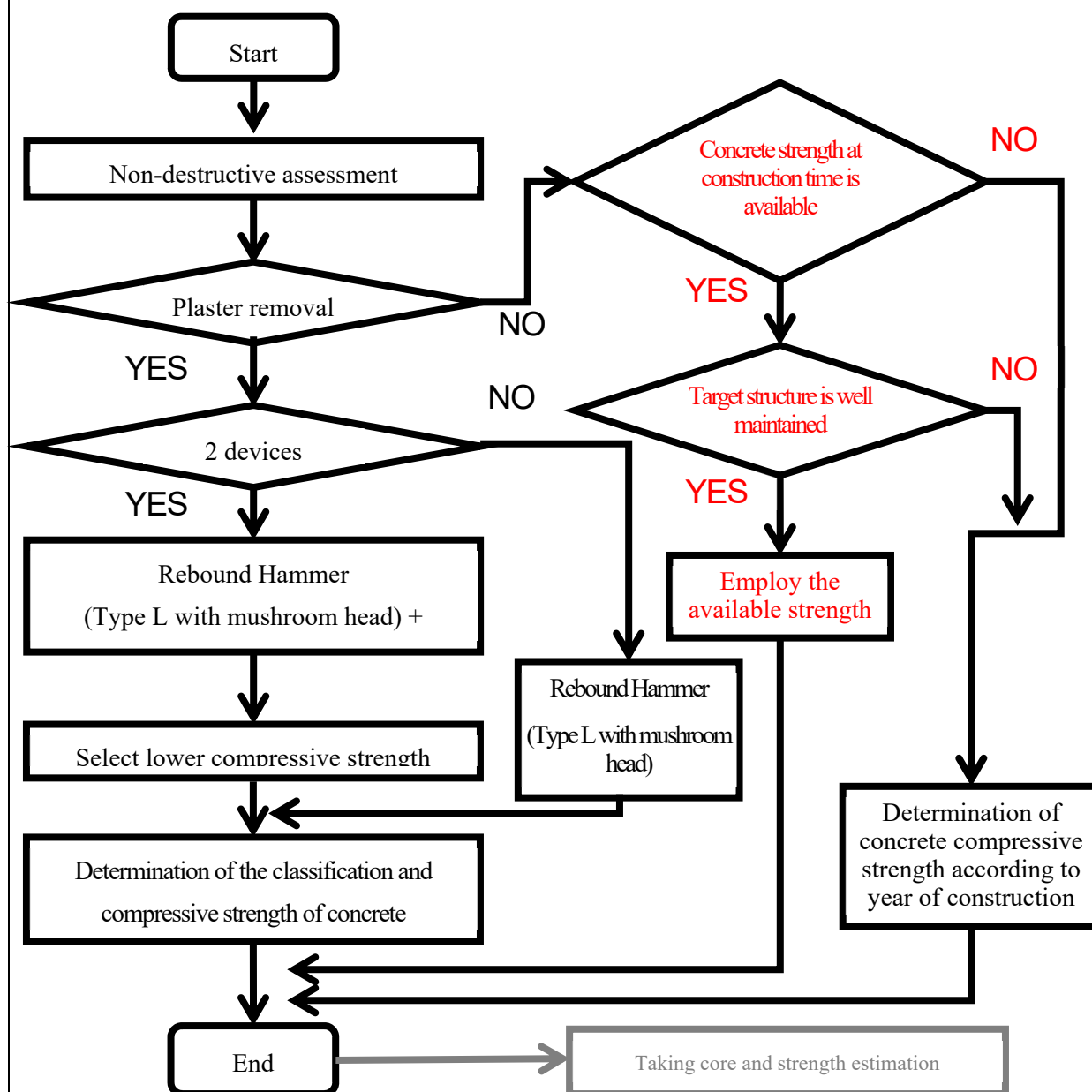


Figure 2.1 Steps during non-destructive assessment of concrete

## C.2.2 [Commentary]

- The proposed methods, rebound hammer type L, associated with a mushroom head, and scratching test device, are surface hardness testing procedures. Based on the NDT results or these combination, concrete strength could be classified.
- On the other hand, most of the buildings in Bangladesh have an outer plaster mortar layer (of 10-20mm thickness) which needs to be peeled off to get contact of the concrete inside. If the test devices are used on the plaster mortar layer, the obtained compressive strength will not be representative of actual concrete. In case of lack of consent of authority to peel off a certain portion (30 cm x30 cm) of the outer plaster layer to successfully perform the tests, the compressive strength should be calculated from the year of construction. According to the proposed visual rating method, we can classify the buildings according to the year of construction and consider the lowest strength in the period. The lowest compressive strength value needs to be considered, to have the most conservative classification. Figure C.2.1 shows the Compressive strength of concrete in surveyed buildings according to the year of construction. Table C.2.1 provides Classification of concrete strength according to construction period.

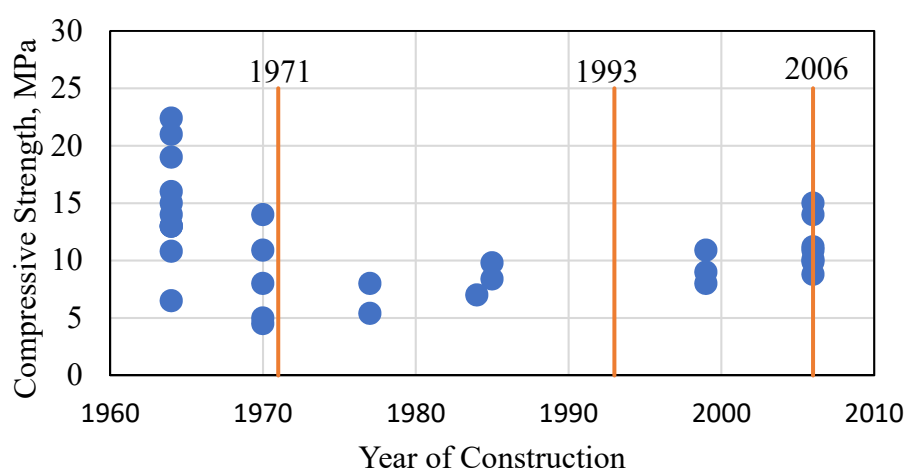


Figure C.2.1 Compressive strength of concrete in surveyed buildings according to the year of construction [2]

Table C.2.1 Classification of concrete strength according to construction period (without testing)

Construction period	Class	Representative compressive strength
Before 1993	Old buildings	Less than 5 MPa
From 1993 to 2006	Middle	Less than 9 MPa
After 2006	New buildings	More than 9 MPa

## 2.3 Procedure to use the rebound hammer

### 2.3.1 Testing device

The procedures to use the rebound hammer can be followed as JIS A 1155:2012 Method of measurement for rebound number on surface of concrete (ISO 1920-7:2004 Testing of concrete — Part 7: Non-destructive tests on hardened concrete).

### 2.3.2 Testing procedures

- i) Bare concrete surface should be exposed by peeling off mortar plaster.
- ii) Make the surface smooth using a stone grinder as long as possible.
- iii) Nine or more points are measured that are 50 mm or more away from the edge of the specimen and by a distance of 30 mm or more away from each other.
- iv) The average value of 9 points excluding the values differ from 20% of the average value of total was used as a result of rebound quotient  $Q$ .

### 2.3.3 Determination of concrete strength class

Concrete strength can be classified by the obtained  $Q$  value according to Table 2.1. If  $GW$  is also available, combination of results by two devices should be employed as more conservative estimation of concrete strength. Note that this section explains a classification method and does not provide an accurate estimate of the compressive strength.

Table 2.1 Division of sample data into 4 zones with boundary values of  $Q$

Classification	Range of compressive strength	Rebound hammer	Mean compressive strength	Standard deviation of compressive strength
	MPa	$Q$	MPa	MPa
Very low	$f_c \leq 9$	$Q \leq 30$	4.76	2.36
Low	$9 < f_c \leq 13.5$	$30 < Q \leq 35$	12.38	2.78
Medium	$13.5 < f_c \leq 21$	$35 < Q \leq 40$	19.12	7.67
Good	$21 < f_c$	$40 < Q$	25.45	6.91

### C.2.3 [Commentary]

- The employed rebound hammer should have low impact energy (0.735 Nm) and the mushroom head to avoid damage of the target concrete, especially in case of low strength concrete. Silver Schmidt type L manufactured by Proceq Co., Ltd., is one of suitable hammers.

## 2.4 Procedure to use the scratching test device

### 2.4.1 Testing device

Scratch test is the surface hardness checking method using a simple spring and needle device which is developed by Japan Society for Finishings Technology, and this test device is certificated by Japan Floor Coating Industry Association. The scratching device make groove on the concrete surface and measuring the groove width (GW) made with the two pins inserted in the plastic material body.

### 2.4.2 Testing procedures

- i) The same surface of the rebound hammer is preferable.
- ii) Bare concrete surface should be exposed by peeling off mortar plaster.
- iii) Make the surface smooth using a stone grinder as long as possible.
- iv) Approximately 10 cm long grooves are made on the concrete surface by scratching at a speed of 2 cm/sec.
- v) GW made by the 9.8 N pin is measured by the various scales available with the device.

### 2.4.3 Determination of concrete strength class

Concrete strength can be classified by the obtained GW value according to Table 2.2. Combination of results by two devices should be employed as more conservative estimation of concrete strength.

Table 2.2 Division of sample data into 4 zones with boundary values of GW

Classification	Range of compressive strength	Scratching test	Mean compressive strength	Standard deviation of compressive strength
	MPa	GW, mm	MPa	MPa
Very low	$f_c \leq 9$	$1 \leq GW$	4.12	1.84
Low	$9 < f_c \leq 13.5$	$0.5 \leq GW < 1$	12.45	4.19
Medium	$13.5 < f_c \leq 21$	$0.4 < GW \leq 0.5$	21.74	3.52
Good	$21 < f_c$	$GW < 0.4$	25.60	6.91

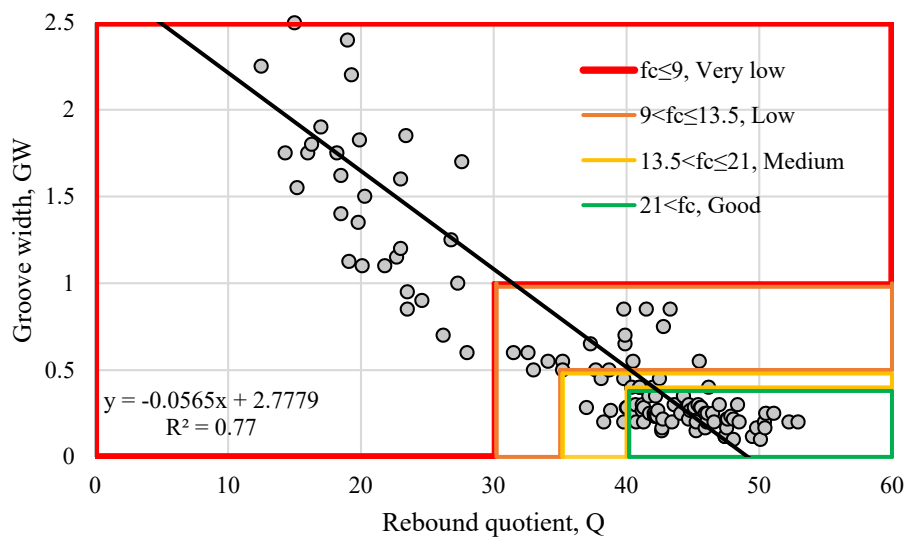
## C.2.4 [Commentary]

- The scratching test device developed by Japan Society for Finishing's Technology has the two pins inside the device when pressed against the surface apply constant load of 9.8 N (1 kg) and 4.9 N (0.5 kg). The pins are made of carbide tungsten alloy which has high hardness and wear resistant. They are inserted in a rectangular prism made of plastic material at the center with 90° angle. Load adjustment is performed by spring coils inside the device installed along the body of pins.

## 2.5 Determination of the classification of concrete

The classification of concrete strength is given by Figure 2.2 which represents four regions. The concrete compressive strength is named as “Good”, when both of the Q and GW values falls within the green region. A red region represents “Very low” condition where the Q is lower than 30 or GW is higher than 1 mm. In this case, concrete compressive strength can be estimate less than 9 MPa. The classification of concrete with upper and lower limits of compressive strength corresponding to Q and GW, are shown in Table 2.1 and 2.2 respectively.

Note that, this classification is not accurate estimation of compressive strength of the target concrete but conservative classification especially for low strength concrete.



Very low		$f_c \leq 9$ MPa
Low	$9 \text{ MPa} < f_c \leq 13.5$ MPa	
Medium	$13.5 \text{ MPa} < f_c \leq 21$ MPa	
Good	$21 \text{ MPa} < f_c$	

Figure 2.2 Classification of concrete into 4 classes depending on Q and GW boundary values

## C.2.5 [Commentary]

- When both rebound hammer and scratching test is performed this classification shows which NDT device gives lower estimation of concrete compressive strength. The calibration equations are given in the Figure C.2.2 and Figure C.2.3. To obtain more conservative results, calibration equation should be chosen from smaller strength estimation among both scratching test and rebound hammer. However, for a point that falls in the green area (‘Good’ strength more than 21 MPa), the compressive strength can be estimated using the rebound hammer only because of difficulty to observe narrow groove widths lower than 0.35 mm.
- Figure C.2.4 shows the normal distribution of compressive strength with upper and lower boundary values for surface hardness NDTs. According to these graphs, the simple NDT method(s) can provide the proper classification of concrete strength.

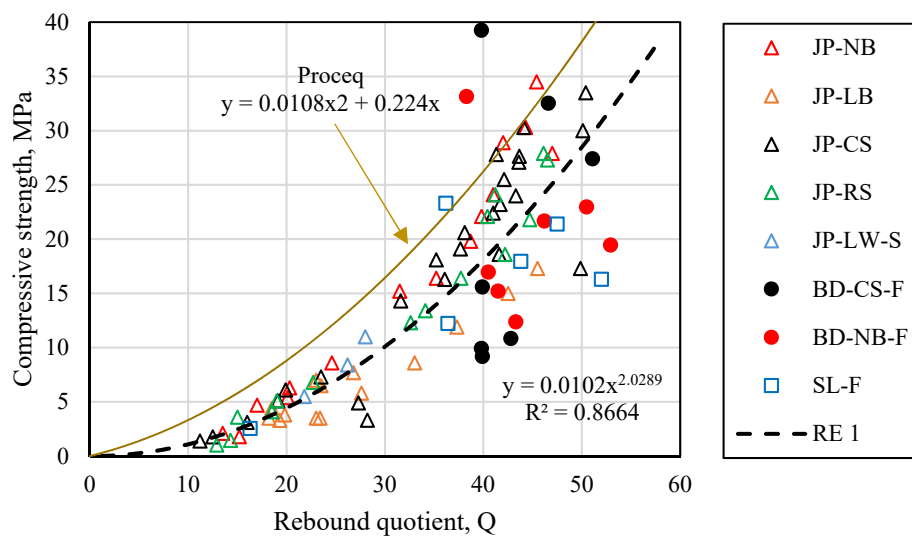


Figure C.2.2 Calibration equation for rebound hammer (Regression equation 1)

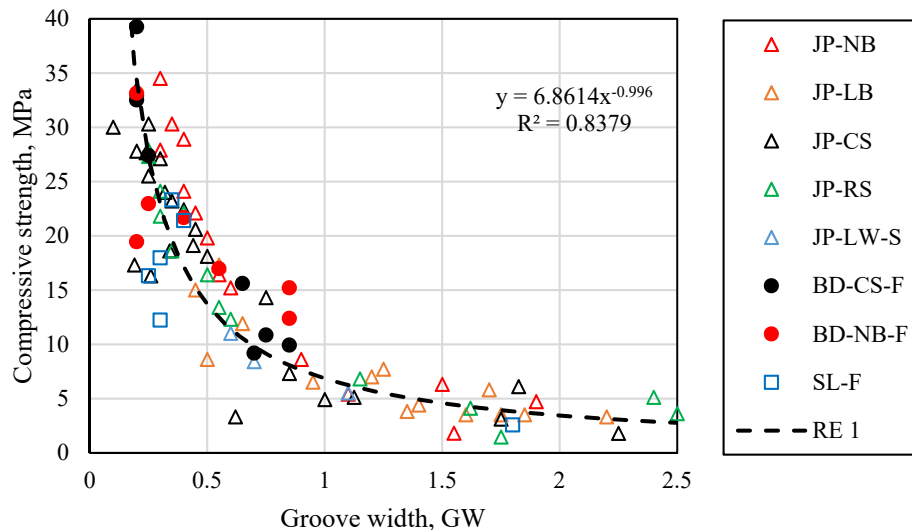


Figure C.2.3 Calibration equation for scratching test (Regression equation 1)

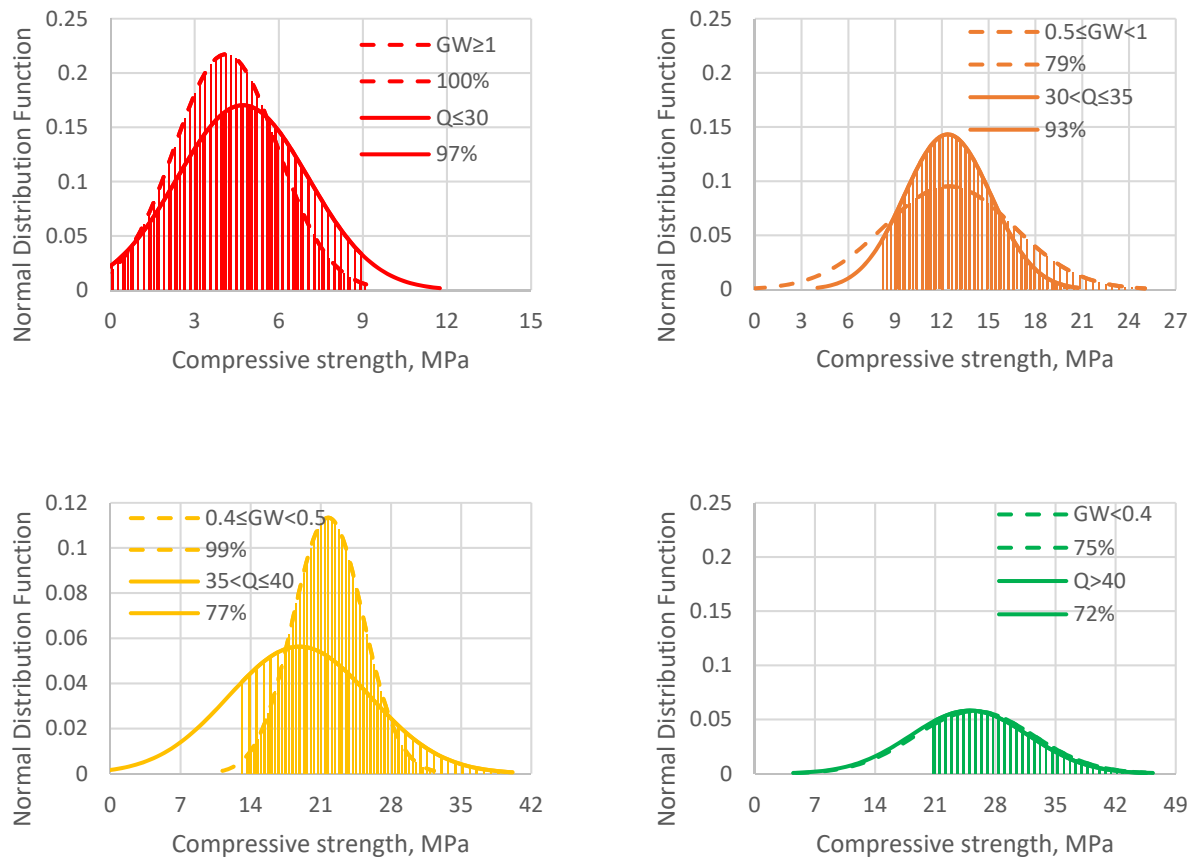


Figure C.2.4 Normal distribution of compressive strength with upper and lower boundary values for surface hardness NDTs.

## References

- [1] N. Yosuke, S. Matsutaro, and M. Atsushi, "Predicting concrete strength using a test hammer for existing reinforced concrete buildings in Bangladesh," *Structure IV*, pp. 513-514(in Japanese), 2016.
- [2] Public Works Department (PWD), "Project for Capacity Disaster-Resistant Techniques of Construction and Retrofitting for Public Buildings in the Government of the People's Republic of Bangladesh. Final Report by Japan International Co-operation Agency," 2015.



## Appendix Scratching device

As showing the following figures, the scratching device is a simple spring and needle device which is developed by Japan Society for Finishings Technology. The surface hardness can be checked by the groove width (GW). The scratching test includes a small portable device with an easier working principle that only requires scratching on the concrete surface and measuring the groove width (GW) made with the two pins inserted in the plastic material body. It is a simple tester that can scratch the concrete surface at a constant angle with loads of 1kg and 0.5 kg. The two pins inside the device when pressed against the surface apply constant stresses of 9.8 N and 4.9 N. The pins are made of carbide tungsten alloy which has high hardness and wear resistant. The pins are inserted in a rectangular prism made of plastic material at the center with 90° angle. Load adjustment is performed by spring coils inside the device installed along the body of pins.



Scratch testing device



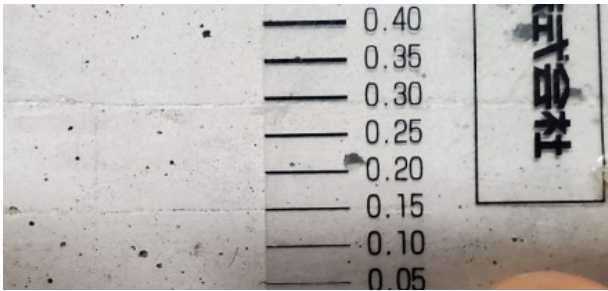
Pins to make grooves by scratching  
the concrete surface

The test procedure of scratching device is following;

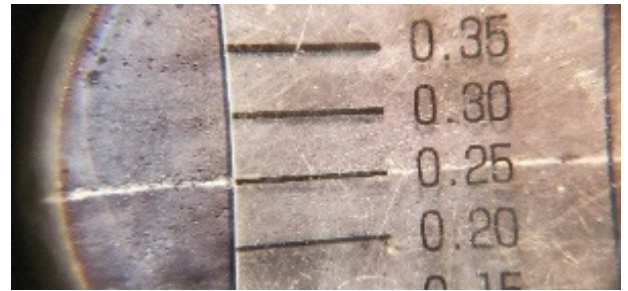
Before performing the scratching, test grind the test surface of concrete with a stone grinder to make it as smooth as possible. Place the pins of the device on the concrete surface steadily. Push the device on the surface and scratch the surface by keeping the speed of scratching as constant as possible (2 cm/s approximately). Place the scale on the scratched groove by aligning the nearest thickness of line drawn on the scale. Use a magnifying glass to match the thickness of the scratched groove with the line of the scale. Choose the nearest thickness of line on the scale and record the thickness. The thickness of the groove can be used to estimate the compressive strength of the tested concrete.



Scratching the concrete surface



Grooves made by scratching



Measuring scale for groove width

## Chapter 3 Columns with Low Strength Concrete and/or High Axial Load

### 3.1 General

In Bangladesh, from recent surveys (JICA, 2015), it is revealed that many old RC buildings in the country have several shortcomings, such as low strength concrete, high axial load ratio, etc. To assess the seismic performance, strength and ductility evaluation of the column with low strength concrete and high axial load ratio is inevitable. In the CNCRP manual (PWD, 2012), the modified equations of the JBDPA standards (JBDPA, 2001) for shear strength of column are proposed to take the shortcomings (especially, for low strength concrete and high axial load, etc.) into account.

In this chapter, alternative equations for the shear strength of RC columns are employed. A set of equations which includes a reduction factor as a function of concrete compressive strength is used to calculate column shear strength. The reduction factor varies linearly with the concrete compressive strength and the calculated shear strength is equal to that of the JBDPA standards and CNCRP equations when concrete strength is approximately 22 MPa or larger. In addition, as mentioned in C.3.1, the employed equations show better agreement with actual shear strength of test specimens with low to medium strength concrete. Therefore, the equations employed in this chapter are applicable for the column with wider range of concrete strength, i.e., both low and medium strength concrete.

Another set of equations are proposed for the calculation of column flexural strength. As mentioned in C.3.2, the JBDPA equations tend to underestimate the flexural strength of columns with high axial load and to overestimate when both low strength concrete and plain bars are simultaneously used. Therefore, factors to take these issues into account are employed.

The other parameters, such as ultimate drift angle  $\epsilon_{Ru}$ , strength index (C-index), ductility index (F-index), etc. are recommended to be evaluated in accordance with the JBDPA standard or the CNCRP manual.

### 3.2. Calculation of Shear Strength (Qsu) and Flexural Strength (Mu)

#### 3.2.1 Shear strength (Qsu)

Shear strength of RC columns shall be calculated by the following Eqs. (3.2.1) and (3.2.2)

$$Q_{su} = \left\{ \frac{0.053 p_t^{0.23} (F_c + 18)}{M / Qd + 0.12} + \alpha_L \sqrt{p_w \sigma_{wy}} + 0.1 \sigma_0 \right\} bj \quad (3.2.1)$$

$$\alpha_L = 0.038 F_c \leq 0.85 \quad (3.2.2)$$

$Q_{su}$ : shear strength of column

$p_t$ : tensile reinforcement ratio (%)

$F_c$ : concrete compressive strength

$d$ : effective depth of column.  $D - 50$  mm shall be applied.

$M/Q$ : Shear span length.  $h_0/2$  shall be applied.  $1.0 \leq M/Qd \leq 3.0$

$b$ : width of column

$D$ : depth of column

$j$ : distance between centroids of tension and compression forces,  $0.8D$  shall be applied.

$p_w$ : transverse reinforcement ratio

$\sigma_{wy}$ : yield strength of transverse reinforcing bars in column

$\sigma_0$ : axial stress in column, not exceeding 8.0MPa

$\alpha_L$ : reduction factor for low strength concrete

$h_0$ : clear height of column

#### 3.2.2 Flexural strength ( $M_u$ )

Flexural strength of columns shall be calculated in accordance with Eqs. (3.2.3) -(3.2.6).

For columns with deformed longitudinal reinforcing bars,

where  $N_{\max} \geq N > 0.4bDF_c$ ,

$$M_u = (0.8a_t \sigma_y D + 0.12bD^2 F_c) \left( \frac{N_{\max} - N}{N_{\max} - 0.4bDF_c} \right) e_h \quad (3.2.3)$$

and where  $0.4bDF_c \geq N > 0$ ,

$$M_u = 0.8a_t \sigma_y D + 0.5ND \left( 1 - \frac{N}{bDF_c} \right) \quad (3.2.4)$$

For columns with plain longitudinal reinforcing bars,

where  $N_{\max} \geq N > 0.4bDF_c$ ,

$$M_u = (0.8a_t \sigma_y D + 0.12bD^2 F_c) \left( \frac{N_{\max} - N}{N_{\max} - 0.4bDF_c} \right) e_h e_p \quad (3.2.5)$$

and where  $0.4bDF_c \geq N > 0$ ,

$$M_u = \left( 0.8a_t\sigma_y D + 0.5ND \left( 1 - \frac{N}{bDF_c} \right) \right) e_p \quad (3.2.6)$$

where

$$e_h = (N/bDF_c + 0.2) / 0.6$$

$$e_p = 0.8 \text{ for } F_c \leq 13.5 \text{ MPa and } 1.0 \text{ for } F_c > 13.5 \text{ MPa}$$

$M_u$ : flexural strength of column

$a_t$ : total area of tensile longitudinal reinforcement

$\sigma_y$ : yield strength of longitudinal reinforcing bars in column

$N_{\max}$ : maximum axial strength of column

$N_{\min}$ : minimum axial strength of column

$N$ : axial load of column

$e_h$ : strength enhancement factor for high axial load

$e_p$ : strength reduction factor for plain bars and low strength concrete

### C.3 [Commentary]

#### C.3.1 Shear strength of RC column

In the JBDPA standard, Eq. (C.3.1.1) is employed to calculate the shear strength of columns. The scope of the equation is to provide conservative shear strength estimation (statistically, 95% exceedance of the actual strength is allowed) to find the columns prone to brittle shear failure. For this purpose, equations for flexural strength of columns are aiming to estimate the mean value. Therefore, the shear strength ratio,  $Q_{su}/Q_{mu}$ , which is an index to find columns prone to fail in shear (when  $Q_{su}/Q_{mu}$  is less than 1.0, the columns are classified as the shear columns), gives a conservative estimation.

Again, Eq. (C.3.1.1) is proposed to predict the lower bound of the test results for RC columns. However, it is not applicable for the columns with low strength concrete column (In JBDPA standard, concrete below 13.5 MPa compressive strength is defined as low strength concrete). The relationship between  $Q_{exp}/Q_{su}$  (the ratio of experimentally obtained to the estimated shear strength.) and  $F_c$  is shown in Figure C.3.1.1, where an overestimation is observed in the low strength concrete zone. Assuming a normal distribution of  $Q_{exp}/Q_{su}$  for specimens having  $F_c$  below 13.5 MPa, 47.3% of the specimens lie below the estimation by Eq. (C.3.1.1), as shown in Figure C.3.1.1 (Kabir et al., 2020).

$$Q_{su} = \left\{ \frac{0.053 p_t^{0.23} (F_c + 18)}{M / Qd + 0.12} + 0.85 \sqrt{p_w \sigma_{wy}} + 0.1 \sigma_0 \right\} bj \quad (C.3.1.1)$$

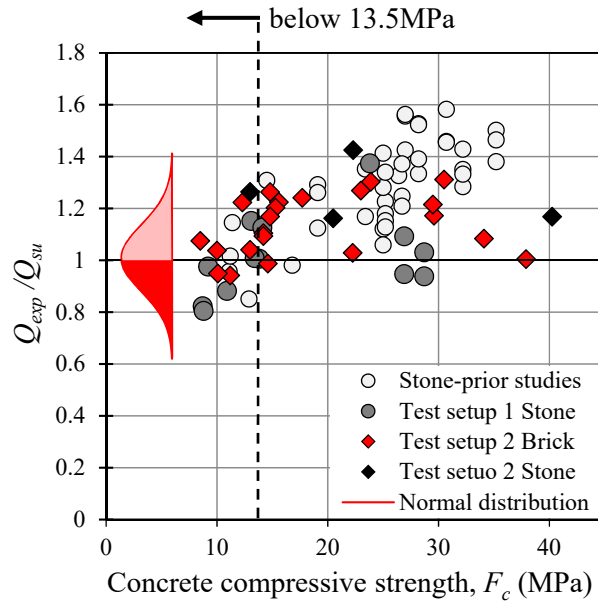


Figure C.3.1.1 Accuracy of the JBDPA shear strength calculation (Kabir et al., 2020)

(Note:  $\sigma_{wy}$  reported in each paper/report is used for the  $Q_{su}$  calculation)

In the CNCRP manual, shear strength of RC columns is estimated by Eq. (C.3.1.2). A reduction factor,  $k_r$  is employed to account for the effect of low strength concrete.

$$Q_{su} = k_r \left\{ \frac{0.053 p_t^{0.23} (F_c + 18)}{M / Qd + 0.12} + 0.85 \sqrt{p_w \sigma_{wy}} + 0.1 \sigma_0 \right\} bj \quad (C.3.1.2)$$

where  $k_r$  is the reduction factor for low strength concrete ( $F_c < 13.5 \text{ MPa}$ ),  $k_r = 0.244 + 0.056 F_c$ .

The application results of Eq. (C.3.1.2) are shown in Figure C.3.1.2. Assuming a normal distribution of  $Q_{exp} / Q_{su}$  for specimens having  $F_c$  below 13.5 MPa, 11.5% of the specimens lie below the estimation by Eq. (C.3.1.2), as shown in Figure C.3.1.2. Although specimens with 10-20 MPa concrete strength are distributed in a range of  $0.88 < Q_{exp} / Q_{su, Kr} < 1.33$ , which are smaller than that of other concrete strength specimens, the results are improved drastically.

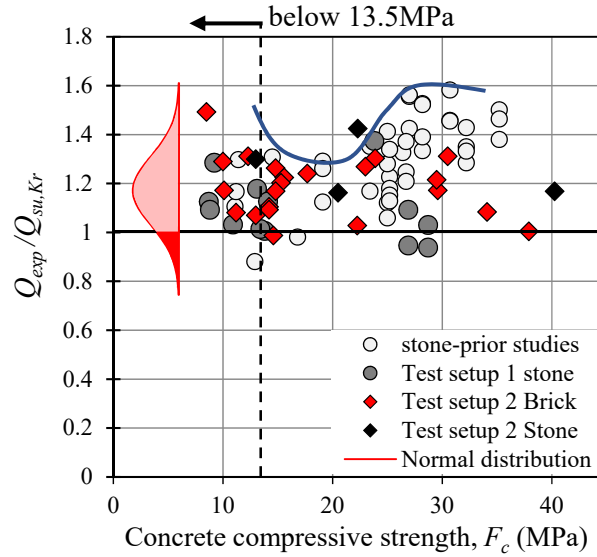


Figure C.3.1.2 Accuracy of the CNCRP shear strength calculation

(Note:  $\sigma_{wy}$  reported in each paper/report is used for the  $Q_{su,Kr}$  calculation)

In this chapter, for calculating the shear strength of low strength concrete columns, Eqs. (3.2.1)- (3.2.2) including a reduction factor  $\alpha_L$  are employed. The factor  $\alpha_L$  is proposed based on a study of tensile stress on transverse reinforcements in low strength concrete columns (Yasojima et al., 2010). The accuracy is shown in Figure C.3.1.3. Assuming a normal distribution of  $Q_{exp}/Q_{su}$  for the specimens having  $F_c$  below 13.5 MPa, 9.3% of the specimens lie below the estimation by Eqs. (3.2.1)- (3.2.2). In addition, the specimens seems to be ranging uniformly along the concrete strength than others results.

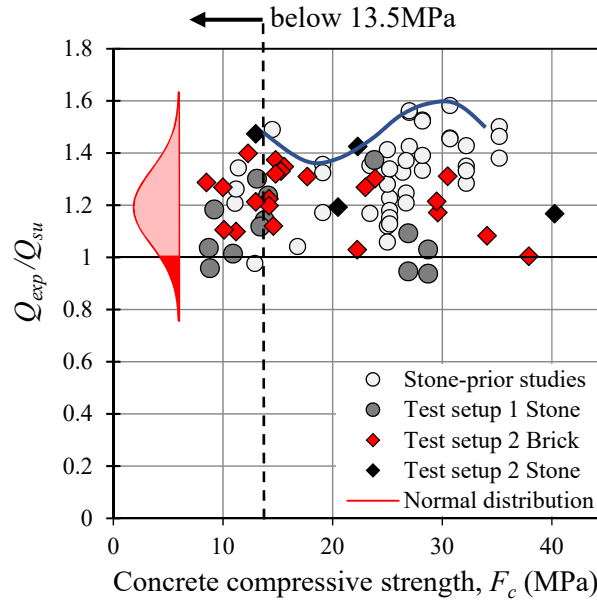


Figure C.3.1.3 Accuracy of the shear strength calculation with  $\alpha_L$  (Kabir et al., 2020)

(Note:  $\sigma_{wy}$  reported in each paper/report is used for the  $Q_{su}$  calculation)

Both Eqs. (C.3.1.2) and (3.2.1) show similar accuracy even in the low strength concrete zone. The CNCRP Eq. (C.3.1.2) multiplies the reduction factor  $k_r$  with the whole shear strength. In contrast, the reduction factor  $\alpha_L$  is multiplied only with  $\sqrt{p_w \sigma_{wy}}$  in Eq. (3.2.1). This is based on the detailed comparison of the stress on the transverse reinforcement of a low strength concrete column specimen and a medium-strength concrete column

specimen. The study showed that the stress level of the low strength concrete column is significantly smaller than that of the medium-strength concrete column (Yasojima et al., 2010), this is the reason why the reduction factor  $\alpha_L$  is multiplied only with the term which refers to the shear strength provided by the transverse reinforcements ( $\sqrt{p_w \sigma_{wy}}$ ).

In addition, the test results are uniformly distributed along the concrete strength when Eq. (3.2.1) is employed, as shown in Figure C.3.1.3. When the CNCRP Eq. (C.3.1.2) is employed, the lower bound of shear strength is captured, however, specimens with 10-20 MPa showed relatively smaller value than others, i.e. not uniform.

Considering the experimentally evident background and uniformity along the concrete strength, Eq. (3.2.1) is employed in this chapter.

In addition, in Figs. (C.3.1.1–3), brick and stone aggregate concrete are shown in different markers. There are some differences between them; however, it is determined to use the Eq. (3.2.1) regardless of the type of aggregate because the lower bound of test results of both concretes is captured well.

### C.3.2 Flexural strength of RC column

In the JBDPA standard, the flexural strength of RC columns is estimated by using Eqs. (C.3.2.1) and (C.3.2.2). As mentioned in C.3.1, the scope of the equations is to estimate the mean flexural strength.

In case of  $N_{\max} \geq N > 0.4bDF_c$ ,

$$M_u = \left( 0.8a_t\sigma_y D + 0.12bD^2 F_c \right) \left( \frac{N_{\max} - N}{N_{\max} - 0.4bDF_c} \right) \quad (C.3.2.1)$$

In case of  $0.4bDF_c \geq N > 0$ ,

$$M_u = 0.8a_t\sigma_y D + 0.5ND \left( 1 - \frac{N}{bDF_c} \right) \quad (C.3.2.2)$$

The equations are examined using test data of low strength concrete specimens with plain bars and deformed bars. The results are shown in Figure C.3.2.1 along with the axial load ratio.



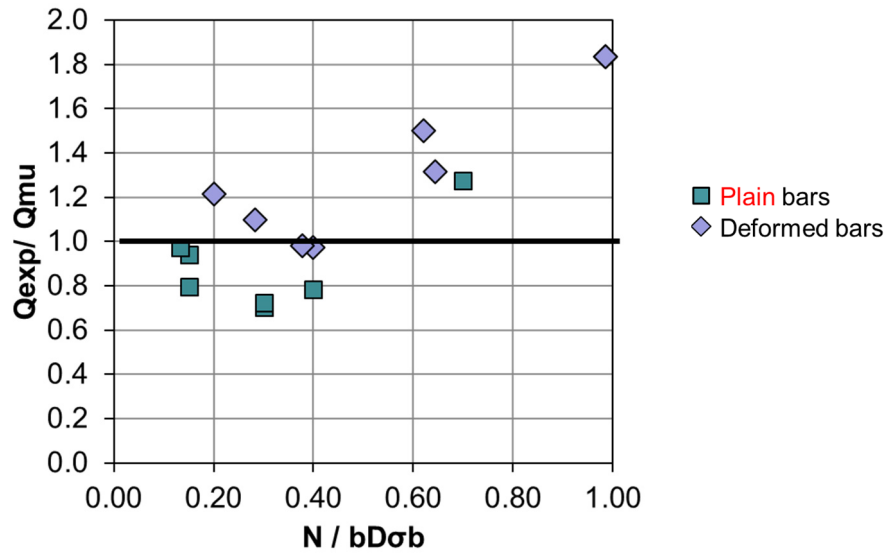


Figure C.3.2.1 Accuracy of the flexural strength calculation using JBDPA equations

(Note:  $\sigma_y$  reported in each paper/report is used for the  $Q_{mu}$  calculation)

The results exhibit two issues; 1) in high axial load zone ( $N/bDF_c > 0.4$ ), test results show much higher strength than calculation, 2) plain bar specimens tend to be lower in strength than the deformed bar specimens. To account for these issues, enhancement factor for high axial load ratio,  $e_h$  and reduction factor for plain bars,  $e_p$  are employed in this chapter.

The strength enhancement in the high axial load zone is known from the experimental studies in the 1980s (Priestly and Park, 1987); therefore, the enhancement factor  $e_h$  is employed in this supplement. Regarding the plain bar issue, another study (Araki et al., 2011) mentions that such trend is observed when both low strength concrete and plain bars are simultaneously used, as shown in Figure C.3.2.2. Employing the enhancement factor,  $e_h$  (for high axial load ratio) and reduction factor,  $e_p$  (for plain bars and low strength concrete), Eqs. (3.2.2)- (3.2.6) are proposed, and the accuracy is improved as shown in Figure C.3.2.3.

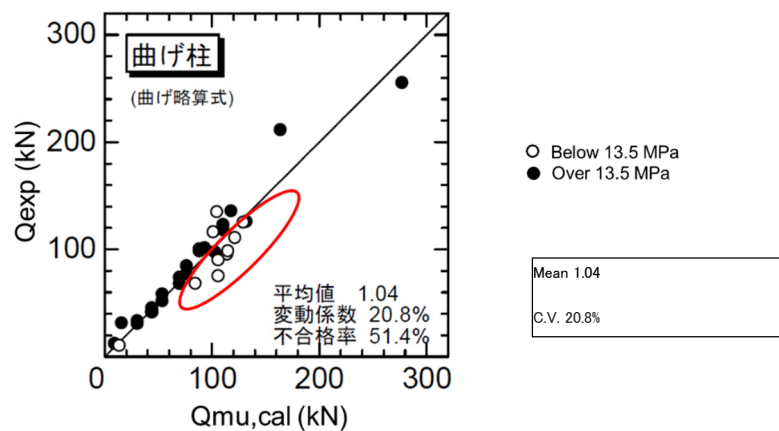


Figure C.3.2.2 Relation between  $Q_{exp}$  and  $Q_{mu}$  for column specimens with plain bars (Araki et al., 2011)

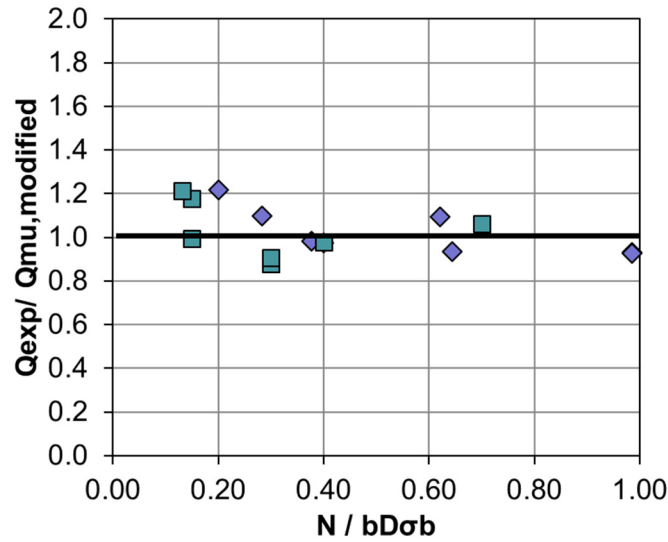


Figure C.3.2.3 Improved accuracy of the flexural strength using enhancement factor,  $e_h$  and reduction factor,

$$e_p$$

(Note:  $\sigma_y$  reported in each paper/report is used for the  $Q_{mu,modified}$  calculation)

### C.3.3: Ductility evaluation of flexural column

In this supplement, ductility evaluation methodologies for columns are not proposed. The reason is that the current JBDPA standard gives reasonable and conservative ductility evaluation even for low strength concrete and high axial load. The CNCRP manual recommends using modified evaluation methods and this gives more conservative ductility than the JBDPA standard. The behaviour of reinforced concrete members/ structures in the inelastic range during earthquakes is complex and still unclear. Therefore, conservative evaluation in ductility is preferred.

In C.3.3, the results of the studies comparing test data and the JBDPA standard calculation are shown.

#### Ultimate flexural drift angle $eR_{mu}$ evaluation

The ultimate flexural drift angle,  $eR_{mu}$  of column specimens with low strength concrete are calculated in accordance with the JBDPA standard and compared with the test results (drift angle at where the shear strength of the specimens deteriorate to 80% of the maximum capacity is defined as  $eR_{mu,exp}$ ). Figure C.3.3.1 shows the comparison.

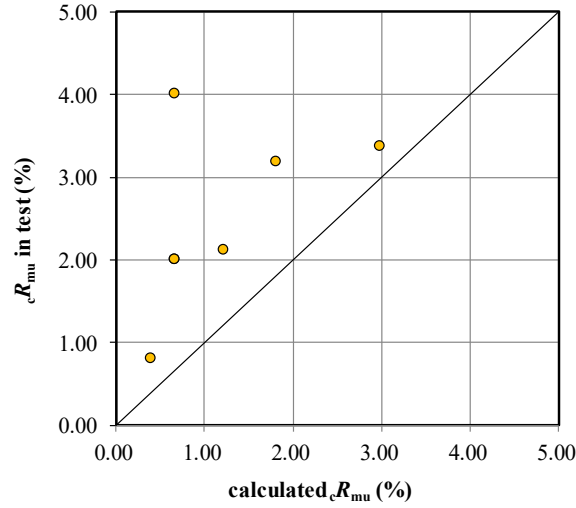


Figure C.3.3.1 Comparison of the calculated  $cR_{mu}$  and  $cR_{mu}$  in test

The JBDPA standard provides reasonable and conservative results even for low strength concrete specimens. In addition, a two-bay two-story bare frame test (Adnan et al, 2020) with  $F_c=4.8$  MPa and  $N/bDF_c (= \eta) = 0.88$  (in the 1<sup>st</sup> story of the center column) showed more than 0.4% drift capacity (calculated  $cR_{mu}$  for this column was 0.4%). Therefore, the CNCRP manual is also expected to work well, even for high axial load columns.

#### Residual axial capacity $N_r$ evaluation

According to the JBDPA standard, the residual axial capacity of columns,  $N_r$  is calculated by multiplying the original axial capacity of concrete ( $=bDF_c$ ) and the residual axial capacity ratio,  $\eta_r$ .  $\eta_r$  is determined based on the failure mode, transverse reinforcement ratio, and  $F$ -index (drift angle).  $\eta_r$  is examined by using test data along with the drift angle and column type. The results are shown in Figures. C.3.3.2–4.

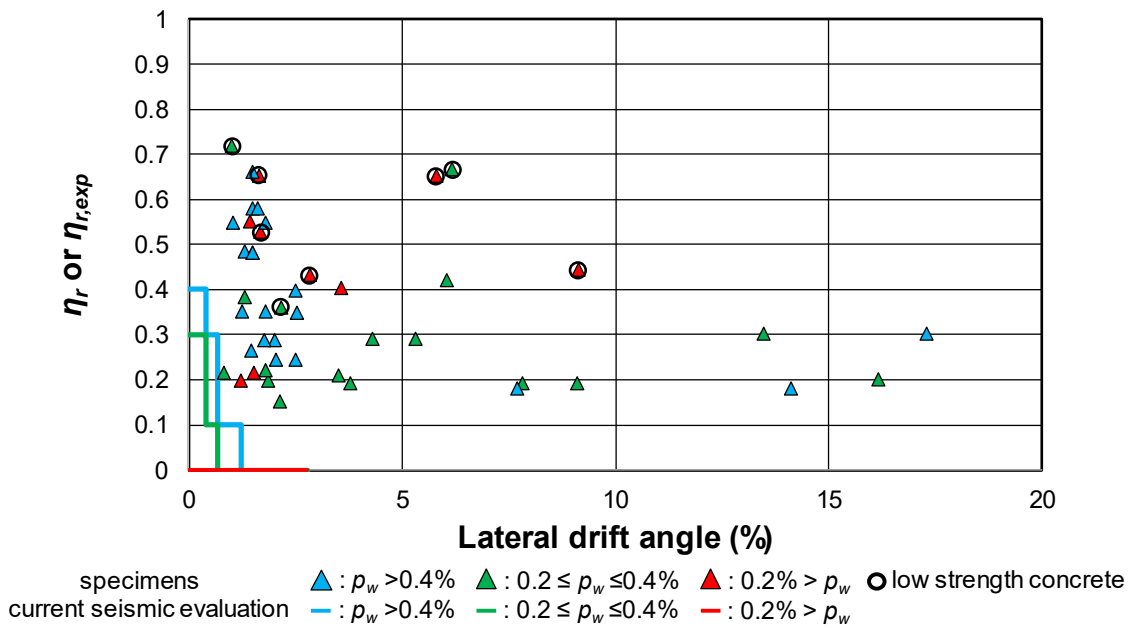


Figure C.3.3.2 Residual axial capacity ratio  $\eta_r$  evaluation for extremely brittle column

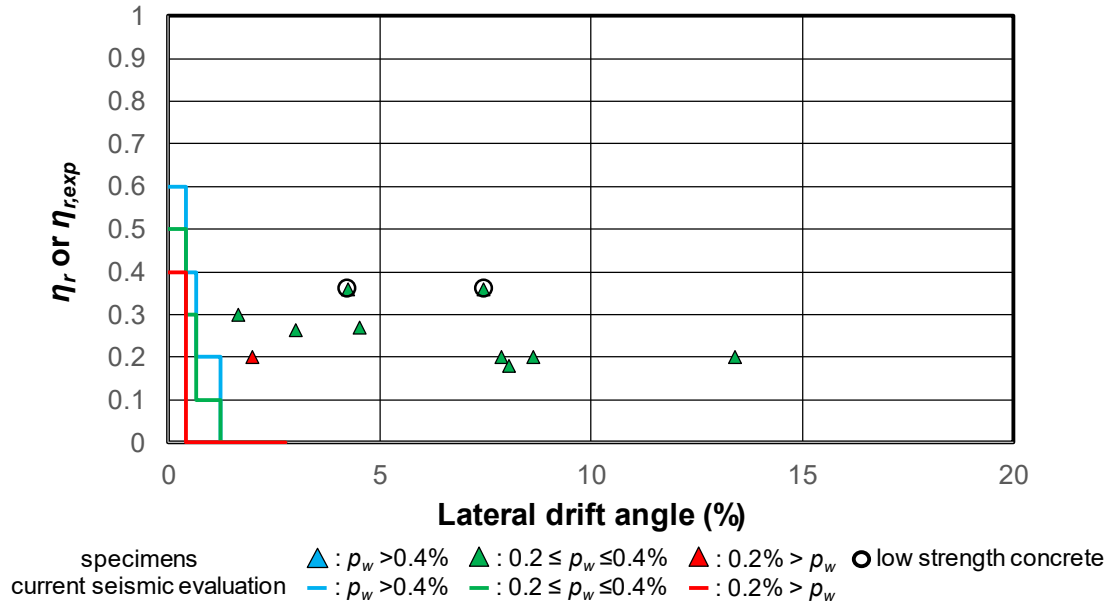


Figure C.3.3.3 Residual axial capacity ratio  $\eta_r$  evaluation for shear column

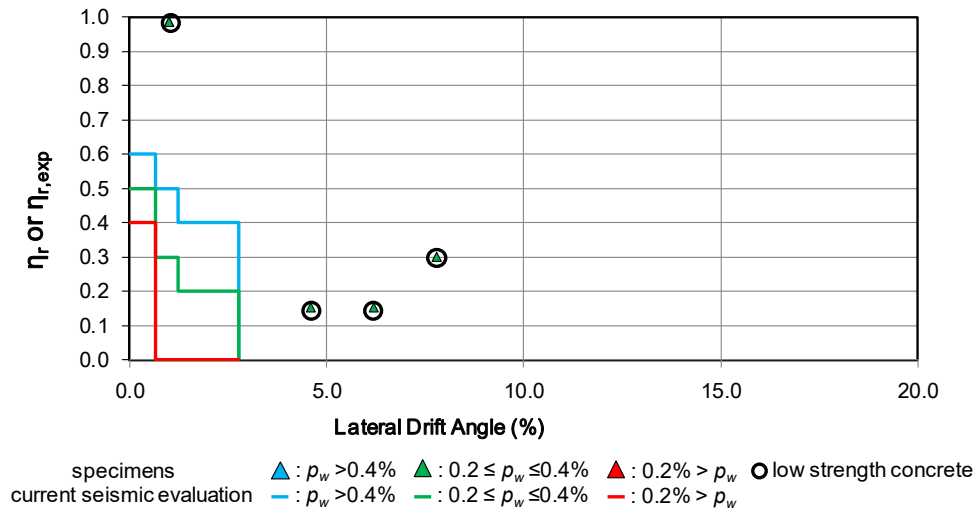
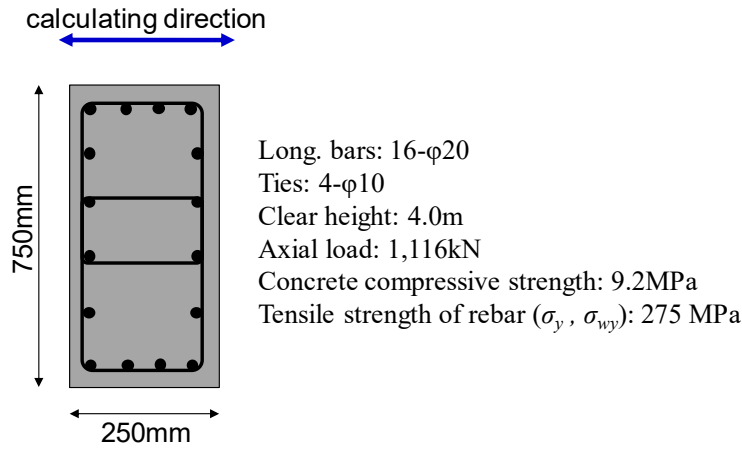


Figure C.3.3.4 Residual axial capacity ratio  $\eta_r$  evaluation for flexural column

The results exhibit that the current residual axial capacity ratio,  $\eta_r$  evaluation as per the JBDPA standard provides conservative estimation.

### 3.3 Example of application: An RC column of a five story office building in Dhaka constructed in 1985

A single RC column with the following dimensions is shown as an example for shear and flexural strength calculation.



Shear strength  $Q_{su}$ :

$$Q_{su} = \left\{ \frac{0.053 p_t^{0.23} (F_c + 18)}{M / Qd + 0.12} + \alpha_L \sqrt{p_w \sigma_{wy}} + 0.1 \sigma_0 \right\} bj \quad (3.2.1)$$

where

$p_t$ : tensile reinforcement ratio (%)

$F_c$ : concrete compressive strength (MPa)

$M/Q$ : shear span length (mm).  $h_0/2$  shall be applied.  $1.0 \leq M/Qd \leq 3.0$ .

$d$ : effective depth of column (mm).  $D - 50$ mm shall be applied.

$D$ : depth of column (mm)

$\sigma_{wy}$ : yield strength of transverse reinforcing bars in columns (MPa)

$\sigma_0$ : axial stress in column (MPa), not exceeding 8 MPa

$\alpha_L$ : reduction factor for low strength concrete

$b$ : width of column (mm)

$j$ : distance between centroids of tension and compression forces (mm),  $0.8D$  shall be applied.

$h_0$ : clear height of column (mm)

$a_t$ : total area of tensile longitudinal reinforcement ( $\text{mm}^2$ )

$$p_t = a_t / bD = 314.2 \text{ mm}^2 \times 6 \text{ nos.} / 750 \text{ mm} \times 250 \text{ mm} \times 100(\%) = 1.01\%$$

$$F_c = 9.2 \text{ MPa}$$

$$D = 250 \text{ mm} - 50 \text{ mm} = 200 \text{ mm}$$

$$M/Qd = h_0/2/d = 4000 \text{ mm}/2/200 \text{ mm} = 10, >3, \text{ therefore } M/Qd = 3.$$

$$p_w = a_w/b/s = 78.54 \text{ mm}^2 \times 4\text{nos.} / 750 \text{ mm}/225 \text{ mm} = 0.00186$$

$$\sigma_{wy} = 275 \text{ MPa}$$

$$\sigma_0 = N/bD = 1116 \times 10^3 \text{ N}/750 \text{ mm}/250 \text{ mm} = 5.95 \text{ MPa} < 8 \text{ MPa}$$

$$\alpha_L = 0.038F_c = 0.3496 < 0.85$$

Finally, the shear strength  $Q_{su}$  is calculated as :

$$Q_{su} = \left\{ \frac{0.053 \cdot 1.01^{0.23} (9.2 + 18)}{3.0 + 0.12} + 0.3496 \sqrt{0.00186 \cdot 275} + 0.1 \cdot 5.95 \right\} 750 \cdot 0.8 \cdot 250 = 196,200 \text{ N}$$

$$= 196.2 \text{ kN}$$

In the CNCRP manual, a calculation example of the same column is shown and the  $Q_{su}$  is 189.9 kN. Due to the difference in both equations, a minor change is observed.

#### Flexural strength $Q_{mu}$

$$N_{\max} = a_g \sigma_y + bDF_c = 314.2 \text{ mm}^2 \times 16\text{nos.} \times 275 \text{ MPa} + 750 \text{ mm} \times 250 \text{ mm} \times 9.2 \text{ MPa} = 3,107 \text{ kN}$$

$$0.4bDF_c = 0.4 \times 750 \text{ mm} \times 250 \text{ mm} \times 9.2 \text{ MPa} = 690 \text{ kN}$$

Eq. (3.2.5) is used because plain bars are used and  $0.4bDF_c \leq N \leq N_{\max}$ .

$$M_u = \left( 0.8a_t \sigma_y D + 0.12bD^2 F_c \right) \left( \frac{N_{\max} - N}{N_{\max} - 0.4bDF_c} \right) e_h e_p \quad (3.2.5)$$

$$a_t = 314.2 \text{ mm}^2 \times 6\text{nos.} = 1885 \text{ mm}^2$$

$$\sigma_y = 275 \text{ MPa}$$

$$e_h = (N/bDF_c + 0.2) / 0.6 = (1116 \times 10^3 \text{ N} / 750 \text{ mm}/250 \text{ mm}/9.2 \text{ MPa} + 0.2) / 0.6 = 1.41$$

$$e_p = 0.8, \text{ because plain bars are used and } F_c \text{ is below } 13.5 \text{ MPa.}$$

Finally, the flexural strength  $M_u$  is calculated as below.

$$M_u = \left( 0.8 \cdot 1885 \cdot 275 \cdot 250 + 0.12 \cdot 750 \cdot 250^2 \cdot 9.2 \right) \left( \frac{3107 - 1116}{3107 - 690} \right) 1.41 \cdot 0.8 = 144,419,084 \text{ N} \cdot \text{mm}$$

$$= 144.4 \text{ kN} \cdot \text{m}$$

$$\text{Therefore, } Q_{mu} = 2M_u / h_0 = 2 \times 144.4 \text{ kNm} / 4.0 \text{ m} = 72.2 \text{ kN}$$

In the CNCRP manual, calculation example of the same column is shown and the  $Q_{mu}$  is 51.16kN. Due to the employment of factors  $e_h$  and  $e_p$ , 141% increase is observed.

## References

1. Japan International Cooperation Agency (JICA), (2015): Project for Capacity Development on Natural Disaster-Resistant Techniques of Construction and Retrofitting for Public Buildings in The People's Republic of Bangladesh Final Report, Japan.
2. JBDPA (2001): Standard for seismic evaluation of existing reinforced concrete buildings, English version, 1<sup>st</sup>, Japan Building Disaster Prevention Association, Japan.
3. PWD (2015): Manual for Seismic Evaluation of Existing Reinforced Concrete Buildings. Public Works Department, The People's Republic of Bangladesh.
4. Kabir, R. T., Hasan, M. K., Adnan, S. M. N., Ahmed M., M. Maliha, M., Barua, S., Ema, A. J., Islam, M. A., Suzuki, R., Matsukawa, K., Nakano, Y., Rahman, M. M., Amin, A. F. M. S. (2020), Tests on Low Strength Concrete Columns under High Axial Compression and Shear, *Proceedings of the 17th World Conference on Earthquake Engineering*, Sendai, Japan, Paper Number C001289.
5. Yasojima, A., Araki, H., Matsui, T., Taniguchi (2010), H., Evaluation of Shear Strength for Low Strength Concrete Members, *AIJ Journal of Technology and Design*, Vol. 16, No. 32, 139-144.
6. Priestly, M. J. N., Park, R. (1987), Strength and Ductility of Concrete Bridge Columns Under Seismic Loading, *ACI Structural Journal*, 61-76.
7. Araki, H., Yasojima, A. (2011), Seismic Performance Evaluation of Low Strength Concrete Members with Plain Round Bar, *AIJ Journal of Technology and Design*, Vol. 16, No. 32, 139-144.
8. Adnan, S. M. N., Fukutomi, Y., Haga, Y., Matsukawa, K., Nakano, Y. (2020), Behavior of Poorly Detailed RC Frames with Low Strength Concrete and URM Infill under High Axial Loads, *Proceedings of the 17th World Conference on Earthquake Engineering*, Sendai, Japan, Paper Number C001287.





## Chapter 4 RC Frame with Masonry Infill Wall

### 4.1 General

- (1) Chapter 4 is applied to the seismic evaluation of RC frame with masonry infill wall. The evaluation method in Chapter 4 is suggested to be applied for frames with an aspect ratio  $h/l$  of 0.5 to 1.
- (2) The general procedure of evaluation is as follows:
- Step 1: Classification into either structural or non-structural elements (Sec. 4.2)
  - Step 2: Judgement of failure mode (Sec. 4.3)
  - Step 3: Evaluation of Strength Index,  $C$  (Sec. 4.4)
  - Step 4: Evaluation of Ductility Index,  $F$  (Sec. 4.5)
  - Step 5: Check for out-of-plane failure (Appendix 4.2)

### C.4.1 [Commentary]

#### C.4.1.1 Scope of application

The Japanese Seismic Evaluation Standard of Existing Reinforced Concrete Buildings (JBDPA, hereafter referred to as “Japanese Seismic Evaluation Standard”) does not account for masonry infill since masonry infill walls are not commonly used in Japan. However, masonry infill is commonly used in RC buildings in other countries and could affect the seismic capacity of RC buildings. Thus, this document is intended to serve as a technical document to evaluate the seismic capacity of RC frame with masonry infill commonly found in other countries, referring to the basic concepts of the Japanese Seismic Evaluation Standard.

#### C.4.1.2 General procedure

The main procedures of seismic evaluation of masonry infill are shown in Figure C.4.1.1.

- Firstly, a masonry infill wall (herein will be referred to as masonry infill) is classified into either a structural element or a non-structural element based on shape, the gap between the RC frame and masonry infill, appearance based on visual inspections.
- Secondly, the failure mode is identified as described in Section 4.3.
- Thirdly, Strength Index ( $C$ ) and Ductility Index ( $F$ ) are evaluated based on Sections 4.4 and 4.5.
- Finally, the out-of-plane behavior is investigated for evaluating these structural walls.

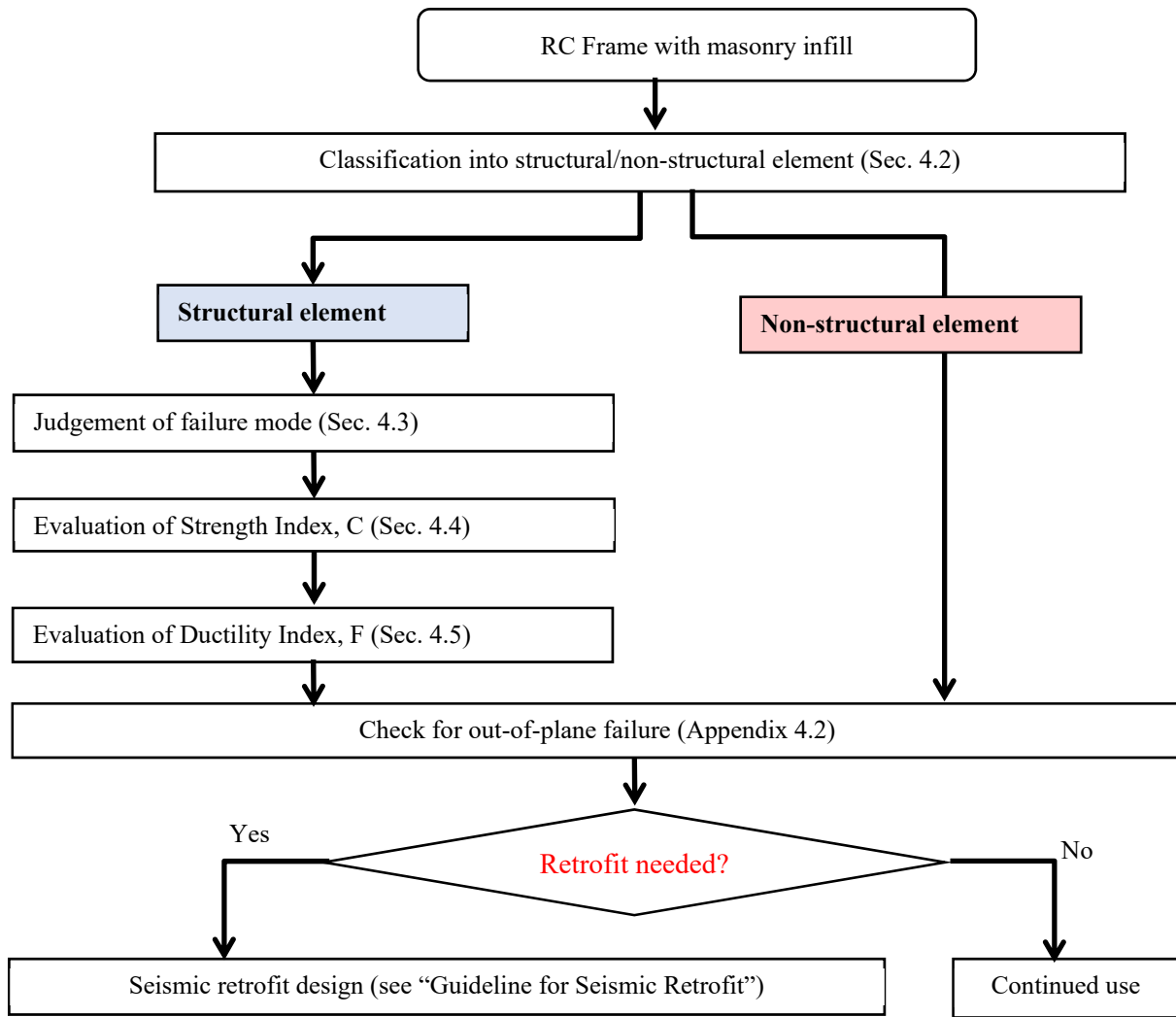


Figure C.4.1.1 Flow of seismic evaluation of RC frame with masonry infill

### C.4.1.3 Definitions

**Strength index  $C$ :** The lateral-load carrying capacity of a member (masonry infill, or RC column) in terms of a shear coefficient, namely the shear capacity normalized by the weight of the building above.

**Ductility index  $F$ :** An index representing the deformation capacity of a structural member.

**$\beta$ -index:** An index representing the confinement of the RC frame defined by the ratio of the boundary frame's lateral strength to masonry infill's shear strength. A larger  $\beta$ -index represents a stronger surrounding RC frame relative to masonry strength.

**$a_c/h_o$  ratio:** The ratio of contact length of masonry infill to column height

**In-plane failure:** A failure mode of masonry infill caused by the load acting horizontally along the wall length.

**Out-of-plane failure:** A failure mode of masonry infill damaged in a perpendicular direction to the wall surface.

**Structural masonry element:** An infill that is deemed to contribute to the lateral capacity of a building.

### C.4.1.4 Notations

$C_{inf}$ : The strength index of a masonry infill wall.

$C_{col}$ : The strength index of a boundary RC column attached to the infill wall.

$F_{inf}$ : The ductility index of a masonry infill wall.

$F_{col}$ : The ductility index of a boundary RC column attached to the infill wall.

$Q_{frame}$  : ( $=lQ_{col}+rQ_{col}$ ) Lateral strength of column calculated as the minimum strength of  $Q_{su}$ ,  $Q_{mu}$ .

$lQ_{col}$ ,  $rQ_{col}$ : Lateral strength of left hand side column and right hand column, respectively

$Q_{expected}$ : Expected lateral strength of masonry infill.

$W$ : The weight of the building including live load for seismic calculation supported by the story concerned.

$Q_{su}$ : Ultimate shear strength of the column.

$Q_{mu}$ : Shear force at the ultimate flexural strength of the column.

$Q_{inf}$ : Lateral in-plane strength of the masonry infill.

$Q_{sla}$ : Sliding lateral strength of masonry infill,

$Q_{dia}$ : Diagonal compression strength of masonry infill.

$f_m$ : Prism compressive strength of masonry infill.

$E_{inf}$ : Young's modulus of masonry infill.

$t_{inf}$ : Thickness of masonry infill.

$l_{inf}$ : Length of masonry infill.

$d_{inf}$ : Diagonal length of masonry infill.

$\theta$ : Inclination angle of masonry wall's diagonal from the horizontal axis.

$E_c$ : Young's modulus of concrete.

$I_c$ : Moment of inertia of RC column.

$M_u$ : Flexural yield moment of the column calculated based on the Japanese standard (JBDPA, 2001).

$h_o$ : Clear height of RC column.

$h_{inf}$ : Height of masonry infill.

$\lambda_{op}$ : Reduction factor to account for opening in masonry infill

$l_o$ : Maximum width of opening measured across a horizontal plane

$Q_{flex-wall}$ : Strength of frame calculated as flexural wall and masonry infill as a rigid panel.

$Q_{punching}$ : Punching shear of an RC column

$Q_{mw}$ : Lateral strength of an RC frame with a masonry infill

$Q_{fw}$ : Lateral strength for overall flexural failure

$Q_{jw}$ : Lateral strength of punching shear failure

$M_{wmu}$ : Flexural Moment capacity for overall flexural failure

$a_{t,col}$ : Area of steel of longitudinal reinforcement in tension column.

$\sigma_y$ : Yield strength of tension reinforcement.

$l_w$ : Center to center span length of RC frame.

$N$ : Total axial force on RC columns on both sides of masonry infill wall.

$Q_{pc}$ : Punching shear strength of column

$K_{inf}$ : Initial stiffness for RC frame with masonry infill

$K_{frame}$ : Initial stiffness of RC frame

$K_{strut}$ : Initial stiffness of masonry infill

$l_b$ : Length of RC beam

$h_c$  = Height of RC column

$W_s/W_{inf}$ : Strut width

$\Gamma$ : A factor to account for the influence of aspect ratio ( $h_{inf}/l_{inf}$ ).

*\*All units are considered as SI unit*

## 4.2 Classification of masonry infill wall

### (1) Judging criteria for a structural element

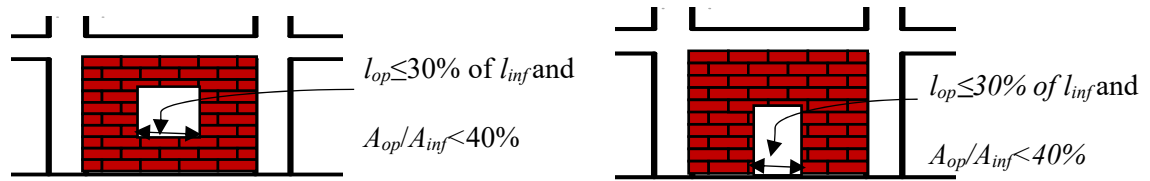
A masonry infill wall is considered as a structural element, in case of satisfying all of the following criteria a) to f) below.

- a) Masonry infill wall is surrounded and confined by RC beams and columns on all sides.
- b) The beam-column joint of the surrounding RC frame is strong and stiff enough with sufficient anchorage capacity as defined in Chapter 5.
- c) In case of a masonry infill wall with a single opening, the area of the opening is less than 40% of the masonry infill and the length of the opening is less than 30% of the wall length.
- d) The slenderness ratio  $h_{inf}/t$  of masonry infill is less than 30.
- e) The masonry infilled frame consists of solid bricks.
- f) The masonry infill does not show cracks nor major damage during a preliminary inspection of the existing building before seismic evaluation as discussed in the BSPP manual Chapter 2, section 2.2.

### C.4.2 [Commentary]

The openings in masonry infill may greatly affect the strength of masonry infill. In order to consider masonry infill as a structural wall, the following points need to be investigated.

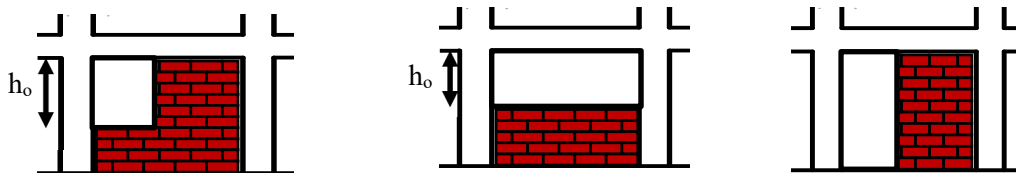
- a) The opening area in the masonry infill should be less than 40% of the masonry infill area. The length of the opening should not exceed 30% of the masonry infill length as shown in Figure C.4.2.1. It should be noted that openings closely adjacent to the frame (large eccentricity) are judged as partial infill as explained in point b) below.
- b) Multiple openings is complex topic that each case need to be studied case by case, thus multiple opening is out of scope in this guideline and need to be evaluated based on the professional judgment for each case.
- c) It should be noted that opening adjacent to column (such as Figure C.4.2.2-a), partial masonry infill (such as Figure C.4.2.2-b), wing walls (such as Figure C.4.2.2-c) are recommended to be ignored as structural elements and the only negative influence of the column such as a short column effect, because of reduced height, need to be considered.
- d) Masonry walls with gaps between frame and masonry infill (detachment) may not work probably as a structural element and are vulnerable to Out of plane failure, therefore are recommended to be ignored as structural elements and Out of plane failure need to be checked.



a) Window opening

b) Door Opening

Figure C.4.2.1 Openings in masonry infill that could be considered as a structural element



a) Position of opening in walls

b) Partial height infill

c) wing wall infill

Figure C.4.2.2 Opening positions and partial masonry infill walls that could not be considered as a structural element

### 4.3 Judgement of failure mode

(1) Failure mode of a RC frame with masonry infill is classified into Type I to Type IV based on the confinement level from the surrounding RC frame. The ratio of contact length to column height ( $a_c/h_o$ ), is used for classification. (Table 4.3.1)

Type I: Diagonal compression failure

Type II: Sliding and diagonal cracking failure

Type III: Overall flexural failure

Type IV: Column punching and joint sliding failure

The failure mode of the surrounding RC column is classified into Type A to Type D.

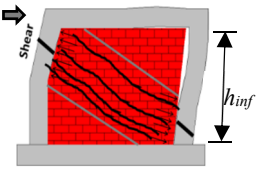
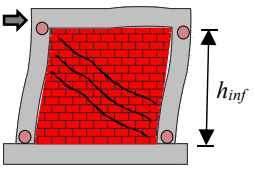
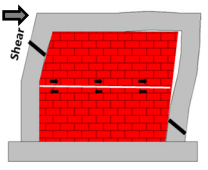
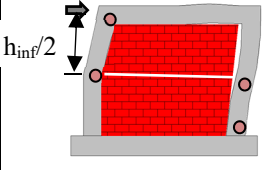
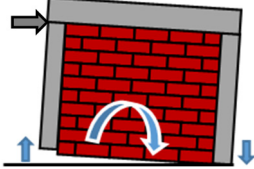
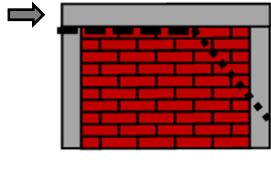
Type A: Column shear failure

Type B: Column flexural failure

Type C: Short column shear failure

Type D: Short column flexural failure

Table 4.3.1 Idealized Failure types of RC frame with masonry infill

	<b>Column</b> $h_o = h_{inf}^{*1}$		<b>Short Column</b> $h_o = h_{inf}/2^{*1}$ (hinge at mid height)	
	<b>Shear</b> <b>Type A</b> $Q_{su}/Q_{mu}^{*2} < 1$	<b>Flexural</b> <b>Type B</b> $Q_{su}/Q_{mu}^{*2} > 1$	<b>Shear</b> <b>Type C</b> $Q_{su}/Q_{mu}^{*2} < 1$ for $h_{inf}/2$	<b>Flexural</b> <b>Type D</b> $Q_{su}/Q_{mu}^{*2} > 1$ for $h_{inf}/2$
<b>Type I</b> <b>Diagonal compression</b> $a_c/h_o \geq 0.30$			N.A.	N.A.
<b>Type II</b> <b>Sliding –diagonal cracking failure</b> $0.2 < a_c/h_o < 0.30$	N.A.	N.A.		
<b>Type III</b> <b>Overall flexural</b> $a_c/h_o \leq 0.2$			N.A.	
<b>Type IV</b> <b>Column punching &amp; joint sliding</b> $a_c/h_o \leq 0.2$	N.A.			

<sup>\*1</sup>  $h_o$ : Clear height of the column (footnote).  $h_{inf}$ : Height of the masonry infill.

<sup>\*2</sup>  $Q_{su}$ : Ultimate shear strength of the column.  $Q_{mu}$ : Shear force at the ultimate flexural strength of the column.  $Q_{su}/Q_{mu}$  is the margin of shear to flexural strength of the column.

(2) Ratio of contact length to column height ( $a_c/h_o$ )

The contact length ratio of masonry infill and RC frame is defined as the ratio of contact length to column height ( $a_c/h_o$ ), which can be calculated through Eqs. (4.3.1) and (4.3.2).

$$\frac{a_c}{h_o} = \frac{\pi}{4\lambda h_o} \quad (4.3.1)$$

$$\lambda = \sqrt[4]{\frac{E_m t_{inf} \cos^2 \theta}{4E_c I_c d_{inf}}} \quad (4.3.2)$$

$E_m$ ,  $E_c$ : Young's modulus of masonry prism and concrete, respectively

(in case of unavailability of masonry material properties,  $E_m$  can be assumed as  $550f_m$ )

$t_{inf}$ : thickness of masonry infill,  $d_{inf}$ : diagonal length of masonry infill,

$I_c$ : moment of inertia of RC column,  $\theta$ : inclination angle of diagonal from the horizontal axis.

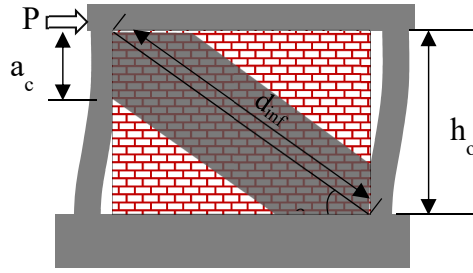


Figure 4.3.1 Contact length of masonry infill

Failure modes are classified according to  $a_c/h_o$  as follows.

- i)  $a_c/h_o \geq 0.3$ , Good confinement/Weak wall: Type I
- ii)  $0.2 < a_c/h_o < 0.3$ , Fair confinement: Type II
- iii)  $a_c/h_o \leq 0.2$ , Poor confinement: Type III or IV

### C.4.3 [Commentary]

#### C.4.3.1 Classification of failure modes

Various types of failure modes of RC frame with masonry infill were observed in previous researches. However, it seems the classification of failure modes has not been studied enough especially based on the theoretical mechanism background. The diagonal compression failure of masonry (Type I) is one of the most popular failure modes when good confinement from the surrounding RC frame is provided. Another popular failure mode is the sliding failure along mortar between bricks or a mixed type of failure with sliding and diagonal cracking is also found in many experiments (Type II). Surrounding RC frame and masonry infill tend to behave separately in these three types of failure modes. Their strength ( $C$  index) and ductility ( $F$  index), therefore, can be evaluated separately.

In case of strong and stiff masonry infill, the masonry infill can be assumed as a rigid wall panel. One possible failure mode is the overall flexural failure mode (Type III) which is a common failure mechanism in the RC wall. If lateral strengths in surrounding columns are insufficient, punching shear in a column and sliding at the top joint between masonry infill and beam may occur (Type IV).

Key parameters to govern these failure modes are the ratio of stiffness and strength of masonry infill to RC frame. Thus,  $a_c/h_o$ , are introduced for the classification of failure modes in this guideline. The contact length ratio  $a_c/h_o$  is an index of confinement by RC frame in terms of contact length of column with masonry infill. Details in  $a_c/h_o$  is described later in this section and the failure mode can be classified based on  $a_c/h_o$ .

#### C.4.3.2 Ratio of contact length to column height, $a_c/h_o$

The most acceptable concept to define the contact length ratio, based on relative stiffness, is to consider the masonry infilled frame is analogous to a beam on an elastic foundation as shown in Figure C.4.3.1. When the beam is subjected to lateral load, lateral deformation of the beam element depends on the relative rigidity of the beam and foundation. According to Hetenyi (1946), the equation of deflection of a finite length beam rests on an elastic foundation (as shown in Figure C.4.3.2) can be written as Eq. (C.4.3.1) based on the theory of elasticity and the relative rigidity can be defined as Eq. (C.4.3.2).



$$y = \frac{P\lambda}{2bk_o} e^{-\lambda x} (\sin\lambda x + \cos\lambda x) \quad (C.4.3.1)$$

$$\lambda = \sqrt[4]{\frac{bk_o}{4EI}} \quad (C.4.3.2)$$

where,  $y$  = deflection of beam element;  $\lambda$  = relative rigidity;  $P$  = lateral load;  $b$  = foundation thickness;  $k_o$  = modulus of foundation, i.e., pressure required to cause unit deflection of foundation;  $E$  = Young's modulus of beam element, i.e., concrete; and  $I$  = moment of inertia of beam element, i.e., RC column.

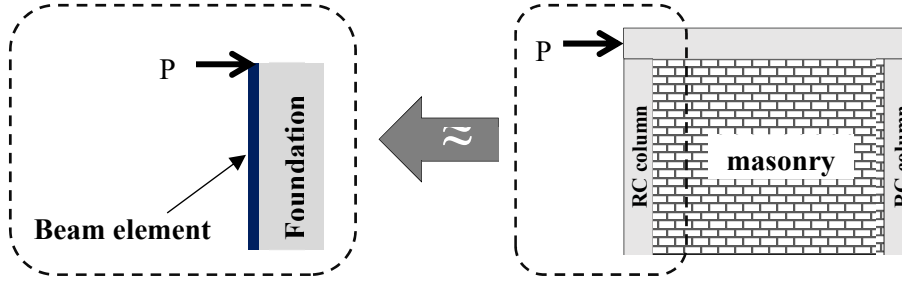


Figure C.4.3.1 Idealization of masonry infilled RC frame

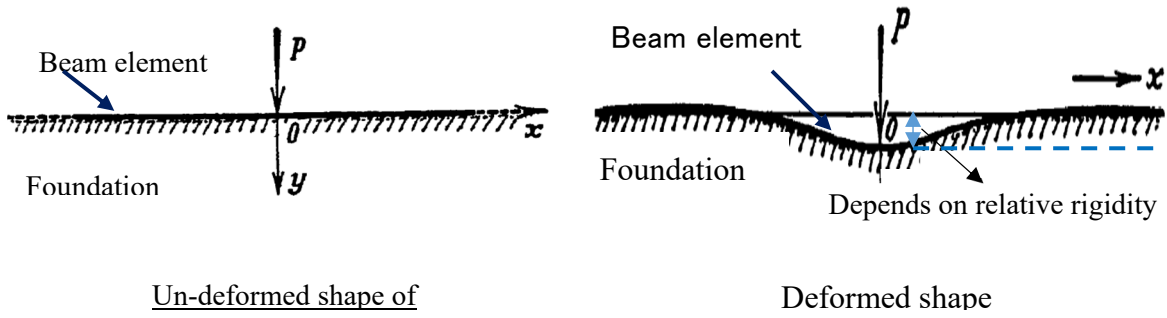


Figure C.4.3.2 Deformation of a beam on an elastic foundation (Hetenyi, 1946)

The relative rigidity ( $\lambda$ ) can easily be defined for the RC column and masonry combination after defining the modulus of foundation ( $k_o$ ) for masonry infill. The modulus of foundation ( $k_o$ ) for masonry infill can be defined as the pressure required to cause a unit deflection of masonry brace in the lateral direction as per Eq. (C.4.3.3).

$$k_o = \frac{E_{inf} \cos^2 \theta}{d_{inf}} \quad (C.4.3.3)$$

where  $E_{inf}$  = Young's modulus of masonry;  $d_{inf}$  = diagonal length of masonry infill; and  $\theta$  = inclination angle of compression diagonal from the horizontal axis.

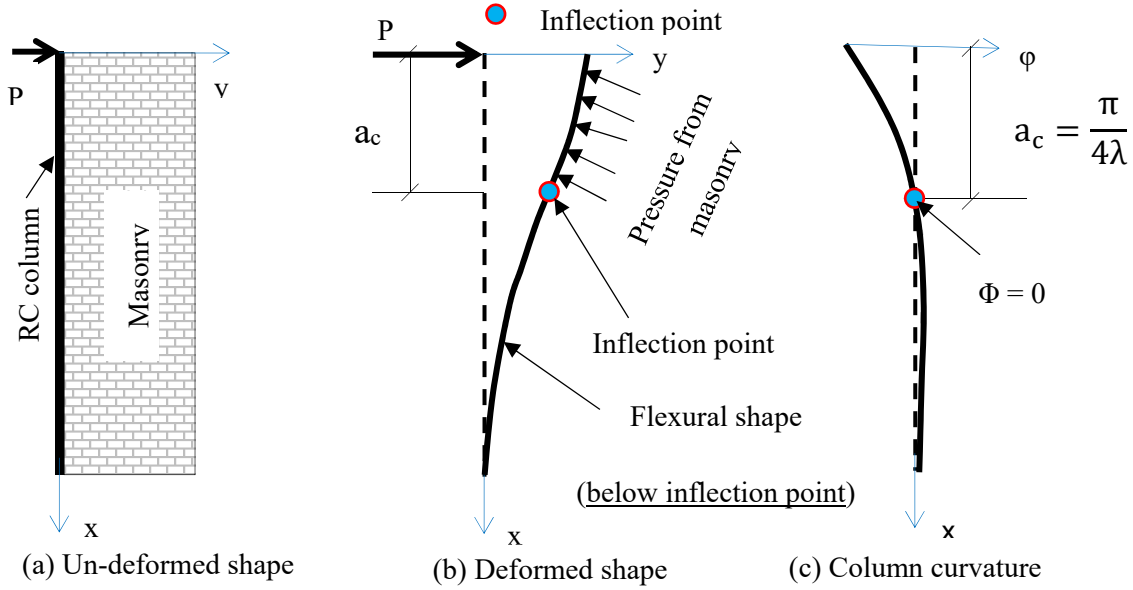


Figure C.4.3.3 Surrounding RC column (a) un-deformed shape, (b) deformed shape and (c) curvature distribution

Therefore, combining Eq. (C.4.3.2) and Eq. (C.4.3.3), the following relative rigidity factor ( $\lambda$ ) for masonry infilled RC frame is defined here as Eq. (C.4.3.4) which has a dimension of per unit length.

$$\lambda = \sqrt[4]{\frac{E_{inf} t_{inf} \cos^2 \theta}{4 E_c I_c d_{inf}}} \quad (C.4.3.4)$$

It is evident from the column deflection shape, as illustrated in Figure C.4.3.3 (b), that the lower portion of the RC column exhibits flexure deflection whereas the deflection mode of its upper part is changed from flexural shape due to the presence of infill masonry, which causes the separation between masonry and RC frame. Based on the deflection shape, it has been considered that the masonry infill of the upper part above the inflection point is attached with the RC frame effectively and considered as contact length ( $a_c$ ) of diagonal strut formed. The height of the inflection point, i.e., contact length ( $a_c$ ) is evaluated from the condition of zero curvature at an inflection point. The curvature of the RC column, as shown in Figure C.4.3.3 (c), is computed from the second derivative of column deflection ( $y$ ) as per Eq. (C.4.3.5). Subsequently, the contact length and contact length ratio are calculated using Eq. (C.4.3.6) and Eq. (C.4.3.7).

$$\frac{d^2 y}{dx^2} = \frac{P \lambda^3}{b k_o} e^{-\lambda x} (\cos \lambda x - \sin \lambda x) \quad (C.4.3.5)$$

$$a_c = \frac{\pi}{4 \lambda} \quad (C.4.3.6)$$

$$\frac{a_c}{h_o} = \frac{\pi}{4 \lambda h_o} \quad (C.4.3.7)$$

where,  $y$  = deflection of beam element (or RC column);  $\lambda$  = relative rigidity of masonry infilled RC frame;  $P$  = lateral load;  $b$  = foundation thickness (or masonry infill, in this case);  $k_o$  = modulus of foundation (in this case, masonry infill), i.e., the pressure required to cause unit deflection of foundation;  $E_c$  = Young's modulus of beam element (or RC column); and  $I_c$  = moment of inertia of RC column and  $a_c$  = contact length.

Failure mechanisms can be differentiated based on the contact length which depends on the relative stiffness of the RC frame and masonry. The idea is illustrated in Figure C.4.3.4, where three different cases are defined based on the contact length. When the masonry infill is very stiff compared to the surrounding RC frame, the RC column cannot deflect easily, therefore, the contact length would be very small. In that case, the masonry infilled RC frame would fail like a structural wall with boundary columns, i.e., punching failure at the top of the column or overall flexural failure of RC frame. On the other hand, when the RC frame is very strong relative to the infill, the RC column can have a long contact length so that it can transfer the lateral load through the diagonal strut and can fail in compression crushing. In the case of intermediate contact length, a compression strut will form, however, the failure would be governed by the sliding of infill masonry or mixed failure (sliding and cracking).

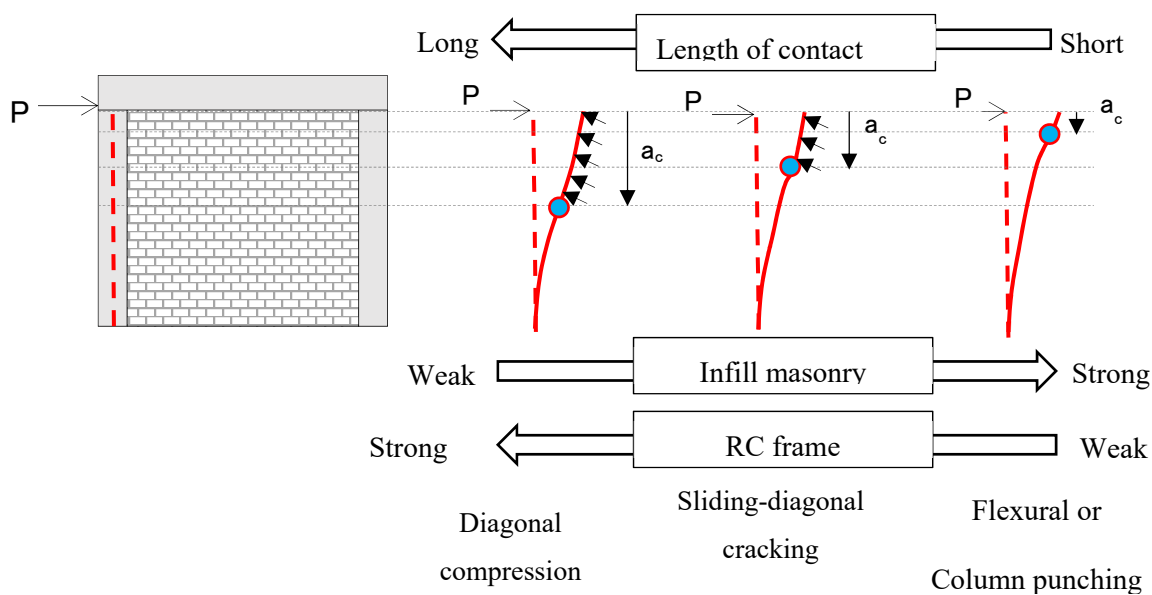


Figure C.4.3.4 Idea to separate failure modes based on contact length

The contact length ( $a_c$ ) of the investigated specimens, collected previously with the failure mechanism, is determined. The ranges of normalized contact length ( $a_c/h_o$ ) are illustrated in Figure C.4.3.5. It is evident that the diagonal compression failure occurred when the normalized contact length ( $a_c/h_o$ ) lay between 0.26 and 0.41. Sliding and mixed failure occurred when normalized contact length ( $a_c/h_o$ ) was most of the specimens were in the range of 0.2 to 0.45, while punching or flexural failure occurred when the normalized contact length ( $a_c/h_o$ ) was less than 0.20.

Therefore, the idea of failure mode separation using the normalized contact length works well, but the determination of the exact contact length ratio for each failure mechanism might be difficult using available experimental data from the literature. Therefore, a further attempt is taken to execute a probabilistic analysis to identify margins for different failure mechanisms which is discussed in the following sub-section.

The log-normal distribution of normalized contact lengths for each cluster of failure mechanisms is shown in Figure C.4.3.6(a). It is evident that the ranges of normalized contact length overlapped for diagonal compression and sliding or mixed failure. Whereas, the distribution for punching or flexural failure is spike-shaped due to the few numbers of data. Hence, the further cumulative distribution of each failure mechanism cluster is drawn in Figure C.4.3.6(b). Afterward, a 90% probability line is drawn to distinguish the failure

mechanisms. Based on the 90% probability line, boundary conditions are proposed and given in Table C.4.3.1 for the separation of failure mechanism of masonry infilled RC frame by analyzing the available data in the literature.

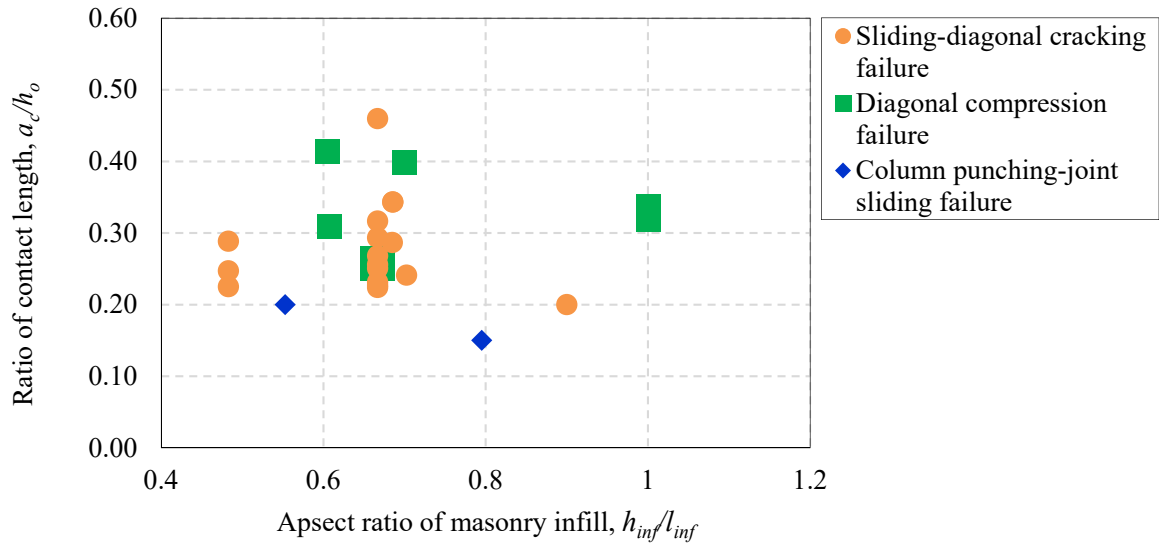


Figure C.4.3.5 Comparison of experimental failure modes and  $a_c/h_o$  ratio

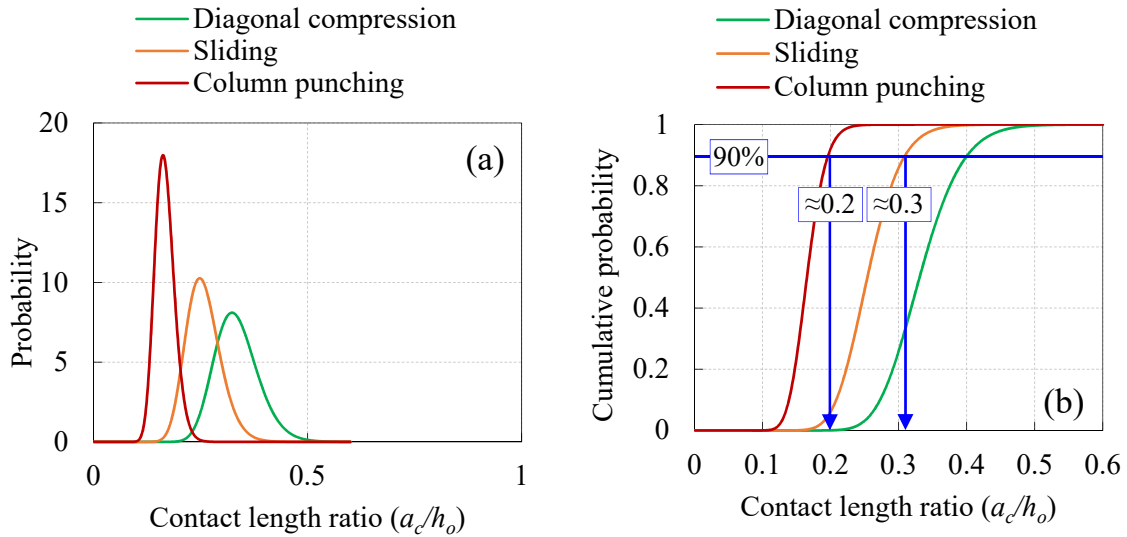


Figure C.4.3.6 (a) Distribution of normalized contact length and (b) Cumulative distribution of normalized contact length for different failure modes

Table C.4.3.1 Boundary for failure mechanism of RC frame with masonry infill

Normalized contact length ( $a_c/h_o$ )	Failure mechanism
$a_c/h_o \leq 0.2$	Punching or Flexural failure
$0.2 < a_c/h_o < 0.3$	Sliding and diagonal cracking
$a_c/h_o \geq 0.3$	Diagonal compression failure

#### C.4.3.3 Prism compressive strength $f_m$

It might be difficult to obtain the prism compressive strength of masonry infill  $f_m$  in the field survey. In this case, the prism compressive strength  $f_m$  could be estimated using the unit compressive strength of brick  $f_u$  obtained from site investigation and/or other methods. Figure C.4.3.7 is reported in MSJC standard 2016. In case of Bangladesh, the masonry brick units are commonly having compressive strengths ranging from 15 to 20 MPa. Using Figure C.4.3.7, the prism compressive strength in Bangladesh will be in the range from 5 MPa to 10MPa.

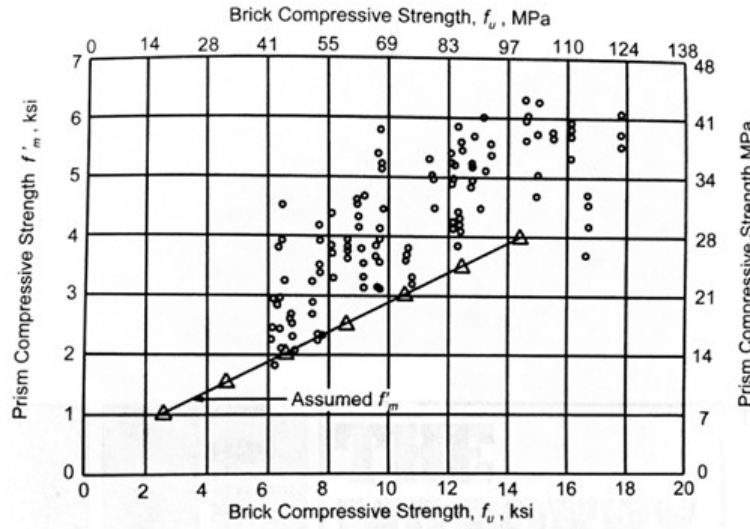


Figure C.4.3.7 Prism compressive strength based on brick strength reported in the Code TMS 402/602-16 (MSJC 2016)

## 4.4 Strength index C

### 4.4.1 General

Strength index  $C_{mw}$  for an RC frame with masonry infill is calculated by Eqs. (4.4.1) and (4.4.2).

$$C_{mw} = \frac{Q_{mw}}{\Sigma W} \quad (4.4.1)$$

Where  $\Sigma W$  is the weight of the building including live load supported by the story concerned.

$$Q_{mw} = \begin{cases} Q_{frame} + Q_{dia} & \text{Type I} \\ Q_{frame} + Q_{sla} & \text{Type II} \\ Q_{fw} & \text{Type III} \\ Q_{jw} & \text{Type IV} \end{cases} \quad (4.4.2)$$

$Q_{mw}$  is the lateral strength of an RC frame with masonry infill.  $Q_{frame}$  is sum of the lateral strength of left-hand side and right-hand side columns of the surrounding frame, smaller of  $Q_{su}$  and  $Q_{mu}$  calculated by BSPP Seismic Evaluation Manual [4.2] with a clear height of  $h_o$  as the height of masonry infill.

$Q_{dia}$  is the lateral strength of a masonry infill wall for Type I.  $Q_{sla}$  is the lateral strength of a masonry infill wall for Type II.  $Q_{fw}$  is Lateral strength for overall flexural failure (Failure Type III),  $Q_{jw}$  is the lateral strength of punching shear failure (Failure Type IV) .

### 4.4.2 Type I (Diagonal compression failure)

- Lateral strength of a frame  $Q_{frame}$  is calculated by BSPP Seismic Evaluation Manual [4.2].

ii) Lateral strength at diagonal compressive failure ( $Q_{dia}$ ) shall be determined using Eq. (4.4.3)

$$Q_{dia} = 0.5f_{m,\theta}W_s t_{mas} \cos\theta \quad (4.4.3)$$

$$W_s = 2a_c \cos\theta$$

$$a_c = \frac{\pi}{4\lambda}$$

$f_{m,\theta}$ : compressive strength of masonry along diagonal ( $= 0.5f_m$ ,  $f_m$  = masonry prism strength)

$W_s$ : strut width;

$a_c$ : contact length

$\lambda$ : relative rigidity of masonry infilled RC frame

$t_{mas}$ : thickness of masonry

$\theta$ : inclination of loaded diagonal with horizontal

#### 4.4.3 Type II (Sliding and diagonal cracking failure)

i) Lateral strength of a frame  $Q_{frame}$  is calculated by BSPP Seismic Evaluation Manual [4.2].

iii) Lateral strength of sliding failure  $Q_{slid}$  is applied Type II given by the Eq (4.4.4).

$$Q_{slid} = \frac{\tau_{inf} \cdot t_{inf} \cdot l_{inf}}{1 - \mu \cdot \frac{h_{inf}}{l_{inf}}} \quad (4.4.4)$$

$\tau_{inf}$ : shear strength of masonry infill taken by in situ tests. In case of unavailable data, it can be taken as  $\tau_{inf} = 0.03f_m$ .

$h_{inf}$ ,  $l_{inf}$ : infill height and length, respectively and for the application limit of this guide of  $0.5 \leq h_{inf}/l_{inf} < 1$

$\mu$ : friction coefficient could be taken as 0.45.

$f_m$ : compressive strength of masonry prism.

#### 4.4.4 Type III (Overall flexural failure of frame)

Surrounding columns and masonry infill work as a solid flexural wall, assuming the masonry infill as a rigid wall panel, and the overall flexural strength  $Q_{fw}$  is given by Eq. (4.4.5).

$$Q_{fw} = M_{wmu}/h_o \quad (4.4.5)$$

$$M_{wmu} = a_{t,col} \sigma_y l_w + 0.5N l_w \quad (4.4.6)$$

$a_{t,col}$ : area of steel of longitudinal reinforcement in tension column.

$\sigma_y$ : yield strength of tension reinforcement.

$l_w$ : center to center span length of RC frame.

$N$ : total axial force on RC columns on both sides of masonry infill wall.

#### 4.4.5 Type IV (Column punching and joint sliding)

Punching shear failure and sliding at the top joint of the masonry infill is considered. Lateral strength  $Q_{fw}$  is calculated by Eq. (4.4.7) by ignoring joint shear strength between masonry infill and beam.

$$Q_{fw} = Q_{pc} + rQ_{col} \quad (4.4.7)$$

i)  $Q_{pc}$  is the punching shear strength of column (left hand side column as shown in Table 4.3.1) calculated by Eq. (4.4.8) in JBDPA Seismic Retrofit Guideline.

$$Q_{pc} = K_{min} \tau_o b D \quad (4.4.8)$$

$$K_{min} = 0.34 / (0.52 + a/D) \quad (4.4.9)$$

$$\tau_o = 0.98 + 0.1f_c + 0.85\sigma \quad \text{in case } 0 \leq \sigma \leq 0.33f_c - 2.75 \quad (4.4.10)$$

$$\tau_o = 0.22f_c + 0.49\sigma \quad \text{in case } 0.33f_c - 2.75 \leq \sigma \leq 0.66f_c$$

$$\tau_o = 0.66f_c \quad \text{in case } 0.66f_c \leq \sigma$$

$$\sigma = \rho_g f_y + \sigma_0 \quad (4.4.11)$$

$$\sigma_0 = \frac{N}{bd} \quad (4.4.12)$$

$$k_{min} = \frac{0.34}{0.52 + a/D} \quad (4.4.13)$$

$K_{min}$  : influence factor considering shear span ratio

$\tau_o$  : basic shear strength of column;  $b$  and  $D$  = width and depth of column

$a$  : shear span taken as  $= D/3$

$\rho_g$  : longitudinal reinforcement ratio of column

$f_c$  : concrete compression strength

$f_y$  : yield strength of longitudinal reinforcement

$N$  : axial load on column.

ii) Lateral strength of a column  $rQ_{col}$  (right hand side column as shown in Table 4.3.1) is calculated by BSPP Seismic Evaluation Manual [4.2].

#### 4.4.6 Summary of strength evaluation

The component strength of RC frame and infill masonry is summarized in the Table 4.4.1. It is to be noted that the frame capacity evaluation needs lateral capacity of the surrounding columns ( $Q_{col}$ ) that should be evaluated as per BSPP manual as mentioned in the following Table 4.4.1.

Table 4.4.1 Summary of strength

	Confinement	$a_c/h_o$	Masonry	Frame
Type I	Good	$0.3 \leq a_c/h_o$	Eq. (4.4.3)	As per BSPP manual ( $Q_{frame}$ )
Type II	Fair	$0.2 < a_c/h_o < 0.3$	Eq. (4.4.4)	
Type III	Poor	$a_c/h_o \leq 0.2$		Eq. (4.4.5)
Type IV				$Q_{pc}$ as per Eq. (4.4.8) and $rQ_{col}$ as per BSPP manual

#### 4.4.7 Strength reduction by opening

Strength of masonry infill should be reduced using a reduction factor  $\lambda_{op}$  as shown in Eq. (4.4.14) and Eq. (4.4.15)

$$C_{inf} = \frac{\lambda_{op} \cdot Q_{inf}}{\sum W} \quad (4.4.14)$$

$$\lambda_{op} = 1 - (1.5 l_o) / l_{inf}; \quad \lambda_{op} \geq 0 \quad (4.4.15)$$

$\lambda_{op}$  : reduction factor to account for opening in masonry infill

$l_o$  : maximum width of opening measured across a horizontal plane

$l_{inf}$  : length of the masonry infill.

In addition to Eq.( 4.4.14), the opening area in the masonry infill should be less than 40% of the masonry infill area. For more details of the background of Eq. (4.4.15), refer to Appendix 4.1.

#### C.4.4 [Commentary]

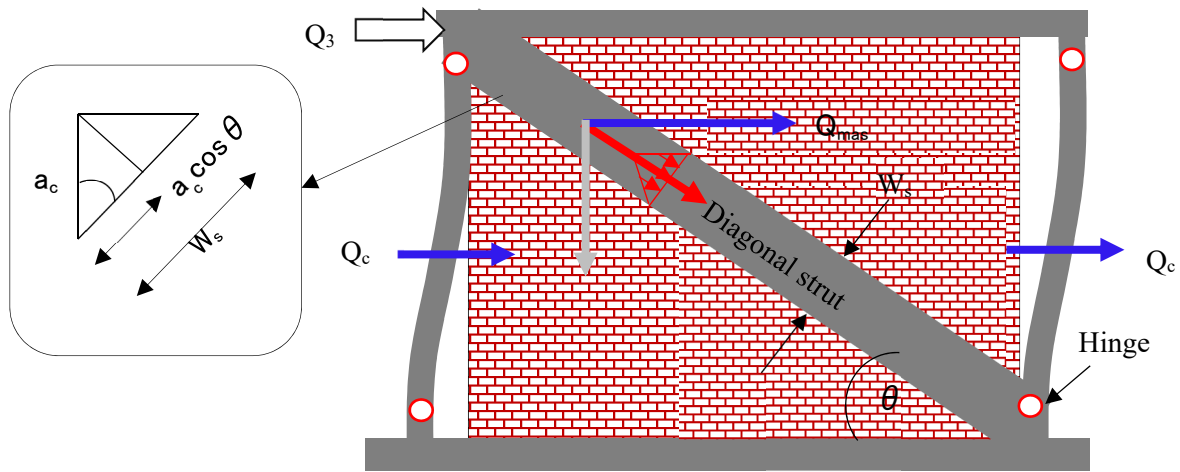
##### C.4.4.1 General

The failure modes (Type I to Type IV) mentioned in Table 4.3.1 in Sec. 4.3 are considered in this Guideline. The lateral strength of the RC frame with masonry infill is calculated according to the classified failure mode. In the case of Types I and II, the masonry infill is relatively weak or relatively similar strength or stiffness to the surrounding RC frame, and the masonry infill wall tends to fail in advance of RC frame. Then the lateral strength for RC frame and masonry infill is evaluated separately and their summation is regarded as the total lateral strength  $Q_{mw}$ .

In the case of Types III and IV, the masonry infill wall is relatively very strong and stiff which behaves as a rigid panel. Then the total lateral strength  $Q_{mw}$  is evaluated as an overall structural component.

##### C.4.4.2 Diagonal compressive strength of masonry infill walls $Q_{dia}$

Diagonal compression failure at peak strength is idealized as illustrated in Figure C.4.4.1(a) considering the formation of a diagonal strut on infill panel. The strut width depends on the relative rigidity of infill material in comparison to surrounding RC column. Under lateral loading, RC column is considered as a beam element resting on infill material, as shown in Figure C.4.4.2 (a), where infill material would act a foundation of the loaded beam element.



(a)



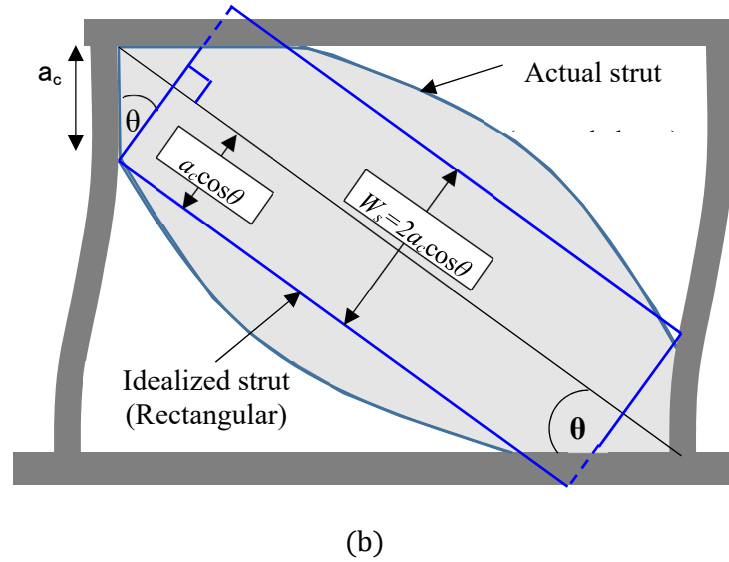


Figure C.4.4.1 (a) Idealized load transfer mechanism of diagonal compression (Type I) (Sen 2020) and (b) concept of idealized diagonal strut width

The lateral deflection ( $y$ ) and curvature ( $\phi$ ) of the RC column could be evaluated considering it is analogous to a beam on elastic foundation. According to the theory of elasticity, general solution of beam deflection ( $y$ ) resting on an elastic foundation can be expressed by Eq. C.4.4.1 [Hetneyi 1946], where, relative rigidity ( $\lambda$ ) of foundation with respect to beam has been defined as Eq. C.4.4.2.

$$y = \frac{P\lambda}{2bk_o} e^{-\lambda x} (\sin \lambda x + \cos \lambda x) \quad (C.4.4.1)$$

$$\lambda = \sqrt[4]{\frac{bk_o}{4EI}} \quad (C.4.4.2)$$

where,  $P$  = lateral load;  $b$  = foundation thickness;  $k_o$  = modulus of foundation i.e. pressure required to get unit deflection of foundation;  $E$  = Young's modulus of beam element i.e. concrete, and  $I$  = moment of inertia of beam element i.e. column.

Considering the flexural rigidity of RC column ( $EI$ ) and modulus of masonry strut following relative rigidity factor ( $\lambda_{mas}$ ) for masonry is defined here as Eq. C.4.4.3.

$$\lambda_{mas} = \sqrt[4]{\frac{(E_{mas} t_{mas}) \cos^2 \theta}{4E_c I_c d_m}} \quad (C.4.4.3)$$

where,  $E_c$ ,  $E_{mas}$ , young's modulus of concrete; masonry, ;  $t_{mas}$  = thickness of masonry;  $I_c$  = moment of inertia of RC column;  $d_m$  = diagonal length of infill panel, and  $\theta$  = inclination of loaded diagonal with horizontal.

It is evident from the column deflection shape, as shown in Figure C.4.4.2(b), that the lower portion of RC column exhibits flexure deflection whereas the deflection mode of upper part is changed from flexural shape due to presence of infill masonry, which actually causes the separation between masonry and RC frame. Based on the deflection shape, it has been considered that the infill panel of the upper part of inflection point is attached with RC frame effectively and considered as contact length ( $a_c$ ) of diagonal strut. The height of inflection point i.e. contact length ( $a_c$ ) has been evaluated from the condition of zero curvature at inflection point, as shown in Figure C.4.4.2(c), using Eq. C.4.4.4. The curvature of RC column, as shown in Figure C.4.4.2(c), has been determined from the second derivative of column deflection ( $y$ ). The diagonal strut width

( $W_s$ ) is considered in reference to Figure C.4.4.1(b). Actual masonry strut is funnel shaped, as discussed by Crisafuli (1997) using stress distribution on masonry diagonal, however the width of strut is considered constant along the diagonal length in capacity evaluation for simplicity. The strut width is considered perpendicular to the diagonal of infill masonry. The half of the strut width is determined as  $a_c \cos \theta$  considering the contact length of masonry with column. Subsequently, width of the diagonal strut ( $W_s$ ) has been calculated by using Eq. C.4.4.5, as shown in Figure C.4.4.1(b). It is to be noted that the considered strut width would overestimate strut width, shown as dotted line in Figure C.4.4.1(b), at the ends of diagonal strut. However, at center of diagonal strut it will give a conservative strut width. The simplified strut width ( $W_s$ ) can give a fair agreement with experimental results that will be discussed in section C.4.4.4.

$$a_c = \frac{\pi}{4\lambda_{mas}} \quad (C.4.4.4)$$

$$W_s = 2a_c \cos \theta \quad (C.4.4.5)$$

where,  $a_c$  = contact length of masonry infill;  $W_s$  = strut width;  $\lambda_{mas}$  = relative rigidity factor for masonry, and  $\theta$  = inclination of loaded diagonal with horizontal.

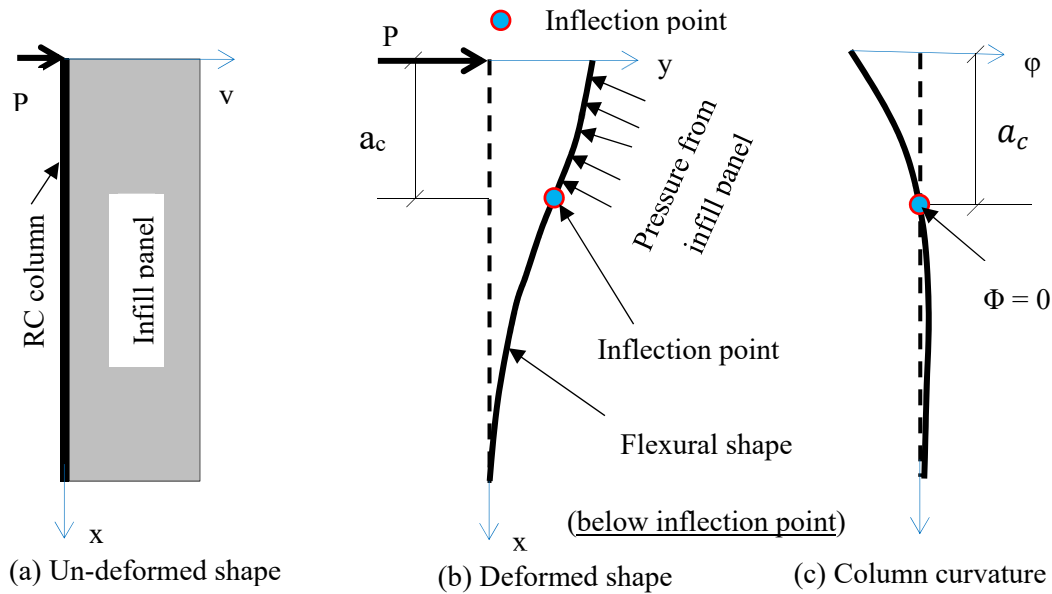


Figure C 4.4.2 Surrounding RC column (a) un-deformed shape, (b) deformed shape and (c) curvature distribution.

#### C.4.4.2 Compressive strength of masonry along diagonal ( $f_{m,\theta}$ )

In general, masonry compressive strength is measured using prism i.e. vertically stacked bricks where mortar joint is perpendicular to the vertical axis of prism. However, the masonry compressive strength in the direction of diagonal strut need to be evaluated to get the diagonal compressive strength of the strut. Several researchers investigated the variation of masonry compressive strength with orientation of mortar joint as shown in Figure C.4.4.3 and Figure C.4.4.4. The compressive strength varies between  $0.25f_m$  to  $0.75f_m$  when mortar joint orientation varies from  $22.5^\circ$  to  $67.5^\circ$  as shown in Figure C.4.4.3. Where  $f_m$  = compressive strength of vertically

stacked masonry prism having  $90^\circ$  angle of mortar joint with vertical axis. For simplicity, the compressive strength along diagonal direction ( $f_{m,\theta}$ ) has been considered as  $0.5 f_m$ , which is the average of the aforementioned range of compressive strength that would occur for  $45^\circ$  orientation.

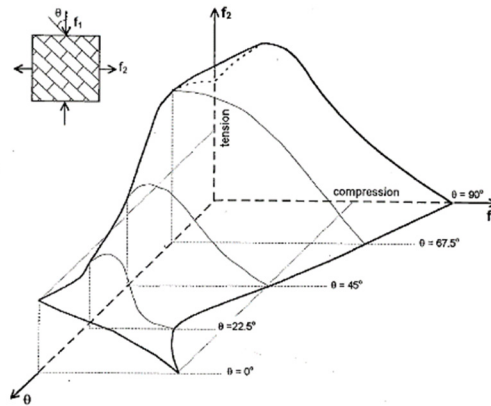


Figure C.4.4.3 Reduction in compressive strength of masonry infill due to orientation by A.W. Page (1981)

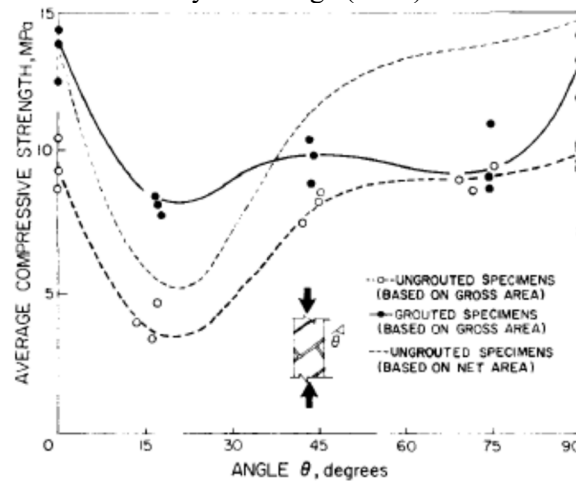


Figure C.4.4.4 Reduction in compressive strength of masonry infill due to orientation by Hamid et al (1980)

#### C.4.4.3 Sliding shear strength of masonry infill walls $Q_{sl}$

This section discusses the basic concept of Eq (4.16) for failure type II (sliding and diagonal cracking failure of masonry infill).

The sliding failure is expressed as the Mohr-Coulomb failure criteria are used as shown in Eq. (C.4.4.6).

$$Q_{sl} = \tau_o \cdot t_{inf} \cdot l_{inf} + \mu N \quad (C.4.4.6)$$

The axial load on the infill,  $N$ , is taken as the summation of gravity load and vertical component of strut force  $C_{strut}$ , as shown in Eq. (C.4.4.7).

$$N = \text{Dead load} + Q_{strut} \cdot \sin \theta \quad (C.4.4.7)$$

Dead load is taken as zero since infill was inserted after the construction of the frame and its self-weight is very small and considered insignificant.  $N$  is taken as the vertical force from compression strut formed as suggested by Paulay and Priestly (1992) and illustrated in Figure C.4.4.5.

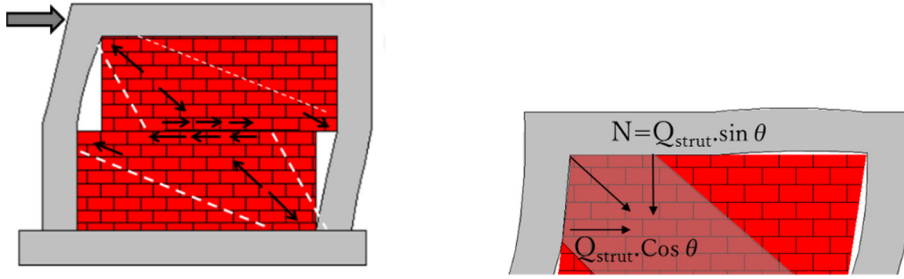


Figure C.4.4.5 Schematic drawing of sliding mechanism and axial load from strut

Substituting a vertical component of  $C_{strut}$  into Eq. (C.4.4.8), then the initial sliding shear strength is given by

$$Q_{sld} = \tau_o \cdot t_{inf} \cdot l_{inf} + \mu \cdot C_{strut} \cdot \sin \theta \quad (C.4.4.8)$$

Knowing that forces of  $Q_{sld} = C_{strut} \cdot \cos \theta$ , as shown in Figure C.4.4.7 and replacing  $Q_{sld}$  in Eq. (C.4.4.9) then,

$$C_{strut} \cdot \cos \theta = \tau_o \cdot t_{inf} \cdot l_{inf} + \mu \cdot C_{strut} \cdot \sin \theta \quad (C.4.4.9)$$

$\cos \theta$  is replaced by  $l_{inf}/d_{inf}$  and  $\sin \theta$  replaced by  $h_{inf}/d_{inf}$ , and rearranging Eq. (C.4.4.9) gives Eq. (C.4.4.10),

$$C_{strut} = \frac{\tau_o \cdot t_{inf} \cdot d_{inf}}{1 - \mu \cdot \tan \theta} \quad (C.4.4.10)$$

Calculating the lateral strength and replacing  $Q_{sld} = C_{strut} \cdot \cos \theta$  in Eq. (C.4.4.11), then:

$$Q_{sld} = \frac{\tau_o \cdot t_{inf} \cdot l_{inf}}{1 - \mu \cdot \tan \theta} \quad (C.4.4.11)$$

The initial cohesive capacity of the mortar beds,  $\tau_o$ , can be taken as a conservative value to be  $0.03f_m$  as recommended by Paulay and Priestly (1992). The friction coefficient of sliding friction,  $\mu$ , greatly varies from a code to another. NZSEE 2006 suggests  $\mu = 0.8$  in the absence of site data. The MSJC standard 2016 states  $\mu = 0.45$ . To be on the conservative side, the lower boundary of  $\mu = 0.45$  is taken in this Guideline.

$$Q_{sld} = \frac{0.03f_m \cdot t_{inf} \cdot l_{inf}}{1 - 0.45 \cdot \tan \theta} \quad (C.4.4.12)$$

For an aspect ratio of  $h_{inf}/l_{inf}$  is of 0.5 to 1.0, then  $Q_{sld}$  is equal to 0.039 to 0.10  $f_m \cdot t_{inf} \cdot l_{inf}$ .

#### C.4.4.4 Comparison between Experimental results and calculation $Q_{mw}$

Figure C.4.4.6 shows a comparison between maximum strength by experimental results as shown in Table

C.4.4.1 and strength calculated using this Guideline's method as per Eq. (4.4.2). As shown in Figure C.4.4.6, the equations proposed in this guideline gave good estimation with some conservativeness were average of experimental results to the proposed calculation method is 1.09 and standard deviation of 0.12.

Table C.4.4.1 Past research database diagonal compression failure

Researcher name	Test specimen name	$h_{inf}$ (m)	$l_{inf}$ (m)	$t_{inf}$ (mm)	Experimental load (kN)	Manual calculated ( $2Q_{col}+Q_{dia}$ )
Mehrabi et al.(1996)	6	1.42	2.13	92	207	258.98
Kakaletsis DJ et al.(2009)	S	0.80	1.20	60	82	69.38
T. Suzuki et al.(2017)	1B-1S-H	0.71	1.16	48	52	42.48
T. Suzuki et al.(2017)	1B-1S-v	0.71	1.16	48	46	42.48
Imran et al.(2009)	Model 1	1.50	1.50	100	111	92.99
Imran et al.(2009)	Model 2	1.50	1.50	100	106	100.86
Alwashali et al.(2018)	SF	1.4	2	100	582	578.19
Bose S. et al(2016)	IF-AAC	1.33	2.2	125	146	130.57
Jin et al.(2016)	IFRB	0.61	0.89	48	61	51.31
Jin et al.(2016)	IFFB	0.61	0.89	48	50	47.30

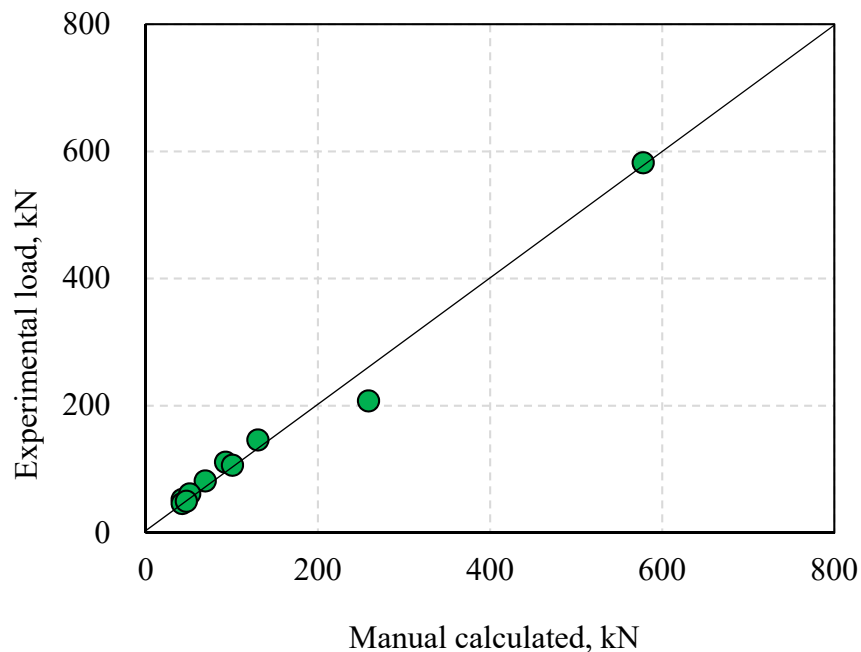


Figure C.4.4.6 Comparison between maximum lateral strength by experiment results and calculated results using this guideline

#### 4.5 Ductility index, $F$

The ductility index  $F$  for each failure mechanism is given below considering masonry infilled RC frame as a unit and considering surrounding columns are flexural columns. However, when the surrounding column is a

shear column ( $Q_{su}/Q_{mu}<1$ ), the ductility index should be considered as unity ( $F=1.0$ ), for failure type except failure type III. The overall idea is summarized in the following Table C.4.5.1.  $F$ -index for masonry infill with openings is recommended to be taken as the lower boundary of  $F=1$ .

Table 4.5.1 Ductility Index corresponding to Failure Mechanism

Failure mechanism	Contact length ratio, $a_c/h_o$	F-index
Diagonal compression (Type I)	$a_c/h_o \geq 0.3$	1.75
Sliding-diagonal cracking (Type II)	$0.2 < a_c/h_o < 0.3$	1.27
Overall flexural (Type III)	$a_c/h_o \leq 0.2$	1.75
Column punching-joint sliding (Type IV)	$a_c/h_o \leq 0.2$	1.00

## C.4.5 [Commentary]

### C.4.5.1 Relationship between Ductility Index and Contact Length Ratio

The  $F$ -index is taken based on experimental observation for each failure mode as shown in Figure C 4.5.1. The lower bound of  $F$ -index of diagonal compression failure as well as overall flexural failure is considered as 1.75, which indicates relatively ductile behaviour. On the other hand, the lower bound of  $F$ -index of diagonal cracking-sliding is considered as 1.27. In case of column punching-joint sliding failure, the  $F$ -index is considered to be a unity ( $F=1$ ), since the failure is governed by shear and the lower bound of  $F$ -index is below 1.27. Idealized C-F relationship of each failure mechanism is shown in Table C 4.5.1.

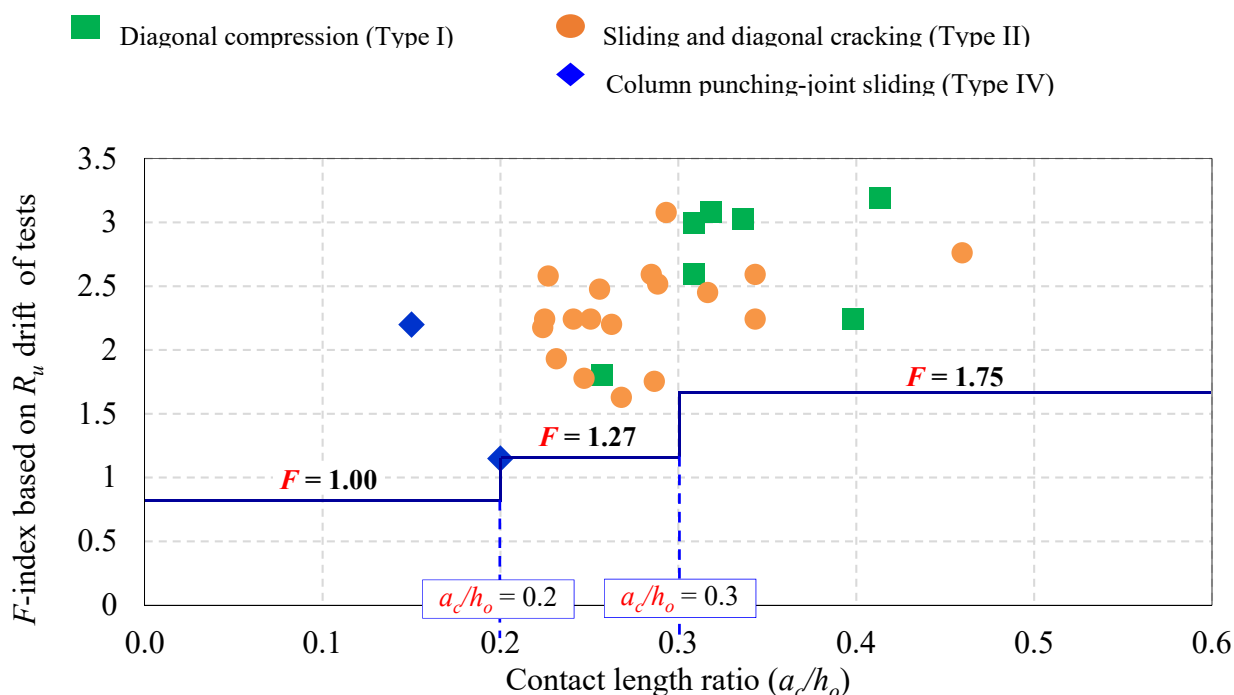
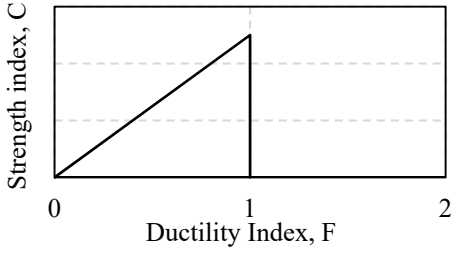
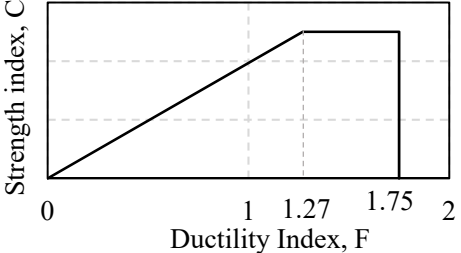
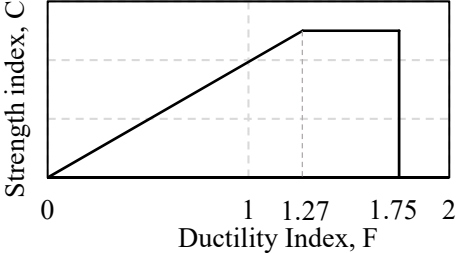
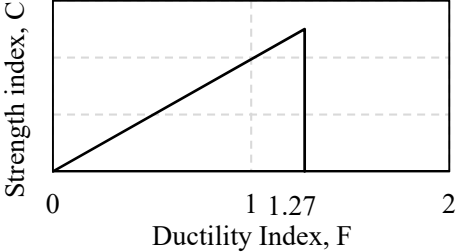
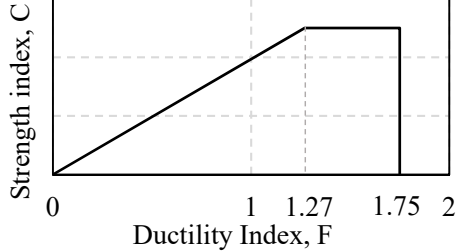
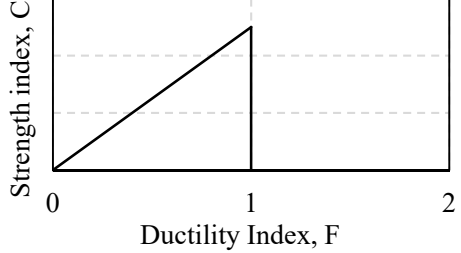


Table C.4.5.1 Idealized C-F relationship of Masonry infilled RC frame

Column type	Failure mode	Idealized C and F relationship
Shear column	Diagonal compression (Type I), Diagonal cracking-sliding (Type II), and Column punching-joint sliding (Type IV)	
	Overall flexural (Type III)	
Flexural column	Diagonal compression (Type I)	
	Sliding-Diagonal cracking (Type II)	
	Overall flexural (Type III)	
	Column punching-joint sliding (Type IV)	

## 4.6 Stiffness evaluation

Stiffness evaluation is required to evaluate the eccentricity due to presence of masonry infill. Therefore, the stiffness evaluation is discussed in this section. The stiffness of the RC frame with masonry infill can be approximated by a simplified method as shown below:

Herein,  $K_{ini}$  is the initial stiffness obtained from the summation of the initial stiffness by RC frame ( $K_{frame}$ ) and the masonry infill ( $K_{strut}$ ) as shown in Eq. (4.6.1).

$$K_{ini} = K_{strut} + K_{frame} \quad (4.6.1)$$

$$K_{strut} = \frac{E_{inf} \cdot W_{inf} \cdot t_{inf} \cdot \cos^2 \theta}{d_{inf}} \quad (4.6.2)$$

$$K_{frame} = \left( \frac{24E_c I_c}{h_c^3} \cdot \frac{12\rho + 1}{12\rho + 4} \right) \quad (4.6.3)$$

$$\rho = \frac{\sum E_c I_b / l_b}{\sum E_c I_c / h_c} \quad (4.6.4)$$

$E_{inf}$ : Young's modulus of masonry infill

$E_c$ : Young's modulus of RC frame

$d_{inf}$ : Diagonal length of masonry infill

$W_{inf}$ : Strut width taken as  $0.2d_{inf}$

$\theta$ : Inclination angle of the diagonal of masonry infill

$I_b$  and  $I_c$ : Second moment of inertia of beam and column respectively.

$l_b$ : Length of RC beam (span length considering center to center of columns)

$h_c$ : Height of RC column

### C.4.6.1 [Commentary]

Herein,  $K_{ini}$  is the initial stiffness obtained from the summation of the initial stiffness by RC frame ( $K_{frame}$ ) and the masonry infill ( $K_{strut}$ ).  $K_{strut}$  is calculated using the axial stiffness of the equivalent diagonal strut. The initial stiffness of the RC frame,  $K_{frame}$ , is calculated by theoretical equations by Chopra (2007) for elastic stiffness of the bare frame, as shown in Eq. (4.6.2) and Eq. (4.6.3).  $I_c$  and  $I_b$  are the moments of inertia of RC column and beam, respectively.

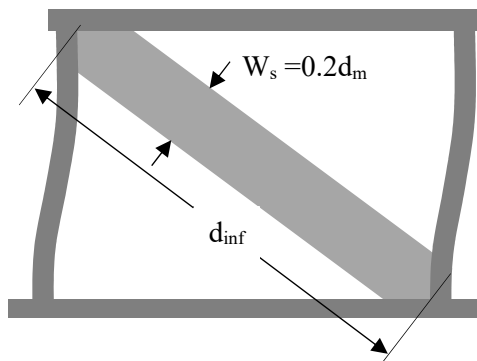


Figure C.4.6.1 Idealization of masonry infilled RC frame as braced RC frame



#### C.4.6.2 Strut width for initial stiffness (Alwashali (2018))

The strut width of masonry infill, based on the experimental study at initial stiffness, ranged between  $0.15d_{inf}$  and  $0.3d_{inf}$  with an average of  $0.2d_{inf}$  (Alwashali (2018)). There was no clear relationship between strut width and the ratio of stiffness of frame to masonry. Paulay and Priestly's method of estimating strut width to be around  $0.25 d_{inf}$  gave relatively good results. However, their proposed strut width tends in several cases to overestimate the initial stiffness. Thus, based on test results, it was found that making a simple assumption of the strut width  $W_{inf}$  to be  $0.2d_{inf}$  ( $d_{inf}$ : diagonal length), which is a slightly modified assumption from Paulay and Priestly (1992), gives a relatively better and conservative estimate for the initial stiffness as shown in Table C.4.6.1. This estimation also showed reasonable agreement with other test data.

Table C.4.6.1 Comparison between experimental initial stiffness and the proposed method

	Experimental stiffness <i>Masonry Infilled RC Frame</i>	Proposed $W_{inf} = 0.2d_{inf}$ <i>Masonry Infilled RC frame Eq. 4.6.1</i>	
Specimen (Alwashali 2018)	Initial stiffness (kN/mm)	Infilled frame (kN/mm)	Ratio
F-0.4	128	126	1.02
F-0.6	145	159	0.91
F-1.5	166	194	0.86
WB	131	152	0.86
WM	128	93	1.38
<b>Average</b>			<b>0.94</b>
<b>Standard deviation</b>			<b>0.19</b>

## 4.7 Application examples

### 4.7.1 Overview of the building

An example of seismic evaluation with masonry infill is described in the following section. A three-storied residential building is selected. Figure 4.7.1 shows the floor plan with the location of the column and masonry infill. The total floor area of the investigated buildings is about  $324.5 \text{ m}^2$ . The sectional properties of column and masonry infill are shown in Table 4.7.1 and Table 4.7.2 respectively.

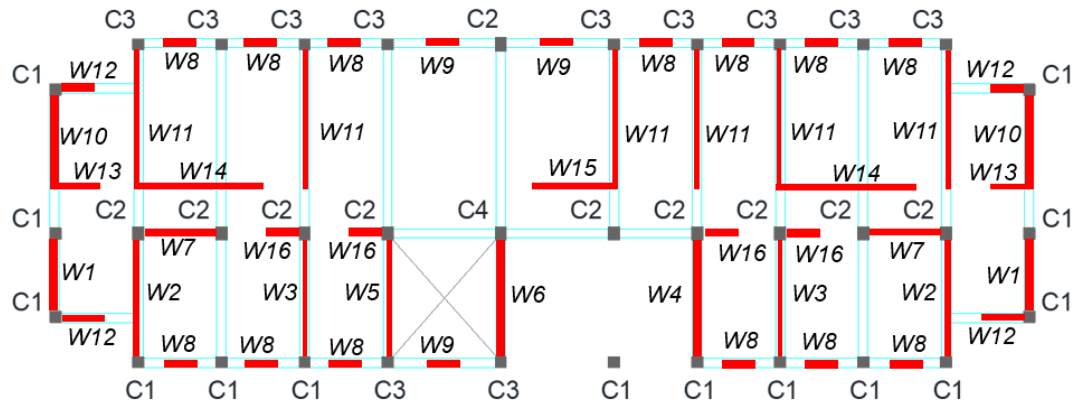


Figure 4.7.1 Architectural plan (dimensions are in mm)

Table 4.7.1 Column dimension

Legend for column	Dimension(mm)
Column (C1,C3)	300×300
Column (C2,C4)	300×375

Table 4.7.2 masonry infill-wall properties

Wall ID	Number	Length (mm)	Thickness (mm)	Surrounding frame	Opening area %	Opening or Solid	Structural wall (yes/no)
W1	2	2750	250	Yes	0%	Solid	Yes
W2	2	3875	125	Yes	0%	Solid	Yes
W3	2	3875	125	Yes	0%	Solid	Yes
W4	1	3875	250	Yes	0%	Solid	Yes
W5	1	3875	125	Yes	0%	Solid	Yes
W6	1	3875	250	Yes	0%	Solid	Yes
W7	2	2400	125	Yes	0%	Solid	Yes
W8	13	2400	250	Yes	>40%	Opening	No
W9	3	3875	250	Yes	>40%	Opening	No
W10	2	2750	250	Yes	>40%	Opening	No
W11	6	4750	125	Yes	>40%	Opening	No
W12	4	2750	250	No	-	Opening	No
W13	2	2750	125	No	-	Opening	No
W14	2	2750	125	No	-	Opening	No
W15	1	2350	125	No	-	Opening	No
W16	4	2750	125	Yes	>40%	Opening	No

#### 4.7.2 Material properties

Both destructive and non-destructive tests are carried out to determine the material properties. The detailed procedure is described in the BSPP manual. The material properties are shown in Table 4.7.3.

Table 4.7.3 Material properties

Material properties	Material strength (MPa)
Concrete strength, $f_c$	17
Yield strength of reinforcement, $f_y$	276
Young's modulus concrete, $E_c$	19378
Young's modulus of masonry, $E_{inf}$	$550 f_m$
Prism strength, $f_m$	8
* Young's modulus of concrete: $4700\sqrt{f_c}$ (unit: MPa) according to ACI318-14	

#### 4.7.3 Evaluation procedures

Evaluation procedures are shown as follows:

##### **Step 1: Classification to structural wall and non-structural wall**

- In the example building, there are two types of masonry infill: solid wall and wall with opening due to window, door, and high window.
- Masonry infill is surrounded and confined by RC frame from all sides.
- A wall with an opening having greater than 40% opening area and that having double openings. These walls are not considered a structural wall.
- The slenderness ratio  $H/t$  of infill wall is 12, which is less than 30.
- Solid brick is used in masonry infill.
- There are no cracks and gaps between frame and masonry infill based on visual inspection according to Chapter 2 of the BSPP seismic evaluation manual.

##### **Step 2: Failure mode identification**

The failure mode is identified based on  $a_o/h_o$  ratio described in Section 4.3.

The calculation procedure of one wall is shown below:

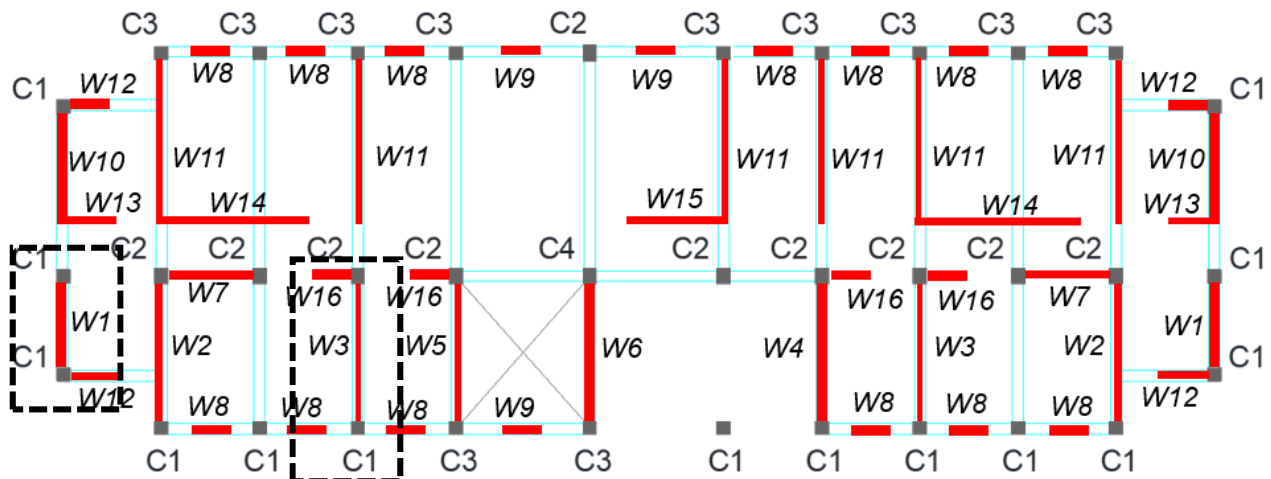


Figure 4.7.2 Location of masonry infill

### Case I: Evaluation of masonry infill wall, W1

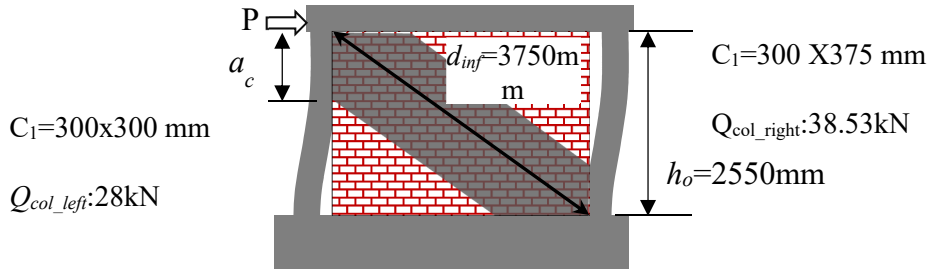


Figure 4.7.3 Masonry Infilled RC Frame  $W_1$

$a_c/h_o$  is calculated using the following procedure:

$(a_c/h_o)$  is calculated through Eqs. (4.3.1) to (4.3.2).

$$\frac{a_c}{h_o} = \frac{\pi}{4\lambda h_o}$$

$$\lambda = \sqrt[4]{\frac{E_{inf} t_{inf} \cos^2 \theta}{4E_c I_c d_{inf}}}$$

where,  $E_{inf}=550 \times 8 = 4400$  MPa

$E_c = 19378$  MPa

Clear height,  $h_o = (3000 - 450)$  mm = 2550 mm

Moment of inertia of RC column,  $I_c = (300 \times 300^3)/12 = 675 \times 10^6$  mm<sup>4</sup>

Note: In case of different column size, the minimum moment of inertia should be considered.

The diagonal length of infill,  $d_{inf} = 3750$  mm

The inclination angle of diagonal from the horizontal axis,  $\theta$  (rad) = 0.75

The contact length ratio:

$$\frac{a_c}{h_o} = 0.23$$

Based on the condition, the failure mode is classified according to  $a_c/h_o$  as follows.

$0.2 < a_c/h_o < 0.3$ , Fair confinement: Type II

### Step3: Strength index ( $C_{mw}$ )

Strength index  $C_{mw}$  for an RC frame with masonry infill is calculated by Eq. (4.4.1).

$$C_{mw} = \frac{Q_{mw}}{\sum W}$$

Where  $\sum W$  is the weight of the building including live load supported by the story concerned.

Since failure mode is Type II, (sliding and diagonal cracking)

the  $Q_{mw}$  is calculated using the following Eq. (4.4.2).

$$Q_{mw} = Q_{frame} + Q_{slid}$$

Where,  $Q_{frame}=28+38.53=66.53$  kN

$Q_{sld}$  will be in the following Eq. (4.4.4)

$$Q_{sld} = \frac{\tau_{inf} \cdot t_{inf} \cdot l_{inf}}{1 - \mu \cdot \frac{h_{inf}}{l_{inf}}}$$

Where  $h_{inf}/l_{inf}$ :  $2550/2750=0.93$

Friction coefficient,  $\mu$ : 0.45 according to ASTM C1531

Prism strength,  $f_m$ : 8 Mpa

Shear strength of infill,  $\tau_{inf}$ :  $0.03 \cdot 8 = 0.24$  MPa

$$Q_{sld} = 0.03 \cdot 8 \cdot 250 \cdot 2750 / (1 - 0.45 \cdot 2550/2750) = 284 \text{ kN}$$

$$\text{Lateral strength, } Q_{mw} = Q_{frame} + Q_{inf} = 66.53 + 284 = 351 \text{ kN}$$

Total building weight,  $W = n \cdot A_f \cdot w$

$n$ =Number of stories=3

$A_f$ =Floor area=324.5 m<sup>2</sup>

$w$ =Floor unit weight=11.20 kN/m<sup>2</sup>

Now total weight,  $W = 3 \cdot 324.5 \cdot 11.20 = 10904$  kN

Strength index,

$$C_{mw} = \frac{Q_{mw}}{\sum W}$$

$$C_{mw} = 351/10904 = 0.032$$

#### **Step4: Ductility index, $F$**

Ductility index is considered based on failure mode,

Failure type: II (Sliding and diagonal cracking failure)

**Ductility index:  $F = 1.27$  ( $0.20 < a_o/h_o \leq 0.3$ )**

#### **Case 2 Evaluation of masonry infill wall, W3:**

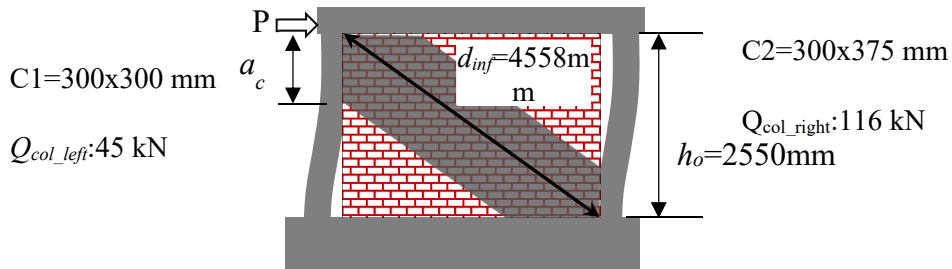


Figure 4.7.4 Masonry Infilled RC Frame W3

$a_c/h_o$  is calculated using the following procedure:

$(a_c/h_o)$  is calculated through Eqs. (4.3.1) to (4.3.2).

$$\frac{a_c}{h_o} = \frac{\pi}{4\lambda h_o}$$

$$\lambda = \sqrt[4]{\frac{(E_{inf} t_{inf} \cos^2 \theta)}{4 E_c I_c d_{inf}}}$$

where,  $E_{inf} = 550 \times 8 = 4400$  MPa

$E_c = 19500$  MPa

Clear height,  $h_o = (3000 - 450) = 2550$  mm

Moment of inertia of RC column C1,  $I_c = (300 \times 300^3) / 12 = 675 \times 10^6$  mm<sup>4</sup>

Moment of inertia of RC column C2,  $I_c = (300 \times 375^3) / 12 = 1318 \times 10^6$  mm<sup>4</sup>

[Note: In case of different column size, the minimum moment of inertia should be considered]

moment of inertia considered,  $I_c = 675 \times 10^6$  mm<sup>4</sup>

The diagonal length of infill,  $d_{inf} = 4558$  mm

The inclination angle of diagonal from the horizontal axis,  $\theta$  (rad) = 0.85

The contact length ratio:

$$\frac{a_c}{h_o} = 0.29$$

Based on the condition, the failure mode is classified according to  $a_c/h_o$  as follows.

$0.2 < a_c/h_o < 0.3$ , Fair confinement: Type II

### **Step3: Strength index ( $C_{mw}$ )**

Strength index  $C_{mw}$  for an RC frame with masonry infill is calculated by Eq. (4.4.1) .

$$C_{mw} = \frac{Q_{mw}}{\Sigma W}$$

Where  $\Sigma W$  is the weight of the building including live load supported by the story concerned.

Since failure mode is II, (sliding and diagonal cracking)

the  $Q_{mw}$  is calculated using the following Eq. (4.4.2).

$$Q_{mw} = Q_{frame} + Q_{sld}$$

Where,  $Q_{frame} = 45 + 116 = 161$  kN

$Q_{sld}$  will be in the following Eq. (4.4.4)

$$Q_{sld} = \frac{\tau_{inf} \cdot t_{inf} \cdot l_{inf}}{1 - \mu \cdot \frac{h_{inf}}{l_{inf}}}$$

Where  $h_{inf} / l_{inf}$ :  $2550 / 3850 = 0.65$

Friction coefficient,  $\mu$  : 0.45 according to ASTM C1531

Prism strength,  $f_m$ : 8 Mpa

Shear strength of infill,  $\tau_{inf}$  :  $0.03 \times 8 = 0.24$  MPa

$Q_{sld} = 0.03 \times 8 \times 125 \times 3850 / (1 - 0.45 \times 2550 / 3850) = 284$  kN

Lateral strength,  $Q_{mw} = Q_{frame} + Q_{sld} = 161 + 164 = 325$  kN

Total building weight,  $W = n \cdot A_f \cdot w$

$n$ =Number of stories=3

$A_f$ =Floor area=324.5 m<sup>2</sup>

$w$ =Floor unit weight=11.20 kN/m<sup>2</sup>

Now total weight,  $W=3*324.5*11.20=10904$  kN

Strength index,

$$C_{mw} = \frac{Q_{mw}}{\sum W}$$

$$C_{mw} = 325/10904 = 0.029$$

#### **Step4: Ductility index, $F$**

Ductility index is considered based on failure mode,

Failure type: II (Sliding and diagonal cracking failure)

**Ductility index:  $F = 1.27$  ( $0.20 < a_o/h_o \leq 0.3$ )**

#### **4.7.4 Summary**

Based on this analysis,

Infill wall  $W_1$  :

The failure mode is considered Type II (Sliding and diagonal cracking failure mode). Strength index,  $C_{mw}$ , is 0.032 and Ductility index,  $F$ , is 1.27, respectively.

Infill wall  $W_3$ :

The failure mode is considered Type II (Sliding and diagonal cracking failure mode). Strength index,  $C_{mw}$ , is 0.029 and Ductility index,  $F$ , is 1.27, respectively.

## Appendix

The commentary section will discuss the background of the proposed method and justification based on past experiments carried under the SATREPS-TSUIB project as well as other references.

### Appendix 4.1 Influence of openings in masonry infill

Masonry infill in RC frame is used as partition walls and thought to be a non-structural element and therefore the presence of openings such as doors and windows is not an exceptional case but it is actually the norm case. Openings in masonry infill are the most significant parameter affecting the strength and seismic capacity. Although the strength of infills with openings could be assessed using strut and tie models as suggested in FEMA 306 (1998), such methods are non-practical since it needs significant knowledge, experiments, and experience to be applied. Therefore, several researchers have proposed simplified method to assess the reduction of strength due to openings.

In this appendix, an outline of several proposed methods to assess opening influence is overviewed and compared to experimental results to check their applicability.

#### C.4.1 (i) Method by Dawe and Seah (1998) and NZSEE (2006)

Based on the work of Dawe and Seah (1998), the New Zealand Society for Earthquake Engineering (NZSEE) (2006) recommended a simplified reduction factor to strength by factor named as  $\lambda_{op}$  as shown in Eq. (C.4.1.1)

$$\lambda_{op} = 1 - \frac{1.5L_o}{L_{inf}}; \quad \lambda_{op} \geq 0 \quad (C.4.1.1)$$

Where  $L_o$  is the maximum width of opening measured across a horizontal plane. It should be noted the Eq. (C.4.1.1) implies that if the opening is greater than two-thirds of the span width, then the infill does not influence the system. In addition, Eq. (C.4.1.1) calculates the reduction factor by the opening width and does not consider the effect of opening height.

#### C.4.1 (ii) Method by FEMA 306 (1998) and ASCE 41/SEE

In both standards (FEMA 306 (1998) and ASCE 41/SEE) there is no simplified method is proposed to assess the influence of openings. However, Strut and Tie models are recommended for calculations, but there are not any provisions or details on how to consider it. Assumptions to consider the Strut and Tie models can vary greatly among engineers or researcher which can cause large variations in results.

#### C.4.1 (iii) Method by Al-Chaar (2003)

Al-Chaar (2003) conducted a large scale experiment and proposed empirical equation for an opening reduction factor to ultimate strength. This is based on the ratio of area of opening to area of masonry infill as in Eq. (C.4.1.2)

$$\lambda_{op} = 0.6 \left( \frac{A_o}{A_p} \right)^2 - 1.6 \left( \frac{A_o}{A_p} \right) + 1 \quad (C.4.1.2)$$

Where  $A_o$  and  $A_p$  are the area of opening and area of masonry infill, respectively.



#### C.4.1 (iv) Method by Tasnimi et al. (2011)

Tasnimi et al. (2011) had experimental results on large-scale steel frames with clay brick masonry infills having openings. They proposed a reduction factor  $\lambda_{op}$  as in Eq. (C.4.1.3) which has a similar concept to the aforementioned Eq. (C.4.1.2) proposed by Al-Chaar (2003).

$$\lambda_{op} = 1.49 \left( \frac{A_o}{A_p} \right)^2 - 2.238 \left( \frac{A_o}{A_p} \right) + 1 \quad (C.4.1.3)$$

#### C.4.1 (v) Comparison of existing methods with past experimental results

Several researchers have done experiments of steel frames having masonry infill with openings. However, only a few researchers have done experiments of RC frames having masonry infill with openings. In a study by Alwashali et al. 2018, a comparative study of 15 specimens consisted of a single span and single story of RC frame with masonry infill having single openings of different sizes and positions was presented. The reduction of strength is calculated based on the ratio of the maximum lateral load of RC frame with masonry infill with an opening to the maximum lateral load of RC frame with solid infill (no opening) which was tested in advance. Figure C.4.1.1 shows the comparison of experimental reduction factor  $\lambda_{op}$  with analytical reduction factor  $\lambda_{op}$  calculated according to Eq. (C.4.1.1) which is proposed by Dawe and Seah (1998), Eq. (C.4.1.2) which is proposed by AlChaar (2003) and Eq. (C.4.1.3) which is proposed by Tasnimi et al (2011).

Dawe and Seah (1998) which is also recommended by (NZSEE) (2006) showed more conservative results which were also proposed in this guideline. The method by AlChaar (2003) as well as Tasnimi et al (2013) showed a good correlation with experimental results but might overestimate the strength as shown by one case in Figure C.4.1.1.

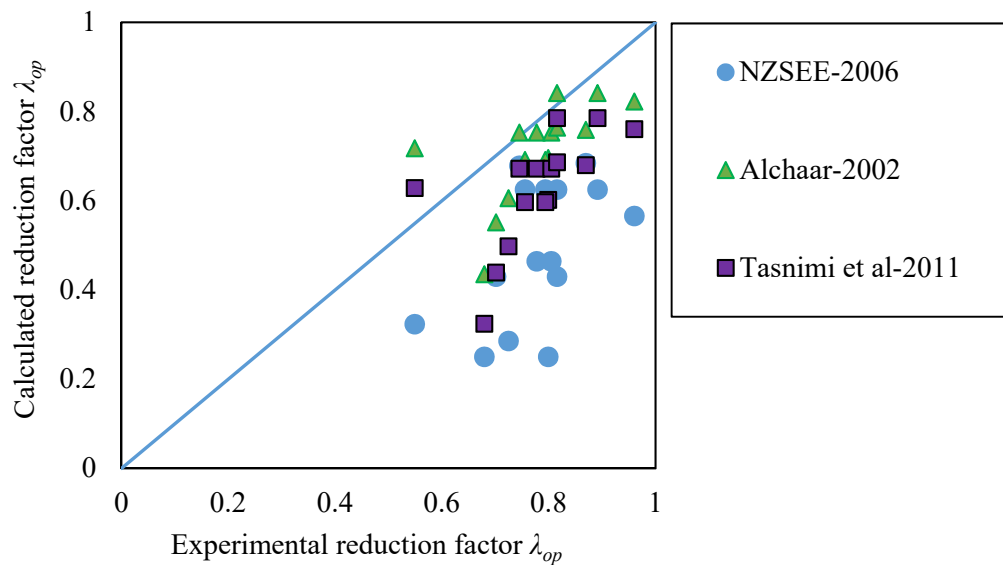


Figure C.4.1.1 Comparison between different methods proposed to calculate the reduction of strength due to openings

It should be noted that this guideline as well as previous studies mentioned above, mainly focused on masonry walls with a single opening. Thus, multiple or several openings is considered out of the scope since it needs

further verification.

#### Appendix 4.2 Out-of-plane capacity

For out-of-plane capacity, this guideline refers to research data by other researchers and several standards. Even though this research focuses on in-plane seismic capacity, out-of-plane behavior is an indispensable subject from the point of view of the seismic evaluation of masonry infilled buildings. Masonry infills might fail in out-of-plane even before it reaches its maximum in-plane seismic capacity. Therefore, to propose a seismic evaluation method for masonry infill which is the final objective of this research, the out-of-plane capacity should also be assessed. The out-of-plane failure of masonry infill is not a crucial failure mode when compared to masonry buildings with no boundary element (RC or steel columns and beams). This is because masonry infill shows relatively a significant increase in strength and displacement capacity to resist out-of-plane failure if compared to masonry buildings with no surrounding frames. Researchers such as Dawe and Seah (1989) and Abrams et al. (1996) indicated that this increase is due to the arching mechanism is shown in Figure 4.2.1.

Studying the out-of-plane capacity is a very essential topic but could not be fully studied experimentally in this study because of time limitations. Therefore, in this section, an overview of out-of-plane assessment methods is reviewed based on the existing literature. Finally, methods to assess out-of-plane capacity are then recommended for the seismic evaluation based on its accuracy, simplicity, and applicability.

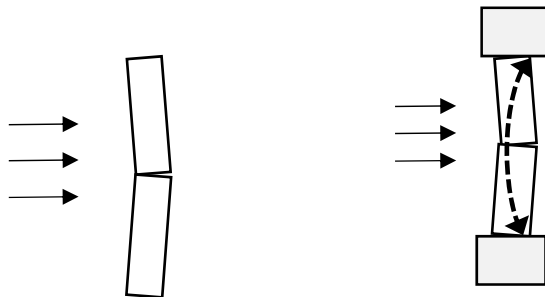


Figure 4.2.1 Out-of-plane failure considering the arching mechanism

##### C.4.2(i) Method by J. L. Dawe and C. K. Seah(1989)

This is one of the most-cited methods when it comes to the out-of-plane capacity of masonry infill since it is based on both experimental and theoretical backgrounds. In their research, they tested nine full-scale concrete masonry infills (3.6m by 2.8m) under uniformly distributed lateral pressure applied incrementally. They also tested masonry infills with openings and having different surface contact conditions with the frame. Figure C.4.2.1 shows theoretical load versus deformation curves of four masonry infills with different boundary conditions. Case 1 represents masonry infills supported at the top and bottom. Case 2 is a masonry infill supported from three sides and free at the top. Therefore, Case 1 and Case 2 allow the arching mechanism to develop only in one direction and the ultimate loads would be lower. Case 3 shows masonry infills with different interface conditions that allow arching action to develop in the vertical span. Based on their results, the masonry infill well attached with all four sides by a frame, as shown by Case 4 of Figure C.4.2.1, results

in a great increase in the ultimate load. Their research investigated showed that boundary conditions are an important parameter in estimating the out-of-plane capacity.

Based on their parametric study and experimental results, they proposed empirical expressions for evaluation of the ultimate out-of-plane load for masonry infills supported on three sides in Eq. (C.4.2.1) and masonry infills supported on four sides in Eq. (C.4.2.2):

$$q_u = 800 \cdot (f_m)^{0.75} t^2 \cdot \alpha / l^{2.5} \quad (\text{C.4.2.1})$$

$$q_u = 800 \cdot (f_m)^{0.75} t^2 \cdot (\alpha / l^{2.5} + \beta / h^{2.5}) \quad (\text{C.4.2.2})$$

$$\alpha = \frac{1}{h} (E \cdot I_c \cdot h^2 + G \cdot J_c \cdot t \cdot h)^{0.25} \leq 50 \quad (\text{C.4.2.3})$$

$$\beta = \frac{1}{l} (E \cdot I_b \cdot l^2 + G \cdot J_b \cdot t \cdot l)^{0.25} \leq 50 \quad (\text{C.4.2.4})$$

Where, the ultimate out-of-plane load  $q_u$  and units in (kPa).  $l$  and  $h$  are the masonry infill length and height and units in (mm).  $I_c$  and  $I_b$  are the moments of inertia of beams and columns.  $E$  and  $G$  are Young's modulus and shear modulus of the frame.  $J_c$  and  $J_b$  are the torsional constants of columns and beams. The out-of-plane capacity depends on the frame stiffness by the coefficients  $\alpha$  and  $\beta$  representing the stiffness of boundary elements, which is based on the results of a parametric study by comparison with an infinitely stiff infilled frame.

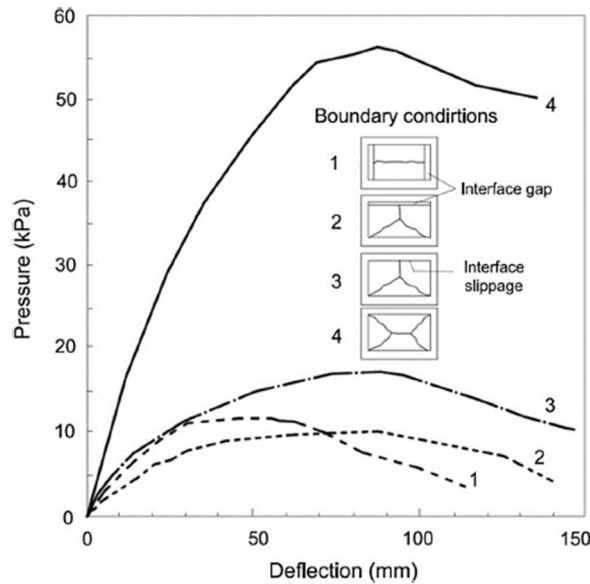


Figure C.4.2.1 Relationship between boundary conditions and the out-of-plane capacity by Dawe and Seah (1989)

#### C.4.2 (ii) Method by Abrams DP, Angel R and Uzarski J. (1996)

They proposed a simple procedure for estimating out-of-plane strength based on an experimental study and an analytical model of the arching theory. Their experimental tests were of eight full-scale RC frames infilled with two types of masonry (concrete blocks and brick masonry).

The interesting new point about their research is that they proposed equations to address the influence of prior in-plane loading effect on out-of-plane strength. Their method depends mainly on two coefficients: coefficient

$R_1$  represents the effect of prior in-plane loading on the out-of-plane strength and  $R_2$  represents the effect of frame rigidity. Here, the method proposed by Abrams et al. (1996) is shown in Eq. (C.4.2.5) which adopted the main concept of theory and equations previously proposed by Dawe and Seah (1989) shown previously and proposed additional reduction factors,  $R_2$ , shown in Eq. (C.4.2.7). The  $\lambda$  is a coefficient mainly dependent on the slenderness ratio and its values are shown in Table C.4.2.1

$$q_u = 2 \cdot \frac{f_m}{\left(\frac{h}{t}\right)} R_1 \cdot R_2 \cdot \lambda \quad (\text{C.4.2.5})$$

$$R_1 = \left[ 1.08 - 0.015 \left(\frac{h}{t}\right) - 0.00049 \left(\frac{h}{t}\right)^2 + 0.000013 \left(\frac{h}{t}\right)^3 \right] \frac{\Delta}{2\Delta_{cracked}} \quad (\text{C.4.2.6})$$

$$R_2 = 0.357 + 7.14 \times 10^{-8} EI \quad (\text{C.4.2.7})$$

Where  $\Delta$  is the maximum in-plane inter-story drift experienced by the infilled frame,  $\Delta_{cracked}$  is the cracking drift and  $EI$  is Young's modulus and moment of inertia of the smallest member of the surrounding frame.

The method of Abrams et al. was also recommended by FEMA 306 (1998) with minor conservative modifications.

#### C.4.2(iii) Method by ASCE/SEI 41-06 (2007)

The ASCE 41 as well as its previous version FEMA 356 (2000) added a condition that if arching actions are to be considered, the lower-bound strength should be taken as recommended by Abrams et al. (1996) as shown in Eq. (C.4.2.8).

$$q_u = 0.7 \frac{f_m \cdot \lambda}{\left(\frac{h}{t}\right)} \times 144 \quad (\text{C.4.2.8})$$

Where  $\lambda$  is the same as in Table C.4.2.1 for Abram's method. The value 144 is a conversion value to give results in the units of lb/ft<sup>2</sup>. In Eq. (C.4.2.5), the  $R_1$  and  $R_2$  shown previously are replaced by a factor 0.7 which is considered the lower bound strength recommended by Abrams et al. (1996) assuming a flexible beam and some prior in-plane damage.

Table C.4.2.1 A factor based on aspect ratio by Abram et al. (1996)

$h/t$	$\lambda$
5	0.129
10	0.06
15	0.034
20	0.021
25	0.013
30	0.008
35	0.005

#### C.4.2(iv) Method by The New Zealand Guidelines for Seismic Assessment of Existing Buildings (2017)

The New Zealand guidelines adopted the modified versions based on equations of Dawe and Seah (1989) as shown previously in Eq. (C.4.2.2) but with the addition of a factor to account for the reduction of capacity due to prior damage as shown below.

$$q_u = 730 \gamma \cdot (f_m)^{0.75} t_{\text{inf}}^2 \cdot (\alpha / l_{\text{inf}}^{2.5} + \beta / h_{\text{inf}}^{2.5}) \quad (\text{C.4.2.9})$$

$$\gamma = 1.1 \left( 1 - \frac{h_{\text{inf}}}{55 \cdot t_{\text{inf}}} \right) \leq 1.0 \quad (\text{C.4.2.10})$$

$$\alpha = \frac{1}{h_{\text{inf}}} (E_c I_c h_{\text{inf}}^2)^{0.25} \leq 50 \quad (\text{C.4.2.11})$$

$$\beta = \frac{1}{l_{\text{inf}}} (E_b I_b l_{\text{inf}}^2)^{0.25} \leq 50 \quad (\text{C.4.2.12})$$

$q_u$ : probable uniformly distributed out-of-plane lateral load capacity (kPa)

$\gamma$ : horizontal arching coefficient

$\beta$ : vertical arching coefficient

$h_{\text{inf}}$ : clear height of masonry infill (mm)

$l_{\text{inf}}$ : length of masonry infill (mm)

$t_{\text{inf}}$ : thickness of masonry infill (mm)

$\alpha$ : in-plane cracking capacity reduction coefficient

In case of the presence of side gaps greater the  $0.02t_{\text{inf}}$ , the coefficient  $\alpha$  should be taken as zero. When a top gap greater than  $0.02t$  is present,  $\beta$  should be taken as zero.

Where  $\gamma$  is the in-plane cracking reduction coefficient. The other coefficients represent the same as Dawe and Seah (1989). The reduction capacity coefficient,  $\gamma$ , to account for the reduction in out-of-plane strength due to prior in-plane cracking is derived by experimental tests by Angel et al. (1994). The NZ Guidelines (2017) also recommended that in case of the presence of side gaps greater the  $0.02t$ , the coefficient  $\alpha$  should be taken as zero. When a top gap greater than  $0.02t$  is present,  $\beta$  should be taken as zero.

#### C.4.2(v) Investigation and comparison of methods of out of plane strength

Flanagan and Bennett (1999) examined 36 experiments to test which method is more applicable. Based on their comparison, the average ratio of experimental to analytical capacities is 1.07 for Dawe and Seah's (1989) method with a coefficient of variations of 42% and the average ratio of experimental to analytical for Abrams et al.'s (1996) is 1.19 with a coefficient of variations of 58%.

In their comparison results, Dawe and Seah's (1989) method provides the best prediction of the out-of-plane capacity of masonry infill.

However, as mentioned earlier the Dawe and Seah's method does not account for prior damage reduction capacity. NZ Guidelines (2017) also adopted Dawe and Seah's method with the additional coefficient to

account for prior damage, which seems to be a logical method to account for out-of-plane capacity with prior damage in the meantime.

In addition, Dawe and Seah's (1989) method gives a ratio of experimental to analytical of 1.07 which might be considered not conservative enough. The NZ method (2017) therefore made a slight reduction of the constant value of 800 in Eq. (C.4.2.2) to a constant value of 730 as shown in Eq. (C.4.2.9), which will give better accuracy and conservative results and is also adopted in this standard.

#### **Appendix 4.3 Alternative method: seismic evaluation of masonry infilled RC frame using relative strength of RC frame to masonry infill ( $\beta$ index)**

This section discusses about seismic evaluation of masonry infilled RC frame using level of confinement from the surrounding RC frame. Here, judgement of failure mode and evaluation of strength and ductility is discussed in the following sections.

##### **4.3.1 Judgement of failure mode**

Failure mode of an RC frame with masonry infill is classified based on the relative strength of RC frame to masonry infill ( $\beta$  index) (Table 4.3.1)

Type I: Diagonal compression failure

Type II: Sliding and diagonal cracking failure

Type III: Overall flexural failure

Type IV: Column punching and joint sliding failure

The failure mode of the surrounding RC column is classified into Type A to Type D.

Type A: Column shear failure

Type B: Column flexural failure

Type C: Short column shear failure

Type D: Short column flexural failure

Table 4.3.1 Idealized Failure types of RC frame with masonry infill

	Column $h_o = h_{inf}^{*1}$		Short Column $h_o = h_{inf}/2^{*1}$ (hinge at mid height)	
	Shear Type A $Q_{su}/Q_{mu}^{*2} < 1$	Flexural Type B $Q_{su}/Q_{mu}^{*2} > 1$	Shear Type C $Q_{su}/Q_{mu}^{*2} < 1$ for $h_{inf}/2$	Flexural Type D $Q_{su}/Q_{mu}^{*2} > 1$ for $h_{inf}/2$
<u>Type I</u> <b>Diagonal compression</b> $\beta \geq 1$			N.A.	N.A.
<u>Type II</u> <b>Sliding –diagonal cracking failure</b> $0.2 < \beta < 1$	N.A.	N.A.		
<u>Type III</u> <b>Overall flexural</b> $\beta \leq 0.2$			N.A.	
<u>Type IV</u> <b>Column punching &amp; joint sliding</b> $\beta \leq 0.2$	N.A.			

\*<sup>1</sup>  $h_o$ : Clear height of the column.  $h_{inf}$ : Height of the masonry infill.

\*<sup>2</sup>  $Q_{su}$ : Ultimate shear strength of the column.  $Q_{mu}$ : Shear force at the ultimate flexural strength of the column.  $Q_{su}/Q_{mu}$  is the margin of shear to flexural strength of the column.

(2) Relative strength of RC frame to masonry infill ( $\beta$  index)

The confinement by RC frame is represented by  $\beta$  index using the following Eq. (4.3.1)

$$\beta = Q_{frame}/Q_{expected} \quad (4.3.1)$$

Where,  $Q_{frame}$ : lateral strength of boundary bare RC frame calculated by Eq. (4.3.2):

$$Q_{frame} = \sum Q_{col} = Q_{col\_left} + Q_{col\_right} \quad (4.3.2)$$

$Q_{col\_left}$ ,  $Q_{col\_right}$ : the lateral strength of boundary columns for the masonry infill calculated as the minimum of  $Q_{mu}$  and  $Q_{su}$  calculated as per the BSPP Seismic Evaluation Manual [4.2], taking a clear height of  $h_o$  as the clear height of masonry infill.

$Q_{expected}$ : expected lateral strength of masonry infill using the following Eq. (4.3.3)

$$Q_{expected} = 0.05 f_m \cdot t_{inf} \cdot l_{inf} \quad (4.3.3)$$

$f_m$  : compressive strength of masonry prism.

$t_{inf}$  : masonry infill thickness.

$l_{inf}$  : masonry infill length.

Failure modes are classified based on  $\beta$  index as follows.

- |   |                |
|---|----------------|
| i) $\beta \geq 1$ , Good confinement/Weak wall: | Type I         |
| ii) $0.2 < \beta < 1$ , Fair confinement:       | Type II        |
| iii) $\beta \leq 0.2$ , Poor confinement:       | Type III or IV |

### C.4.3 [Commentary]

#### C.4.3.1 Classification of failure modes

Various types of failure modes of RC frame with masonry infill were observed in previous researches. However, it seems the classification of failure modes has not been studied enough especially based on the theoretical mechanism background. The diagonal compression failure of masonry (Type I) is one of the most popular failure modes when good confinement from the surrounding RC frame is provided. Another popular failure mode is the sliding failure along mortar between bricks or a mixed type of failure with sliding and diagonal cracking is also found in many experiments (Type II). Surrounding RC frame and masonry infill tend to behave separately in these three types of failure modes. Their strength ( $C$  index) and ductility ( $F$  index), therefore, can be evaluated separately.

In case of strong and stiff masonry infill, the masonry infill can be assumed as a rigid wall panel. One possible failure mode is the overall flexural failure mode (Type III) which is a common failure mechanism in the RC wall. If lateral strengths in surrounding columns are insufficient, punching shear in a column and sliding at the top joint between masonry infill and beam may occur (Type IV).

#### C.4.3.2 $\beta$ index

In general, a strong RC frame surrounding the masonry infill would increase the confinement of the masonry infill and affect its failure mode. To classify the frames as a weak or strong frame, the  $\beta$  index is used which is defined as the ratio of the expected bare frame's lateral strength to the expected masonry infill's strength as shown in Eq. (4.3.1).

$Q_{frame}$  is the lateral strength of the boundary frame calculated as a minimum of flexural capacity or shear strength.

$Q_{expected}$  is the expected lateral capacity of the masonry infill computed by Eq. (4.3.3). This is a simple prediction assuming  $\tau_{inf}$  is equal to  $0.05f_m$ , where  $f_m$  is the prism compressive strength. Obtaining  $f_m$  might be difficult in a field survey and a method to estimate  $f_m$  is discussed in a later section (C.4.3.2). Assuming  $0.05f_m$  is a simple prediction model that showed fair compatibility with the average of the experimental database of 24 specimens of masonry infill within the range of  $f_m = 3$  MPa to 20 MPa and aspect ratio ( $h/l$ )



= 0.5 to 1., observed in a study by Alwashali et al. (2018). Figure C.4.3.1 shows that Eq. (4.3.3) can roughly estimate the lateral strength of masonry infill with an average ratio of analytical to the experimental ratio of 0.8.

A  $\beta$  index larger than 1 indicates that the RC frame is stronger than the masonry infill and thus having good confinement. The relationship of  $\beta$  index and failure modes was investigated in a study by Alwashali et al. (2018) and showed that the  $\beta$  index greater than 1 is an important parameter in determining the failure mechanism of masonry infill as well as RC frame. Other parameters such as very weak mortar and workmanship quality may have some influence on failure modes. Those parameters are, however, difficult to incorporate during seismic evaluation in the field, thus this guideline considers only two main key parameters, i.e.,  $\beta$  index and contact length ratio ( $a_c/h_o$ ) that will be discussed in a later section.

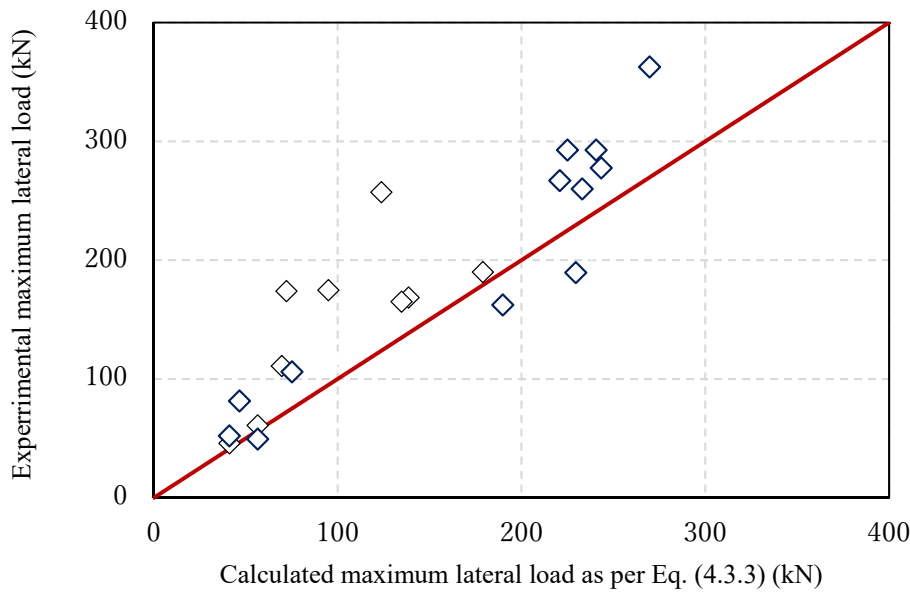


Figure C.4.3.1 Comparison of experimental results and calculated results based on Eq. (4.3.3) [Alwashali et al. (2018)]

Figure C.4.3.2 shows a comparison of failure modes observed in past experimental tests of 26 specimens (details of specimens shown in Alwashali et al. (2018)) and  $\beta$  index. As shown in Figure C.4.3.2, most of the specimens having values of  $\beta$  index  $> 1$  had failure type I (diagonal compression). On the other hand, specimens with  $\beta$  index  $< 1$  had failure Type II (Sliding-diagonal cracking failure).

The idea of failure mode separation using the  $\beta$  index length works well, but the determination of the  $\beta$  index ratio for each failure mechanism might be difficult using available experimental data from the literature. Therefore, a further attempt is taken to execute a probabilistic analysis to identify boundaries for different failure mechanisms. The log-normal distribution of normalized  $\beta$  index for each cluster of failure mechanisms is shown in Figure C.4.3.3(a). The ranges of  $\beta$  index overlapped for diagonal compression and sliding-diagonal failure. Whereas, the distribution for punching or flexural failure is spike-shaped due to the few numbers of available data. Hence, the further cumulative distribution of each failure mechanism cluster is drawn in Figure C.4.3.3(b). Afterward, a 90% probability line is drawn to distinguish the failure mechanisms. Based on the 90% probability line, boundary conditions are proposed as of i)  $\beta$  index  $> 1$  had failure type I (diagonal compression) ii)  $0.2 < \beta$  index  $< 1$  is the boundary for failure Type II (Sliding-diagonal cracking failure and iii)

$0.2 < \beta$  index is boundary failure for column-punching shear failure.

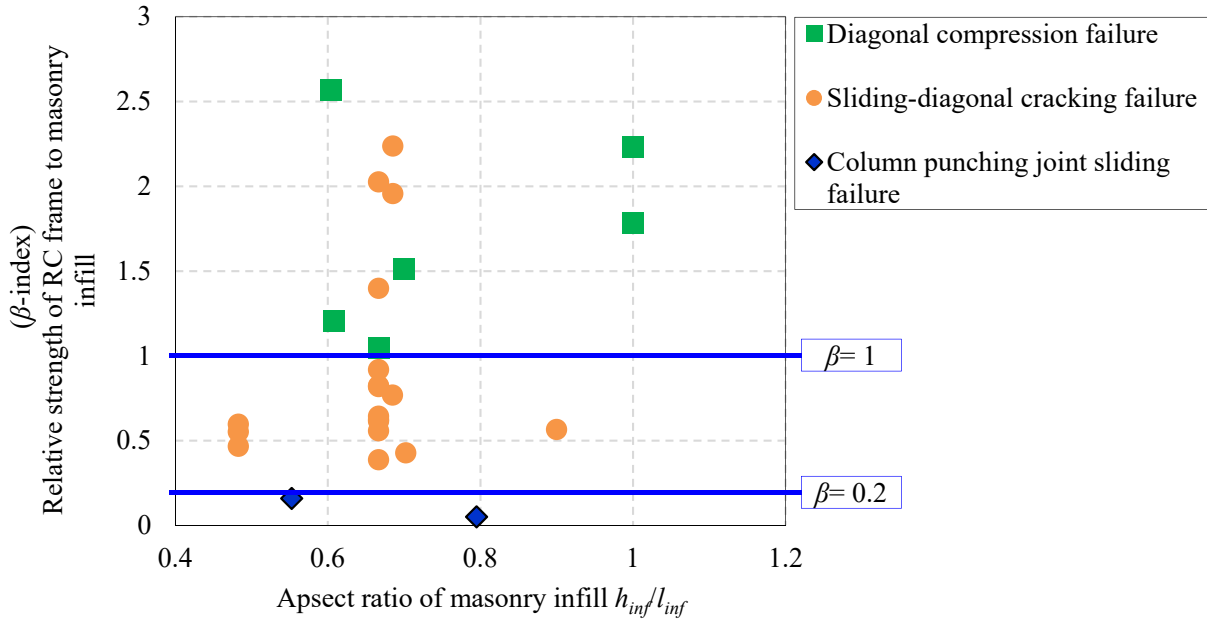


Figure C.4.3.2 Comparison of experimental failure modes and  $\beta$ -index

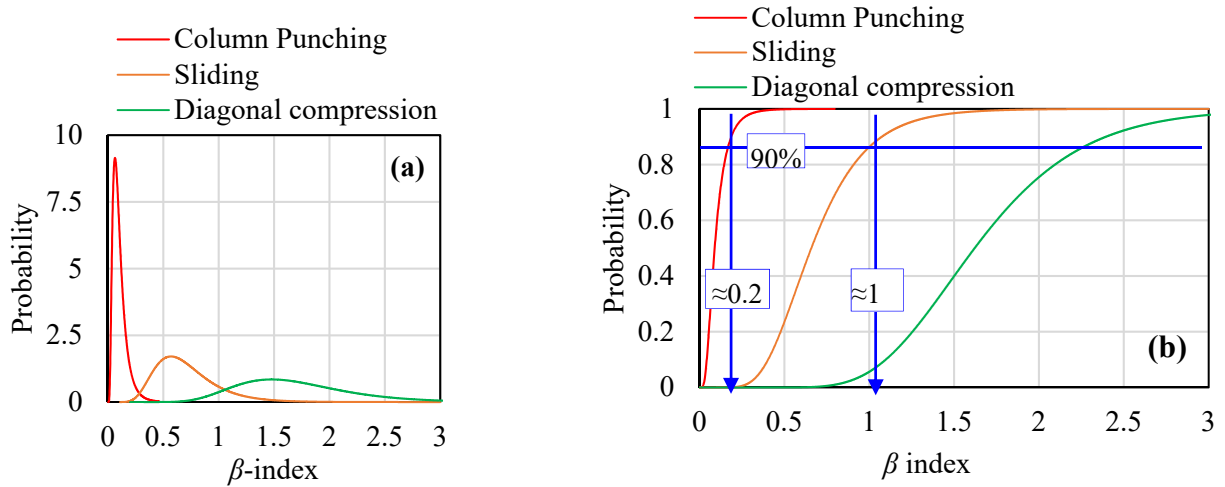


Figure C.4.3.3 (a) Distribution of  $\beta$  index with different failure mode  
(b) Cumulative distribution of  $\beta$  index for different failure modes

### C.4.3.3 Correlation between $\beta$ -index and contact length ratio

Figure C.4.3.4 shows a comparison between failure modes and boundaries suggested for each failure type proposed by this guideline.

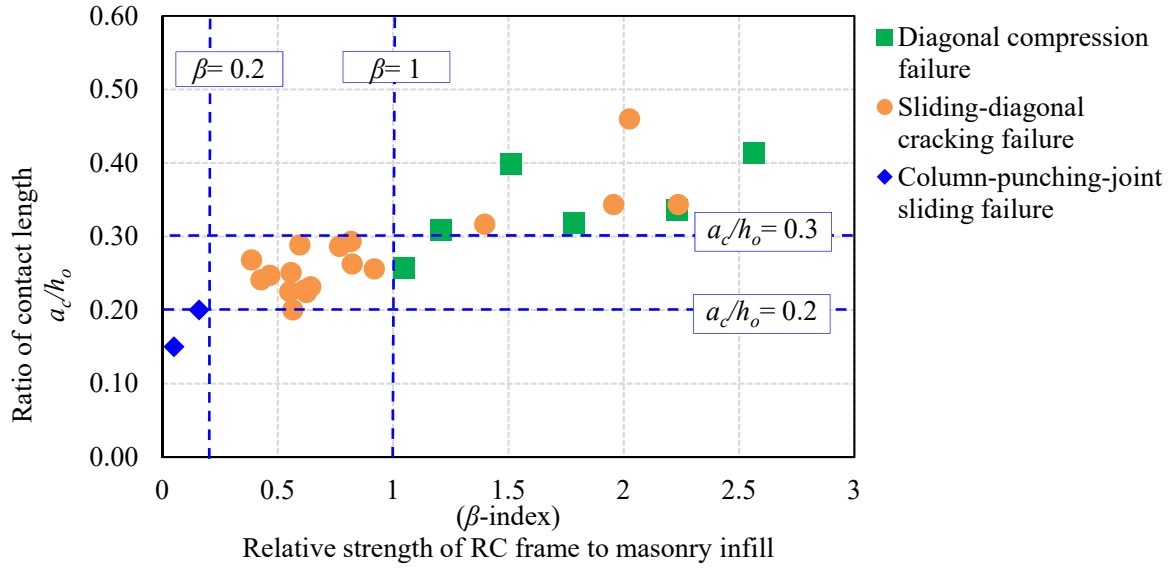


Figure C.4.3.4 Correlation between  $\beta$  index and contact length ratio

### 4.3.2 Strength index $C$

#### General

Strength index  $C_{mw}$  for an RC frame with masonry infill is calculated by Eqs. (4.3.4) and (4.3.5).

$$C_{mw} = \frac{Q_{mw}}{\Sigma W} \quad (4.3.4)$$

Where  $\Sigma W$  is the weight of the building including live load supported by the story concerned.

$$Q_{mw} = \begin{cases} Q_{frame} + Q_{dia} & \text{Type I} \\ Q_{frame} + Q_{sld} & \text{Type II} \\ Q_{fw} & \text{Type III} \\ Q_{jw} & \text{Type IV} \end{cases} \quad (4.3.5)$$

$Q_{mw}$  is the lateral strength of an RC frame with masonry infill.  $Q_{frame}$  is the lateral strength of left hand side and right hand side columns of the surrounding frame, smaller of  $Q_{su}$  and  $Q_{mu}$  calculated by BSPP Seismic Evaluation Manual [4.2] with a clear height of  $h_o$  as the height of masonry infill.

$Q_{dia}$  is the lateral strength of a masonry infill wall for Type I.  $Q_{sld}$  is the lateral strength of a masonry infill wall for Type II.  $Q_{fw}$  is Lateral strength for overall flexural failure (Failure Type III),  $Q_{jw}$  is the lateral strength of punching shear failure (Failure Type IV) .

#### Type I (Diagonal compression failure)

i) Lateral strength of a frame  $Q_{frame}$  is evaluated with a clear height  $h_o$ .

iv) Lateral strength of masonry infill  $Q_{inf}$  is evaluated as diagonal compression strength  $Q_{dia}$  by Eq. (4.3.6).

$$Q_{dia} = (0.06\beta - 0.01) \cdot \gamma \cdot f_m \cdot t_{inf} \cdot l_{inf} \quad (\text{for the case } 1 < \beta < 1.5) \quad (4.3.6)$$

$$Q_{dia} = 0.08 \cdot \gamma \cdot f_m \cdot t_{inf} \cdot l_{inf} \quad (\text{for the case } \beta \geq 1.5)$$

$f_m$ : compressive strength of masonry prism.

$t_{inf}$ : infill thickness

$l_{inf}$ : infill length

$\gamma$  : a factor to account for the influence of aspect ratio. Is taken as 1 in case of  $h_{inf}/l_{inf}=1.0$  and 0.8 in case of  $h_{inf}/l_{inf}=0.5$ . For other cases, interpolation between  $h_{inf}/l_{inf}=0.5$  and 1.0

**Type II (Sliding and diagonal cracking failure)** Lateral strength of sliding failure  $Q_{sld}$  is applied Type II given by the Eq (4.3.7).

$$Q_{sld} = \frac{\tau_{inf} \cdot t_{inf} \cdot l_{inf}}{1 - \mu \frac{h_{inf}}{l_{inf}}} \quad (4.3.7)$$

$\tau_{inf}$ : shear strength of masonry infill taken by in situ tests. In case of unavailable data, it can be taken as  $\tau_{inf} = 0.03f_m$ .

$h_{inf}, l_{inf}$ : infill height and length, respectively and for the application limit of this guide of  $0.5 \leq h_{inf}/l_{inf} < 1$

$\mu$ : friction coefficient could be taken as 0.45.

$f_m$ : compressive strength of masonry prism.

### **Type III (Overall flexural failure of frame)**

Surrounding columns and masonry infill work as a solid flexural wall, assuming the masonry infill as a rigid wall panel, and the overall flexural strength  $Q_{fw}$  is given by Eq. (4.3.8).

$$Q_{fw} = M_{wmu}/h_o \quad (4.3.8)$$

$$M_{wmu} = a_{t.col} \sigma_y l_w + 0.5N l_w \quad (4.3.9)$$

$a_{t.col}$ : area of steel of longitudinal reinforcement in tension column.

$\sigma_y$ : yield strength of tension reinforcement.

$l_w$ : center to center span length of RC frame.

$N$ : total axial force on RC columns on both sides of masonry infill wall.

### **Type IV (Column punching and joint sliding)**

Punching shear failure and sliding at the top joint of the masonry infill is considered. Lateral strength  $Q_{fw}$  is calculated by Eq. (4.3.10) by ignoring joint shear strength between masonry infill and beam.

$$Q_{fw} = Q_{pc} + rQ_{col} \quad (4.3.10)$$

i)  $Q_{pc}$  is the punching shear strength of column (left hand side column as shown in Table 4.3.1) calculated by Eq. (4.3.11) in JBDPA Seismic Retrofit Guideline.

$$Q_{pc} = K_{min} \tau_o bD \quad (4.3.11)$$

Where according to JBDPA Seismic Retrofit Guideline,

$$K_{min} = 0.34/(0.52 + a/D) \quad (4.3.12)$$

$$\tau_o = 0.98 + 0.1f_c + 0.85\sigma \quad \text{in case } 0 \leq \sigma \leq 0.33f_c - 2.75 \quad (4.3.13)$$

$$\tau_o = 0.22f_c + 0.49\sigma \quad \text{in case } 0.33f_c - 2.75 \leq \sigma \leq 0.66f_c$$

$$\tau_o = 0.66f_c \quad \text{in case } 0.66f_c \leq \sigma$$

$$\sigma = \rho_g f_y + \sigma_0 \quad (4.3.14)$$

$$\sigma_0 = \frac{N}{bd} \quad (4.3.15)$$

$$k_{min} = \frac{0.34}{0.52 + a/D} \quad (4.3.16)$$

$K_{min}$  : influence factor considering shear span ratio

$\tau_o$  : basic shear strength of column

$b$  and  $D$  : width and depth of column

$a$  : shear span taken as  $= D/3$

$\rho_g$  : longitudinal reinforcement ratio of column

$f_c$  : concrete compression strength

$f_y$  : yield strength of longitudinal reinforcement

$N$  : axial load on column.

ii) Lateral strength of a column  $rQ_{col}$  (Right hand side column as shown in Table 4.3.1) is evaluated with clear height  $h_0$ .

### Summary of strength evaluation

The component strength of RC frame and infill masonry is summarized in the Table 4.3.2. It is to be noted that the frame capacity evaluation needs lateral capacity of the surrounding columns ( $rQ_{col}$ ) that should be evaluated as per BSPP manual as mentioned in the following Table 4.3.2.

Table 4.3.2 Summary of calculation of  $C$  index

	Confinement	$\beta$	Masonry	Frame
Type I	Good	$1.0 < \beta$	Eq. (4.3.6)	As per BSPP manual ( $Q_{frame}$ )
Type II	Fair	$0.2 < \beta < 1.0$	Eq. (4.3.7)	
Type III	Poor	$\beta \leq 0.2$		Eq. (4.3.8)
Type IV				$Q_{pc}$ as per Eq. (4.3.10) and $rQ_{col}$ as per BSPP manual

### C.4.3.2 [Commentary]

#### C.4.3.2.1 General

The failure modes (Type I to Type IV) mentioned in Table 4.3.1 in Sec. 4.3.1 are considered in this Guideline. The lateral strength of the RC frame with masonry infill is calculated according to the classified failure mode. In the case of Types I and II, the masonry infill is relatively weak or relatively similar strength or stiffness to the surrounding RC frame, and the masonry infill wall tends to fail in advance of RC frame. Then the lateral strength for RC frame and masonry infill is evaluated separately and their summation is regarded as the total lateral strength  $Q_{mw}$ . In the case of Types III and IV, the masonry infill wall is relatively very strong and stiff which behaves as a rigid panel. Then the total lateral strength  $Q_{mw}$  is evaluated as an overall structural component.

#### C.4.3.2.2 Diagonal compressive strength of masonry infill walls $Q_{dia}$

Figure C.4.3.5 shows the diagonal compression strut of a masonry infilled RC frame. The width of the strut changes during loading and might not be the same as that at initial stiffness. The main reason is that with the increase of the lateral load, masonry infill and RC frame are detached and a gap is formed, which is due to the deformation of the frame and masonry infill as shown in Figure C.4.3.5-a). This also indicates that the weaker is the frame (more flexible), the greater is the deformation and the larger is the gap between frame and infill.

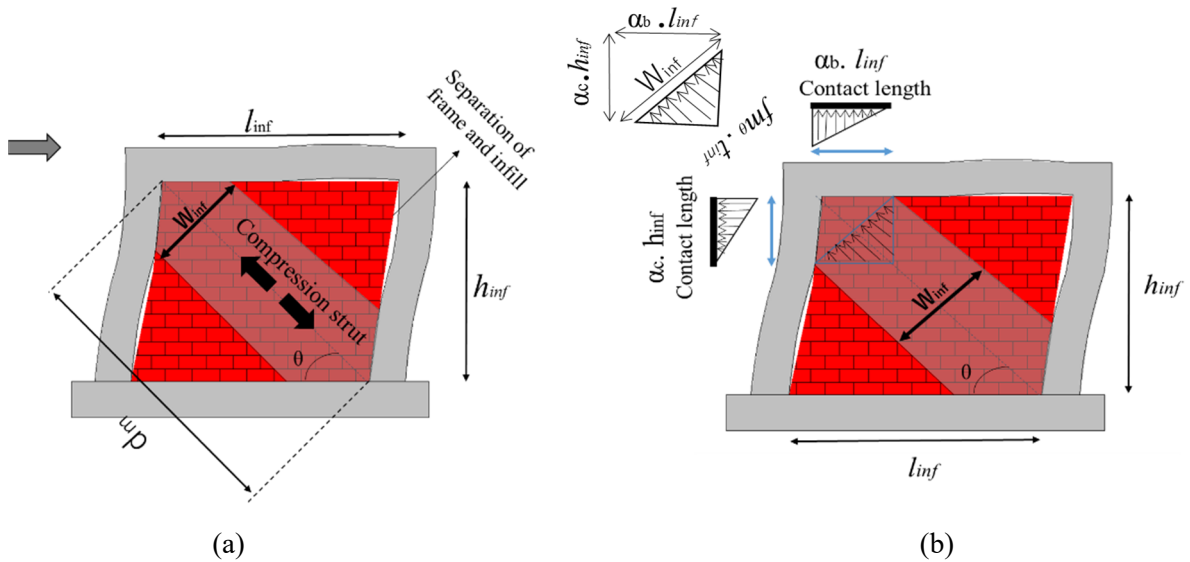


Figure C.4.3.5 Strut width and contact length at maximum strength

Herein, the maximum lateral load of the infill was taken as a horizontal component of the diagonal compression strut, as shown in Eq. (C.4.3.1).

$$Q_{dia} = C_{strut} \cos \theta \quad (C.4.3.1)$$

Where  $C_{strut}$  is the diagonal forces of the infill strut and  $\theta$  is the diagonal strut angle.

In addition, the compressive stress distribution in the strut is not uniform having a shape of parabolic or triangular distribution with the maximum stress at the corner. In this Guideline, for simplicity, the stress distribution is proposed as a triangular shape with the maximum at the corner, as shown in Figure C.4.3.5 (b). The  $C_{strut}$  is the product of triangle stress distribution area ( $0.5f_m\theta$ ), strut width ( $W_{inf}$ ), and infill thickness ( $t_{inf}$ ),

as shown in Eqs. (C.4.3.2) to (C.4.3.3).

$$C_{strut} = 0.5 f_{m\theta} \cdot t_{inf} \cdot W_{inf} \quad (C.4.3.2)$$

$$f_{m\theta} = f_m \cdot \eta \quad (C.4.3.3)$$

where  $t_{inf}$  is the infill thickness,  $W_{inf}$  is the width of the compression strut.  $f_{m\theta}$  is the compressive strength of masonry infill based on the orientation angle due to anisotropic characteristics.  $\eta$  is a reduction index to consider the reduction of compressive strength due to the orientation of loading.

The reduction index,  $\eta$ , could be estimated based on results of intensive material experimental results conducted by Page (1981) and Hamid (1980) which are shown in Figure C.4.3.6 and Figure C.4.3.7, respectively.

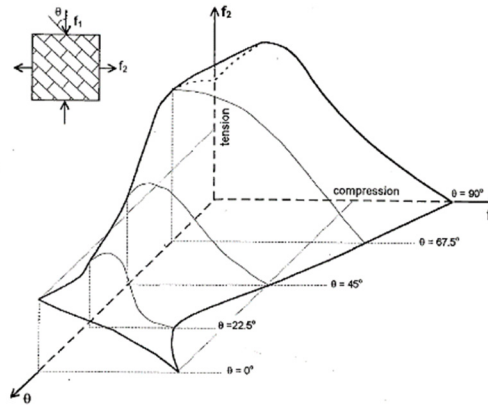


Figure C.4.3.6 Reduction in compressive strength of masonry infill due to orientation by A.W. Page (1981)

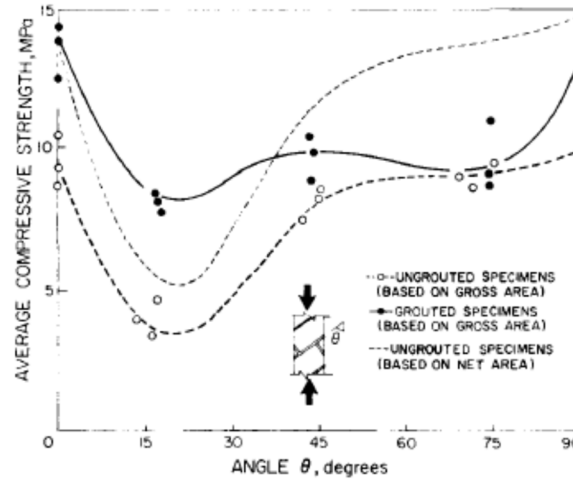


Figure C.4.3.7 Reduction in compressive strength of masonry infill due to orientation by Hamid et al (1980)

Based on Figure C.4.3.6 and Figure C.4.3.7, the reduction index  $\eta$  could be estimated using Eq. (C.4.3.4),

$$\eta = 0.5\theta + 0.2 \quad (C.4.3.4)$$

Where  $\theta$  is the diagonal strut angle in radians and diagonal angles ranging from 0.4 to 1.0 radians (23 to 60 in degree).

The width of the compression strut is affected by several factors such as the strength ratio of the frame to the masonry infill, interface condition between masonry infills and frames, and loading level. The effective contact length reduces with the increasing lateral load due to separation between frame and masonry infill. The stronger is the boundary frame relative to the masonry infill, the less is the deformation of the frame, and thus smaller is the separation between frame and masonry infill which increases the contact length between the infill and frame which increases the width of compression strut. On the other hand, a flexible or a weak frame has greater deformation and greater separation between the frame and the infill, and thus shorter contact length and smaller strut width. Figure C.4.3.8 and Figure C.4.3.9 show the relationship between  $\beta$  index (the expected strength ratio of frame to masonry infill) and the strut width at maximum strength and shear strength based on experimental results (Alwashali et al. 2018). The strut width and shear strength increased with the increase of the  $\beta$  index. It is thought that the larger  $\beta$  index resembles a stronger frame and stiffer boundary RC frame which will increase the compression strut width of masonry infill which increases infill's shear strength. In this guideline, estimation of width of the strut for the Type I failure i.e, diagonal compression failure is proposed as the lower boundary of width strut that is shown by the green dotted line in Figure C.4.3.8. Transformation of the strut width of Figure C.4.3.8 into lateral shear strength (normalized by masonry compressive strength,  $f_m$ ) is shown in Figure C.4.3.9. The green dotted line in Figure C.4.3.9 represents the Eq.( 4.3.6) proposed in this guideline for failure Type I for  $\beta$  index  $>1$ . To account for the aspect ratio influence shown in Figure C.4.3.8, a factor  $\gamma$  is introduced as in the Eq.( 4.3.6). It should be noted that values of  $\beta$  index  $< 1$ , the failure type is not failure Type I (Type II sliding and diagonal cracking failure), this is not shown in the line of Eq. (4.3.6) in Figure C.4.3.8 and will be discussed in next section.

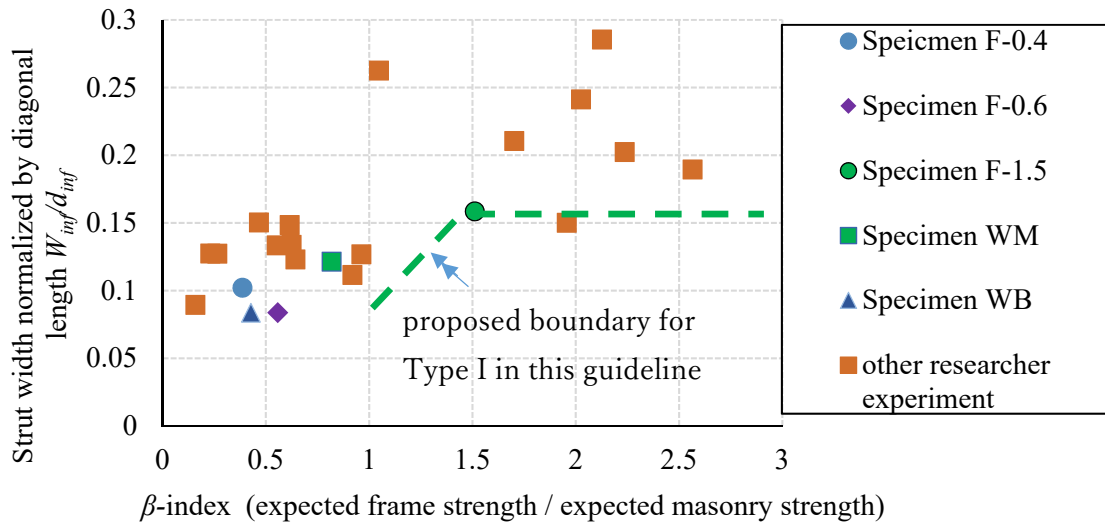


Figure C.4.3.8 Relationship between ratio of strut width to diagonal length and  $\beta$ -index based on experimental results (Alwashali et al. 2018)



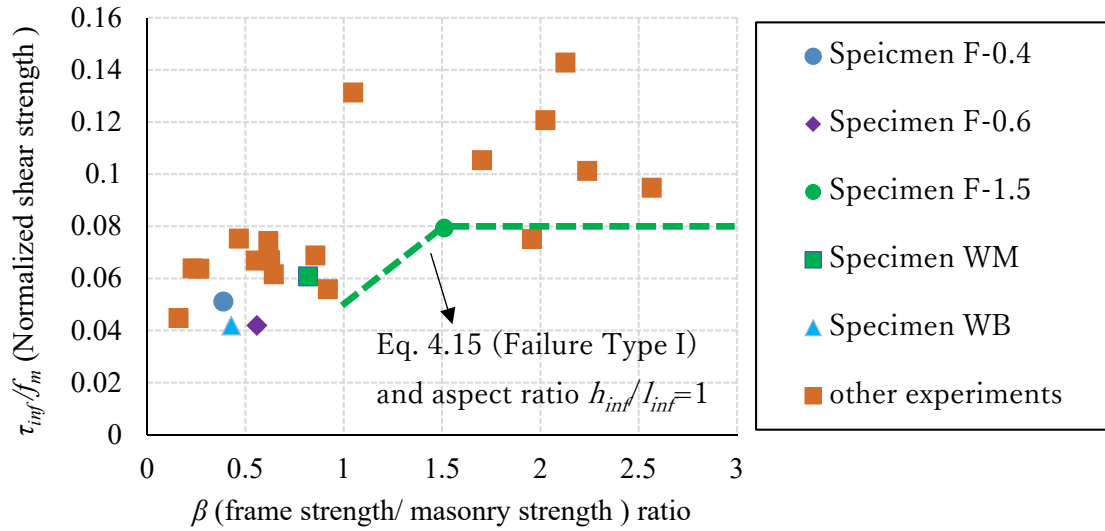


Figure C.4.3.9 Relationship between shear strength and  $\beta$ -index based on other past experimental data

#### C.4.3.2.2 Sliding shear strength of masonry infill walls $Q_{slid}$

This section discusses the basic concept of Eq (4.3.7) for failure Type II (sliding and diagonal cracking failure of masonry infill).

The sliding failure is expressed as the Mohr-Coulomb failure criteria are used as shown in Eq. (C.4.3.5).

$$Q_{slid} = \tau_o \cdot t_{inf} \cdot l_{inf} + \mu N \quad (C.4.3.5)$$

The axial load on the infill,  $N$ , is taken as the summation of gravity load and vertical component of strut force  $C_{strut}$ , as shown in Eq. (C.4.3.6).

$$N = \text{Dead load} + Q_{strut} \cdot \sin \theta \quad (C.4.3.6)$$

Dead load is taken as zero since infill was inserted after the construction of the frame and its self-weight is very small and considered insignificant.  $N$  is taken as the vertical force from compression strut formed as suggested by Paulay and Priestly (1992) and illustrated in Figure C.4.3.10.

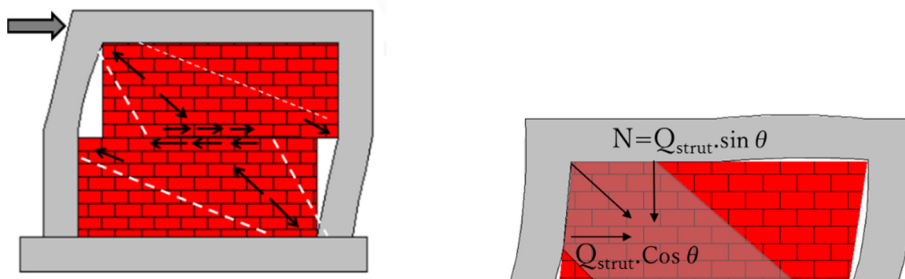


Figure C.4.3.10 Schematic drawing of sliding mechanism and axial load from strut

Substituting a vertical component of  $C_{strut}$  into Eq. (C.4.3.7), then the initial sliding shear strength is given by

$$Q_{sld} = \tau_o \cdot t_{inf} \cdot l_{inf} + \mu \cdot C_{strut} \cdot \sin\theta \quad (C.4.3.7)$$

Knowing that forces of  $Q_{sld} = C_{strut} \cdot \cos\theta$ , as shown in Figure C.4.3.10 and replacing  $Q_{sld}$  in Eq. (C.4.3.8) then,

$$C_{strut} \cdot \cos\theta = \tau_o \cdot t_{inf} \cdot l_{inf} + \mu \cdot C_{strut} \cdot \sin\theta \quad (C.4.3.8)$$

$\cos\theta$  is replaced by  $l_{inf}/d_{inf}$  and  $\sin\theta$  replaced by  $h_{inf}/d_{inf}$ , and rearranging Eq. (C.4.3.8) gives Eq. (C.4.3.9),

$$C_{strut} = \frac{\tau_o \cdot t_{inf} \cdot d_{inf}}{1 - \mu \cdot \tan\theta} \quad (C.4.3.9)$$

Calculating the lateral strength and replacing  $Q_{sld} = C_{strut} \cdot \cos\theta$  in Eq. (C.4.3.10), then:

$$Q_{sld} = \frac{\tau_o \cdot t_{inf} \cdot l_{inf}}{1 - \mu \cdot \tan\theta} \quad (C.4.3.10)$$

The initial cohesive capacity of the mortar beds,  $\tau_o$ , can be taken as a conservative value to be  $0.03f_m$  as recommended by Paulay and Priestly (1992). The friction coefficient of sliding friction,  $\mu$ , greatly varies from a code to another. NZSEE 2006 suggests  $\mu = 0.8$  in the absence of site data. The MSJC standard 2016 states  $\mu = 0.45$ . To be on the conservative side, the lower boundary of  $\mu = 0.45$  is taken in this Guideline.

$$Q_{sld} = \frac{0.03f_m \cdot t_{inf} \cdot l_{inf}}{1 - 0.45 \cdot \tan\theta} \quad (C.4.3.11)$$

For an aspect ratio of  $h_{inf}/l_{inf}$  is of 0.5 to 1.0, then  $Q_{sld}$  is equal to  $0.039$  to  $0.10 f_m \cdot t_{inf} \cdot l_{inf}$ .

#### C.4.3.2.3 Average shear strength of the masonry infill, $\tau_{inf}$ , in Eq. (4.3.3)

Figure C.4.3.11 shows the relationship between the shear strength of the masonry infill and the masonry prism compressive strength,  $f_m$ , based on a database of experimental results from nine different researchers, and details of specimens are summarized in the study by Alwashali et.al (2018). The database consists of single-story, single-span RC frames with masonry infill tested under static cyclic loading with several types of masonry bricks. As shown in Figure C.4.3.11, the shear strength of the masonry infill,  $\tau_{inf}$ , generally ranges between  $0.2$  and  $1 \text{ N/mm}^2$ . The shear strength,  $\tau_{inf}$ , commonly ranges between  $0.04f_m$  and  $0.1f_m$ .

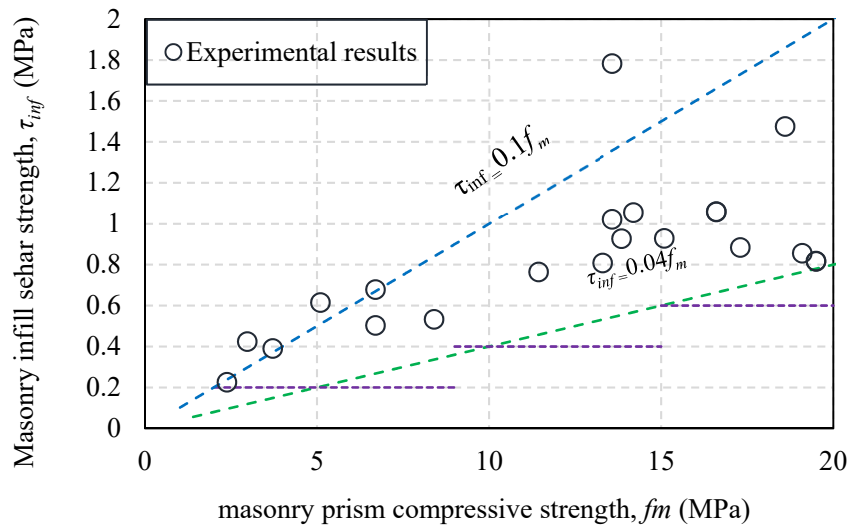


Figure C.4.3.11 Relationship between prism compressive strength and shear strength of masonry infill

Assuming the  $\tau_{inf}$  as  $0.05f_m$ , Eq. (4.3.3) gives a good and conservative approximation for shear strength with an average ratio of analytical to experimental of 0.83 as shown in the study Alwashali et al. (2018).

#### 4.3.3 Ductility index $F$

The ductility index  $F$  for each failure mechanism is given below considering masonry infilled RC frame as a unit and considering surrounding columns are flexural columns. However, when the surrounding column is a shear column ( $Q_{su}/Q_{mu} < 1$ ), the ductility index should be considered as unity ( $F=1$ ), for failure type except failure Type III. The overall idea is summarized in the following Table 4.3.3.

$F$ -index for masonry infill with openings is recommended to be taken as the lower boundary of  $F=1$ .

Table 4.3.3 Ductility Index corresponding to Failure Mechanism

Failure mechanism	$\beta$ index	F-index
Diagonal compression (Type I)	$\beta \geq 1$	1.75
Sliding-diagonal cracking (Type II)	$0.2 < \beta < 1$	1.27
Overall flexural (Type III)	$\beta \leq 0.2$	1.75
Column punching-joint sliding (Type IV)	$\beta \leq 0.2$	1.00

#### C.4.3.3 [Commentary]

The F-index is taken based on experimental observation for each failure mode as shown in Figure C 4.3.12. The lower bound of F-index of diagonal compression failure as well as overall flexural failure is considered as 1.75, which indicates relatively ductile behaviour. On the other hand, the lower bound of F-index of diagonal cracking-sliding is considered as 1.27. In case of column punching-joint sliding failure, the F-index is considered to be a unity ( $F=1$ ), since the failure is governed by shear and the lower bound of F-index is below 1.27. Idealized C-F relationship of each failure mechanism is shown in Table C 4.3.1.

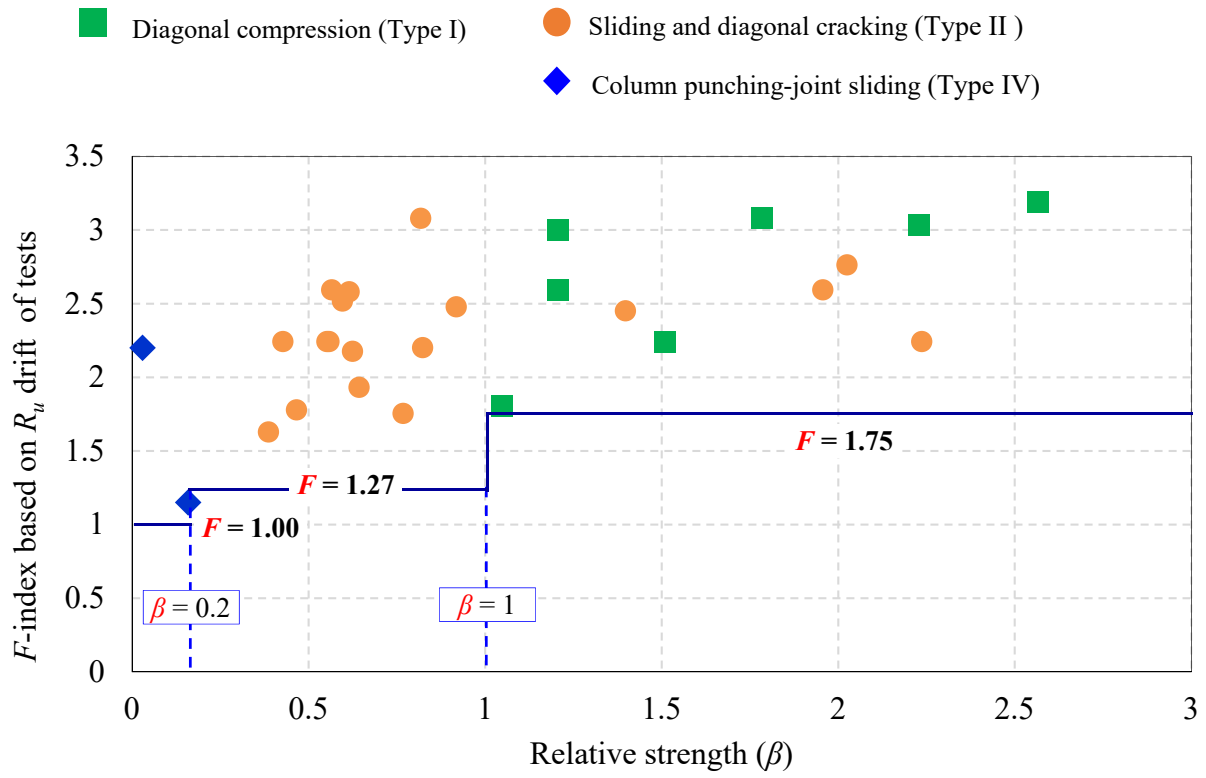
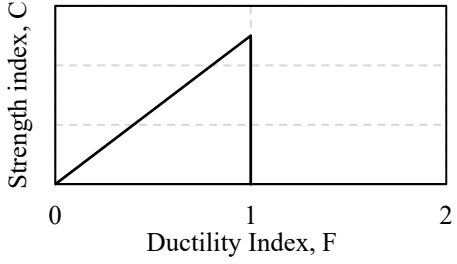
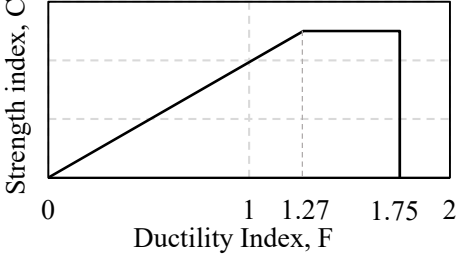
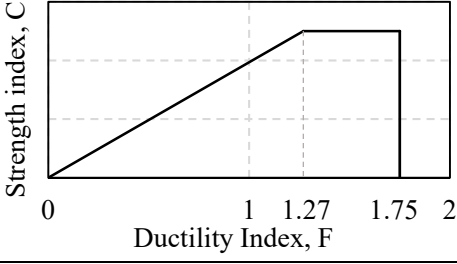
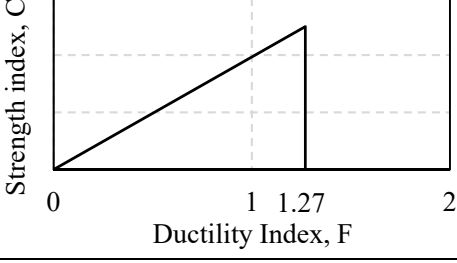
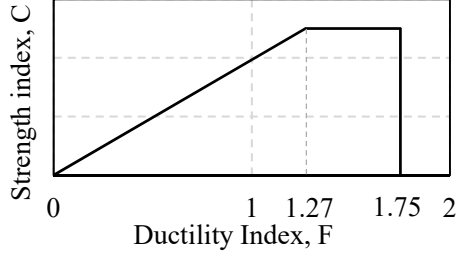
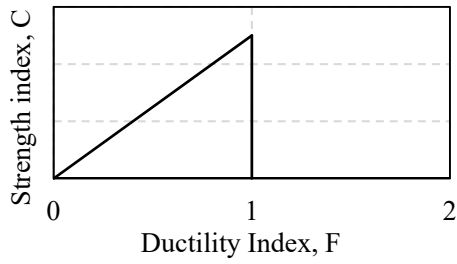


Figure C.4.3.12 Relationship of experimental  $F$ -index with relative strength ( $\beta$ )

Table C 4.3.1 Idealized C-F relationship of FC strengthened Masonry infilled RC frame

Column type	Failure mode	Idealized C and F relationship
Shear column	Diagonal compression (Type I), Diagonal cracking-sliding (Type II), and Column punching-joint sliding (Type IV)	
	Overall flexural (Type III)	
Flexural column	Diagonal compression (Type I)	
	Diagonal cracking-sliding (Type II)	
	Overall flexural (Type III)	
	Column punching-joint sliding (Type IV)	

#### 4.3.4 Application examples of alternative method of seismic evaluation

##### 4.3.4 Overview of the building

An example of seismic evaluation with masonry infill is described in the following section. A three-storied residential building is selected. Figure 4.3.4.1 shows the floor plan with the location of the column and masonry infill. The total floor area of the investigated buildings is about 324.5 m<sup>2</sup>. The sectional properties of column and masonry infill are shown in Table 4.3.4.1 and 4.3.4.2.

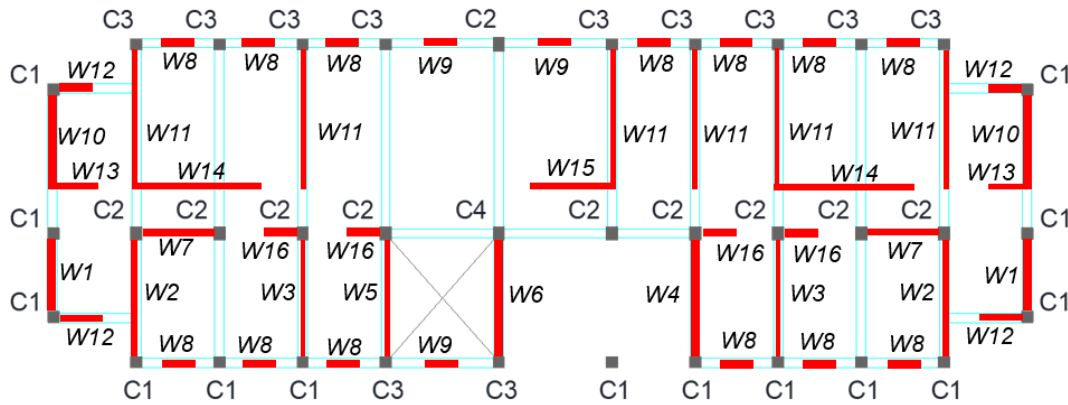


Figure 4.3.4.1 Architectural plan (dimensions are in mm)

Table 4.3.4.1 Column dimension

Legend for column	Dimension(mm)
Column (C1,C3)	300×300
Column (C2,C4)	300×375

Table 4.3.4.2 masonry infill-wall properties

Wall ID	Number	Length (mm)	Thickness (mm)	Surrounding frame	Opening area %	Opening or Solid	Structural wall (yes/no)
W1	2	2750	250	Yes	0%	Solid	Yes
W2	2	3875	125	Yes	0%	Solid	Yes
W3	2	3875	125	Yes	0%	Solid	Yes
W4	1	3875	250	Yes	0%	Solid	Yes
W5	1	3875	125	Yes	0%	Solid	Yes
W6	1	3875	250	Yes	0%	Solid	Yes
W7	2	2400	125	Yes	0%	Solid	Yes
W8	13	2400	250	Yes	>40%	Opening	No
W9	3	3875	250	Yes	>40%	Opening	No
W10	2	2750	250	Yes	>40%	Opening	No
W11	6	4750	125	Yes	>40%	Opening	No
W12	4	2750	250	No	-	Opening	No
W13	2	2750	125	No	-	Opening	No
W14	2	2750	125	No	-	Opening	No
W15	1	2350	125	No	-	Opening	No
W16	4	2750	125	Yes	>40%	Opening	No

#### 4.3.4.2 Material properties

Both destructive and non-destructive tests are carried out to determine the material properties. The detailed procedure is described in the BSPP manual. The material properties are shown in Table 4.3.4.3.

Table 4.3.4.3 Material properties

Material properties	Material strength (MPa)
Concrete strength, $f_c$	17
Yield strength of reinforcement, $f_y$	276
Young's modulus concrete, $E_c$	19378
Young's modulus of masonry, $E_{inf}$	$550 f_m$
Prism strength, $f_m$	8
* Young's modulus of concrete: $4700\sqrt{f_c}$ (unit: MPa) according to ACI318-14	

#### 4.3.4.3 Evaluation procedures

Evaluation procedures are shown as follows:

##### **Step 1: Classification to structural wall and non-structural wall**

- In the example building, there are two types of masonry infill: solid wall and wall with opening due to window, door, and high window.
- Masonry infill is surrounded and confined by RC frame from all sides.
- A wall with an opening having greater than 40% opening area and that having double openings. These walls are not considered a structural wall.
- The slenderness ratio  $H/t$  of infill wall is 12, which is less than 30.
- Solid brick is used in masonry infill.
- There are no cracks and gaps between frame and masonry infill based on visual inspection according to Chapter 2 of the BSPP manual.

##### **Step 2: Failure mode identification**

The failure mode is identified based on the  $\beta$ -index in Section 4.3.1.

The calculation procedure of one wall is shown below:

i)  $\beta$ -index is calculated using the following procedure:

$$\beta = Q_{frame} / Q_{expected}$$

$$Q_{frame} = \sum Q_{col} = Q_{col\_left} + Q_{col\_right}$$

$Q_{col\_left}$  and  $Q_{col\_right}$  are calculated based on the BSPP seismic evaluation manual (BSPP Evaluation manual).

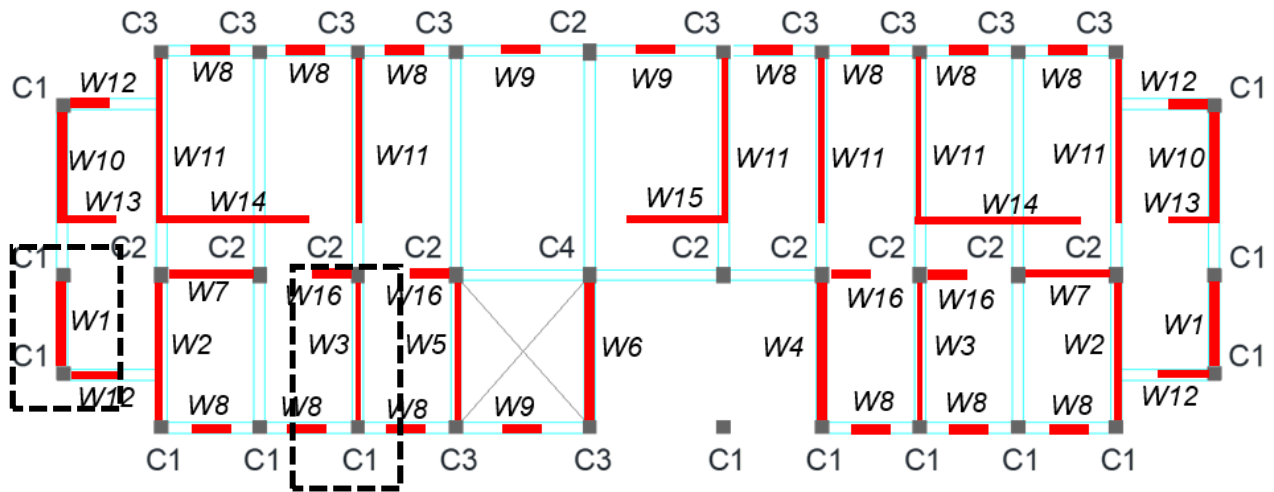


Figure 4.3.4.2 Location of masonry infill

### Case 1: Masonry Infilled RC Frame, W1

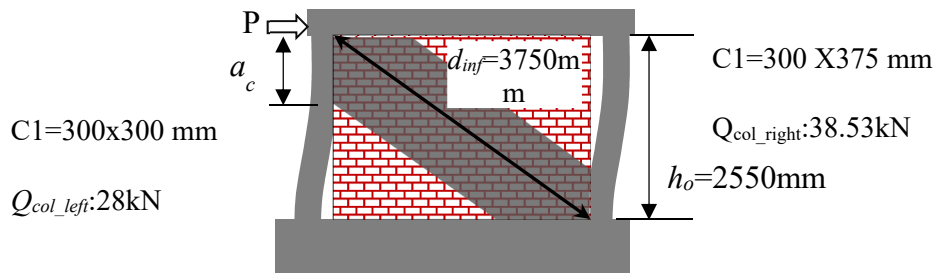


Figure 4.3.4.3 Masonry Infilled RC Frame W1

$$Q_{frame} = 28 + 38.53 = 66.53 \text{ kN}$$

$Q_{expected}$  is calculated using Eq. (4.3.3) in Section 4.3.1

- Prism strength,  $f_m = 8 \text{ MPa}$
- Thickness,  $t_{inf} = 250 \text{ mm}$
- Length of infill,  $l_{inf} = 2750 \text{ mm}$

$$Q_{expected} = 0.05 f_m \cdot t_{inf} \cdot l_{inf} = 0.05 \cdot 8 \cdot 250 \cdot 2750 = 275 \text{ kN}$$

$$\beta = Q_{frame} / Q_{expected} = 0.242$$

From the condition,  $0.2 < \beta < 1$ , Fair confinement: Type II

### Step3: Strength index ( $C_{mw}$ )

Strength index  $C_{mw}$  for an RC frame with masonry infill is calculated by Eq. (4.3.4).

$$C_{mw} = \frac{Q_{mw}}{\sum W}$$



Where  $\Sigma W$  is the weight of the building including live load supported by the story concerned.

Since failure mode is Type II (sliding and diagonal cracking)  
the  $Q_{mw}$  is calculated using the following Eq. (4.3.5).

$$Q_{mw} = Q_{frame} + Q_{sld}$$

Where,  $Q_{frame} = 28 + 38.53 = 66.53$  kN

$Q_{sld}$  will be in the following Eq. (4.3.7)

$$Q_{sld} = \frac{\tau_{inf} \cdot t_{inf} \cdot l_{inf}}{1 - \mu \cdot \frac{h_{inf}}{l_{inf}}}$$

Where  $h_{inf} / l_{inf}$ :  $2550 / 2750 = 0.93$

Friction coefficient,  $\mu$ : 0.45 according to ASTM C1531

Prism strength,  $f_m$ : 8 MPa

Shear strength of infill,  $\tau_{inf}$ :  $0.03 \cdot 8 = 0.24$  MPa

$$Q_{sld} = 0.03 \cdot 8 \cdot 250 \cdot 2750 / (1 - 0.45 \cdot 2550 / 2750) = 284 \text{ kN}$$

$$\text{Lateral strength, } Q_{mw} = Q_{frame} + Q_{sld} = 66.53 + 284 = 351 \text{ kN}$$

Total building weight,  $W = n \cdot A_f \cdot w$

$n$  = Number of stories = 3

$A_f$  = Floor area =  $324.5 \text{ m}^2$

$w$  = Floor unit weight =  $11.20 \text{ kN/m}^2$

Now total weight,  $W = 3 \cdot 324.5 \cdot 11.20 = 10904 \text{ kN}$

Strength index,

$$C_{mw} = \frac{Q_{mw}}{\Sigma W}$$

$$C_{mw} = 351 / 10904 = 0.032$$

#### **Step4: Ductility index, $F$**

Ductility index is considered based on failure mode,

Failure type: II (Sliding and diagonal cracking failure)

**Ductility index:  $F = 1.27$  ( $0.2 < \beta \leq 1$ )**

### **Case 2: Masonry Infilled RC Frame, W3**

Evaluation of masonry infill, W3

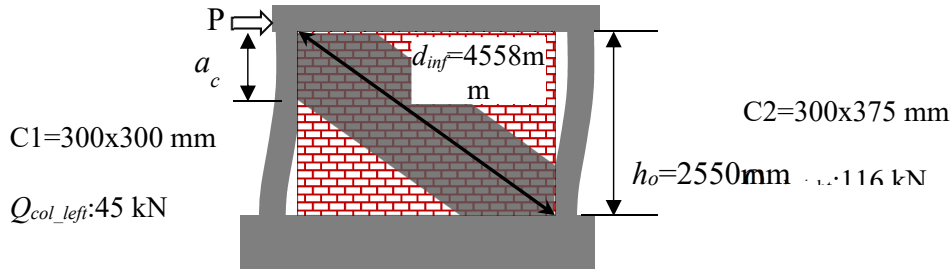


Figure 4.3.4.4 Masonry Infilled RC Frame W3

$$Q_{frame} = 45 + 116 = 161 \text{ kN}$$

$Q_{expected}$  is calculated using Eq. (4.3.1) in Section 4.3.1

- Prism strength,  $f_m = 8 \text{ MPa}$
- Thickness,  $t_{inf} = 250 \text{ mm}$
- Length of infill,  $l_{inf} = 3875 \text{ mm}$

$$Q_{expected} = 0.05 f_m \cdot t_{inf} \cdot l_{inf} = 0.05 \cdot 8 \cdot 125 \cdot 3875 = 194 \text{ kN}$$

$$\beta = \frac{Q_{frame}}{Q_{expected}} = 0.83$$

From the condition,  $0.2 < \beta < 1$ , Fair confinement: Type II

### Step3: Strength index ( $C_{mw}$ )

Strength index  $C_{mw}$  for an RC frame with masonry infill is calculated by Eq. (4.3.4).

$$C_{mw} = \frac{Q_{mw}}{\Sigma W}$$

Where  $\Sigma W$  is the weight of the building including live load supported by the story concerned.

Since failure mode is II, (sliding and diagonal cracking)

the  $Q_{mw}$  is calculated using the following Eq. (4.3.5).

$$Q_{mw} = Q_{frame} + Q_{sld}$$

Where,  $Q_{frame} = 45 + 116 = 161 \text{ kN}$

$Q_{sld}$  will be in the following Eq. (4.3.7)

$$Q_{sld} = \frac{\tau_{inf} \cdot t_{inf} \cdot l_{inf}}{1 - \mu \cdot \frac{h_{inf}}{l_{inf}}}$$

Where  $h_{inf} / l_{inf} : 2550 / 3875 = 0.65$

Friction coefficient,  $\mu : 0.45$  according to ASTM C1531

Prism strength,  $f_m : 8 \text{ MPa}$

Shear strength of infill,  $\tau_{inf} : 0.03 \cdot 8 = 0.24 \text{ MPa}$

$$Q_{sld} = 0.03 \cdot 8 \cdot 125 \cdot 3875 / (1 - 0.45 \cdot 2550 / 3875) = 284 \text{ kN}$$

$$\text{Lateral strength, } Q_{mw} = Q_{frame} + Q_{sld} = 161 + 164 = 325 \text{ kN}$$

Total building weight,  $W = n \cdot A_f \cdot w$

$n$ =Number of stories=3

$A_f$ =Floor area=324.5 m<sup>2</sup>

$w$ =Floor unit weight=11.20 kN/m<sup>2</sup>

Now total weight,  $W=3*324.5*11.20=10904$  kN

Strength index,

$$C_{mw} = \frac{Q_{mw}}{\sum W}$$

$$C_{mw} = 325/10904 = 0.029$$

#### **Step4: Ductility index, $F$**

Ductility index is considered based on failure mode,

Failure type: II (Sliding and diagonal cracking failure)

**Ductility index:  $F = 1.27$  ( $0.2 < \beta \leq 1$ )**

#### **4.3.4.4 Summary**

Based on this analysis,

Infill wall  $W_1$  :

The failure mode is considered Type II (Sliding and diagonal cracking failure mode). Strength index,  $C_{mw}$ , is 0.032 and Ductility index,  $F$ , is 1.27, respectively.

Infill wall  $W_3$ :

The failure mode is considered Type II (Sliding and diagonal cracking failure mode). Strength index,  $C_{mw}$ , is 0.029 and Ductility index,  $F$ , is 1.27, respectively.

#### **References:**

Abrams DP, Angel R, Uzarski J (1996). Out-of-plane strength of unreinforced masonry infill panels. Earthquake Spectra; 12(4):825–844

Al-Chaar G, Lamb GE, Issa MA. (2003). Effects of openings on structural performance of unreinforced masonry infilled frames. ACI Special Publication. SP-211-12; 247–261

Alwashali H., Sen D., Jin K. and Maeda M, Experimental investigation of influences of several parameters on seismic capacity of masonry infilled reinforced concrete frame. Engineering Structures 189 (2019) 11–24. doi.org/10.1016/j.engstruct.2019.03.020

Alwashali H., “Seismic Capacity Evaluation of Reinforced Concrete Buildings with Unreinforced Masonry Infill in Developing Countries”, Ph.D. Thesis, Tohoku Univ. 10/2018

American Society of Civil Engineers (ASCE) (2007). Seismic Rehabilitation of Existing Buildings. Reston, Virginia (ASCE/SEI 41-06)

Angel R, Abrams D, Shapiro D, Uzarski J & Webster M. (1994). Behaviour of reinforced concrete frames with masonry infills. Report No. UILU - ENG - 94 - 2005. Department of Civil Engineering, University of Illinois, Urbana - Champaign, IL, USA.

Public Works Department “Manual for Seismic Evaluation of Existing Reinforced Concrete Buildings (Second edition),” Prepared under the Project on Promoting Building Safety for Disaster Risk Reduction (BSPP), A Technical Cooperation Project between PWD and JICA, November 2021.

Bose S, Rai DC (2016) Lateral load behavior of an open-ground-story RC building with AAC infills in upper stories. *Earthq Spectra* 32(3):1653–1674. doi:10.1193/121413EQS295M.

Chopra Anil. K. (2007). Dynamics of Structures, Theory and Application to Earthquake Engineering. 3rd edition, Upper-Saddle River, NJ: Pearson Prentice Hall.

Dawe JL & Seah CK. Behaviour of masonry infilled steel frames. *Journal of the Canadian Society of Civil Engineering* 1989; 16: 865–876.

Flanagan, R. D., and Bennett, R. M. (1999). Arching of masonry infilled frames: Comparison of analytical methods. *Pract. Period. Struct. Des. Constr.*, 4(3), 105–110.10.1061/(ASCE)1084-0680(1999)4:3(105)

Hamid AA & Drysdale RG (1981). Concrete masonry under combined shear and compression along the mortar joints. *ACI Journal*, 1314–320

Hetenyi, M. (1946). Beams On Elastic Foundation Theory with applications in the fields of civil and mechanical engineering (1st ed.). Michigan, USA: The University of Michigan Press.

Imran L, Aryanto A (2009) Behavior of reinforced concrete frames in-filled with lightweight materials under seismic loads. *Civil Eng Dimens* 11(2):69–77.

Japan Building Disaster Prevention Association (JBDPA) (2001). Standard for Seismic Evaluation of Existing Reinforced Concrete Buildings.

Jin KW, Choi H, Nakano Y (2016) Experimental study on lateral strength evaluation of unreinforced masonry-infilled RC frame. *Earthq Spectra* 32:1725–1747. doi:10.1193/00714EQS152M.

Kakaletsis D. J, Karayannis CG (2009) Experimental investigation of infilled reinforced concrete frames with openings. *ACI Struct J* 106(2):132–141.

Masonry Standards Joint Committee (MSJC) (2016). Building Code Requirements and Specification for Masonry Structures and Related Commentaries. Farmington Hills, MI.

Mehrabi AB, Shing PB, Schuller M, Noland J. (1996). Experimental Evaluation of Masonry infilled RC Frames. *Journal of Structural Engineering*, ASCE, Vol. 122, No. 3.

New Zealand Society for Earthquake Engineering (NZSEE) (2006). *Assessment and Improvement of the Structural Performance of Buildings in Earthquakes*. NZSEE, Wellington, New Zealand, Section 9.

New Zealand Society for Earthquake Engineering (2017). *The seismic assessment of existing buildings*. July, 2017, Section C7, Moment Resisting Frames with Infill Panels

Masonry Standards Joint Committee (MSJC) (2016). *Building Code Requirements and Specification for Masonry Structures and Related Commentaries*. Farmington Hills, MI.

Paulay T, Priestley MJN (1992) *Seismic Design of Reinforced Concrete and Masonry Buildings*. John Wiley & Sons.

Saneinejad A, Hobbs B (1995). Inelastic Design of Infilled Frames. *Journal of Structural Engineering*, (121) 4: 634-650, 1995.

Suzuki T, Choi H, Sanada Y, Nakano Y, Matsukawa K, Paul D, Gülkan P, Binici B (2017) Experimental evaluation of the in-plane behavior of masonry wall infilled RC frames. *Bull Earthq Eng*. doi:10.1007/s10518-017-0139-1

Tasnimi AA, Mohebkah A. (2011). Investigation on the behavior of brick-infilled steel frames with openings, experimental and analytical approaches. *Engineering Structures* 33: 968–980.



## Chapter 5 RC Beam-Column Joint

### 5.1 General

The seismic performance of RC buildings in Bangladesh shall be evaluated considering a potential risk of pull-out failure of beam longitudinal rebar from exterior beam-column joint.

#### C.5.1 [Commentary]

One of the specific problems that exist in RC buildings in Bangladesh is a lack of the structural integrity of exterior beam-column joint (Figure C.5.1 shows a typical exterior beam-column joint under construction in 2017). In Bangladesh, plain bar (round bar) was common for RC construction more or less before 1995 and was gradually replaced by deformed bar after 1995. After the advent of deformed bar in construction, beam longitudinal rebar began to be anchored without end hook (by straight anchorage) to exterior beam-column joint in many buildings which were constructed under poor construction management until 2006 when Bangladesh National Building Code (BNBC) was enforced by the government. Such poorly anchored beam longitudinal rebar has a potential risk of pull-out failure. Therefore, detailed inspection is recommended to clarify anchorage details of beam longitudinal rebar to exterior beam-column joint for the seismic evaluation of the existing buildings; however, destructive tests cannot be performed in many of the buildings because of the building owners' opinion.

Considering the above background, estimating the structural performance of exterior beam-column joint with poor anchorage of beam longitudinal rebar was an urgent issue to appropriately evaluate the seismic performance of Bangladeshi RC buildings. The supplement presents a flow of the seismic evaluation based on some experimental investigations performed under the SATRTEPS-TSUIB project, as shown in Figure C.5.2. This procedure considers the ductility (deformation capacity) limit,  $F_{limit}$  ( $= 2.2$ ) to occur brittle pull-out failure. The ordinary procedure can be applied to the seismic evaluation within the proposed  $F_{limit}$ , while the following procedure shall be followed beyond the limit.



Figure C.5.1 Typical exterior beam-column joint under construction in 2017.

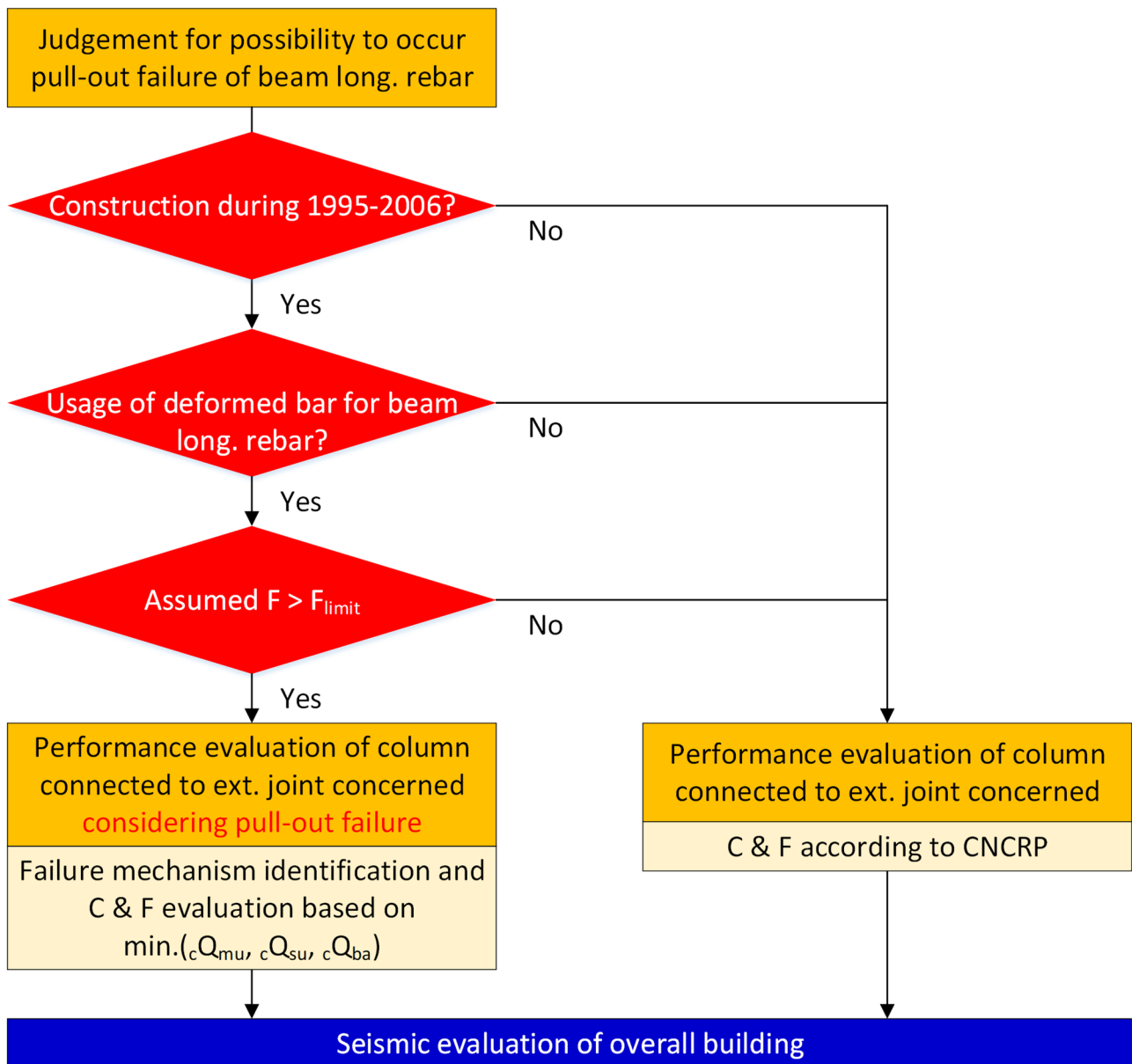


Figure C.5.2 Flow of the seismic performance evaluation considering existence of exterior beam-column joint with poor anchorage of beam longitudinal rebar.

## 5.2 Scope

The scope is limited to exterior beam-column joints in RC buildings with insufficient anchorage of beam longitudinal rebar.



### C.5.2 [Commentary]

The procedure presented in Figure 2 evaluates the seismic performance of RC columns connected to exterior beam-column joints which possibly have poor anchorage of beam longitudinal rebar showing brittle pull-out failure. Therefore, the scope is mainly limited to exterior beam-column joints in RC buildings constructed within 1995 to 2006 because those contain deformed bar with straight anchorage.

#### 5.3 Failure mechanism identification

The following procedure is for the case satisfying the conditions having a possibility to occur pull-out failure of beam longitudinal rebar presented in Figure 2.

A failure mechanism of joint affects the column shear resistance consist of the joint,  $C_c$ , then the strength index of building concerned,  $C$ . Therefore, the column failure mechanism shall be identified as that showing the minimum of the following column shear resistances:  ${}_cQ_{mu}/{}_cQ_{su}$ , and  ${}_cQ_{ba}$ .

${}_cQ_{mu}/{}_cQ_{su}$  are evaluated according to the CNCRP manual.

$${}_cQ_{ba} = \frac{{}_bM_{ba} \frac{L_b}{L_b - D_c}}{L_c} \quad (1)$$

$${}_bM_{ba} = 0.9 \cdot T_{ba} \cdot d \quad (2)$$

$$T_{ba} = \sum \pi \cdot d_b \cdot l_{ba} \cdot \tau_{ba} \quad (3)$$

$$\tau_{ba} = 0.7 \left( 1 + \frac{\sigma_0}{\sigma_B} \right) \sigma_B^{2/3} \quad (4)$$

where

${}_cQ_{mu}$ :	column shear resistance at the flexural yielding.
${}_cQ_{su}$ :	column shear strength at the shear failure.
${}_cQ_{ba}$ :	column shear resistance at pull-out failure of beam connected to the column.
${}_bM_{ba}$ :	flexural strength of beam at pull-out failure
$L_b$ :	Span length of beam
$L_c$ :	column height (= story height)
$D_c$ :	column depth
$d$ :	beam effective depth
$d_b$ :	diameter of beam longitudinal rebar
$l_{ba}$ :	anchorage length of beam longitudinal rebar; when $l_{ba}$ is unknown $l_{ba} = \frac{2}{3} D_c$
$\sigma_0$ :	axial force on the joint (N/mm <sup>2</sup> )
$\sigma_B$ :	compressive strength of concrete (N/mm <sup>2</sup> )

#### 5.4 C-index

The  $C$ -index of exterior column is evaluated as follows:

$$C_c = \frac{\min({}_cQ_{mu}, {}_cQ_{su}, {}_cQ_{ba})}{\sum W} \quad (5)$$

where

$\sum W$ : total weight supported by the story concerned

#### 5.5 F-index

The  $F$ -index of exterior column is evaluated as follows:

In the case that the failure mode is flexural yielding/shear failure (the min.(  $cQ_{mu}$ ,  $cQ_{su}$ ,  $cQ_{ba}$ ) is  $cQ_{mu}$  or  $cQ_{su}$ ), the  $F$ -index follows that of column provided in the CNCRP manual.

Otherwise, the  $F$ -index is  $F_{limit}$ .

### C.5.3-C.5.5 [Commentary]

The ordinary procedure considers two patterns of column failure mode: flexural failure or shear failure when the lateral resistance of a building concerned is evaluated. However, brittle pull-out failure of beam longitudinal rebar may result in lower lateral force-resisting capacity of the column, as illustrated in Figure C.5.3. Therefore, when satisfying the conditions having a possibility to occur pull-out failure of beam longitudinal rebar, the column failure mechanism shall be appropriately identified considering the pull-out failure of beam longitudinal rebar from the joint connecting to the column concerned.

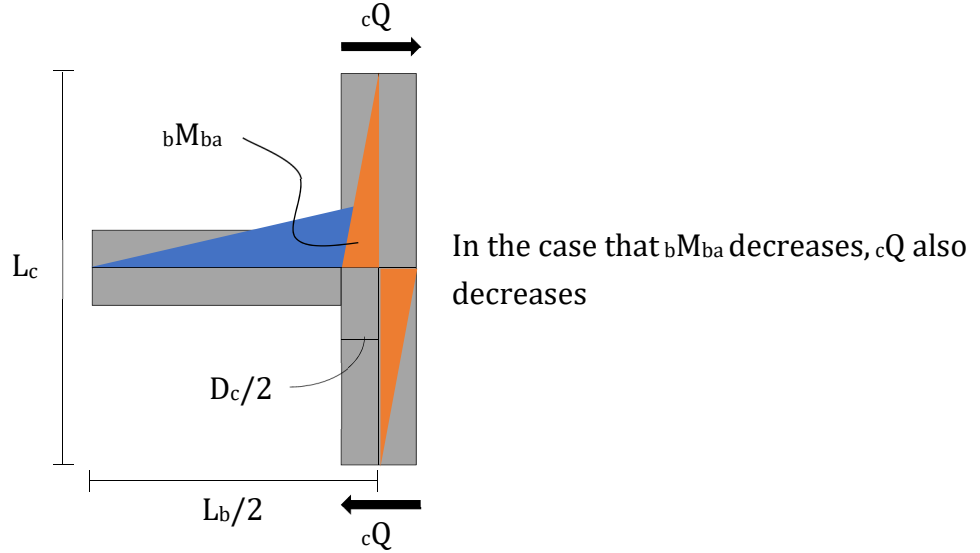
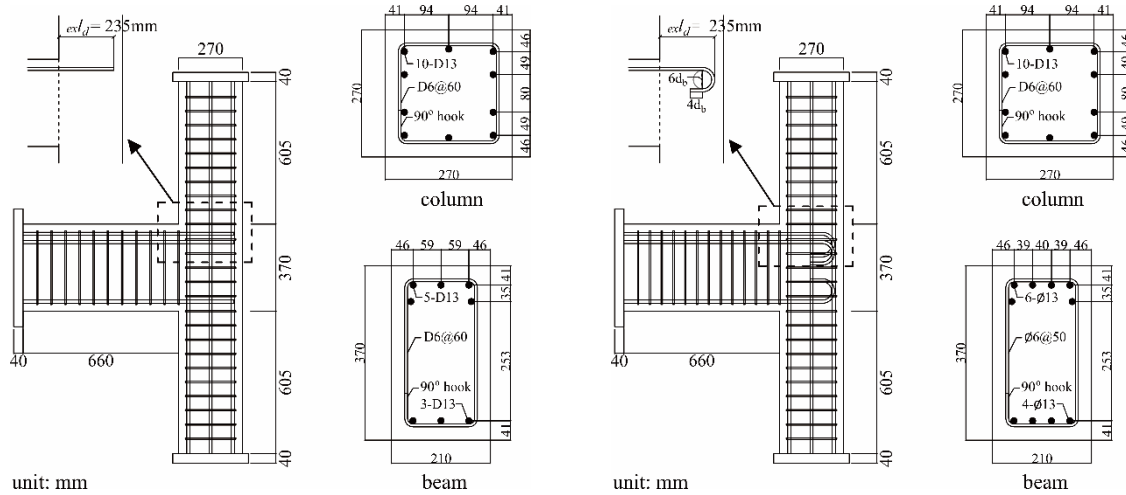


Figure C.5.3 Equilibrium of moment/force at beam-column joint for equation (1).

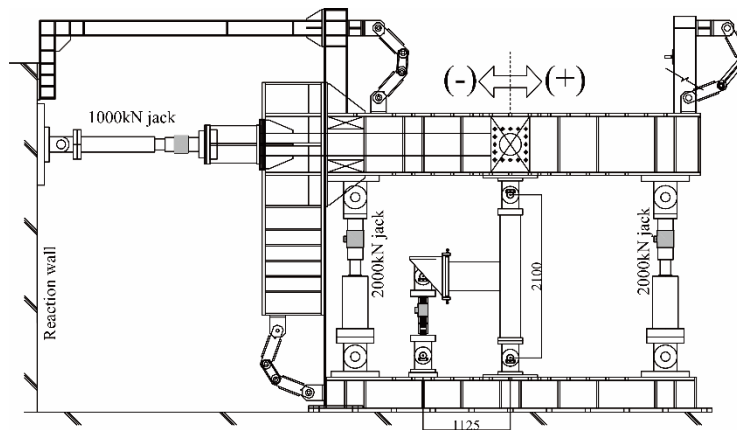
Figure 4 summarizes the structural tests on typical beam-column joints in Bangladeshi RC buildings performed in the SATREPS-TSUIB project<sup>1)</sup>. The specimens were 70% scale models representing two types of typical beam-column joints in Bangladesh: Figure 4a with straight anchorage at the end of beam deformed rebar used after 1995 (hereafter J1) and Figure 4b with 180° degree end hook at the end of beam plain rebar used before 1995 (hereafter J2). Figure 5 compares the test results between both specimens applied static cyclic loading by the apparatus shown in Figure 4c. The specimen J1 showed more brittle behavior in the negative loading direction with pull-out failure, as shown in the photograph, while the lateral resistance gradually degraded with joint shear failure in the positive loading direction. The pull-out failure initiated at a drift angle of -1.5% rad, thus the ductility limit,  $F_{limit}$  was proposed at 2.2 consistent to the 1.5% drift angle. In addition, an initial yielding of the beam longitudinal rebar was observed during the loading cycle to 0.75%; thus, the beam ductility ratio at the pull-out failure was approximately 2.0, which was consistent to the  $F_{limit}$  of 2.2. On the other hand, the specimen J2 behaved in a similar manner to that of J1 in the positive loading direction showing joint shear failure. The ductility of J2 was 4.0% rad ( $F > 3.2$ ); thus, the evaluation of joint shear failure was not considered in this procedure. Furthermore, the specimen J1 was modeled and analyzed using FEM. Bond strength on the FE model was determined using the design formula by equation (4)<sup>2)</sup>. The analytical result is compared to the experimental one in Figure 6. The FEM analysis reproduced similar brittle pullout failure which was observed in the experiment, while the estimation was conservative in both loading directions. Thus, the pull-out capacity of the beam was conservatively evaluated by the FE model applied the bond strength by

equation (4). Based on the above experimental and analytical studies, the supplement recommends to evaluate the flexural strength of beam at pull-out failure by equations (2) to (4) when satisfying the conditions having a possibility to occur pull-out failure of beam longitudinal rebar. In practical application, however, the existing anchorage length of beam longitudinal rebar may be unclear; thus, the supplement suggests to apply two third of the depth of column concerned to the anchorage length. This value was adopted for conservative evaluation of the resistance to pull-out failure after discussions with Bangladeshi expert engineers.



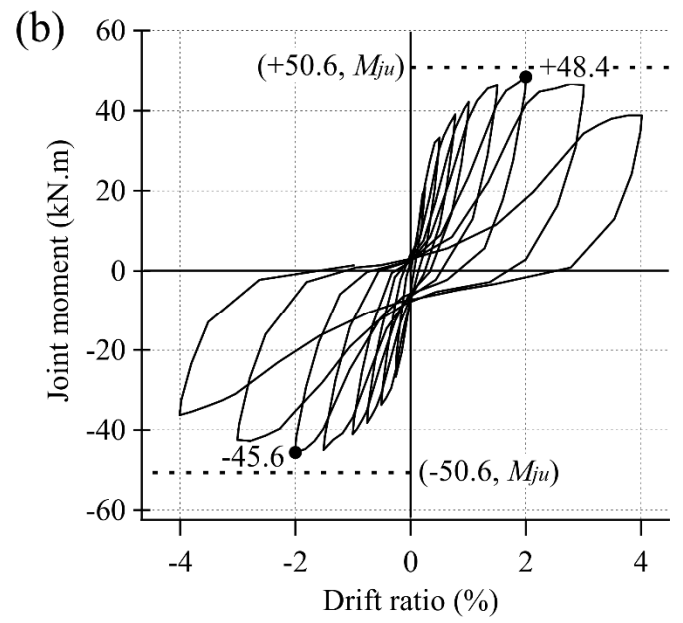
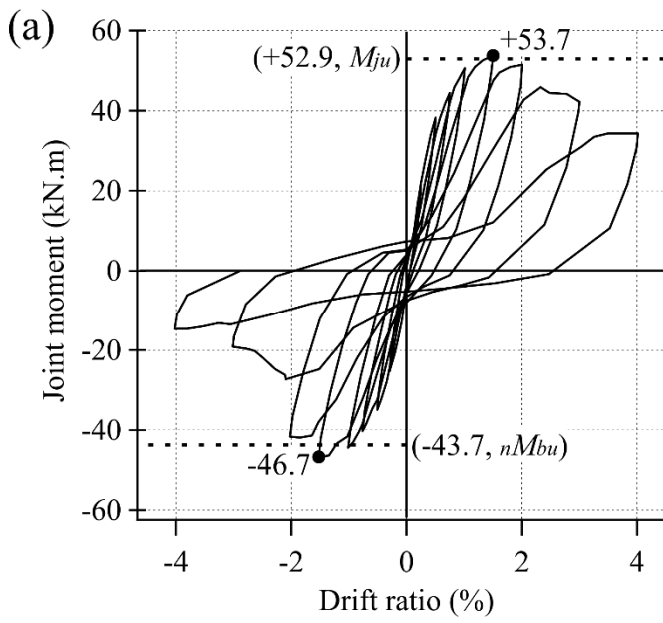
(a) Specimen representing construction after 1995

(b) Specimen representing construction before 1995



(c) Loading apparatus

Figure C.5.4 Test specimens and loading scheme.



(a) Specimen representing construction after 1995

(b) Specimen representing construction before 1995

Figure C.5.5 Comparisons of the seismic performance.

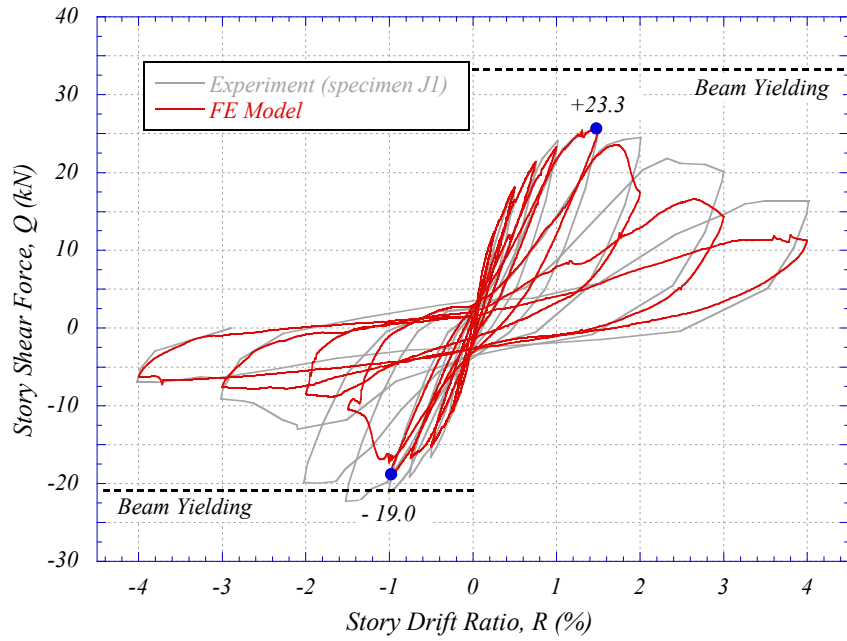
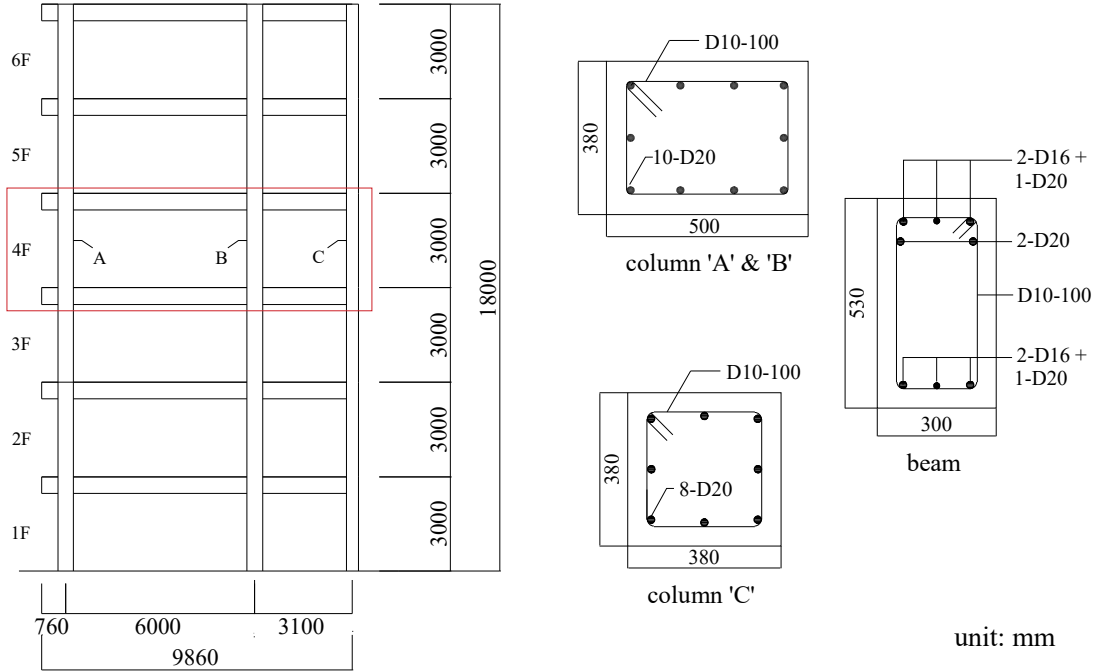


Figure C.5.6 Comparison between the experiment and FE analysis.

In the SATREPS project, however, a smaller drift angle of approximately 0.5% at pull-out failure of beam longitudinal rebar was also observed in another test using the moment-resisting frame specimen representing a typical Bangladeshi RC building<sup>3)</sup>. However, the present supplement tentatively adopted the  $F_{limit}$  of 2.2 corresponding to the drift angle of 1.5% because the scale of the test specimen was much small at 40%. Therefore, more experimental studies are recommended to strengthen experimental data and the  $F_{limit}$  should be modified based on future findings.

## 5.6 Example of exterior beam-column joint capacity estimation

The above evaluation procedure is applied to a sample building, as shown in Figure C.5.6, focusing on the plane frame consisting of three columns on the 4<sup>th</sup> floor. The detailed calculation is shown only for the column 'C' which is also a component of the exterior beam-column joint on the 5<sup>th</sup> floor.



### Other specifications:

Concrete strength,  $\sigma_B = F_c = 10 \text{ MPa}$ ;

Rebar strength,  $\sigma_y = 275 \text{ MPa}$ ;

Axial load  $N$  for the column 'C' = 289.9 kN;

Constructed in 2001.

Figure 5.7 Sample building.

### Flexural capacity evaluation according to the CNCRP manual.

$${}_cQ_{mu} = \frac{2M_u}{h_0}$$

$$\text{for } 0.4b \cdot D \cdot F_c \geq N > 0$$

$$M_u = 0.8a_t \cdot \sigma_y \cdot D + 0.5N \cdot D \cdot \left(1 - \frac{N}{b \cdot D \cdot F_c}\right)$$

where,

$$M_u = 122.8 \text{ kN} \cdot \text{m}$$

thus

$${}_cQ_{mu} = \frac{2M_u}{h_0} = 99.4 \text{ kN}$$

### Shear capacity evaluation according to the CNCRP manual

$${}_cQ_{su} = k_r \cdot \left\{ \frac{0.053p_t^{0.23}(18 + \sigma_B)}{M/(Q \cdot d) + 0.12} + 0.85\sqrt{p_w \cdot s_{wy} + 0.1\sigma_0} \right\} \cdot b \cdot j$$

where

$$k_r = 0.244 + 0.056\sigma_B$$

$$M/Q = h_0/2$$

thus

$${}_cQ_{su} = 143.1 \text{ kN}$$

### C-index and F-index evaluation according to the CNCRP manual

$${}_cQ_u = \min\{ {}_cQ_{mu}, {}_cQ_{su} \} = 99.4 \text{ kN}$$

Following the procedure explained in the CNCRP manual, the C-index and F-index can be evaluated and the following C-F relationship can be found, as shown in Table 5.1 and Figure 5.8.

Table 5.1 List of the C-index and F-index according to the CNCRP manual.

Column ID	$Q_u$ (kN)	$\Sigma W$ (kN)	C-index	F-index
<b>A</b>	166.7	1771	0.094	2.32
<b>B</b>	165.2		0.093	1.04
<b>C</b>	99.4		0.056	3.17

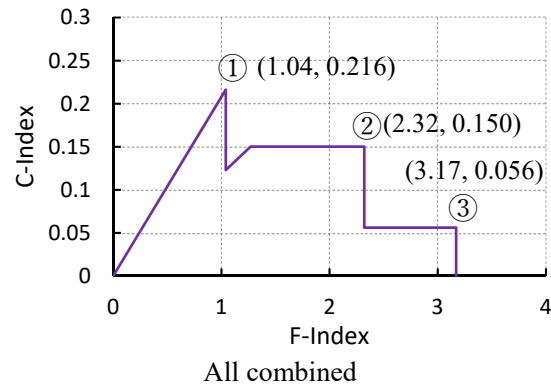
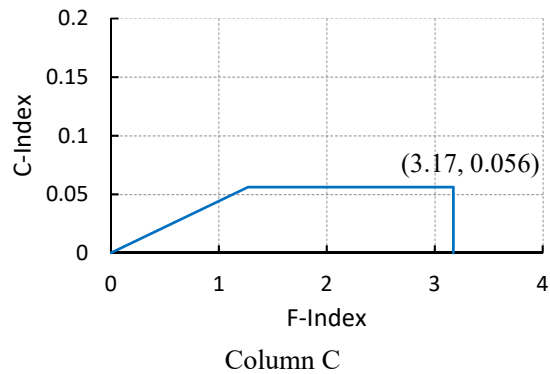
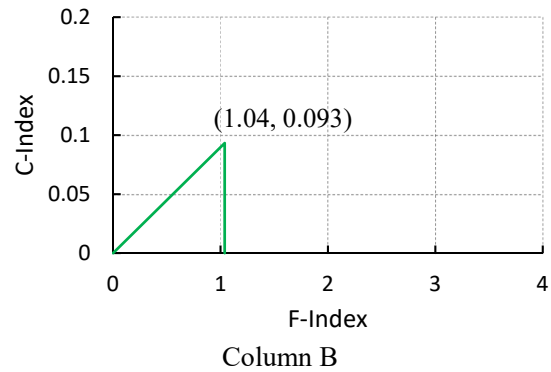
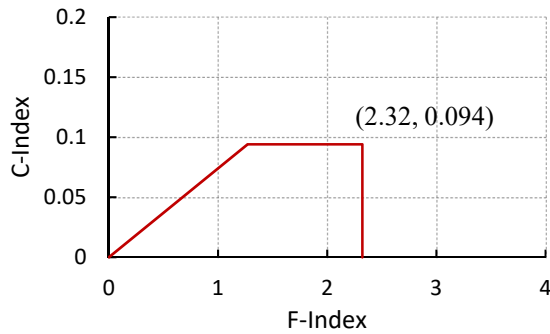


Figure 5.8 C-F relationship according to the CNCRP manual.

### E<sub>0</sub>-index evaluation according to the CNCRP manual



From Eq. (4) for the ductile-dominant basic seismic index  $E_0$  in the CNCRP manual,

$$E_0 = \frac{n+1}{n+i} \left( \sqrt{E_1^2 + E_2^2 + E_3^2} \right) = 0.316$$

where

$$n = \text{number of story} = 6$$

$$i = \text{concerned story} = 4$$

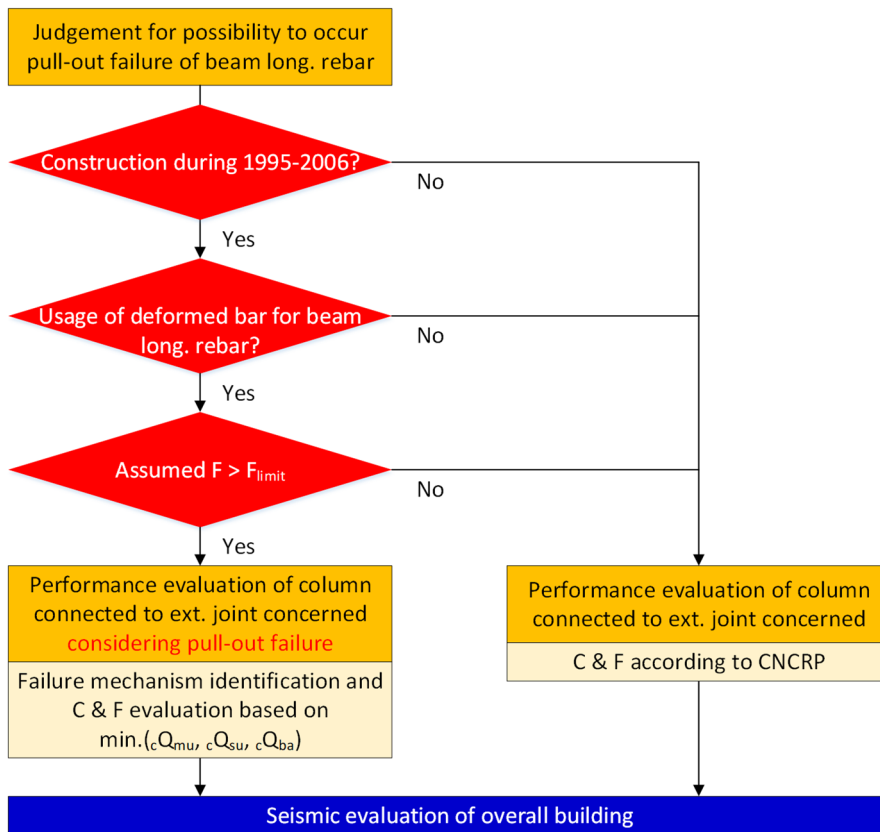
From Eq. (5) for the strength-dominant basic seismic index  $E_0$  in the CNCRP manual, the maximum value is obtained at  $F = 2.32$ , as shown in Figure C.5.8:

$$E_0 = \frac{n+1}{n+i} \left( C_1 + \sum_j \alpha_j C_j \right) \cdot F_1 = 0.244$$

$E_0$  is the larger one between Eq. (4) and Eq. (5); thus,  $E_0 = 0.316$ .

### **Judgement for possibility of pull-out failure**

According to Figure C.5.2 also shown below, a possibility of pull-out failure at the exterior beam on the 5<sup>th</sup> floor is judged. Consequently, the building has the possibility because of the construction year of 2001, usage of deformed rebar, and the adopted  $F$ -index of 2.32 beyond the  $F_{limit}$  of 2.2.



### Pull-out capacity evaluation

$${}_cQ_{ba} = \frac{{}_bM_{ba} \frac{L_b}{L_b - D_c}}{L_c}$$

where

$${}_bM_{ba} = 0.9 \cdot T_{ba} \cdot d$$

$$T_{ba} = \sum \pi \cdot d_b \cdot l_{ba} \cdot \tau_{ba}$$

$$\tau_{ba} = 0.7 \left( 1 + \frac{\sigma_0}{\sigma_B} \right) \sigma_B^{2/3} = 3.90 \text{ N/mm}^2$$

Span length of beam,  $L_b = 3100 \text{ mm}$

Column height,  $L_c = 3000 \text{ mm}$

Column depth,  $D_c = 380 \text{ mm}$  Anchorage length of beam longitudinal rebar,  $l_{ba} = \frac{2}{3} D_c$   
 $= \frac{2}{3} \times 380 = 253.3 \text{ mm}$

$$\text{Axial stress of column, } \sigma_0 = \frac{N}{b \cdot D_c} = \frac{289.9 \times 1000}{380 \times 380} = 2.01 \text{ N/mm}^2$$

As shown above, the anchorage length of beam longitudinal rebar is unknown; thus, the anchorage length should be assumed to be  $\frac{2}{3}$  depth of the column.

In the case of the positive loading from left to right in Figure 7,

Diameter of beam longitudinal rebar,  $d_b = 16 \text{ mm}$  (two rebars) &  $20 \text{ mm}$  (three rebars)

$$\sum \pi \cdot d_b = 2 \times (\pi \times 16) + 3 \times (\pi \times 20) = 289 \text{ mm}$$

Effective beam depth,  $d = 436 \text{ mm}$

$$T_{ba} = 285.7 \text{ kN}$$

$${}_bM_{ba} = 112.1 \text{ kN} \cdot \text{m}$$

thus

$${}_c^+Q_{ba} = 42.6 \text{ kN}$$

In the case of the negative loading from right to left in Figure 7,

Diameter of beam longitudinal rebar,  $d_b = 16 \text{ mm}$  (two rebars) &  $20 \text{ mm}$  (one rebar)

$$\sum \pi \cdot d_b = 2 \times (\pi \times 16) + (\pi \times 20) = 163 \text{ mm}$$

Effective beam depth,  $d = 457 \text{ mm}$

$$T_{ba} = 161.5 \text{ kN}$$

$${}_bM_{ba} = 66.4 \text{ kN} \cdot \text{m}$$

thus

$${}_c^-Q_{ba} = 25.2 \text{ kN}$$

The pull-out capacity is lower in the case of the negative loading; thus, the following evaluation is performed in this case. Since the  $F$ -index is larger than  $F_{limit}$ , as mentioned above, the capacity of column 'C' should be

reduced to  $\bar{c}Q_{ba}$  from  $cQ_u$ . Thus, the structural performance is modified from Table 5.1 and Figure 5.8 to Table 5.2 and Figure 5.9.

Table 5.2. List of the modified C-index and F-index.

Column ID	$Q_u$ (kN)	$\Sigma W$ (kN)	C-index	F-index
<b>A</b>	166.7	1771	0.094	2.32 $\rightarrow$ 2.2
<b>B</b>	165.2		0.093	1.04
<b>C</b>	99.4 $\rightarrow$ 25.2		0.056 $\rightarrow$ 0.014	2.2 ( $F_{limit}$ )

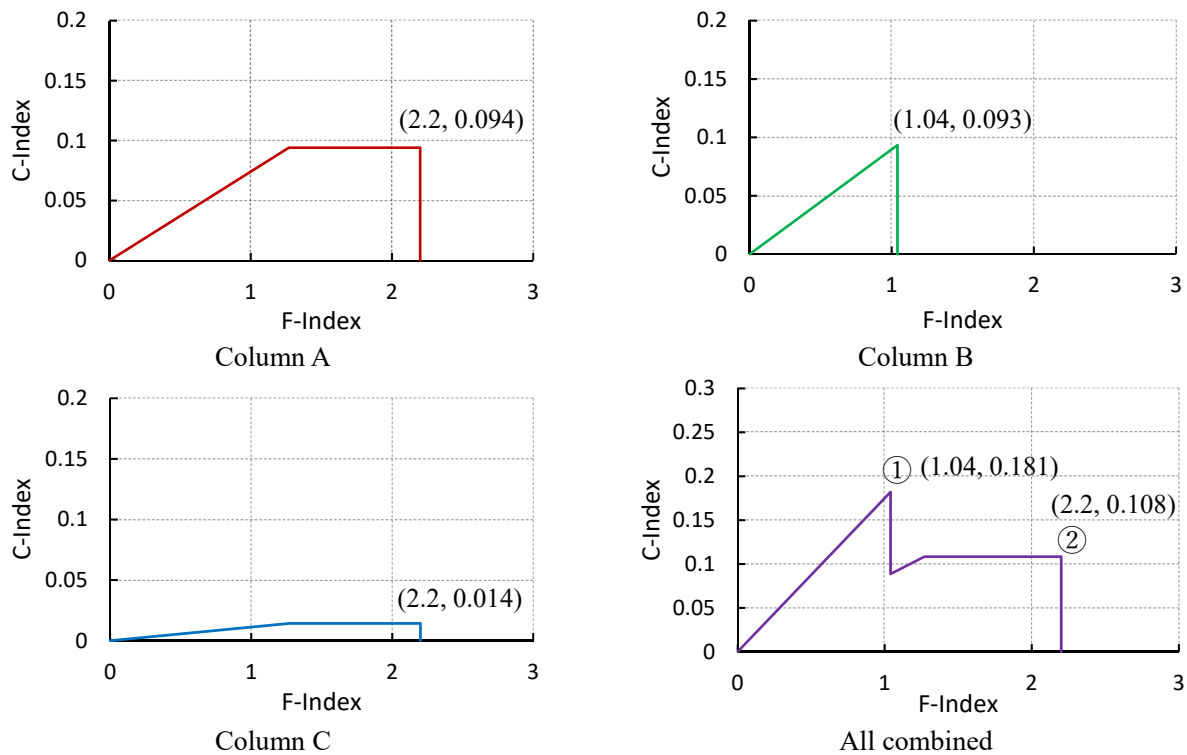


Figure 5.9 Modified C-F relationship.

### E<sub>0</sub>-index modification

From Eq. (4) for the ductile-dominant basic seismic index  $E_0$  in the CNCRP manual,

$$E_0 = \frac{n+1}{n+i} \left( \sqrt{E_1^2 + E_2^2 + E_3^2} \right) = 0.212$$

where

$n$  = number of story = 6

$i$  = concerned story = 4

From Eq. (5) for the strength-dominant basic seismic index  $E_0$  in the CNCRP manual, the maximum value is obtained at  $F = 2.2$ , as shown in Figure 5.9:

$$E_0 = \frac{n+1}{n+i} \left( C_1 + \sum_j \alpha_j C_j \right) \cdot F_1 = 0.166$$

$E_0$  is the larger one between Eq. (4) and Eq. (5); thus, the seismic performance of the sample building is evaluated as  $E_0 = 0.212$ .

### References:

1. Syafri Wardi, Yasushi Sanada, Nandita Saha and Susumu Takahashi: Improving integrity of RC beam-column joints with deficient beam rebar anchorage, *Earthquake Engineering & Structural Dynamics*, Vol. 49, Issue 3, pp. 234-260, Mar. 2020, DOI: 10.1002/eqe.3229.
2. Architectural Institute of Japan: Design Guidelines for Earthquake Resistant Reinforced Concrete Buildings Based on Inelastic Displacement Concept, Sep. 1999.
3. S M Naheed Adnan, Yuji Haga, Kazuto Matsukawa and Yoshiaki Nakano: Behavior of RC Frame with Low Strength Concrete and Straight Anchorage under Extremely High Axial Loads, *Proceedings of the 14th Annual Meeting of Japan Association for Earthquake Engineering*, Sep. 2019.

## Chapter 6 Flat Plate Structures

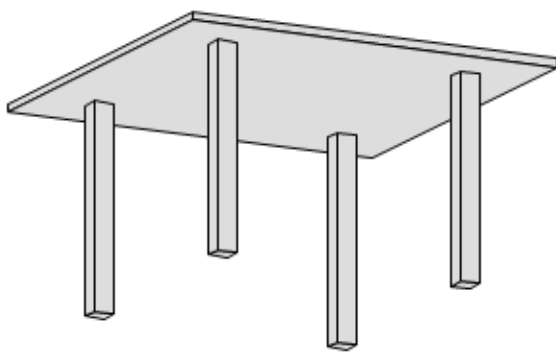
### 6.1 General

Flat plate structure is consisting of flat plate and columns (Figure 6.1.1) and is able to reduce the height of the building, provides flexible spatial planning due to absence of beams. Moreover, absence of beams makes it easy to set up formwork. However, flat plate structure has a risk to fail in punching shear failure which is a brittle failure and harm structural integrity. To prevent this failure, drop panel is used as shown Figure 6.1.2 and this structure is called flat slab structure.

The Japanese seismic evaluation standard of existing reinforced concrete buildings (JBDPA, 2001), does not include flat plate structures in the scope of application. Therefore, this chapter is intended to be as supplement document in order to evaluate the seismic capacity of flat plate structures commonly used in Bangladesh, based on concepts of the Japanese seismic evaluation standard of existing reinforced concrete buildings (JBDPA, 2001).

In Bangladesh, flat plate structures have beams in perimeter frame and interior columns are not connected to beams (Figure 6.1.3). Because flat plate part (interior columns) are flexible (described in detail later), only the contributions of exterior columns with beams can be considered to evaluate seismic capacity of flat plate structures.

Exterior columns are connected to beams, therefore, the seismic capacity of these members can be calculated same as columns of moment resisting frame. However, flat plate structures have a risk to fail in punching shear failure of interior columns as mentioned above. This supplement prescribes upper limit of deformation to prevent punching shear failure for the calculation of seismic capacity of exterior columns of flat plate structures.

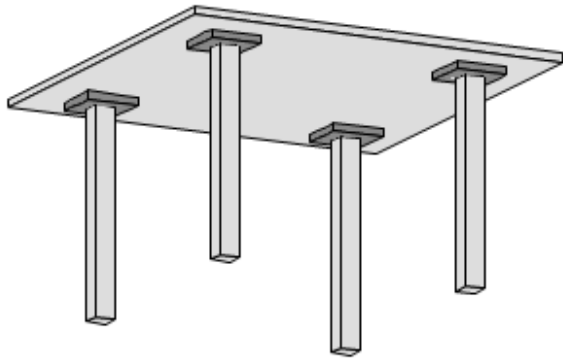


(a) Image of a flat plate structure



(b) An example building in Dhaka

Figure 6.1.1 Flat plate structure

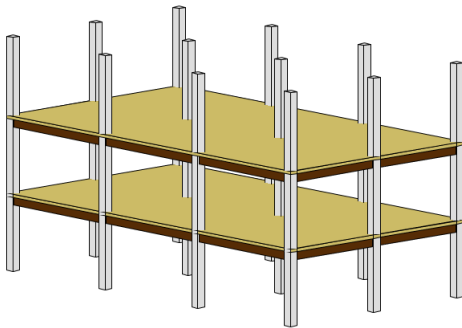


(a) Image of a flat slab structure

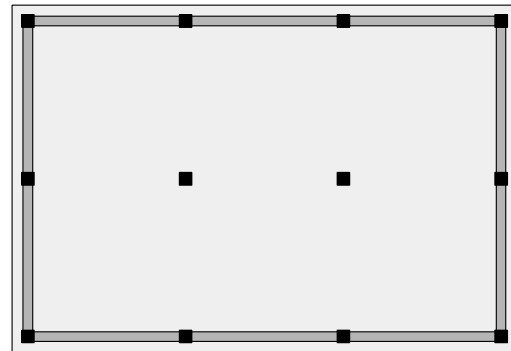


(b) An example building in Dhaka

Figure 6.1.2 Flat slab structure



(a) Isometric view



(b) Beam layout

Figure 6.1.3 Flat-plate structure with beams in perimeter frame

## 6.2 Scope

This supplement is intended to be used in the second level screening procedure (JBDPA, 2001) for flat plate structures with beams on their perimeter. Pure flat plate structures (no beam even in perimeter) are out of scope because the seismic capacity of pure flat plate structures is calculated as zero according to this supplement. The procedures specified in this supplement should be used in principle for seismic evaluation of existing low-rise and medium-rise reinforced concrete buildings of maximum height around six stories.

### 6.3 Judgement of failure mode

#### 6.3.1 Column shear resistance

The exterior column shear resistance  ${}_eQ_u$  is calculated by the following equation according to BSPP Seismic Evaluation Manual.

$${}_eQ_u = \min(Q_{mu}, Q_{su}) \quad (6.3.1)$$

where,  $Q_{mu}$  is column shear force at the flexural yielding of column

$Q_{su}$  is column shear strength at the shear failure

The interior column shear resistance  ${}_iQ_u$  is assumed to be zero in the evaluation of story shear. However, judgement of failure mode of interior column should be done to determine  $F$  index of exterior column.

#### 6.3.2 Lateral Strength of each failure mechanism

For exterior column, two types of failure modes, i. e., (a) flexural yielding and (b) shear failure are considered. The strength of each failure mechanism is calculated as follows. Based on the calculated strengths, the failure mode can be determined by taking the minimum value.

(a)  $Q_{mu}$ : column shear resistance based on the flexural yielding at the top and bottom of a column

$Q_{mu}$  can be calculated same as Chapter 3, Eqs. (3.2.3)-(3.2.6).

(b)  $Q_{su}$ : column shear resistance based on the shear failure of column

$Q_{su}$  can be calculated same as “Manual for seismic evaluation of existing reinforced concrete buildings (CNCRP, p. 48)”.

For interior column, (c) flexural yielding of floor slab and (d) punching shear failure of slab are considered in addition to (a) and (b). The strength of each failure mechanism is calculated as follows. Based on the calculated strengths, the failure mode can be determined by taking the minimum value.

(a)  $Q_{mu}$ : column shear resistance based on the flexural yielding at the top and bottom of a column

$Q_{mu}$  can be calculated same as Chapter 3, Eqs. (3.2.3)-(3.2.6).

(b)  $Q_{su}$ : column shear resistance based on the shear failure of column

$Q_{su}$  can be calculated same as “Manual for seismic evaluation of existing reinforced concrete buildings (CNCRP, p. 48)”.

(c)  $Q_{slab}$ : column shear resistance based on the flexural yielding of slab

$$Q_{slab} = \frac{{}_sM_y}{h_0 / 2} \quad (6.3.2)$$

where,  ${}_sM_y$ : flexural yielding capacity of slab

$h_0$ : clear height of column

Note that, bending moment of slab can be assumed as antisymmetric bending moment and  ${}_sM_y$  is defined as the nodal moment.

For normal strength concrete, flexural capacity of slab  ${}_sM_y$  is calculated by the following equation in which full slab width is assumed to be effective.

$${}_sM_y = 0.9a_t\sigma_y d \quad (6.3.3)$$

where,  $a_t$ : cross section area of tensile reinforcement

$\sigma_y$ : yield stress of reinforcement

$d$ : effective depth of slab

For low strength concrete, flexural capacity of slab  ${}_sM_y$  is calculated based on the following assumptions instead of Eq. (6.3.3).

1. Maximum strain at the extreme concrete compression fiber shall be 0.003.
2. Tensile strength of concrete shall be neglected.
3. Concrete stress distribution is replaced with the equivalent rectangular.

For reinforcement, the following assumptions are used.

1. Reinforcement resist tensile or compressive force.
2. Stress-strain relationship of reinforcement is idealized as bi-linear relationship using the yield stress  $\sigma_y$  and Young's modulus  $E_s$ .

(d)  $Q_{punch}$ : column shear resistance based on the punching shear failure

$$Q_{punch} = \frac{M_u}{h_0} = \left(1 - \frac{V_u}{V_0}\right) \frac{M_0}{h_0} \quad (6.3.4)$$

where,  $V_u$ : vertical load at the ultimate state

$M_u$ : bending moment at the ultimate state

$V_0$ : capacity of vertical load



$$V_0 = \tau_u A_c \quad (6.3.5)$$

$A_c$ : the area of critical section

$$A_c = 2d(c_1 + c_2 + 2d) \quad (6.3.6)$$

$\tau_u$ : direct shear strength of concrete

$$\tau_u = 0.335\sqrt{\sigma_B} \quad \text{for } \sigma_B \geq 13.5 \text{ MPa} \quad (6.3.7)$$

$$\tau_u = \frac{0.38\sqrt{13.5}}{13.5} \sigma_B \quad \text{for } \sigma_B < 13.5 \text{ MPa} \quad (\text{Miyauchi et al., 2009}) \quad (6.3.8)$$

$\sigma_B$ : compressive strength of concrete

$M_0$ : capacity of bending moment

$$M_0 = M_f + M_s + M_t \quad (6.3.9)$$

$M_f$ : bending moment due to the flexural resistance of slab at the critical section

$$M_f = 0.9a_{0t}\sigma_y d \frac{c_2 + d}{x_t} + 0.9a_{0b}\sigma_y d \frac{c_2 + d}{x_b} \quad (6.3.10)$$

$a_{0t}$ : sectional area of a reinforcing bar of slab top layer

$a_{0b}$ : sectional area of a reinforcing bar of slab bottom layer

$x_t$ : space of reinforcing bars of slab top layer

$x_b$ : space of reinforcing bars of slab bottom layer

$\sigma_y$ : yield strength of slab reinforcement

$d$ : effective depth of slab

$c_1$ : column depth

$c_2$ : column width

Note that, for low strength concrete,  $M_f$  should be calculated based on the assumption used in the calculation of  $sM_y$ .

$M_s$ : bending moment due to the shear resistance of slab at the critical section

$$M_s = \tau_u (c_2 + d)d(c_1 + d) \quad (6.3.11)$$

$M_t$ : bending moment due to the torsional resistance of slab at the critical section

$$M_t = \tau_{tu} \frac{d^2}{2} \left\{ (c_1 + d) - \frac{d}{3} \right\} \cdot 2 \quad (6.3.12)$$

$\tau_{tu}$ : torsional shear strength of concrete

$$\tau_{tu} = 6\tau_u \quad (6.3.13)$$

In this supplement, shear resistance of interior columns is assumed to be zero because an experimental study indicates that a connection between interior columns and flat plates are flexible. Figure C.6.3.1 is an example. As seen in Figure C.6.3.2, the applied nodal moment at a drift of 0.4 % was 1.98 kN·m. The specimen was a half scaled model. If story height is assumed to be 3 m, the corresponding height in scaled specimen is 1.5 m. Therefore, when double curvature is assumed, shear force of column at a drift of 0.4 % is  $1.98 \text{ kN} \cdot \text{m} \times 2 / 1.5 \text{ m} = 2.64 \text{ kN}$ . The column size in this experiment was 175mm × 175mm. Shear stress of column was  $2640 \text{ kN} / (175\text{mm} \times 175\text{mm}) = 0.086 \text{ MPa}$ , and it is negligibly small. The contribution of interior columns is assumed to be zero, and shear resistance of exterior columns are calculated by Eq. (6.3.1).



124

moment of slab and shear span length of column is assumed to be a half of clear height of column. The bending moment of the bottom of a column is not equal to  $sM_y$  rigorously, however, this assumption is used for simplification.

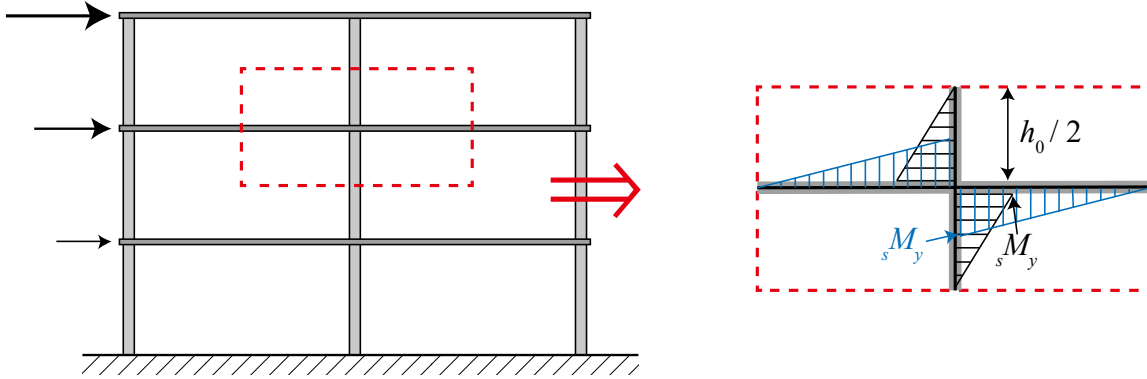


Figure C. 6.3.3 Assumed moment diagram

In the Japanese standard for calculation of reinforced concrete structures (AIJ, 2018), the capacity of connection between column and flat plate is assumed to be consumed by vertical load and bending moment. The vertical load carrying capacity  $V_0$  is shear capacity of connection under vertical load only. Therefore,  $(1 - V_u/V_0)$  in Eq. (6.3.4) is the ratio of the capacity used by the applied vertical load  $V_u$ . Similarly, the capacity of bending moment  $M_0$  is the capacity of connection when it is consumed by bending moment only. Therefore,  $(1 - V_u/V_0) M_0$  is the capacity which can be consumed by bending moment.

The capacity of vertical load  $V_0$  can be calculated as the product of the shear strength of concrete and the area of critical section. The critical section is located  $d/2$  away from the column edge (Figure C.6.3.4).

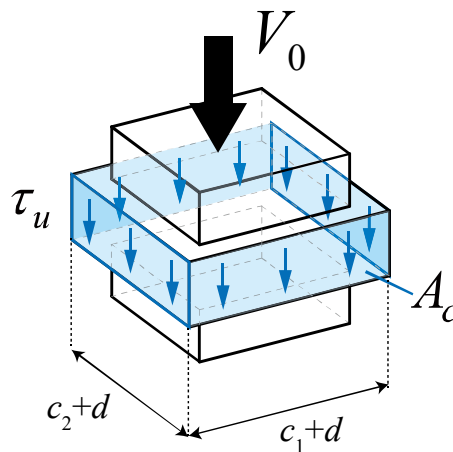


Figure C.6.3.4 Capacity of vertical load

The capacity of bending moment  $M_0$  can be calculated as sum of three components ( $M_f$ ,  $M_s$  and  $M_t$ ) at the critical section as shown in Figure C.6.3.5. The contribution of each component is shown in Eqs. (6.3.10)-

(6.3.12). These equations are sited from the Japanese standard. However, low strength concrete is out of scope of the standard, therefore, a modification on the shear stress of concrete is applied by Eqs. (6.3.7)-(6.3.8) in this supplement.

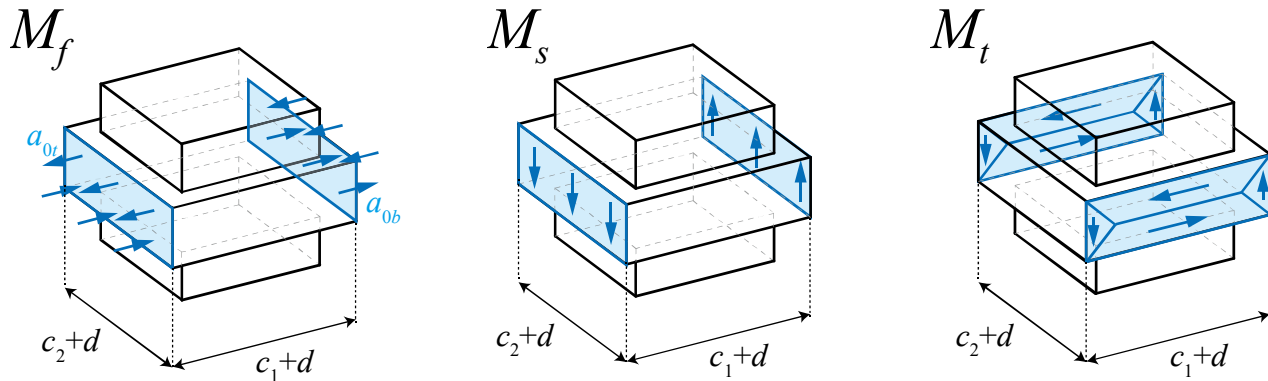


Figure C.6.3.5 Capacity of bending moment

## 6.4 Strength index C

### 6.4.1 C-index of a column

Strength index, C-index of an exterior column with beam is calculated by the following equation.

$$C = Q_u / \Sigma W \quad (6.4.1)$$

where  $\Sigma W$  is the weight supported by the story concerned

C-index of interior column without beam is zero.

## 6.5 Ductility index F

### 6.5.1 F-index of a column

Ductility index, F-index of an exterior column can be determined according to “Manual for seismic evaluation of existing reinforced concrete buildings (CNCRP, pp. 50-58)”. However, if the expected failure mode of interior column without beam is punching shear failure, drift angle of exterior column  $cR_{max}$  cannot exceed 1/50 rad in the evaluation of F-index.

## C.6.5 [Commentary]

As seen in Figs. C.6.4.1 and C.6.4.2, the punching shear failure of a flat plate specimens was observed at 1/50 of a drift in two specimens whereas the concrete strength of these specimens were different. Based on the result, the upper limit of  $cR_{max}$  is determined.

As seen in Figure C.6.4.2, the punching shear failure of a flat plate specimens was observed at 2 % of a drift in two specimens whereas the concrete strength of these specimens were different. Based on the result, the upper limit of F-index is determined.

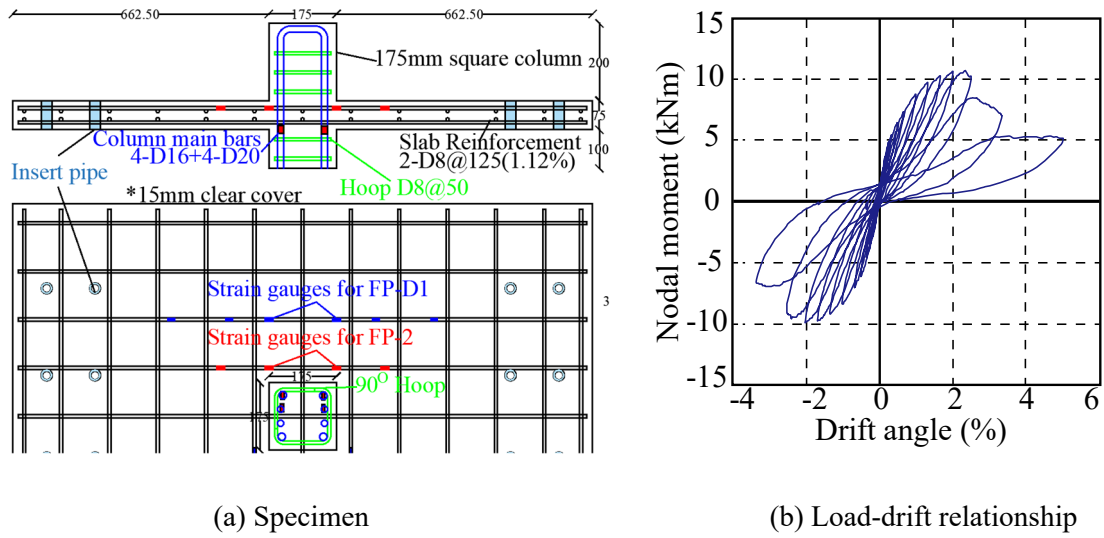


Figure C.6.4.3 Experimental result (Specimen FP-C2)

## 6.6 Limitations

In the experimental study, the ratio of slab reinforcement was around 1 %. Flat plate in which the ratio of slab reinforcement is much different from this value, the upper limit of the drift angle of exterior column  $cR_{max}$  should be carefully determined.

## 6.7 Example of Application

### [Column]

$b \times D$ : 381 mm  $\times$  254 mm (15"  $\times$  10")

$a_t$ : 5-D20 ( $5 \times 314 = 1570 \text{ mm}^2$ )

$\sigma_y$ : 420 MPa (Grade 60)

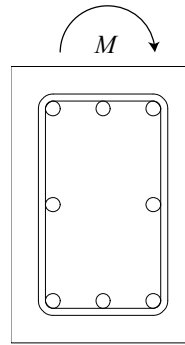
$f'_c$ : 24 MPa

Axial Force: 234 kN ( $\phi = 0.1$  is assumed)

$h_0$ : 3 m

Tie bar: D10@150

$\sigma_{sy}$ : 420 MPa



### [Slab]

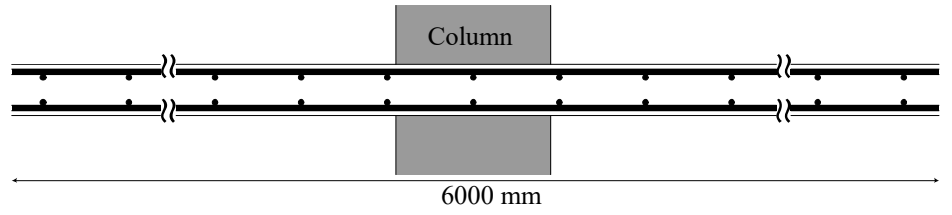
Thickness: 125 mm

Span: 6 m

Reinforcement: D12@125

$\sigma_y$ : 420 MPa

$f'_c$ : 24 MPa



(a)  $Q_{mu}$ : column shear resistance based on the flexural yielding of column

In the case of this example, axial load  $N$  satisfy the following relation.

$$0.4bDf'_c > N > 0$$

Therefore,

$$\begin{aligned} M_u &= 0.8a_t\sigma_y D + 0.5ND \left( 1 - \frac{N}{bDf'_c} \right) \\ &= 0.8 \times 1570 \times 420 \times 254 + 0.5 \times 234000 \times 254 \times \left( 1 - \frac{234000}{381 \times 254 \times 24} \right) \\ &= 160713985 \text{ (N} \cdot \text{mm)} \\ &= 161 \text{ (kN} \cdot \text{m)} \end{aligned}$$

$$Q_{mu} = M_u / (h_0 / 2) = 161 / 1.5 = 107 \text{ (kN)}$$

(b)  $Q_{su}$ : column shear resistance based on the shear failure of column

$$\begin{aligned} Q_{su} &= \left\{ \frac{0.053p_t^{0.23}(f'_c + 18)}{M / (Qd) + 0.12} + 0.85\sqrt{p_w\sigma_{wy}} + 0.1\sigma_0 \right\} bj \\ &= \left\{ \frac{0.053 \times 0.97^{0.23}(24 + 18)}{3} + 0.85\sqrt{0.00248 \times 420} + 0.1 \times 2.4 \right\} 381 \times 200 \\ &= 140537 \text{ (N)} \\ &= 141 \text{ (kN)} \end{aligned}$$

(c)  $Q_{slab}$ : column shear resistance based on the flexural yielding of slab

$$\begin{aligned} {}_sM_y &= 0.9a_t\sigma_y d = 0.9 \times 48 \times 113 \times 420 \times 112.5 \\ &= 230655600 \text{ (N} \cdot \text{mm)} \\ &= 231 \text{ (kN} \cdot \text{m)} \end{aligned}$$

$$\begin{aligned}
Q_{slab} &= M_y / (h_0 / 2) \\
&= 231 / 1.5 \\
&= 154 \text{ (kN)}
\end{aligned}$$

(d)  $Q_{punch}$ : column shear resistance based on the punching shear failure

$$\begin{aligned}
M_f &= 0.9a_{0t}\sigma_y d \frac{c_2 + d}{x_t} + 0.9a_{0b}\sigma_y d \frac{c_2 + d}{x_b} \\
&= 0.9 \times 113 \times 420 \times 112.5 \times \frac{381 + 112.5}{125} + 0.9 \times 113 \times 420 \times 112.5 \times \frac{381 + 112.5}{125} \\
&= 37942846 \text{ (N} \cdot \text{mm)} \\
&= 37.9 \text{ (kN} \cdot \text{m)}
\end{aligned}$$

$$\begin{aligned}
M_s &= \tau_u (c_2 + d) d (c_1 + d) \\
&= 0.335 \sqrt{24} (381 + 112.5) \times 112.5 \times (254 + 112.5) \\
&= 33393665 \text{ (N} \cdot \text{mm)} \\
&= 33.4 \text{ (kN} \cdot \text{m)}
\end{aligned}$$

$$\begin{aligned}
M_t &= \tau_u \frac{d^2}{2} \left\{ (c_1 + d) - \frac{d}{3} \right\} \cdot 2 \\
&= 6 \times 0.335 \sqrt{24} \times \frac{112.5^2}{2} \left\{ (254 + 112.5) - \frac{112.5}{3} \right\} \cdot 2 \\
&= 41001771 \text{ (N} \cdot \text{mm)} \\
&= 41.0 \text{ (kN} \cdot \text{m)}
\end{aligned}$$

$$M_0 = M_f + M_s + M_t = 37.9 + 33.4 + 41.0 = 112.3 \text{ (kN} \cdot \text{m)}$$

$$\begin{aligned}
V_0 &= \tau_u A_c = 0.335 \sqrt{24} \times \{ (381 + 112.5) \times 2 + (254 + 112.5) \times 2 \} \times 112.5 \\
&= 317564 \text{ (N)} \\
&= 318 \text{ (kN)}
\end{aligned}$$

$$\begin{aligned}
\frac{V_u}{V_0} + \frac{M_u}{M_0} &= \frac{234}{318} + \frac{M_u}{112.3} = 1 \\
M_u &= 29.7 \text{ (kN} \cdot \text{m)}
\end{aligned}$$

$$\begin{aligned}
Q_{punch} &= \frac{M_u}{h_0} \\
&= \frac{29.7}{3} = 9.9 \text{ (kN)}
\end{aligned}$$

$${}_i Q_u = \min(Q_{mu}, Q_{su}, Q_{slab}, Q_{punch}) = Q_{punch} = 9.9 \text{ (kN)}$$

Therefore, the failure mode of the interior column is punching shear failure.

F-index of the exterior columns (with beam) of this building should be determined by using the upper limit of the drift angle of exterior column  $cR_{max} = 1/50$ .

## References

1. Architectural Institute of Japan (2018): AIJ Standard for Structural Calculation of Reinforced Concrete Structures.
2. JBDPA (2001): Standard for Seismic Evaluation of Existing Reinforced Concrete Buildings; Guidelines for Seismic Retrofit of Existing Reinforced Concrete Buildings.
3. Miyauchi Y, Fukuhara T, Kei T (2009): Experimental study on seismic performance of retrofitted reinforced concrete member with low-strength concrete (in Japanese). *Proceedings of the Japan Concrete Institute*, Vol. 31, No. 2, pp. 1015-1020
4. Public Works Department (2015): Manual for seismic evaluation of existing reinforced concrete buildings.



## Chapter 7 Example building

### 7.1 General

The example buildings are prepared only for describing the general procedure of the manual to professional engineers and practitioners. The example buildings are chosen which are similar building in BSPP manual (Ref). **modified** The calculation procedure is followed from BSPP manual.

#### 1.1 Objectives

- To describe the general procedure of SATREPS-TSUIB Guidelines by the sample building.
- To understand the procedure of evaluation among professional engineer and investigators.
- To understand the effectiveness of the proposed manual

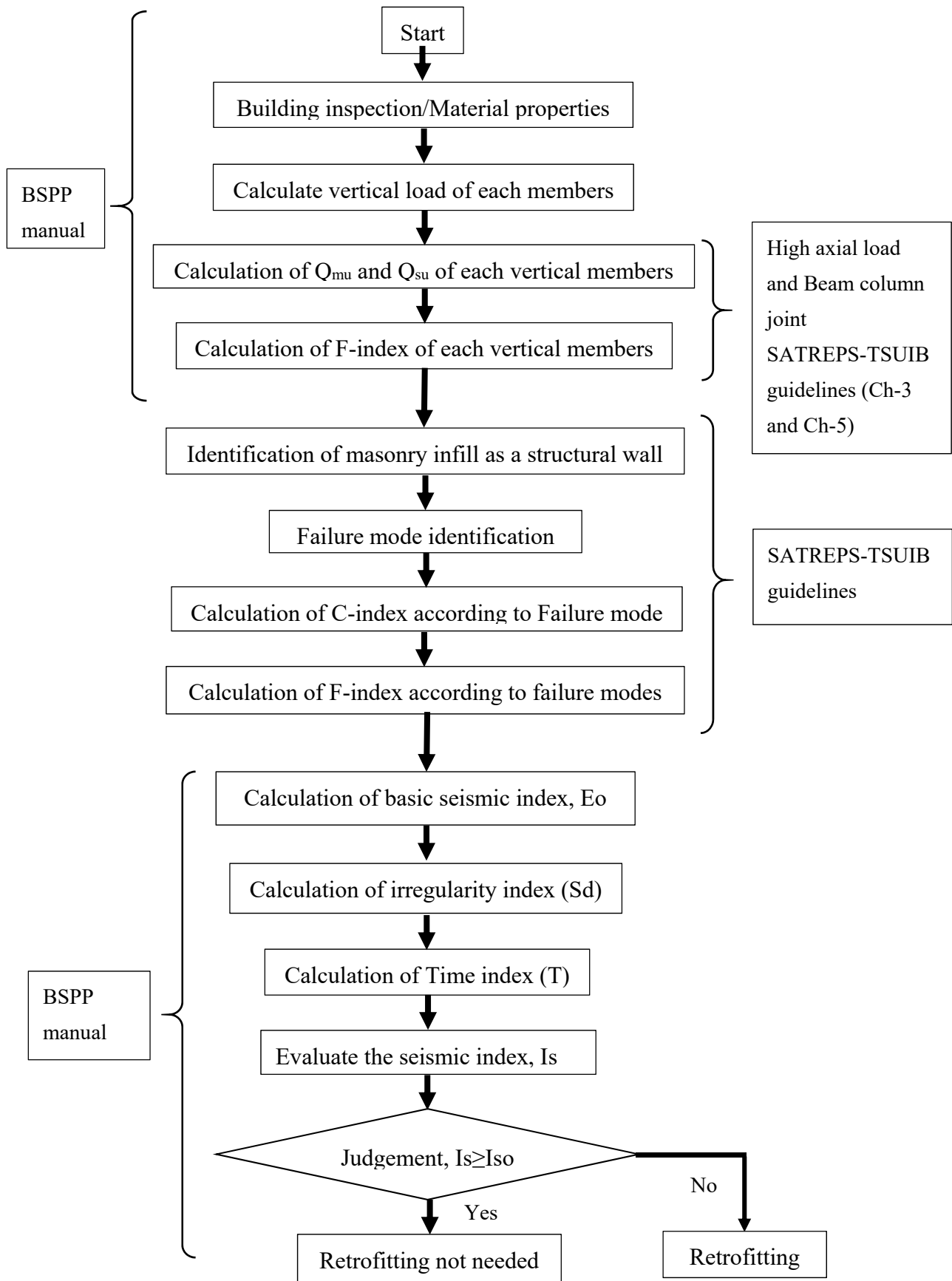


Figure: General flow of evaluation

### 7.1.1 Overview of the building

An example of detailed seismic evaluation has been described in following section. In this regard, a ten storied office building has been selected as mentioned as Bangladesh Betar Bhaban located at Dhaka. A general information is showing in Table A1 describing overview of the building.

Table A1 General Information

Item	
Location	Dhaka
Structure type	RC with masonry infill
Year of construction	1990
Number of story	10
Soil type	SD type
Foundation type	Shallow foundation
Floor area (part 1)	471 m <sup>2</sup>
Floor height	3500mm

Figure A2 and Figure A3 show the floor plan of first and the location of column and masonry infill.

The total floor area of the investigated buildings is about 471 m<sup>2</sup>.

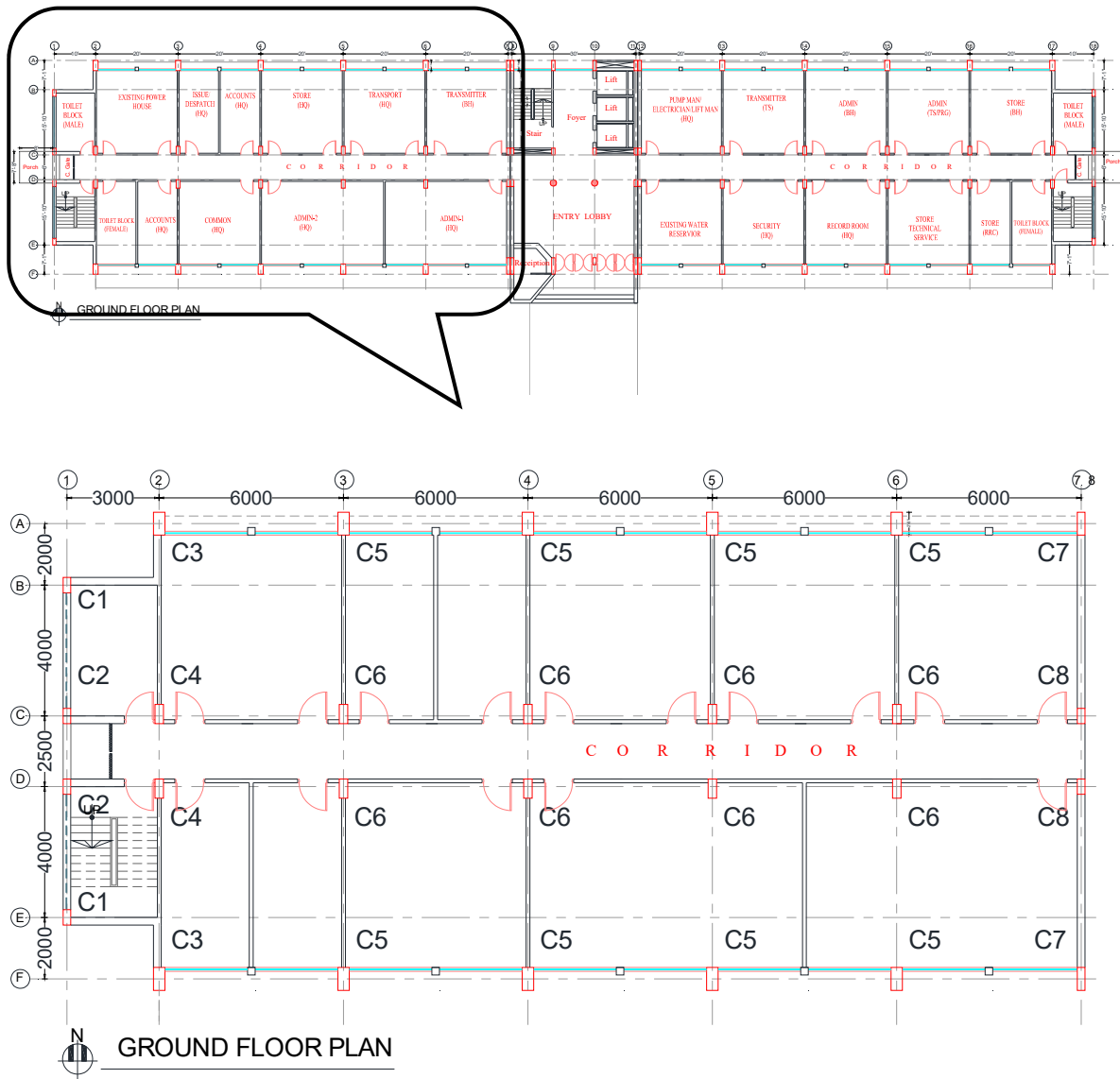


Figure A3 Floor plan with column layout

Table A2: Dimension and Reinforcement in X direction

Column Id	No of column	B (mm)	D (mm)	No. of Main Rebar	Dia of Main Rebar (mm)	No. of Main Rebar	Dia of Main Rebar (mm)	$a_g$ (mm <sup>2</sup> )
C1	2	500	250	6	22	8	20	4794.07
C2	2	500	250	12	22	2	20	5189.91
C3	2	750	300	24	20	-	-	7539.82
C4	2	750	300	20	25	4	20	11074.11
C5	8	750	300	20	25	4	20	11074.11
C6	8	750	450	24	25	4	20	13037.61
C7	2	750	250	12	22	4	16	5365.84
C8	2	750	250	12	25	4	16	6694.73

Table A3: Tension and Shear rebar in x-direction

Column Id	Tension rebar						Shear rebar (10mm dia)	
	No. of Tension Rebar	Dia of Tension Rebar (mm)	No. of Tension Rebar	Dia of Tension Rebar (mm)	$a_t$ (mm <sup>2</sup> )	$\rho_t$ (%)	Hoop spacing (mm)	$\rho_w$ (%)
C1	2	22	3	20	1702.74	1.36	250	0.31
C2	4	22	1	20	1834.69	1.47	250	0.31
C3	10	20	-	-	3141.59	1.40	300	0.21
C4	8	25	2	20	4555.31	2.02	300	0.21
C5	8	25	2	20	4555.31	2.02	300	0.21
C6	8	25	2	20	4555.31	1.35	300	0.21
C7	4	22	2	16	1922.65	1.03	250	0.25
C8	4	25	2	16	2365.62	1.26	250	0.25

Beam depth: 600 mm

### 7.1.2 Site investigation/Material properties (according to BSPP manual)

#### 3.1 Material properties

Both destructive and non-destructive test are carried out to determine the material properties. The detailed procedure is described in BSPP manual. However, the material properties are shown in Table A4.

Table A4 Material properties

Material properties	Strength
Concrete strength, $f_c$	19 MPa (Ground to 5 <sup>th</sup> floor) 25 MPa (6 <sup>th</sup> floor to roof)
Yield strength of reinforcement, $f_y$	400 MPa (All floor)
Young modulus concrete, $E_c$	22000 MPa
Young modulus of masonry, $E_m$	550 $f_m$
Prism strength, $f_m$	8 MPa
<i>*For young modulus of concrete, <math>4700\sqrt{f_c}</math> according to ACI318-14</i>	

### 7.1.3. Seismic evaluation

**Basic principle includes seismic index ( $I_s$ ) and  $I_{so}$  calculation procedure described in BSPP manual)**

#### 4.2 Seismic evaluation considering bare frame in X direction (BSPP manual)

Second level evaluation considering bare frame has been done as per BSPP seismic evaluation manual.

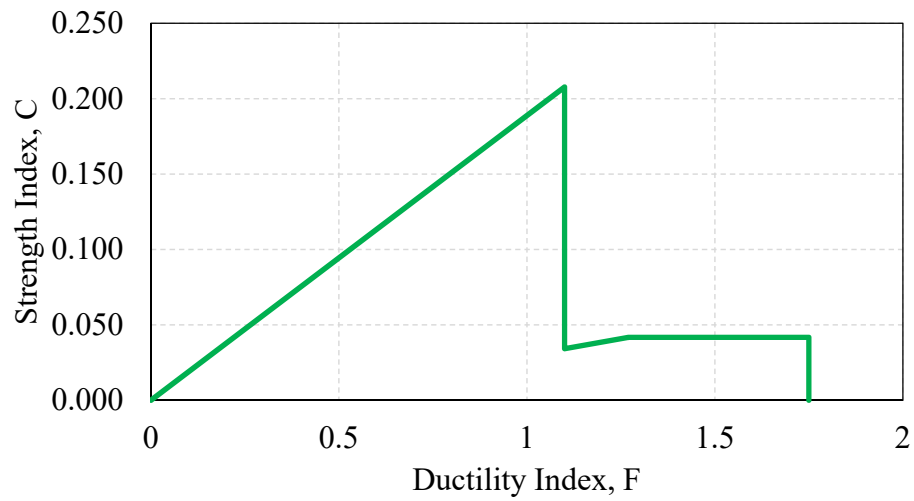


Figure A5 C-F relationship in x direction at ground floor

#### **7.1.4 Seismic evaluation considering proposed Guidelines**

##### **7.1.4.1 Low strength concrete**

The material properties is shown in Table A4. It has been observed that the concrete strength is higher than 13.5 MPa. Hence this building does not require to investigate for low strength concrete.

##### **7.1.4.2 Beam column joint investigation.**

According to chapter 5 beam column joint the evaluation flow diagram as shown in Figure C.5.2. The following conditions meets:

- The building has been constructed after 2006
- The rebar used in the building is deformed bar.
- The ductility index is less than the F limit.

So, there is no possibility to occur pull-out failure of beam longitudinal rebar. Therefore beam-column joint investigation is not required in these buildings.

Flow of the seismic performance evaluation considering existence of exterior beam-column joint with poor anchorage of beam longitudinal rebar.

### 7.1.4.3 Seismic evaluation with masonry infill (SATREPS Guidelines)

#### 1) Location of infill

Figure A6 shows the floor plan with the location of column and masonry infill.

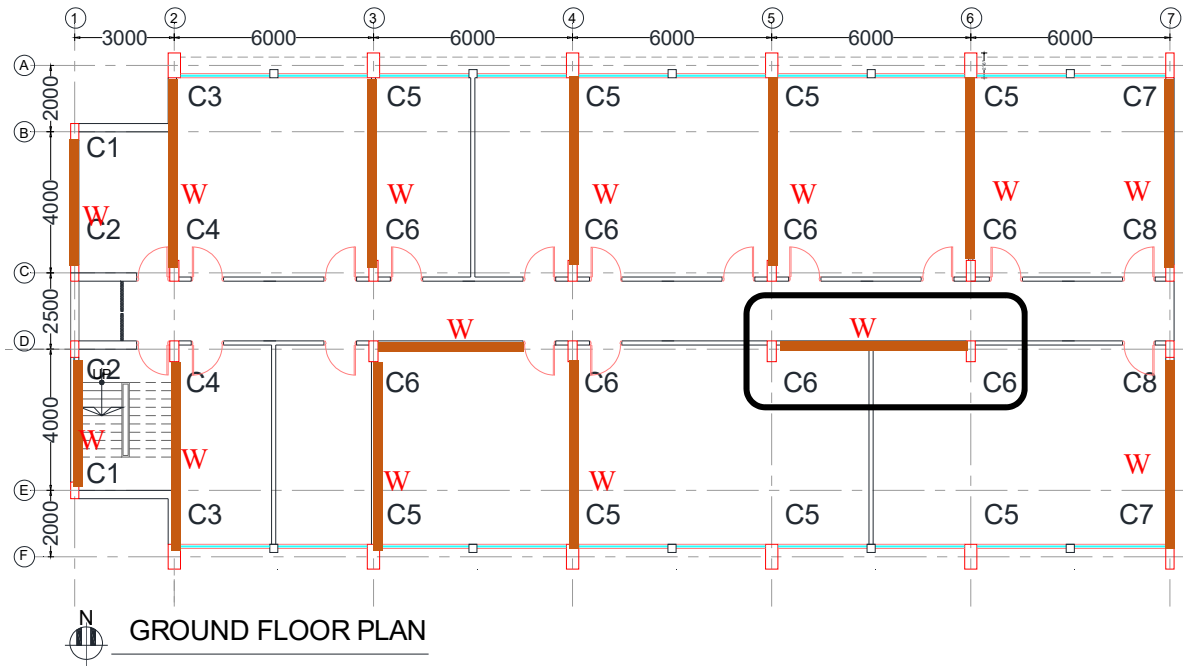


Figure A6 Architectural plan (dimensions are in mm)

Table A5 Masonry infill-wall properties

	Wall ID	Number	Length (mm)	Thickness (mm)	Opening area %	Structural wall (yes/no)
X-direction	W1	1	2750	250	0%	Yes
	W2	2	3875	125	Less than 40%	Yes
	W3	1	3875	125	Less than 40%	Yes
Y-direction	W4	2	3875	250	0%	Yes
	W5	2	3875	125	0%	Yes
	W6	6	3875	250	0%	Yes
	W7	2	2400	125	0%	Yes

#### **Step 1: Classification of structural wall and non-structural wall**

- In the example building, there are two types of masonry infill: solid and with opening due to window, door and high window.
- Masonry infill wall is surrounded and confined by RC frame from all sides.



- It has been observed that wall with opening has more than 40% opening area and some of them are double opening. These walls are not considered as structural wall.
- Slenderness ratio is  $H/t$  of infill wall is 20, which is less than 30.
- Solid brick is used in masonry infill.
- There are no cracks, and gap between frame and masonry infill based on visual inspection according to **BSPP manual chapter 2**.

The calculation procedure of a masonry infilled wall ‘W’ is shown in this section.

### **Step 2: Failure mode identification**

Failure mode is identified based on  $\beta$  index and  $a_c/h_o$  ratio are described in Section 4.3.

Calculation procedure of one wall is shown in below:

1)  $\beta$  index is calculated using the following procedure:

$$\beta = Q_{frame} / Q_{exp}$$

$$Q_{frame} = \sum Q_{col} = Q_{col\_left} + Q_{col\_right}$$

$Q_{col\_left}$  and  $Q_{col\_right}$  is calculated based on BSPP seismic evaluation manual(Ref).

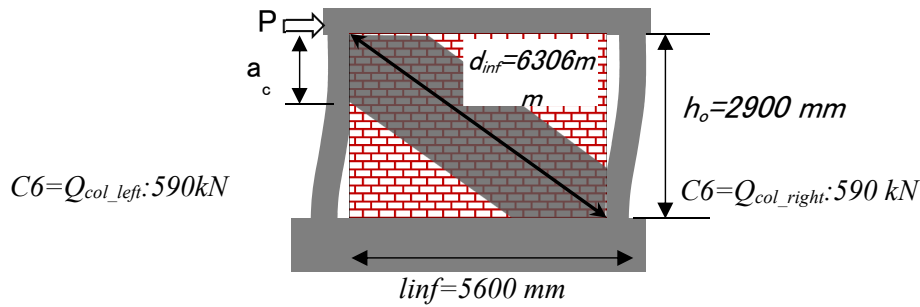


Figure A7 Masonry infill wall W

$$Q_{frame} = 590 + 590 = 1180 \text{ kN}$$

$Q_{exp}$  is calculated using Eq (4.3) is section 4.3

- Prism strength,  $f_m = 8 \text{ MPa}$
- Thickness,  $t_{inf} = 125 \text{ mm}$
- Length of infill,  $l_{inf} = 5600 \text{ mm}$

$$Q_{exp} = 0.05 f_m \cdot t_{inf} \cdot l_{inf} = 0.05 \cdot 8 \cdot 125 \cdot 5600 = 280 \text{ kN}$$

$$\beta = Q_{frame} / Q_{exp} = 4.46$$

From the condition,  $1 < \beta$ , Good confinement: Type I

2)  $a_c/h_o$  is calculated using the following procedure:

$(a_c/h_o)$  is calculated through Eqs. (4.4)- (4.5).

$$\frac{a_c}{h_o} = \frac{\pi}{4\lambda h_o} \quad (4.4)$$

$$\lambda = \sqrt[4]{\frac{(E_m t_{inf} \cos^2 \theta)}{4 E_c I_c d_{inf}}} \quad (4.5)$$

where,  $E_m = 550 \times 8 = 4400$  MPa

$E_c = 20486$  MPa

Clear height,  $h_o = 3500 - 600 = 2900$  mm

Moment of inertia of RC column,  $I_c = (750 \times 450^3) / 12 = 5.69 \times 10^9$  mm<sup>4</sup>

Note: In case of different column size, the minimum moment of inertia should be considered.

Diagonal length of infill,  $d_{inf} = 6306$  mm

Inclination of diagonal with horizontal,  $\theta$  (rad) = 0.47

The contact length ratio:

$$\frac{a_c}{h_o} = 0.44$$

Based on condition, Failure mode is classified according to  $a_c/h_o$  as follows.

$0.3 < a_c/h_o$ , Good confinement: Type I

Based on both criteria, it has been observed that the failure type: I, diagonal compression failure mode for infill wall, **W1**.

By the same procedure, the other walls are as follows:

Table A6 Failure mode of all wall in x-direction

Direction	Wall ID	$a_c/h_o$	$\beta$ index	Failure type	Failure mode
X-direction	W1	0.44	4.21	I	Diagonal compression
	W2	0.44	4.465	I	Diagonal compression
	W3	0.30	2.800	I	Diagonal compression

$\beta$  index and  $a_c/h_o$  are calculated for all masonry infill, based on figure, it has been observed that the failure type: I, diagonal compression failure mode.

### **Step3: Strength index ( $C_{mw}$ )**

Strength index  $C_{mw}$  for a RC frame with masonry infill is calculated by Eq. (4.6).

$$C_{mw} = \frac{Q_{mw}}{\sum W} \quad (4.6)$$

Where,  $\sum W$  is weight of the building including live load supported by the story concerned.

Since failure mode is II and III, (sliding and mixed types of failure)

the  $Q_{mw}$  is calculated using the following Eq.4.7

$$Q_{mw}=Q_{frame}+Q_{inf}$$

Where,  $Q_{frame}=590+590=1180$  kN

$Q_{inf}$  will be  $Q_{diagonal}$  in the following EQ.4.9

$$Q_{dia}=0.08 f_m \cdot t_{inf} \cdot l_{inf} = 0.08 \cdot 8 \cdot 125 \cdot 5600 = 448 \text{ kN}$$

Lateral strength,  $Q_{mw}=Q_{frame}+Q_{inf}=1180+448=1628$  kN

Total building weight,  $W=49004$  kN

Strength index,

$$C_{mw} = \frac{Q_{mw}}{\sum W}$$

$$C_{mw} = 1628/49004 = 0.0332$$

By calculation, strength index of W1 is of 0.0332

Using similar procedure, Strength index are as follows:

Table A7: Strength index of all wall in x-direction

Direction	Wall ID	$Q_{frame}$	$Q_{inf}$	$C_{mw}$
X-direction	W1	1180	448	0.0332
	W2	1180	422	0.0327
	W3	740	422	0.0237

#### **Step4: Ductility index, F**

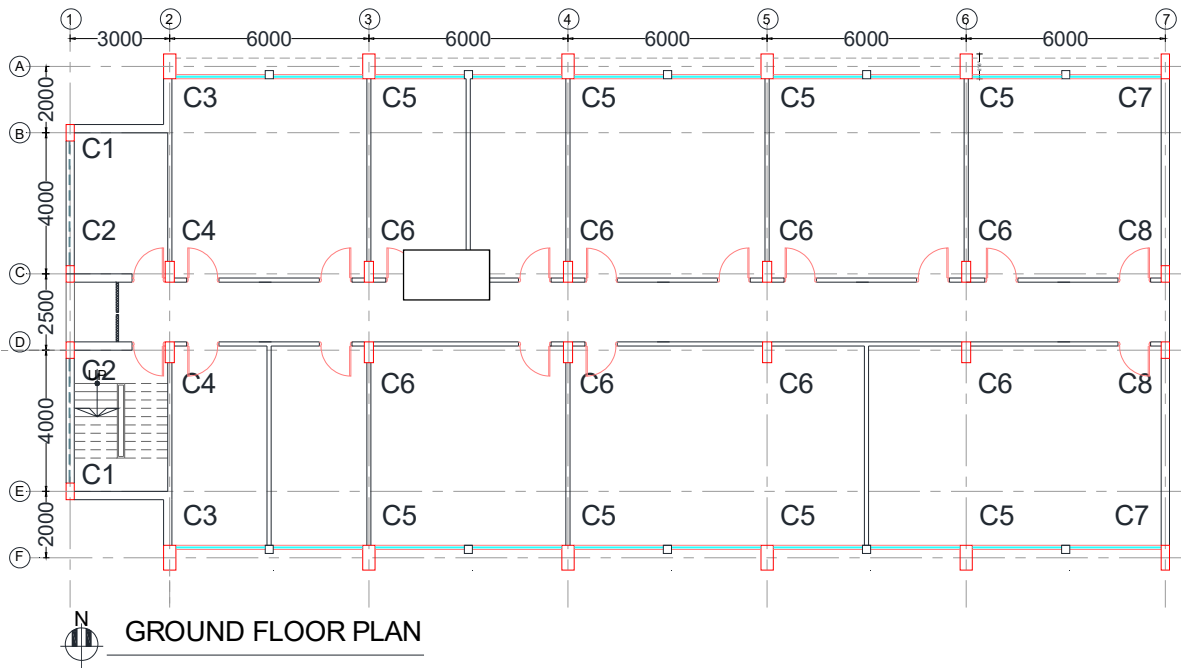
Ductility index is considered based on failure mode,

Table A8: Ductility index of wall in x-direction

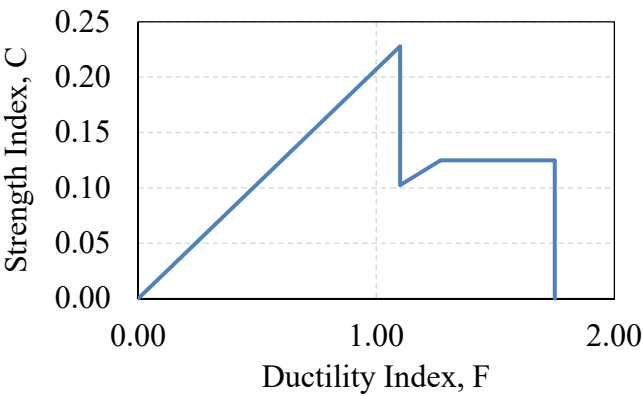
Direction	Wall ID	Failure type	Failure mode	Ductility index
X-direction	W1	I	Diagonal compression	1.75
	W2	I	Diagonal compression	1.75
	W3	I	Diagonal compression	1.75

**5. Summary:**

**X-direction evaluation:**



Based on this analysis, Seismic evaluation results: C and F relationships in x-direction



- **Seismic index with masonry infill**

Table A9: Basic seismic index ( $E_0$ ) using Equation 4 in x-direction

C-index	F-index	Basic seismic index ( $E_0$ )
0.125	1.10	0.258
0.125	1.75	

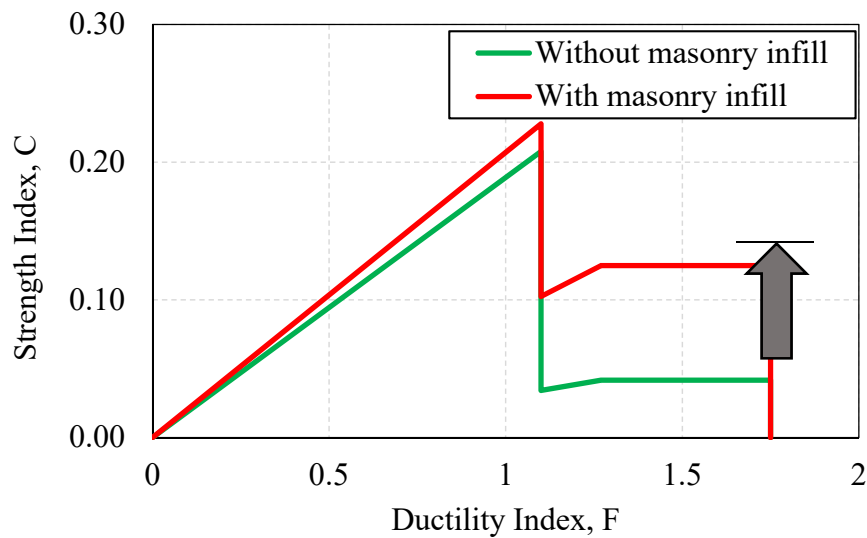
Table A10: Basic seismic index ( $E_o$ ) using Equation 5 in x-direction

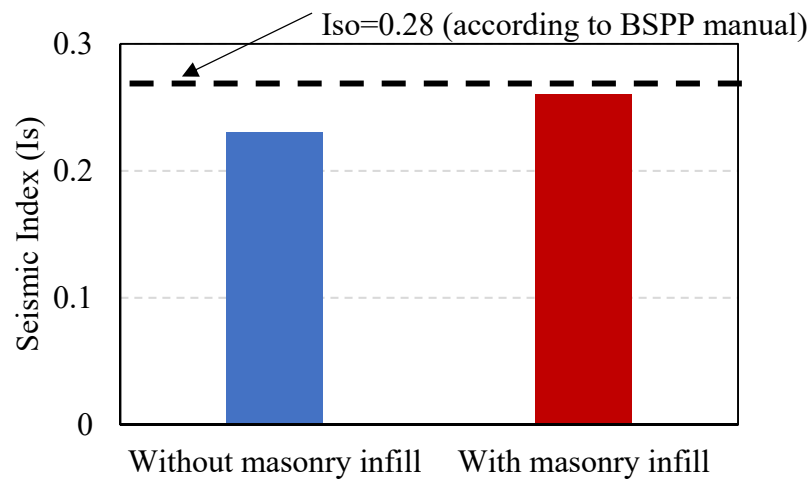
C- index	F-index	Eq.5	Basic seismic index ( $E_o$ )
0.228	1.10	0.251	0.251
0.125	1.75	0.218	

Table A11: Seismic index of the building in both directions

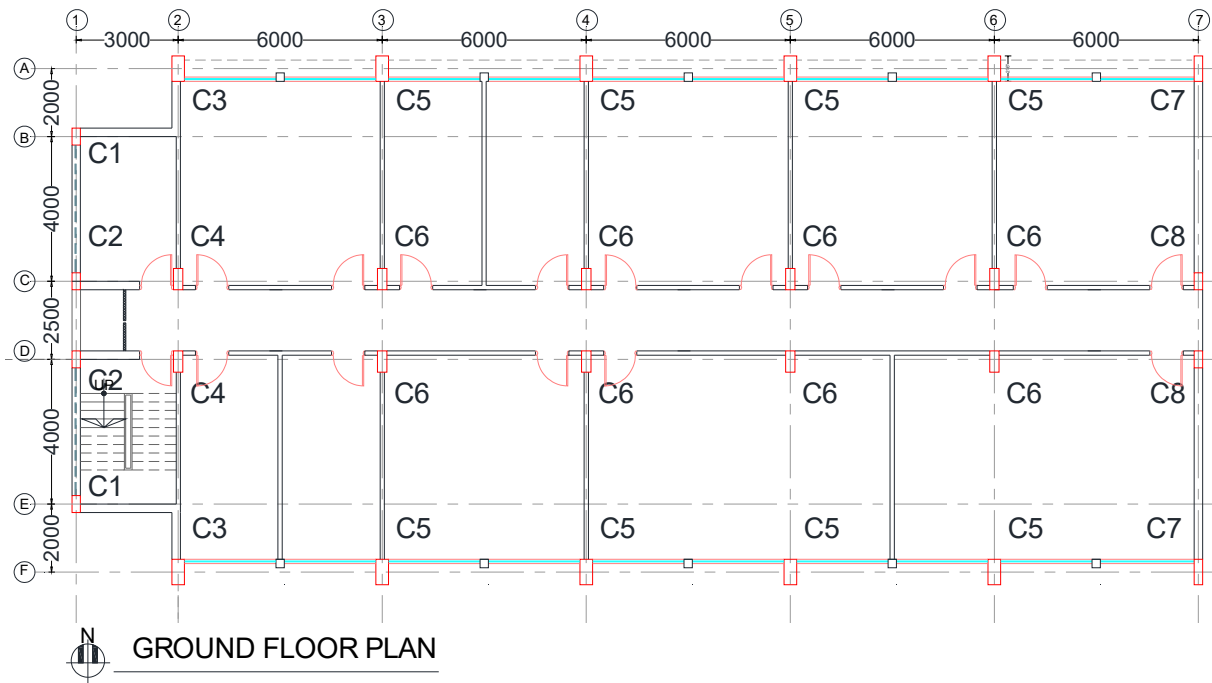
Basic Seismic Index, $E_o$		Irregularity index, $S_d$	Time index, $T$	Seismic Index, $I_s$	
Without masonry infill	With masonry infill			Without masonry infill	With masonry infill
0.23	0.258	1.00	1.00	0.23	0.258

Seismic index ( $I_{s2}$ ) has been calculated considering masonry infill for X direction. It has been observed that the contribution of masonry infill increased seismic capacity of existing RC building.





### Y-direction seismic evaluation



F index of all column is 1.0

Floor plan with the location of column and masonry infill.

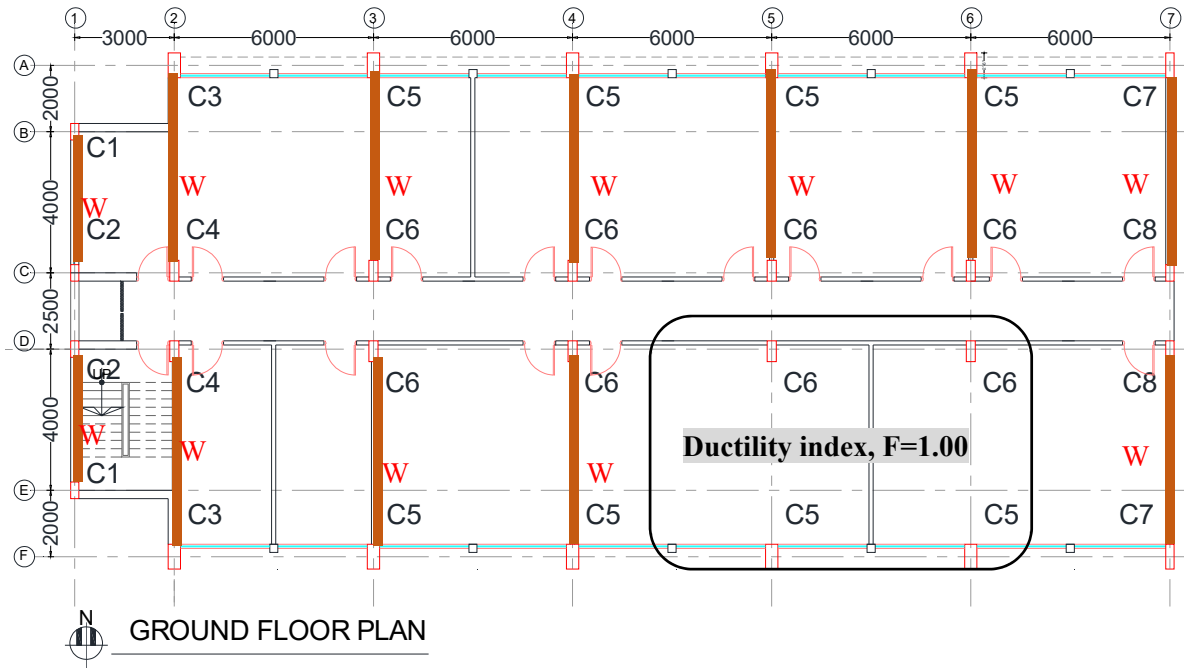


Figure A6: Architectural plan (dimensions are in mm)

#### Summary of wall C and F

Wall Id	No of wall	$V_{frame}$	$Q_{inf}$	$C_{mw}$ of each one	Failure mode	Ductility, F
W4	2	361.10	608.00	0.02	Diagonal compression	1.75
W5	2	847.81	286.00	0.023	Diagonal compression	1.75
W6	6	1093.20	448.00	0.031	Diagonal compression	1.75
W7	2	713.79	896.00	0.033	Diagonal compression	1.75

Table A9: Basic seismic index ( $E_0$ ) using Equation 4 in x-direction

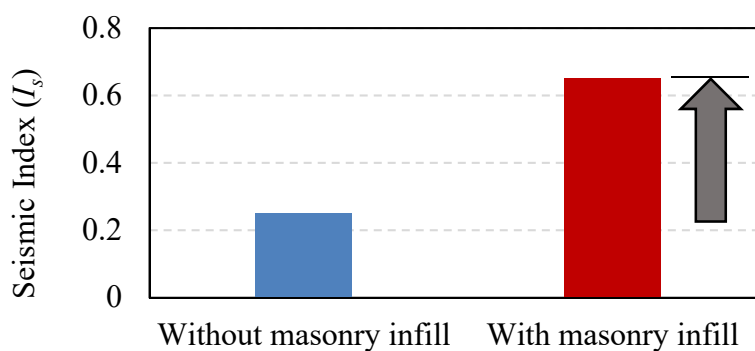
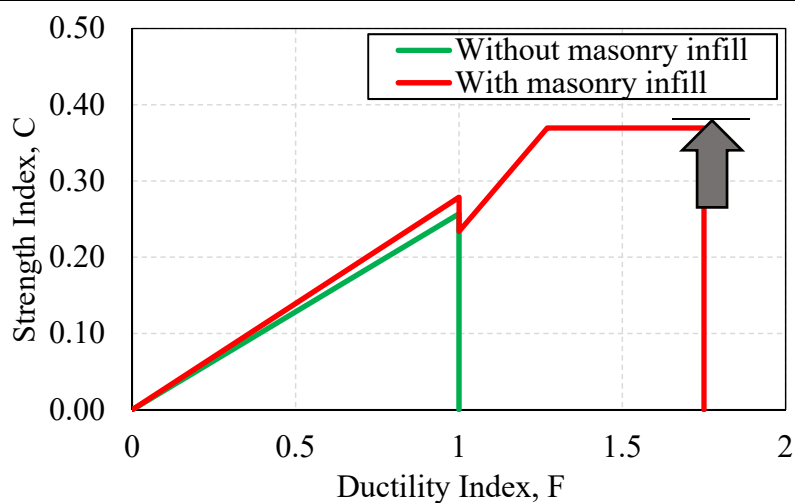
C-index	F-index	Basic seismic index ( $E_0$ )
0.045	1.00	0.57
0.325	1.75	

Table A10: Basic seismic index ( $E_o$ ) using Equation 5 in x-direction

C- index	F-index	Eq.5	Basic seismic index ( $E_o$ )
0.28	1.00	0.28	0.65
0.37	1.75	0.65	

Table A11: Seismic index of the building in both directions

Basic Seismic Index, $E_o$		Irregularity index, $S_d$	Time index, $T$	Seismic Index, $I_s$	
Without masonry infill	With masonry infill			Without masonry infill	With masonry infill
0.26	0.65	1.00	1.00	0.26	0.65



Based on this analysis, Seismic evaluation results: C and F relationships in x-direction



## 7.2 Moment-resisting frame structure

### 7.2.1 General

The procedure of the seismic evaluation is illustrated through an example of existing moment-resisting frame building which is outlined in this section. The main purpose of this example calculation is to show the process of determining the seismic performance based on CNCRP/BSPP Manuals & SATREPS-TSUIB Guidelines and to show how to apply the present guidelines for seismic evaluation.

### 7.2.2 Scope

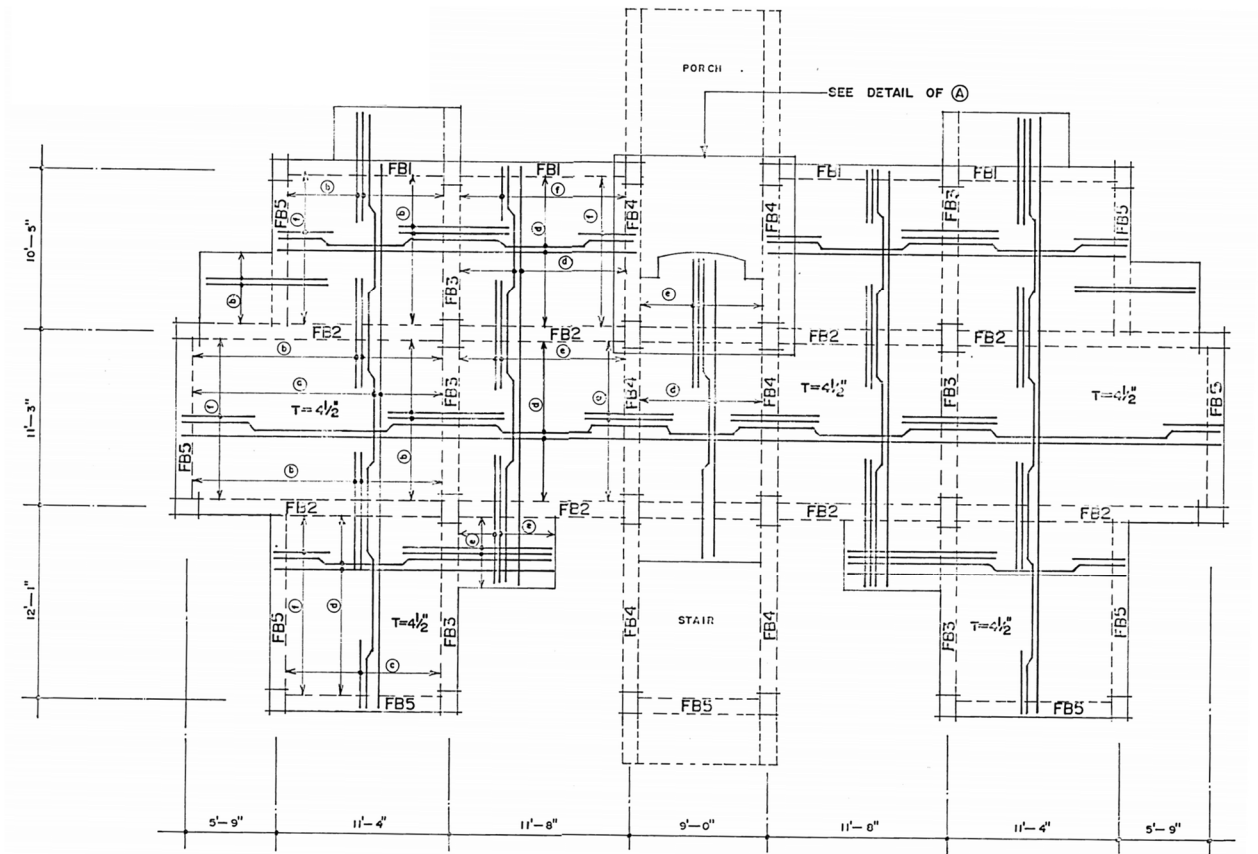
The following sample calculation flow mainly focuses on and illustrates several procedures and/or schemes presented in both SATREPS-TSUIB Guidelines for the seismic evaluation. Assumptions of evaluation are made according to CNCRP/BSPP Manuals & SATREPS-TSUIB Guidelines.

### 7.2.3 Outline of the structure

The example building is a multi-storey RC building located in Dhaka city. The structure has no load-bearing infill walls. It represents a typical Bangladeshi moment-resisting frame structure. The building is used for residential purposes. The floor plan, column schedule and material property are shown in the following tables and figures.

Table 7.2.1 Summary

Usage	Residential building
Number of stories	Six
Structure type	Moment-resisting frame
Foundation type	Pile foundation
Construction year	2002
Building constructor	GoB PWD (Public)
Building location	Dhaka city



Unit: Feet-inch

Figure 7.2.1 Typical floor plan

	UP TO F.G.L	UP TO 2 <sup>ND</sup> FLOOR	UP TO 4 <sup>TH</sup> FLOOR	UP TO ROOF LEVEL
C1	<p>6 - 20 mm <math>\phi</math></p>	<p>6 - 20 mm <math>\phi</math></p>	<p>4 - 20 mm <math>\phi</math> (corner) 2 - 16 mm <math>\phi</math></p>	<p>6 - 16 mm <math>\phi</math></p>
C2	<p>4 - 20 mm <math>\phi</math> (corner) 6 - 16 mm <math>\phi</math></p>	<p>4 - 20 mm <math>\phi</math> (corner) 6 - 16 mm <math>\phi</math></p>	<p>10 - 20 mm <math>\phi</math></p>	<p>10 - 16 mm <math>\phi</math></p>
C3	<p>10 - 20 mm <math>\phi</math></p>	<p>10 - 20 mm <math>\phi</math></p>	<p>4 - 20 mm <math>\phi</math> (corner) 6 - 16 mm <math>\phi</math></p>	<p>10 - 16 mm <math>\phi</math></p>

Figure 7.2.2 Column schedule

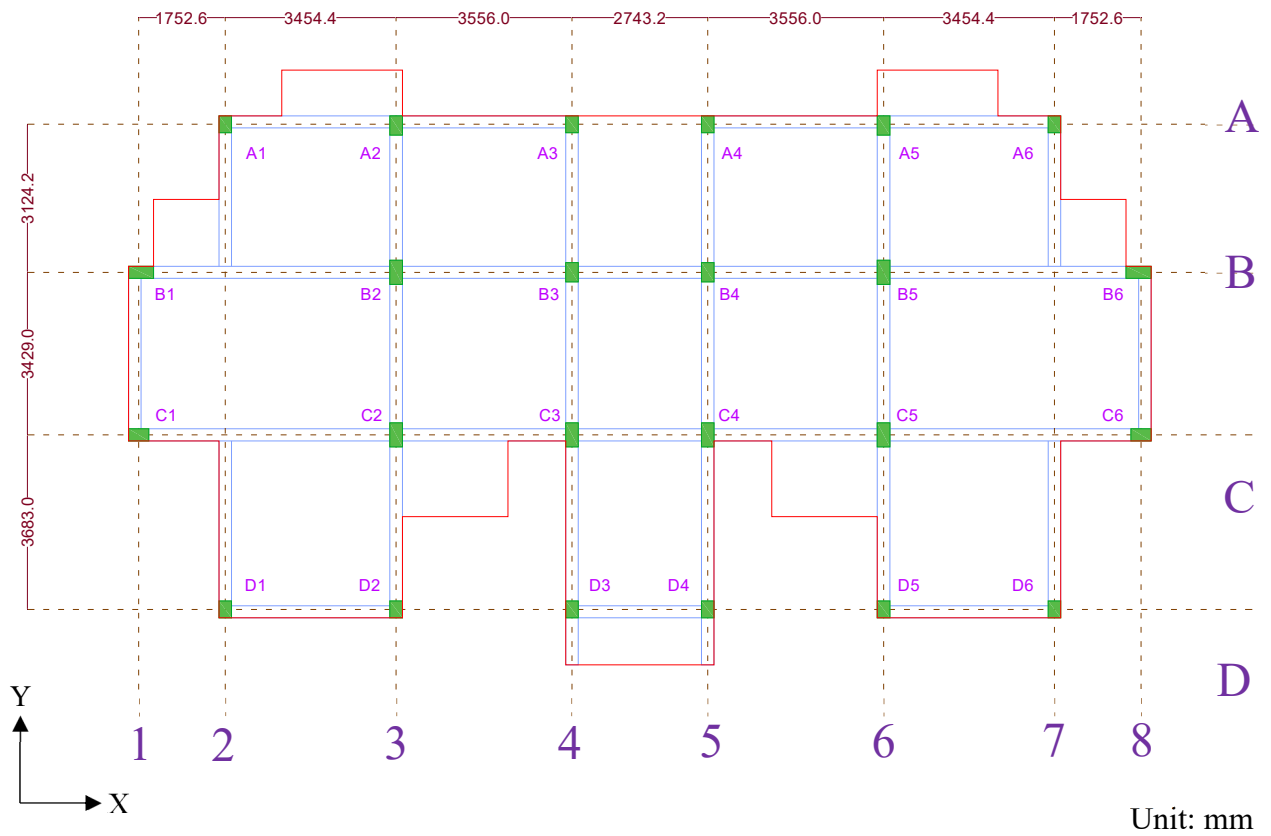


Figure 7.2.3 Column layout

Table 7.2.2 Column Layout

Column Layout						
Frame	1	2	3	4	5	6
<b>A</b>	A1	A2	A3	A4	A5	A6
<b>B</b>	B1	B2	B3	B4	B5	B6
<b>C</b>	C1	C2	C3	C4	C5	C6
<b>D</b>	D1	D2	D3	D4	D5	D6

Table 7.2.3 Material property

Type of concrete	Normal strength concrete
Concrete strength	25 MPa (28 days cylinder test)
Type of rebar	Deformed
Rebar yield stress	415 MPa (billet steel)

As-built drawing, in situ material strengths and soil type data were unavailable for this example building. As a result, design drawings and design material strengths were considered for the seismic evaluation of the building. Also considering the lack of availability of in situ soil type data, conservative estimation was made assuming SD as soil type.

**Note:** Conservative estimations should be adopted when some data/information is not available.

The building had a possibility of brittle pullout failure at exterior beam-column joints because the structural specification corresponded to some items: construction year and type of rebar, indicating possible pullout failure of beam longitudinal rebar, as listed in Section 3.1.

#### 7.2.4 Seismic demand index

The seismic demand of the structure,  $I_{S0}$  is evaluated according to the CNCRP/BSPP Manuals for Seismic Evaluation of Existing Reinforced Concrete Buildings as

$$I_{S0} = 0.8 \times \frac{2}{3} Z \cdot I \cdot C_S$$

$$C_S = 2.5S\eta$$

For this example building,

$$S = 1.35 \text{ [for SD type soil]}$$

$$\eta = 0.55 \text{ [considering 5\% viscous dampening]}$$

$$\text{So, } I_{S0} = 0.8 \times \frac{2}{3} \times 0.2 \times 1.0 \times 3.375$$

$$= 0.36$$

## 7.2.5 Seismic evaluation of the building

### Outlines

The seismic evaluation of the above structure was performed according to the CNCRP Manual for Seismic Evaluation, however, several new proposals by the SATREPS-TSUIB Guidelines are mainly focused on and illustrated in the following. In particular, the seismic performance evaluation on beam-column joints is newly presented in the Guidelines.

### Member strength

Member strength is determined based on the equations listed in, “*Technical Guidelines for Seismic Evaluation of Existing Reinforced Concrete Buildings for Extended Application of BSPP Seismic Evaluation Manual*”.

#### (1) Ultimate flexural strength

The equations listed in the Technical Guidelines for Seismic Evaluation of Existing RC Building manual are applied in this example.

$$Q_{mu} = \frac{2M_u}{h_0}$$

$$\text{for, } N_{max} \geq N > 0.4b \cdot D \cdot f_c'$$

$$M_u = (0.8a_t \cdot \sigma_y \cdot D + 0.12b \cdot D^2 \cdot f_c') \times \left( \frac{N_{max} - N}{N_{max} - 0.4b \cdot D \cdot f_c'} \right)$$

$$\text{for, } 0.4b \cdot D \cdot f_c' \geq N > 0$$

$$M_u = 0.8a_t \cdot \sigma_y \cdot D + 0.5N \cdot D \cdot \left( 1 - \frac{N}{b \cdot D \cdot f_c'} \right)$$

$$\text{for, } 0 > N \geq N_{min}$$

$$M_u = 0.8a_t \cdot \sigma_y \cdot D + 0.4N \cdot D$$

For A1 column on 1<sup>st</sup> floor [X-direction],

Column width,  $b = 355.6 \text{ mm}$

Column depth,  $D = 254 \text{ mm}$

Column height,  $H = 3048 \text{ mm}$

Clear height,  $h_0 = 2692.4 \text{ mm}$

Gross reinforcement area,  $a_g = 1884.96 \text{ mm}^2$

Tensile reinforcement area,  $a_t = 942.48 \text{ mm}^2$

Concrete strength,  $f_c' = 25 \text{ N/mm}^2$

Reinforcement strength,  $\sigma_y = 415 \text{ N/mm}^2$

floor weight = Slab area  $\times 12 \text{ kN/m}^2$  [conservative estimation]

Effective slab area tranfering load on the selected column =  $3.76644 \text{ m}^2$

Axial load,  $N = 3.76644 \times 12 \times 6 = 271.2 \text{ kN}$

$N_{max} = b \cdot D \cdot f_c' + a_g \cdot \sigma_y = 3040.3 \text{ kN}$

$0.4b \cdot D \cdot f_c' = 0.4 \times 355.6 \times 254 \times 25 = 903.22 \text{ kN}$

$M_u = 0.8a_t \cdot \sigma_y \cdot D + 0.5N \cdot D \cdot \left(1 - \frac{N}{b \cdot D \cdot f_c'}\right)$

$= 0.8 \times 942.48 \times 415 \times 254 + 0.5 \times 271.2 \times 1000 \times 254 \times \left(1 - \frac{271.2 \times 1000}{355.6 \times 254 \times 25}\right)$

$= 109.783 \text{ kN.m}$

$Q_{mu} = \frac{2M_u}{h_0} = \frac{2 \times 109.783}{\frac{2692.4}{1000}} = 81.55 \text{ kN}$

The ultimate flexural strength of each column can be calculated in the same procedure.

Calculation results for the whole structure is shown in the appendix.

## (2) Ultimate shear strength

The equations listed in the Technical Guidelines for Seismic Evaluation of Existing RC Building manual are applied in this example.

$$Q_{su} = k_r \cdot \left\{ \frac{0.053 p_t^{0.23} (18 + f_c')}{M/(Q \cdot d) + 0.12} + 0.85 \sqrt{p_w \cdot s \sigma_{wy} + 0.1 \sigma_0} \right\} \cdot b \cdot j$$

$$k_r = 0.244 + 0.056 f_c' \text{ [for, } f_c' > 13 \text{ N/mm}^2 \text{]}$$

$$M/Q = h_0/2$$

For B1 column on 1<sup>st</sup> floor [X-direction],

Column width,  $b = 254 \text{ mm}$

Column depth,  $D = 508 \text{ mm}$

Column height,  $H = 3048 \text{ mm}$

Clear height,  $h_0 = 2590.8 \text{ mm}$

Gross reinforcement area,  $a_g = 3141.6 \text{ mm}^2$

Tensile reinforcement area,  $a_t = 942.48 \text{ mm}^2$

Longitudinal reinforcement ratio (in %),  $p_t = \frac{a_t}{b \cdot D} = \frac{942.48}{254 \times 508} \times 100 = 0.7304235\%$

Transvers reinforcement ratio (in %),  $p_w = \frac{\text{hoop area}}{b \cdot \text{hoop spacing}} = \frac{2 \times 78.54}{254 \times 125}$

$= 0.0049474\% (\leq 0.012)$

$M/(Q \cdot d) = h_0/2/d = 2590.8/2/(508 - 50) = 2.82838$

\* $d$  = effective depth of column;  $D - 50$  maybe applied

$$s\sigma_{wy} = \sigma_y = 415 \text{ MPa}$$

$$\text{Axial load, } N = 8.2374 \times 12 \times 6 = 593.1 \text{ kN}$$

$$\sigma_0 = \frac{N}{b \cdot D} = \frac{593.1 \times 1000}{254 \times 508} = 4.59653 \text{ N/mm}^2 \quad (\leq 8 \text{ N/mm}^2)$$

$$j = 0.8D = 0.8 \times 508 = 406.4$$

$$Q_{su} = \left\{ \frac{0.053p_t^{0.23}(18 + f_c')}{M/(Q \cdot d) + 0.12} + 0.85\sqrt{p_w \cdot s\sigma_{wy} + 0.1\sigma_0} \right\} \cdot b \cdot j$$

$$= \left\{ \frac{0.053 \times 0.7304235^{0.23}(18 + 25)}{2.82838 + 0.12} + 0.85\sqrt{0.0049474 \times 415 + 0.1 \times 4.59653} \right\} \times 254$$

$$\times 406.4$$

$$= 247.4 \text{ kN}$$

The ultimate shear strength of each column can be calculated in the same procedure

Calculation results for the whole structure is shown in the appendix.

### **Strength index C**

The strength index is determined according to the methods described in, “*Technical Guidelines for Seismic Evaluation of Existing Reinforced Concrete Buildings for Extended Application of BSPP Seismic Evaluation Manual*”. Ultimate flexural strength and ultimate shear strength for each member are determined, and the governing strength is taken as member strength. The strength index of the structure is obtained by the following equation;

$$C_c = \frac{\min. ({}_cQ_{mu}, {}_cQ_{su})}{\Sigma W}$$

where,



$\Sigma W$ : total weight supported by the storey concerned

Total weight of one storey = 2247.5 kN

Total weight of whole building = 13485.1 kN

For B1 column in the X-direction for 1<sup>st</sup> floor,

$$\text{Strength index, } C = \frac{\min(cQ_{mu}, cQ_{su})}{\Sigma W} = \frac{81.55}{13485.1} = 0.006$$

Similarly, strength index can be obtained for all the column in either direction for all stories.

Calculation results for the whole structure is shown in the appendix.

### **Ductility index F**

The  $F$  index for the independent column is calculated according to its failure mode, considering the strength margin for shear failure (ultimate shear strength/shear force at ultimate flexural strength) and deflection angle. The deflection angles to be considered are as follows; the maximum deflection angle of the column to the deformable length  $cR_{max}$ , the deflection angle of the column at the yielding  $cR_{my}$ , the plastic deflection angle of the column  $cR_{mp}$ , the deflection angle of the column at the ultimate flexural strength  $cR_{mu}$ , the deflection angle of the storey at flexural yielding modified by the clear height ( $h_0$ ) and standard height ( $H_0$ )  $R_{my}$ , the deflection angle of the storey at ultimate flexural strength  $R_{mu}$ , the deflection angle of the storey at the ultimate shear strength  $R_{su}$ , and the deflection angle at storey yielding  $R_y$ . The process for determining the  $F$  index of the structure is explained in details in CNCRP.

For column A2 in the Y-direction for 1<sup>st</sup> floor,

Dimension  $b \times D = 254\text{mm} \times 406.4\text{mm}, j = 325.12\text{mm}$

Hoops D10 @ 125mm c/c

$$N = 564.8 \text{ kN}$$

Concrete strength,  $f_c' = 25 \text{ MPa}$

Moment capacity,  $M_u = 201.55 \text{ kN.m}$

Shear force at the moment capacity,  $cQ_{mu} = 149.72 \text{ kN}$

Ultimate shear strength,  $cQ_{su} = 203.12 \text{ kN}$

a) Upper limit of the deflection angle of flexural column  $cR_{max}$ ,

$$cR_{max} = \min[ cR_{\max(n)}, cR_{\max(s)}, cR_{\max(t)}, cR_{\max(b)}, cR_{\max(h)}]$$

--  $cR_{\max(n)}$

Since  $s > 100\text{mm}, \eta_L = 0.2, \eta_H = 0.4$

$$\eta = \frac{N_s}{bDf_c'} = \frac{564.8 \times 1000}{254 \times 406.4 \times 25} = 0.2189$$

$$n' = (\eta - \eta_L)/(\eta_H - \eta_L) = 0.0943$$

$$cR_{\max(n)} = R_{30} \times \left( R_{250}/R_{30} \right)^{n'} = 1/30 \times \left( \frac{1}{250} / \frac{1}{30} \right)^{0.0943} = 0.0273$$

--  $cR_{\max(s)}$

$$c\tau_u = \frac{149.72 \times 1000}{254 \times 325.12} = 1.813$$

Since  $s = \frac{c\tau_u}{F_c} = 0.0725, s < 0.2, cR_{\max(s)} = 1/30$

--  $cR_{\max(t)}$

$$t = P_t = 0.80(\%)$$

Since  $t < 1.0(\%)$ ,  ${}_cR_{\max(t)} = 1/30$

--  ${}_cR_{\max(b)}$

$$b = \frac{s}{d_b} = \frac{125}{20} = 6.25$$

Since  $\frac{s}{d_b} < 8$ ,  ${}_cR_{\max(b)} = 1/30$

--  ${}_cR_{\max(h)}$

$$h = \frac{h_0}{D} = \frac{2692.4}{406.4} = 6.625$$

Since  $h > 2$ ,  ${}_cR_{\max(b)} = 1/30$

$$\therefore {}_cR_{\max} = \min[{}_cR_{\max(n)}, {}_cR_{\max(s)}, {}_cR_{\max(t)}, {}_cR_{\max(b)}, {}_cR_{\max(h)}] = 0.0273$$

b) The yielding deflection angle of the column  ${}_cR_{\text{my}}$

since,  $\frac{h_0}{D} > 3.0$ ,  ${}_cR_{\text{my}} = R_{150} = 1/150$

since,  ${}_cR_{\max} > {}_cR_{\text{my}}$ ,  ${}_cR_{\text{my}} = 1/150$

c) Failure mode categorization according to the strength margin for shear failure

The ultimate shear strength:  ${}_cQ_{su} = 203.12 \text{ kN}$

The shear force at flexural yielding:  ${}_cQ_{mu} = 149.72 \text{ kN}$

$$\frac{{}_cQ_{su}}{{}_cQ_{mu}} = \frac{203.12}{149.72} = 1.36 > 1.0$$

Therefore, the failure mode of the column is categorized as flexural yielding.

d) Extremely brittle column check

$$\frac{h_0}{D} = \frac{2692.4}{406.4} = 6.625 > 2.0$$

Therefore, the ductility index for the flexural column is applied.

e) The yielding inter-storey deflection angle of the column  $R_{my}$

$$\text{since, } R_{my} = (h_0/H_0) \times {}_cR_{my} \geq \frac{1}{250}, \quad R_{my} = 1.0 \times 1/150$$

f) The effective strength factor of the column  ${}_c\alpha$  to calculate  $R_{su}$

$${}_c\alpha = 0.3 + 0.7 \times \left( \frac{1/250}{R_{my}} \right) = 0.3 + 0.7 \times \left( \frac{1/250}{1/150} \right) = 0.72$$

g) The inter-storey deflection angle at the ultimate limit state of the shear column  $R_{su}$

$${}_c\alpha \cdot {}_cQ_{mu} = 0.72 \times 86.62 = 62.37 < {}_cQ_{su} (= 158.23)$$

$$R_{su} = \frac{{}_cQ_{su} / {}_cQ_{mu} - 0.3}{0.7} \cdot R_{my} = \frac{\frac{203.12}{149.72} - 0.3}{0.7} \cdot \frac{1}{150} = 0.0101$$

h) Plastic deformation angle of column  ${}_cR_{mp}$

$$s = 125 > 100mm, q = 1.1$$

$$\text{Hence, } {}_cR_{mp} = 10 \left( \frac{{}_cQ_{su}}{{}_cQ_{mu}} - q \right) \cdot {}_cR_{my} = 10 \left( \frac{203.12}{149.72} - 1.1 \right) \cdot \frac{1}{150} = 0.017$$

i) Inter-storey drift angle at the ultimate flexural strength of column  $R_{mu}$

$${}_cR_{mu} = {}_cR_{my} + {}_cR_{mp} = 1/150 + 0.017 = 0.024$$

$${}_cR_{mu} \leq {}_cR_{max}, \text{ so, } {}_cR_{mu} = {}_cR_{max} = 0.024$$

$$R_{mu} = (h_0/H_0) \times {}_cR_{mu} \geq R_{250} = 1.0 \times 0.024 = 0.024$$

j) The ductility index, F

since  $R_{mu} > R_y$

$$F = \frac{\sqrt{2R_{mu}/R_y - 1}}{0.75 \times (1 + 0.05R_{mu}/R_y)} = \frac{\sqrt{2 \times \frac{0.024}{1/150} - 1}}{0.75 \times \left(1 + 0.05 \times \frac{0.024}{1/150}\right)} = 2.8$$

Similarly, ductility index value can be evaluated for all the columns for all stories.

Calculation results for the whole structure is shown in the appendix.

### **Structure performance**

Figure 7.2.5 shows the seismic evaluation results of the structure by the C-F relationships according to the CNCRP/BSPP Manuals for Seismic Evaluation of Existing Reinforced Concrete Buildings.

*C – F* relationship of the example building:

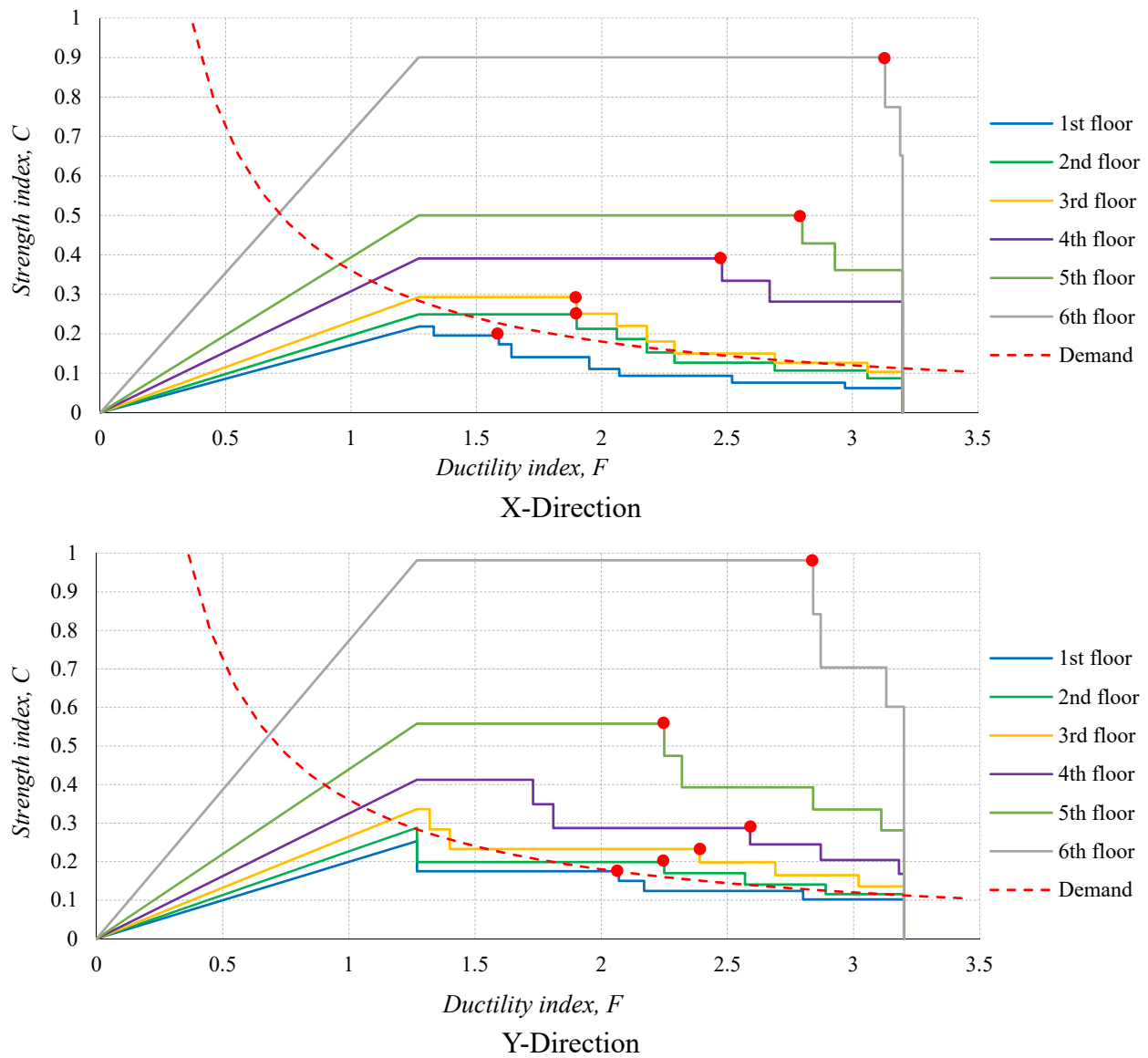


Figure 7.2.5 Seismic evaluation results according to the CNCRP/BSPP Manuals.

Basic seismic index  $E_0$  is evaluated for each direction of loading in each storey to determine failure point according to the CNCRP/BSPP Manuals for Seismic Evaluation of Existing Reinforced Concrete Buildings. An example for 2<sup>nd</sup> floor in the Y-Direction is shown below.  $E_0$  values are calculated at each peak of peak of the structural performance curve ( $C - F$  relationship).

Table 7.2.3 Basic seismic index  $E_0$  of 2<sup>nd</sup> floor in the Y-Direction

Peak	$\frac{n + 1}{n + i}$	Strength index, $C$	Ductility index, $F$	Basic seismic index, $E_0$
1	0.875	0.288	1.27	0.322

2	0.875	0.199	2.25	0.393
3	0.875	0.170	2.57	0.385
4	0.875	0.141	2.89	0.358
5	0.875	0.115	3.2	0.325

So, the maximum value of  $E_0$  is 0.393 which is obtained at  $F = 2.25$  for the 2<sup>nd</sup> floor in the Y-direction.

The possibility of pullout failure at exterior beam-column joints of the structure should be judged according to the SATREPS-TSUIB Guidelines for Seismic Evaluation of Existing RC Buildings.

Since this building was constructed between 1995-2006 and deformed rebar was used in construction, this building has a risk of pullout failure at the exterior beam-column joints. Thus, the seismic evaluation results of the structure was modified considering the deformation limit of 2.2 without any retrofitting and re-checked against the demand

Table 7.2.4 Basic seismic index  $E_0$  of 2<sup>nd</sup> floor in the Y-Direction up to  $F_{limit}$

Peak	$\frac{n+1}{n+i}$	Strength index, $C$	Ductility index, $F$	Basic seismic index, $E_0$
1	0.875	0.288	1.27	0.322
2	0.875	0.199	2.2*	0.382
3	0.875	0.170	2.2*	0.327
4	0.875	0.141	2.2*	0.271
5	0.875	0.115	2.2*	0.221

\*Considering the structural performance up to deformation limit of 2.2 according to “*Technical Guidelines for Seismic Evaluation of Existing Reinforced Concrete Buildings for Extended Application of BSPP Seismic Evaluation Manual*”.

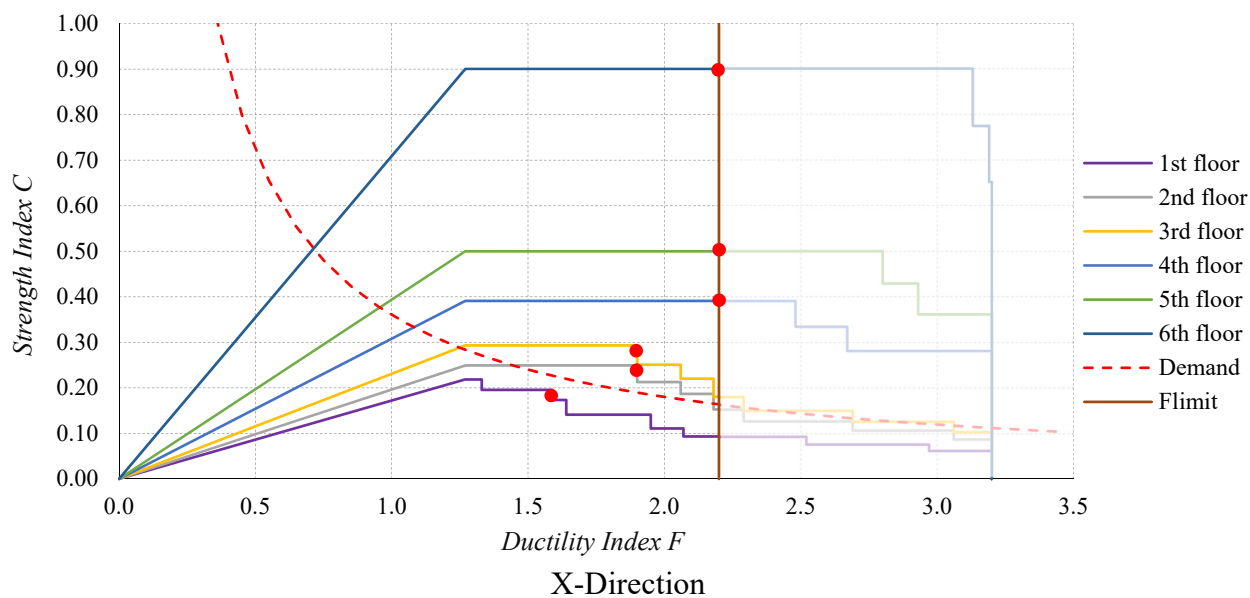
Basic seismic index  $E_0$  was evaluated by EQ.4 and Eq.5 as described in CNCRP/BSPP manuals.

Similarly, basic seismic index  $E_0$  values can be evaluated for each storey in both directions.

Table 7.2.5 Basic seismic index  $E_0$  of whole building

Storey	$\frac{n+1}{n+i}$	X-Direction			Y-Direction		
		Basic seismic index $\max E_0$		Corresponding ductility index	Basic seismic index $\max E_0$		Corresponding ductility index
		EQ. 4*	EQ. 5		EQ. 4*	EQ. 5	
6	0.583	0.866	1.155	2.2	0.823	1.260	2.2
5	0.636	0.524	0.700	2.2	0.440	0.781	2.2
4	0.7	0.449	0.602	2.2	0.300	0.416	2.2
3	0.778	0.219	0.433	1.90	0.263	0.398	2.2
2	0.875	0.209	0.414	1.90	0.260	0.382	2.2
1	1	0.176	0.311	1.59	0.261	0.362	2.07

\*  $F_{limit} = 2.2$  was used while evaluating the  $E_0$  value by EQ.4, deformation capacity ( $F$ ) of any member beyond 2.2 was considered as 2.2 for the evaluation process.





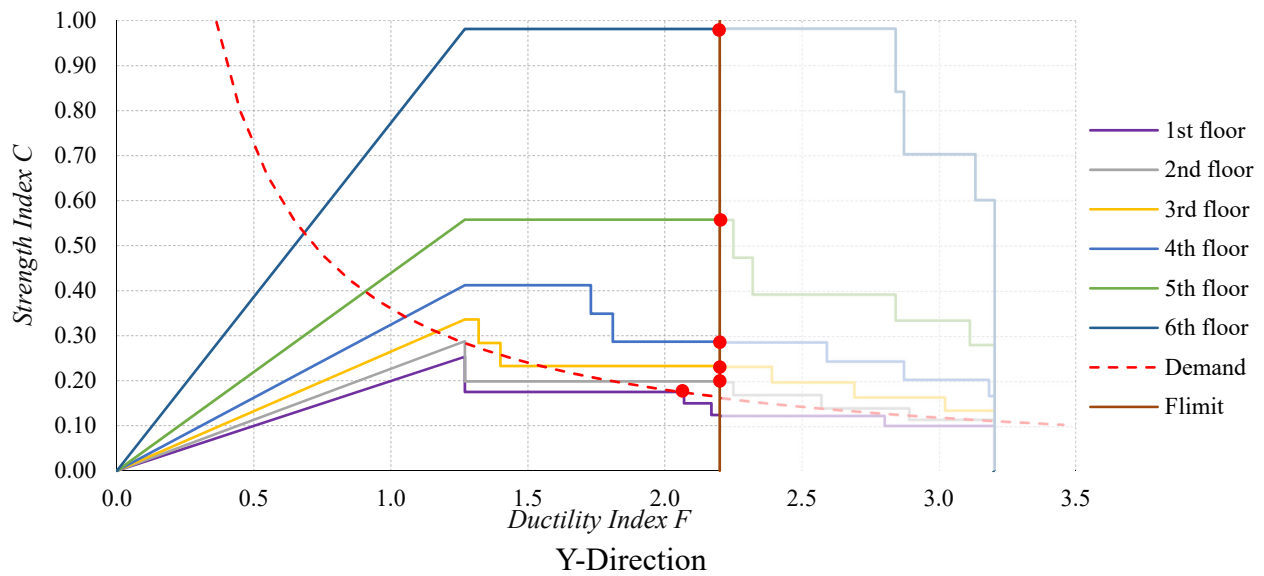


Figure 7.2.6 Structural performance curve

For this structure irregularity index  $S_D = 1.0$  and time index  $T = 1.0$

The seismic capacity of this structure on the 2<sup>nd</sup> floor in the Y-direction is  $I_S = E_0 \cdot S_D \cdot T = 0.382$  [at  $F = 2.2$ ]

Similarly,  $I_S$  index can be calculated for each storey in both directions.

Table 7.2.6 Seismic performance judgment

Storey	Seismic demand $I_{S0}$	X-Direction			Y-Direction		
		Seismic capacity $I_S$	Corresponding ductility index	Judgment	Seismic capacity $I_S$	Corresponding ductility index	Judgement
6	0.360	1.155	2.2	OK	1.260	2.2	OK
5		0.700	2.2	OK	0.781	2.2	OK
4		0.602	2.2	OK	0.416	2.2	OK
3		0.433	1.90	OK	0.398	2.2	OK
2		0.414	1.90	OK	0.382	2.2	OK
1		0.311	1.59	Not Good	0.362	2.07	OK

Only the seismic capacity index  $I_s$  of the 1<sup>st</sup> floor was lower than the seismic demand index  $I_{s0}$ , while other storey's seismic capacity exceeded the demand within the limited ductility limit of 2.2.

Seismic capacity of 1<sup>st</sup> floor was obtained at a ductility index of 1.59 while considering the structural performance up to ductility limit of 2.2. Hence, the 1<sup>st</sup> floor in the X-Direction of the building is expected to fail before the initiation of pullout failure on exterior beam-column joint. Thus, structural strengthening to prevent pullout failure i.e. installation of wing walls on exterior column is not required for this building. Other retrofitting scheme focusing on increasing the structural performance is required.

## References

1. Technical Guidelines for Seismic Evaluation of Existing Reinforced Concrete Buildings in Bangladesh for Extended Application of BSPP Seismic Evaluation Manual, 2021.
2. Public Works Department (PWD). Manual for seismic evaluation of existing reinforced concrete buildings, Manual for seismic retrofit design of existing reinforced concrete buildings, Manual for seismic design of existing reinforced concrete buildings (CNCRP manual). Published online 2015.
3. JBDPA. Standard for seismic evaluation of existing reinforced concrete buildings, 2001, Guidelines for seismic retrofit of existing reinforced concrete buildings, 2001 and Technical manual for seismic evaluation and seismic retrofit of existing reinforced concrete. Published online 2005.
4. HBRI. Bangladesh National Building Code (BNBC 2020).

### **7.3 Seismic evaluation considering Beam-column joints**

## **Appendix C: Application Example: 3**

### ***Seismic evaluation of Flat plate structures***

#### **Contents:**

#### **7.3 Example calculation of flat plate structure**

7.3.1. General

7.3.2. Overview of the Example building

7.3.3. Seismic evaluation of the building

### **7.3 Example calculation of flat plate structure**

#### **7.3.1 General**

The procedure of the seismic evaluation is demonstrated in this section through an example of flat plate structure. The main purpose of the example is to show how to calculate the seismic index  $I_s$  based on the “*Technical guidelines for seismic evaluation of reinforced concrete buildings for extended application of BSPP seismic evaluation manual* (chapter 6)”. The calculation procedure is explained, considering the 1<sup>st</sup> story in X-direction only, since the detailed calculation was provided in the CNCRP manuals.

#### **Objectives and Scope**

To determine the Seismic capacity of the flat plate building by detail seismic evaluation and compare that with required seismic capacity as per BNBC 2020.

The CNCRP/BSPP Manuals does not include a sample calculation for the flat plate structure in the scope of application. Therefore, the following sample calculation is intended to be a supplement document to evaluate the seismic capacity of flat plate structures commonly used in Bangladesh. Evaluation assumptions are established in accordance with the CNCRP/BSPP Manuals and the SATREPS-TSUIB Guidelines.

#### **Flow Chart/Diagram of Seismic Evaluation**

The Seismic Evaluation flow diagram is shown in Figure C1. The evaluation method is based on the “*Technical guidelines for seismic evaluation of reinforced concrete buildings for extended application of BSPP seismic evaluation manual* (chapter 6)” published by HBRI.

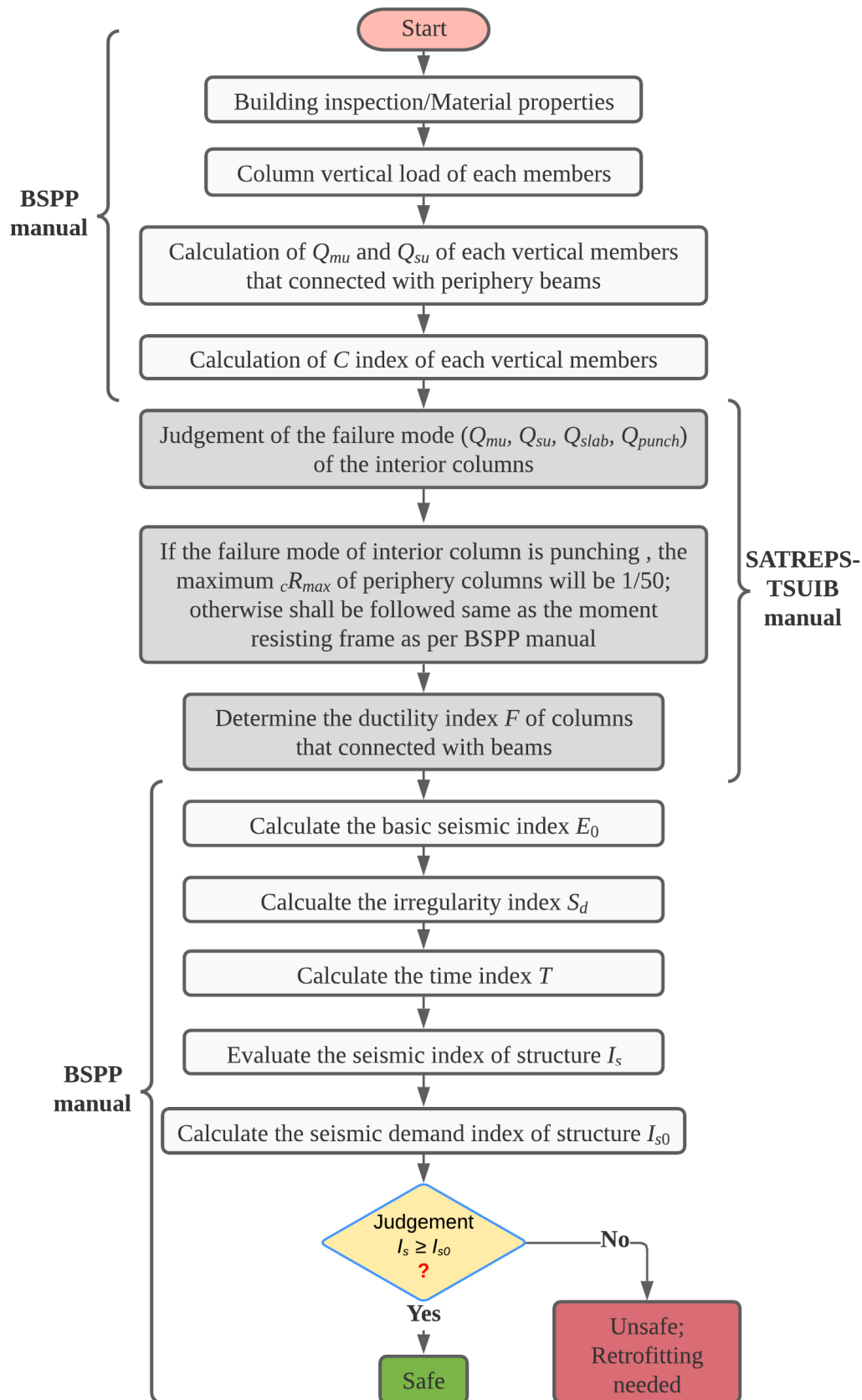


Figure C1 Flow Diagram of Seismic Evaluation

### 7.3.2 Overview of the Example Building

The sample building is assumed to be a 6-storey typical Bangladeshi flat plate structure located in Dhaka city.

The floor plan and column schedule of the existing building are shown in Figures C2 and C3, respectively.

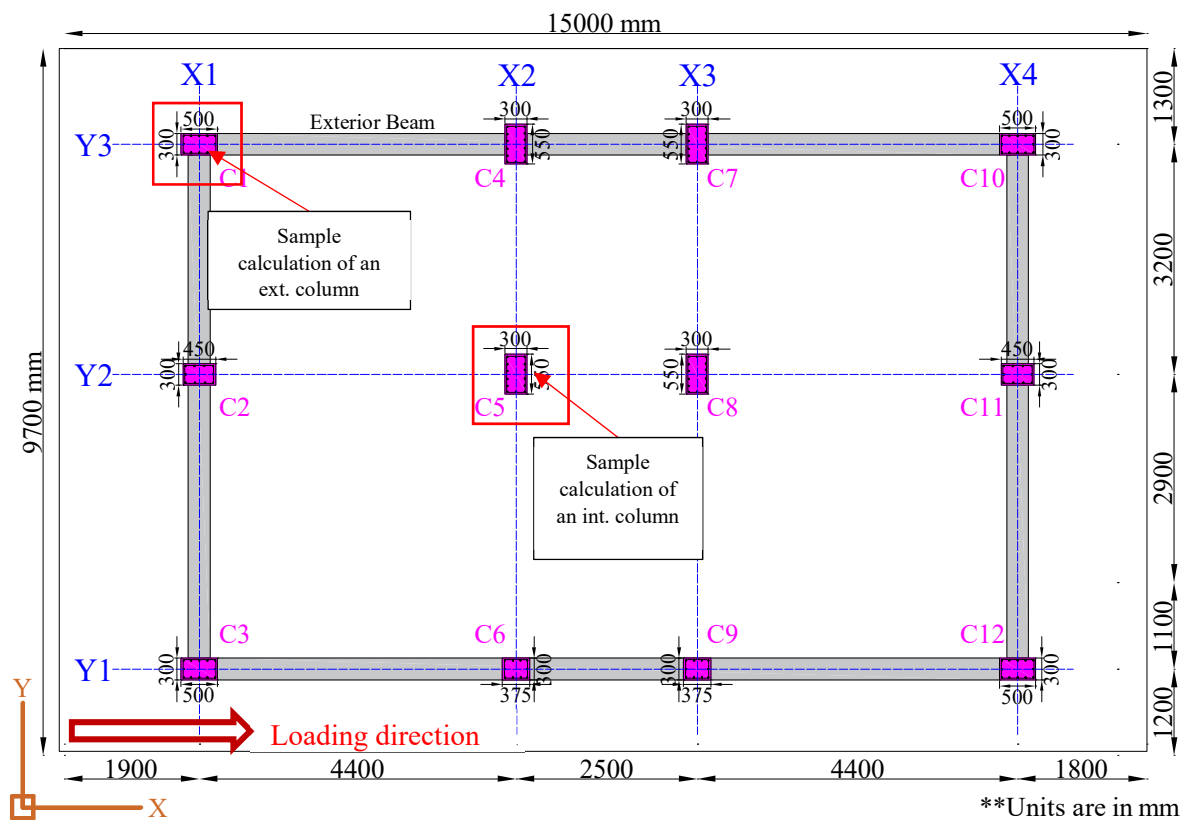
#### Characteristics of the building

Some of the important specifications of the building are listed below:

- 1) Typical flat plate structure
- 2) No earthquake resisting design performed
- 3) Exterior beams exist

Table C1 Summary of materials

Concrete Strength	24 (N/mm <sup>2</sup> ) for column and 20 (N/mm <sup>2</sup> ) for slab
Rebar yield stress	400 (N/mm <sup>2</sup> )
Type of rebar	Deformed



\*\*Slab thickness = 200mm

\*\*12mm @ 100 mm C/C STR top bar

\*\*12mm @ 200 mm C/C STR bottom bar

\*\*Clear cover at bottom 25mm, top 18mm

Figure C2 Typical floor layout with exterior beams

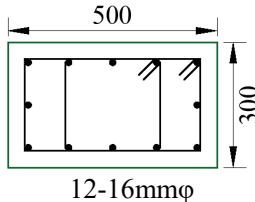
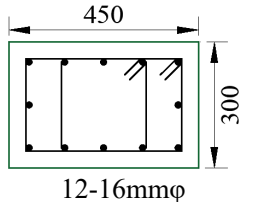
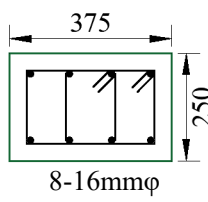
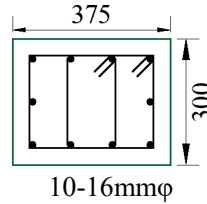
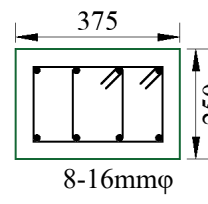
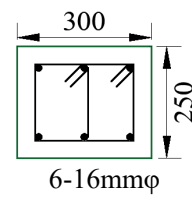
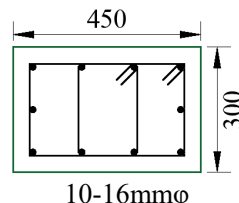
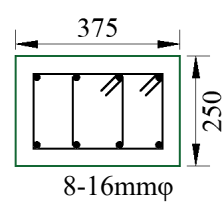
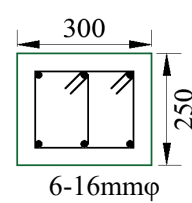
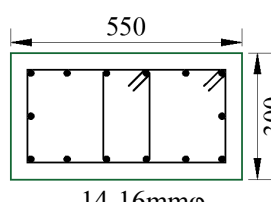
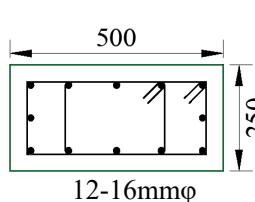
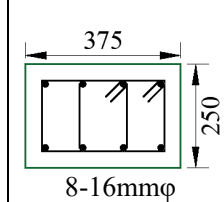
Column Type	Column Size Below EGL	Main Reinforcement			TIES
		Above EGL to 1st Floor	2nd Floor to 3rd Floor	4th Floor to Onward	
C1	300 × 500 (mm)	 12-16mmφ	 12-16mmφ	 8-16mmφ	All TIES will be provided as 10mmφ @ 100mm C/C at joint zone and 10mmφ @ 200mm C/C at mid zone
C2	300 × 375 (mm)	 10-16mmφ	 8-16mmφ	 6-16mmφ	
C3	300 × 450 (mm)	 10-16mmφ	 8-16mmφ	 6-16mmφ	
C4	300 × 550 (mm)	 14-16mmφ	 12-16mmφ	 8-16mmφ	

Figure C3 Column schedule of the existing structure

### Preliminary Calculation

The assumed typical floor weight is 12.0 kN/m<sup>2</sup>.

Table C2 Summary of Floor weight of the structure

Storey	Floor Area (m <sup>2</sup> )	Floor Weight $W_i$ (kN)	Total weight (kN)
6	145.5	1746	1746
5	145.5	1746	3492
4	145.5	1746	5238
3	145.5	1746	6984
2	145.5	1746	8730
1	145.5	1746	10476

Storey shear modification factors for calculating  $E_0$  are listed as follows. However, the calculation procedures are shown for 1<sup>st</sup> storey only; thus, the factor value will be 1.

Table C3 Storey modification factor

Storey	Modification factor
6	0.583
5	0.636
4	0.700
3	0.778
2	0.875
1	1.000

Table C4 Summary of Sustaining Force of Columns

Column ID	Story	Tributary area (m <sup>2</sup> )	Weight $W_i$ (kN)	Sustaining force (kN)
C1	1	11.9	143	856
C2	1	14.8	177	1063
C3	1	13.1	157	945
C4	1	10.0	120	720
C5	1	12.4	149	894
C6	1	11.0	133	795
C7	1	10.0	120	720
C8	1	12.4	149	894
C9	1	11.0	133	795
C10	1	11.6	139	835
C11	1	14.4	173	1063
C12	1	12.8	154	922

### 7.3.3 Seismic evaluation of the building

The shear resistance of the exterior columns connected to beams only contributes to the seismic performance of the building according to the current guidelines because those of the interior columns shall be zero. However, the failure modes of interior columns should be judged because they affect the  $F$  index of the building.

**Judgement of the failure mode for interior column according to the “Technical guidelines for seismic evaluation of reinforced concrete buildings for extended application of BSPP seismic evaluation manual (chapter 6).”**

For the interior column, four types of failure modes were considered. The strength of each failure mechanism was calculated as the following. Based on the calculated strengths, the failure mode was determined by taking that showing the minimum value.

The general procedure for the judgment of the failure mode of the interior column C5 is shown as below:

$${}_iQ_u = \min (Q_{mu}, Q_{su}, Q_{slab}, Q_{punch})$$

where  $Q_{mu}$  is column shear resistance at flexural yielding of the column

$Q_{su}$  is column shear resistance at shear failure of the column

$Q_{slab}$  is column shear at flexural yielding of slab adjacent to the column

$Q_{punch}$  is column shear at punching shear failure of slab adjacent to the column



### [Column]

$b \times D$ : 550 mm  $\times$  300 mm (22"  $\times$  12")

$a_t$ : 6-D16 (6  $\times$  201 = 1206 mm<sup>2</sup>)

$\sigma_y$ : 400 (N/mm<sup>2</sup>) (Grade 60)

$f'_c$ : 24 (N/mm<sup>2</sup>)

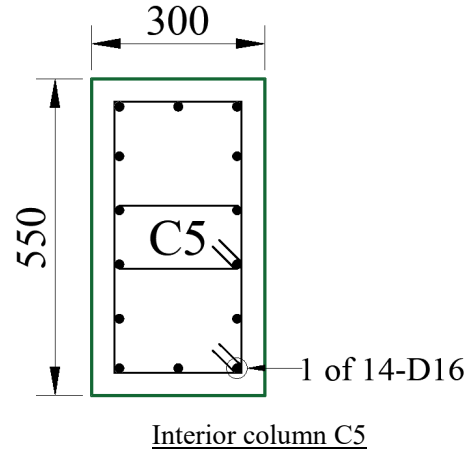
Axial Force: 894240 (N)

$h_0$ : 3.6 (m) (1<sup>st</sup> floor)

$H_0$ : 3.6 - 0.575 = 3.025 (m) (1<sup>st</sup> floor)

Tie bar: D10@100

$\sigma_y$ : 400 (N/mm<sup>2</sup>)



### [Slab]

Thickness: 200 (mm)

Span: (4400 + 2500) / 2 = 3.45 (m)

Reinforcement: D12@200 (extra top 1-D12)

$\sigma_y$ : 275 (N/mm<sup>2</sup>)

$f'_c$ : 20 (N/mm<sup>2</sup>)

**(b)  $Q_{mu}$ :** Column shear resistance based on the flexural yielding at the top and bottom of column

In the case of this example, axial load  $N$  satisfies the following relation.

$$0.4bDf'_c = 0.4 \times 550 \times 300 \times 24 = 1584,000 \text{ (N)}$$

$$0.4bDf'_c > N > 0$$

Storey height: 3.6 (m)

Clear height of column,  $h_0$  = 3.6 - 0.575 = 3.025 (m)

Therefore,

$$\begin{aligned}
M_u &= 0.8a_t\sigma_yD + 0.5ND \left( 1 - \frac{N}{bDf'_c} \right) \\
&= 0.8 \times 1206 \times 400 \times 300 + 0.5 \times 894240 \times 300 \times \left( 1 - \frac{894240}{550 \times 300 \times 24} \right) \\
&= 219621652 \text{ (N} \cdot \text{mm)}
\end{aligned}$$

$$= 219.6 \text{ (kN} \cdot \text{m)}$$

$$Q_{mu} = M_u / (h_0 / 2) = 2 \times 219.6 / 3.025 = 145.2 \text{ (kN)}$$

(c)  $Q_{su}$ : Column shear resistance based on the shear failure of column

$$p_t = \frac{1206}{550 \times 300} = 0.00731 = 0.731\%$$

$$d = 300 - 40 - 10 - \frac{16}{2} = 242 \text{ (mm)}$$

$$\frac{M}{Q \cdot d} = \frac{h_0}{2 \cdot d} = \frac{3.025 \times 1000}{2 \times 242} = 6.25 > 3; \text{ use } 3$$

$$p_w \sigma_{wy} = \frac{2 \times 78.5}{550 \times 100} \times 400 = 1.14;$$

$$0.1 \sigma_0 = 0.1 \times \frac{N}{b \cdot j} = 0.1 \times \frac{894240}{550 \times 0.8 \times 300} = 0.677$$

Therefore,

$$Q_{su} = \left\{ \frac{0.053 p_t^{0.23} (f_c' + 18)}{M / (Qd) + 0.12} + 0.85 \sqrt{p_w \sigma_{wy}} + 0.1 \sigma_0 \right\} \cdot b \cdot j$$

$$= \left\{ \frac{0.053 \times 0.731^{0.23} \times (24 + 18)}{3 + 0.12} + 0.85 \sqrt{1.14 + 0.677} \right\} 550 \times 240$$

$$= 296789 \text{ (N)}$$

$$= 296.8 \text{ (kN)}$$

(d)  $Q_{slab}$ : Column shear resistance based on the flexural yielding of slab

Reinforcement: D12@200 alt. with extra top 1-D12@200

Number of reinforcement = transverse span length / spacing of rebar =  $6100 / 2 \times 100 = 31 + 1 = 32$  rebar for top slab and 18 rebar for bottom slab.

$$Q_{slab} = \frac{M_{slab}}{h_0}$$

where,  $M_{slab}$ : flexural yielding capacity of slab perspective with the nodal moment

$$h_0: \text{clear height of column} = 3.025 \text{ (m)}$$

The flexural yielding capacity of slab,  $M_{slab}$ :

$$M_{slab} = 0.9 a_t \sigma_y d = 0.9 \times 32 \times 113.1 \times 275 \times 182$$

$$= 163026864 \text{ (N} \cdot \text{mm)} = 163.0 \text{ (kN} \cdot \text{m)}$$

$$rM_{slab} = 0.9a_t\sigma_y d = 0.9 \times 16 \times 113.1 \times 275 \times 182$$

$$= 81513432 \text{ (N} \cdot \text{mm)} = 81.5 \text{ (kN} \cdot \text{m)}$$

$$M_{slab} = \frac{\frac{4025 + 300}{2}}{\frac{4025}{2}} \times 163 + \frac{\frac{2200 + 300}{2}}{\frac{2200}{2}} \times 81.5 \text{ (right)} = 267.7 \text{ (kN.m)}$$

$$Q_{slab} = M_{slab}/h_0$$

$$= 267.7 / 3.025$$

$$= 88.5 \text{ (kN)}$$

To calculate  $Q_{slab}$ , the bending moment diagram (Grid Y2) was assumed as shown in Figure C4 in the seismic evaluation guidelines. Different amounts of the slab top and bottom reinforcement lead to different moment resistances for the left and right slabs.

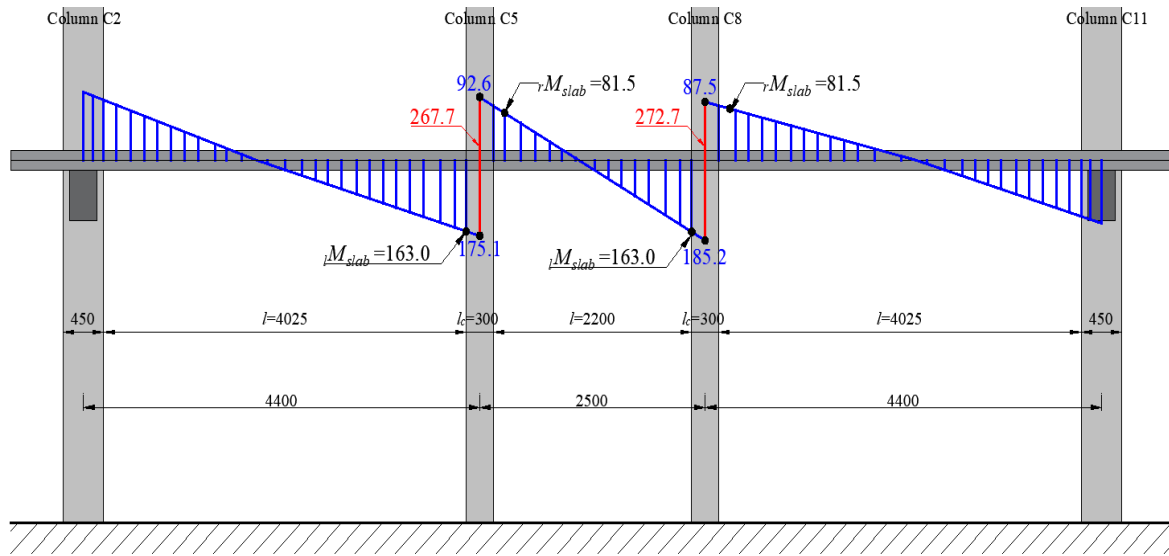


Figure C4 Assumed moment diagram at slab yielding (Grid Y2)

(e)  $Q_{punch}$ : Column shear resistance based on the punching shear failure

Thickness: 200 (mm) Reinforcement: D12@200 alt. with extra top 1-D12@200

$c_1$  = column depth = 300 (mm)

$c_2$  = column width = 550 (mm)

$\sigma_y$  : 275 (MPa) for slab (400 MPa for column)

$F_c$  : 20 (MPa) for slab (24 MPa for column)

Axial load (one storey)  $V_u=149.0$  (kN)

$d$  : effective depth =200-18 =182 (mm)

$$\begin{aligned} M_f &= 0.9a_{0t} \cdot \sigma_y \cdot d \cdot \frac{c_2+d}{x_t} + 0.9a_{0b} \cdot \sigma_y \cdot d \cdot \frac{c_2+d}{x_b} \\ &= 0.9 \times 113.1 \times 275 \times 182 \times \frac{550+182}{100} + 0.9 \times 113.1 \times 275 \times 182 \times \frac{550+182}{200} \\ &= 55938593 \text{ (N} \cdot \text{mm)} \\ &= 55.9 \text{ (kN} \cdot \text{m)} \end{aligned}$$

$$\begin{aligned} M_s &= \tau_u \cdot (c_2 + d) \cdot d \cdot (c_1 + d) \\ &= 0.335 \times \sqrt{20} \times (550 + 182) \times 182 \times (300 + 182) \\ &= 96203154 \text{ (N} \cdot \text{mm)} \\ &= 96.2 \text{ (kN} \cdot \text{m)} \end{aligned}$$

$$\begin{aligned} M_t &= \tau_{tu} \frac{d^2}{2} \left\{ (c_1 + d) - \frac{d}{3} \right\} \cdot 2 \\ &= 6 \times 0.335 \times \sqrt{20} \times \frac{182^2}{2} \left\{ (300 + 182) - \frac{182}{3} \right\} \cdot 2 \\ &= 125452600 \text{ (N} \cdot \text{mm)} \\ &= 125.5 \text{ (kN} \cdot \text{m)} \end{aligned}$$

$$M_0 = M_f + M_s + M_t = 55.9 + 96.2 + 125.4 = 277.6 \text{ (kN} \cdot \text{m)}$$

$$\begin{aligned} V_0 &= \tau_u A_c = 0.335 \sqrt{20} \times \{ (300 + 182) \times 2 + (550 + 182) \times 2 \} \times 182 \\ &= 662033362 \text{ (N)} = 662.0 \text{ (kN)} \end{aligned}$$

$$\frac{V_u}{V_0} + \frac{M_u}{M_0} = \frac{149.0}{662.03} + \frac{M_u}{277.6} = 1$$

$$M_u = 215.1 \text{ (kN} \cdot \text{m)}$$

$$\therefore Q_{punch} = \frac{M_u}{h_0} = \frac{M_u(top) + M_u(bottom)}{h_0} = \frac{M_u(top)}{h_0/2} = \frac{215.1}{3.025} = 71.1 \text{ (kN)}$$

Therefore,  $iQ_u = 71.1$  (kN); **punching failure mode**

To calculate  $Q_{punch}$ , the bending moment diagram was assumed, as shown in Figure C5 in the seismic evaluation guidelines.

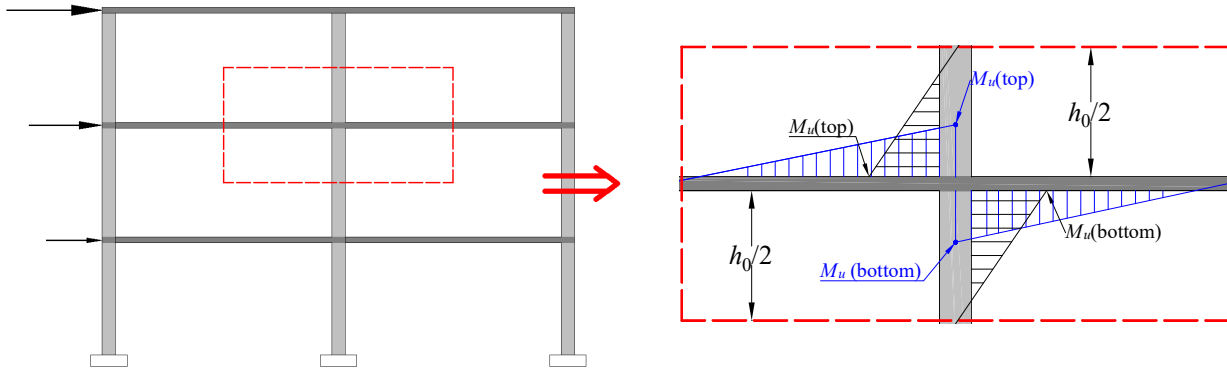


Figure C5 Assumed moment diagram for slab punching

The failure mode of the interior column was punching shear failure. Therefore, the  $F$ -index of the exterior columns (with beam) of this building should consider the upper limit of the drift angle of an exterior column  ${}_eR_{max}$  of 1/50, which will be described later in this section.

**Column shear resistance for exterior column according to the “Technical guidelines for seismic evaluation of reinforced concrete buildings for extended application of BSPP seismic evaluation manual (chapter 6)”**

The exterior column shear resistance  ${}_eQ_u$  was calculated by the following equation according to the “Technical guidelines for seismic evaluation of reinforced concrete buildings for extended application of BSPP seismic evaluation manual”. Based on the calculated strengths, the failure mode can be determined by taking that showing the minimum value.

$${}_eQ_u = \min (Q_{mu}, Q_{su})$$

where  $Q_{mu}$  is column shear force at the flexural yielding

$Q_{su}$  is column shear strength at the shear failure

**Typical Floor dimensions:**  $15 \times 9.7 = 145.5 \text{ (m}^2\text{)}$

Total weight of the building  $= 15 \times 9.7 \times 12 \times 6 = 10476 \text{ (kN)}$

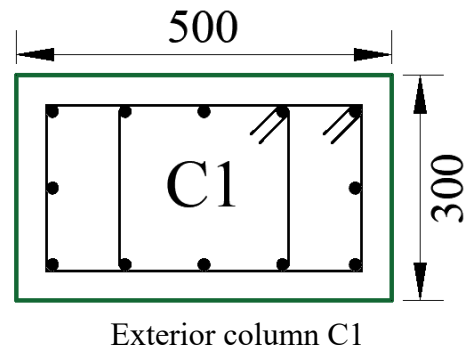
**(a)  $Q_{mu}$**

In the case of this example, axial load  $N$  satisfies the following relation.

Axial load,  $N = 4.1 \times 2.9 \times 6 \times 12 = 856080 \text{ (N)}$

$b \times D = 300 \text{ (mm)} \times 500 \text{ (mm)}$

$0.4bDf'_c = 0.4 \times 300 \times 500 \times 24 = 1440,000 \text{ (N)}$



$$0.4bDf'_c > N > 0$$

Therefore,

$$\begin{aligned} M_u &= 0.8a_t\sigma_y D + 0.5ND \left(1 - \frac{N}{bDf'_c}\right) \\ &= 0.8 \times 603 \times 400 \times 500 + 0.5 \times 856080 \times 500 \times \left(1 - \frac{856080}{500 \times 300 \times 24}\right) \\ &= 259.6 \text{ (kN} \cdot \text{m)} \end{aligned}$$

$$Q_{mu} = \frac{M_u}{\frac{h_0}{2}} = \frac{259.6}{3.025} \times 2 = 171.7 \text{ (kN)}$$

(b)  $Q_{su}$

$$p_t = \frac{603}{500 \times 300} = 0.004 = 0.4\%$$

$$d = 500 - 40 - 10 - \frac{16}{2} = 442 \text{ (mm)}$$

$$\frac{M}{Q \cdot d} = \frac{h_0}{2 \cdot d} = \frac{3.025 \times 1000}{2 \times 442} = 3.42 > 3; \text{ use } 3$$

$$p_w\sigma_{wy} = \frac{2 \times 78.5}{300 \times 100} \times 400 = 2.09;$$

$$0.1\sigma_0 = 0.1 \times \frac{N}{b \cdot D} = 0.1 \times \frac{856080}{300 \times 500} = 0.57$$

$$j = 0.8 \times 500 = 400 \text{ (mm)}$$

$$\begin{aligned} \text{Therefore,} \quad Q_{su} &= \left\{ \frac{0.053p_t^{0.23}(f'_c + 18)}{M/(Qd) + 0.12} + 0.85\sqrt{p_w\sigma_{wy}} + 0.1\sigma_0 \right\} \cdot b \cdot j \\ &= \left\{ \frac{0.053 \times 0.4^{0.23} \times (24 + 18)}{3 + 0.12} + 0.85\sqrt{2.09} + 0.57 \right\} 300 \times 400 \\ &= 285.2 \text{ (kN)} > 171.7 \text{ (kN)}; \text{ Flexural column} \end{aligned}$$

The ultimate shear strength of each exterior column was calculated in the same procedure. The calculated strength of each member is listed below.

Table C5 Summary of the column lateral resistances

Column ID	Floor	$M_u$ (kN.m)	$Q_{mu}$ (kN)	$Q_{su}$ (kN)	$Q_{slab}$ (kN)	$Q_{punch}$ (kN)	$Q_u$ (kN)	Failure mode	Remarks
C1	1	259.6	171.7	285.2	-	-	171.7	Flexure	Ext. column with beam
C2	1	Ignoring shear resistance							Ext. column without beam
C3	1	270.7	179.0	292.6	-	-	179.0	Flexure	Ext. column with beam

C4	1	204.2	135.0	265.2	-	-	135.0	Flexure	Ext. column with beam
C5	1	219.6	145.2	296.8	88.5	71.1	74.3	Punching	Int. column
C6	1	177.5	117.4	229.9	-	-	117.4	Flexure	Ext. column with beam
C7	1	204.2	135.0	265.2	-	-	135.0	Flexure	Ext. column with beam
C8	1	219.6	145.2	279.1	90.1	71.1	74.3	Punching	Int. column
C9	1	177.5	117.4	229.9	-	-	117.4	Flexure	Ext. column with beam
C10	1	256.9	169.8	283.8	-	-	169.8	Flexure	Ext. column with beam
C11	1	Ignoring shear resistance							Ext. column without beam
C12	1	267.9	177.1	290.7	-	-	177.1	Flexure	Ext. column with beam

### **Calculation of C index of the column C1 according to the CNCRP Manual**

The strength index  $C$  was calculated as follows:

$$C = \frac{\min(Q_{mw}, Q_{su})}{\Sigma W}$$

$\Sigma W$  =total weight of the building

Thus,  $C$  index of  $C_1$  column =  $171.7/10476 = 0.0164$

### **Calculation of F index of the column C1 according to the CNCRP Manual**

The ductility index calculation of the vertical members with the perimeter beams shall follow the CNCRP manual. In principle, the upper limit of the drift angle of flexural column shall be calculated with the following equations. The CNCRP/BSPP Manuals provided detailed calculations; thus, the typical calculations are omitted in this extensive procedure.

$${}_cR_{max} = \min \{ {}_cR_{max(n)}, {}_cR_{max(s)}, {}_cR_{max(t)}, {}_cR_{max(b)}, {}_cR_{max(h)} \}$$

$$\therefore {}_cR_{max} = \min \left\{ \frac{1}{33}, \frac{1}{30}, \frac{1}{30}, \frac{1}{30}, \frac{1}{30} \right\} = 1/33$$

${}_cR_{max}$ , the upper limit of the deflection angle of an exterior flexural column shall be determined by the failure mode of an interior column according to the “Technical guidelines for seismic evaluation of reinforced concrete buildings for extended application of BSPP seismic evaluation manual (chapter 6)”. Therefore,  ${}_cR_{max(punch)}$  shall be considered when the failure mode of an interior column is punching.

$$\text{So, } {}_cR_{max(punch)} = \frac{1}{50}$$

Here,  $cR_{\max} = \frac{1}{33} > cR_{\text{punch}} = \frac{1}{50}$ ; (Since the failure mode of an interior column is punching, the upper limit of the drift angle of members shall be  $cR_{\max} = 1/50 = 0.02$ .)

$$\text{Therefore, } cR_{\max} = \frac{1}{50}$$

$$\text{And, } cR_{\text{my}} = \frac{1}{150}, R_{\text{mu}} = \frac{1}{50}$$

#### The ductility index:

Since  $R_{\text{mu}} \geq R_y$

$$\text{Therefore, } F = \frac{\sqrt{2R_{\text{mu}}/R_y - 1}}{0.75(1 + 0.05R_{\text{mu}}/R_y)} \leq 3.2 \text{ for } R_{\text{mu}} \geq R_y$$

$$F = \frac{\sqrt{2 \times \frac{1}{50} \times \frac{1}{150} - 1}}{0.75(1 + 0.05 \times \frac{1}{50} \times \frac{1}{150})} = 2.6$$

The strength index  $C$  and ductility index  $F$  of each exterior column can be calculated in the same procedure. The calculated index of each member is listed below.

Table C6 Ductility index  $F$  and strength index  $C$

Column ID	Storey	Weight of the building	$Q_u$ (kN)	$C$	$Q_{su}/Q_{mu}$	$F$	Remarks
C1	1	10476	171.7	0.0164	1.66	2.6	Ext. column with beam
C2	1		Ignoring shear resistance				Ext. column <b>without</b> beam
C3	1		179.0	0.0171	1.63	2.6	Ext. column with beam
C4	1		135.0	0.0129	1.96	2.6	Ext. column with beam
C5	1		-	-	-	-	Int. col. (punching)
C6	1		117.4	0.0113	1.96	2.6	Ext. column with beam
C7	1		135.0	0.0129	1.96	2.6	Ext. column with beam
C8	1		-	-	-	-	Int. col. (punching)
C9	1		117.4	0.0113	1.96	2.6	Ext. column with beam
C10	1		169.8	0.0162	1.67	2.6	Ext. column with beam
C11	1		Ignoring shear resistance				Ext. column <b>without</b> beam
C12	1		177.1	0.0169	1.64	2.6	Ext. column with beam

[**Note:** The columns without being connected to beams are flexible in their respective directions; thus, only the contributions of perimeter columns with beams can be considered to evaluate the seismic capacity of the structure. [For example: in this sample building, C2 and C11 columns are not connected with beams in the X-direction; thus, their contributions shall be ignored along with the interior columns of C5 and C8]

Therefore, the summation of  $C$  from all contributed columns is 0.117.

The seismic capacity of the building structure is expressed by the structural seismic index  $I_s$  calculated form:

$$I_s = E_0 \times S_d \times T$$



Here, the basic seismic index,  $E_0 = C \cdot F = 0.1168 \cdot 2.59 = 0.303$ , as shown in Figure C6 (since, there is one group only)

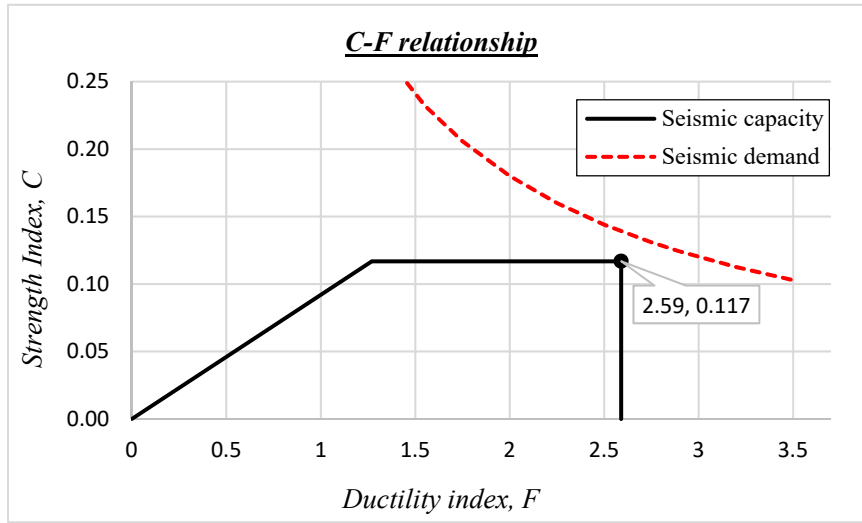


Figure C6 Relationship between strength index  $C$  and ductility index  $F$

Therefore, the seismic index,  $I_s = E_0 \times S_d \times T = 0.303 \times 1 \times 1 = 0.303$  (story modification factor = 1)

Where,  $E_0$  = Basic seismic index,  $S_d = 1.0$  (Irregularity index),  $T = 1.0$  (time index)

### Seismic demand index

Seismic demand index  $I_{s0}$  is determined as per the requirement of BNBC 2020.

$$I_{s0} = \frac{0.8 \times 2}{3} \cdot Z \cdot I \cdot C_s$$

Where:

$Z$ : Seismic zone coefficient, as defined in Section 2.5.4.2 of BNBC (2020)

$I$ : Structure importance factor, as defined in Section 2.5.5.1 of BNBC (2020)

$C_s$ : Normalized acceleration response spectrum, which is a function of structure (building) period and soil type (site class), as defined by Eqs. 6.2.35a to 6.3.35d of BNBC (2020)

$Z$ : 0.2 (zone coefficient)

$I$ : 1.0

Therefore,

$$I_{s0} = 0.8 \times 2 / 3 \times Z \times I \times C_s$$

$Z = 0.2$ ,  $I = 1.0$ , Soil type-soft (SD) = 1.5,  $h_n = 18.6$  (m)

$T = C_t (h_n)^m = 0.0446 (h_n)^{0.9} = 0.619s$  (according to Section 2.5.7.2; Tables 6.2.16, 6.2.20 of BNBC 2020)

$C_s = 2.5 S_\mu = 2.5 * 1.35 * 1 = 3.375$ ; Table 6.2.13 (assuming soil type SD)

$I_{s0} = 0.8 \times 2/3 \times 0.2 \times 1.0 \times 3.375 = \mathbf{0.36}$  (low-rise residential building on soil type SD)

Therefore, seismic index of this building,  $I_s = 0.303 < I_{s0} = 0.36$  (**Not safe**) (X-direction). Hence, more strengthening should be carried out, either installing by wing walls or drop panel, or shear wall as much as needed and possible.

Finally, seismic evaluation is done for each major direction and floor of the building (shown in table C7 and Figure C7). The proposed  $I_{s0}$  is 0.36 for buildings located in Dhaka based on soil type SD of BNBC 2020. However, it was evaluated that the building was not safe in any direction. Therefore, it is desirable to establish some retrofit plans that will ensure that  $I_s > 0.36$  is achieved at each floor level and in each direction.

Table C7 Summary of the seismic evaluation

Storey	Seismic demand index $I_{s0}$	X-direction			Y-direction		
		Seismic capacity $I_s$	Corresponding ductility index	Judgement	Seismic capacity $I_s$	Corresponding ductility index	Judgement
6	0.36	0.405	2.59	OK	0.330	2.59	Not OK
5		0.279	2.59	Not OK	0.215	2.59	Not OK
4		0.239	2.59	Not OK	0.179	2.59	Not OK
3		0.310	2.59	Not OK	0.222	2.59	Not OK
2		0.305	2.59	Not OK	0.214	2.59	Not OK
1		0.303	2.59	Not OK	0.189	2.59	Not OK

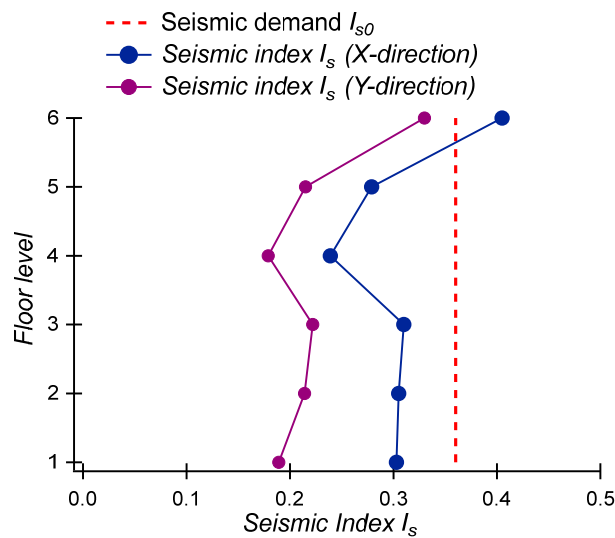


Figure C7 Comparison between seismic demand and capacity

## **References:**

1. Technical guidelines for seismic evaluation of existing reinforced concrete buildings in Bangladesh for extended application of BSPP seismic evaluation manual, 2021.
2. JBDPA. Standard for seismic evaluation of existing reinforced concrete buildings, 2001, Guidelines for seismic retrofit of existing reinforced concrete buildings, 2001 and Technical manual for seismic evaluation and seismic retrofit of existing reinforced concrete. Published online 2005.
3. Public Works Department (PWD). Manual for seismic evaluation of existing reinforced concrete buildings, Manual for seismic retrofit design of existing reinforced concrete buildings, Manual for seismic design of existing reinforced concrete buildings (CNCRP manual). Published online 2015.
4. Samdani HMG, Takahashi S, Yoon R, Sanada Y: Strengthening seismically vulnerable reinforced concrete flat plate-column connections by installing wing walls, *Japan Architectural Review*, Vol. 4; Issue 3, pp. 442–454, June 2021, <http://dx.doi.org/10.1002/2475-8876.12232>.
5. AIJ. AIJ Standard for structural calculation of reinforced concrete structures, revised 2010; 2010 (in Japanese).
6. HBRI. Bangladesh National Building Code (BNBC 2020).

End Page